PROPERTIES OF SELF-COMPACTING CONCRETE INCORPORATING RICE HUSK ASH AND WASTE FOUNDRY SAND

A Thesis

Submitted in fulfilment of the requirement for the award of the degree of

DOCTOR OF PHILOSOPHY

IN

CIVIL ENGINEERING

Submitted By

Ravinder Kaur Sandhu

Registration No. 951402001

THAPAR INSTITUTE
OF ENGINEERING & TECHNOLOGY
(Deemed to be University)

DEPARTMENT OF CIVIL ENGINEERING
THAPAR INSTITUTE OF ENGINEERING AND TECHNOLOGY
PATIALA, PUNJAB (INDIA)-147004
2022

CERTIFICATE

Certify that the thesis entitled "Properties of Self-Compacting Concrete Incorporating Rice Husk Ash and Waste Foundry Sand" which is submitted by Ravinder Kaur Sandhu, in fulfilment of the requirements for the award of degree of Doctor of Philosophy in the Department of Civil Engineering, Thapar Institute of Engineering and Technology, Patiala, is a record of candidate's own original and independent research work carried out by her under my supervision and guidance. The matter embodied in this thesis has not been submitted in part or full to any other University or Institute for the award of any degree.

(Dr. Rafat Siddique)
Dean of Research and Sponsored Projects & Senior Professor
Department of Civil Engineering
Thapar Institute of Engineering and Technology, Patiala
Punjab, India.

DECLARATION

I hereby declare that the research work presented in this thesis entitled "Properties of Self-Compacting Concrete Incorporating Rice Husk Ash and Waste Foundry Sand" submitted for the award of the degree of Doctor of Philosophy in the department of Civil Engineering, Thapar Institute of Engineering and Technology, Patiala is an authenticated record of my own research work carried out under the supervision of Dr. Rafat Siddique, Senior Professor, Department of Civil Engineering and refers other researcher's work are duly listed in reference section. The matter presented in this thesis has not previously been submitted in part or full to any other University or Institution for award of any degree in India or Abroad.

(Ravinder Kaur Sandhu)

ACKNOWLEDGEMENT

- *It has been a really life-changing experience for me to pursue this PhD, and I could not have done it without the support and direction I received from so many people. Many people have supported and encouraged me as I've walked with them throughout the years.*
- *I would like to express my gratitude to my supervisor, Dr. Rafat Siddique, senior professor in the department of civil engineering at the Thapar Institute of Engineering and Technology in Patiala, for his invaluable advice, moral support, and encouragement throughout the entire period of this research.*
- *I would like to extend my acknowledgement to my advisory committee members Dr. Kulvir Singh, Dr. Shweta Goyal and Dr. Heaven Singh for their valuable suggestions and feedbacks. The inputs provided by Dr. P.P Bansal, Head, Department of Civil Engineering, his interest and critical appraisal during the early stages of this research are invaluable. I express my regards to Dr. A.B Danie Roy, PhD coordinator for suggestions and taking interest in the progress of work along with valuable suggestions.*
- *I extend my thanks to all the faculty members of Department of Civil Engineering, Thapar Institute, and Patiala for providing necessary guidance during my research work.*
- *Er. Varinder Kumar Sharma and Shri Ram Simran, technical personnel, are to be commended for their assistance and support during the whole research period. I am thankful to non-teaching staff, Department of Civil Engineering, for the constant official help and cooperation.*

- *I especially thank my family for standing by me through all the joys and sorrows that research scholar life had to offer. My parents have provided unconditional love, moral support and care. Their permanent love and confidence in me have encouraged me to go ahead in my study and career. My heartfelt thanks to my elder sister Gurpinder Kaur Sandhu and younger brother Karan Singh Sandhu for all their constant support and encouragement. They have been my best friends all my life and thank them for all their advice and support. I know I always have my family to count on when times are rough and I would not have made it this far without them. A special thanks to all my friends who have given me many life experiences and immense support during this journey. Their timely help and friendship shall always be remembered.*

(Ravinder Kaur Sandhu)

RESEARCH PUBLICATIONS

- Strength properties and microstructural analysis of self-compacting concrete incorporating waste foundry sand. RK Sandhu, R Siddique, ***Construction and Building Materials*** 225, 371-383, 2019. ***IMPACT FACTOR - 7.693***

- Properties of sustainable self-compacting concrete made with rice husk ash, RK Sandhu, R Siddique, ***European Journal of Environmental and Civil Engineering***, 1-25, 2021. ***IMPACT FACTOR – 2.187***

- Durability performance of self-compacting concrete made with waste foundry sand, RK Sandhu, R Siddique, ***Structural Concrete*** 23 (2), 722-738, 2022. ***IMPACT FACTOR – 2.793***

- Influence of rice husk ash (RHA) on the properties of self-compacting concrete: A review, RK Sandhu, R Siddique, ***Construction and Building Materials*** 153, 751-764, 2017. ***IMPACT FACTOR - 7.693***

ABSTRACT

The widely available rice husk (RH) is burned to produce rice husk ash (RHA), an agricultural by-product that may be used in place of cement which will limit environmental hazards. Worldwide, the casting industry produces more than 60 million metric tonnes of Waste Foundry Sand (WFS) each year, causing environmental issues. Disposal of WFS generated from the casting industry poses serious environmental problems. On the other hand, continuous extraction of natural resources is depleting the environment at a rapid pace increasing the cost of production due to an insufficiency of natural resources. These issues may be resolved with the use of waste materials in concrete. The present study has been carried out to explore the use of RHA and WFS as partial replacement of cement and fine aggregates in SCC.

In this research study, RHA up to 30% by weight is used as a partial replacement for cement as one of the ingredients in self-compacting concrete (SCC). The fresh properties of SCC were investigated by experimental programmes. Compressive strength, splitting tensile strength, sorptivity, water absorption and porosity, rapid chloride permeability test (RCPT), and sulphate resistance were all assessed up to a 365-day curing period. It was determined that the strength properties improved with replacement of cement with RHA. RHA up to 15% replacement level yielded the maximum value. While the durability properties increased noticeably at all replacement levels of RHA. The results of the compressive strength tests were confirmed by X-ray diffraction (XRD) and scanning electron microscope (SEM) microstructure analysis.

Waste Foundry Sand (WFS) has been studied for use in SCC to test its strength and durability. Self-Compacting Concrete prepared with various proportions (0-30%) of WFS as a partial replacement of fine aggregates. In this study, its fresh, strength, durability, and microstructural properties were investigated at 28, 90 and 365 days of curing. Fine aggregates were substituted with 5, 10, 15, 20, 25, and 30% of WFS by volume after control mix design of SCC. Testing was performed for the following characteristics: fresh properties, compressive strength, splitting tensile strength, water absorption, sorptivity, rapid chloride permeability, sulphate resistance, SEM, and XRD. According to EFNARC, all SCC mixes confirmed fresh state properties such as slump flow, T500, V-funnel box, and U-box test. There was a

marginal reduction in compressive strength with the inclusion of WFS up to 10% as compared to the control mix at 28, 90, and 365 days of curing. Incorporating WFS up to 30% increase the volume of permeable pore space from 13.43 to 16.67%, water absorption increased by 2.11 to 3.07 mm, chloride permeability decreased by 2119 to 3553 Coulombs, and compressive strength of samples cured with sulphate decreased nearly 5% when compared to samples cured with water at 28 days of curing. The concrete samples improved in terms of pore structure, permeation, sulphate attack, and chloride permeability after 90 and 365 days of curing. With the usage of 5 to 30% WFS at 28 days, the strength of SCC was reduced from 6.38 to 18.76%. The experimental results are validated by the microstructural results of XRD and SEM. It was observed that by utilizing WFS up to 10%, cost-effective SCC with performance comparable to control mix could be obtained.

In this research study, the effects of RHA as a partial substitute for cement and WFS as a partial replacement for fine aggregates in the SCC mix have also been examined. After 7, 28, 90, and 365 days of curing, percentage variation in compressive strength for the mixes R0WFS0, R5WFS5, R10WFS10, R15WFS15, R20WFS20, R25WFS25, and R30WFS30 was observed. Increased compressive strength was obtained with inclusion of RHA and WFS up to 10% in comparison to control mix at 28, 90, and 365 days of curing. It was possible to prepare SCC of the strength above 49 MPa with utilization of RHA and WFS up to 30% as a replacement of cement and fine aggregates. Sorptivity value decreased up to 10% partial replacement levels at all ages and thereafter values increased for 15% to 30% of replacement levels. At ages 28, 90, and 365 days, the water absorption of the control mix was 4.64%, 4.23%, and 1.40%, respectively, whereas it was 5.07%, 4.47%, and 1.59% for mix R30WFS30. Additionally, research has been done to determine the relationships between the compressive and tensile strengths of all blends which have been cured for 7, 28, 90, and 365 days. SEM images of the SCC mixes with RHA and WFS were obtained to investigate the microstructure aspects in the transition zone and paste around the aggregates. It was found that the permeability of RHA and WFS blended SCC mixes decreased at all ages, up to 15% replacement levels. SCC specimens that had been cured in a sulphate solution showed compressive strengths that were comparable to control mixes up to 10% replacement levels of RHA and WFS blends at all ages.

TABLE OF CONTENTS

LIST OF TABLES

LIST OF FIGURES

ABBREVIATIONS

Abbreviations		Word(s)
ACI	-	American Concrete Institute
ASTM	-	American Society for Testing and Materials
CASH	-	Calcium Aluminium Silicate Hydrate
CEB	-	COMIT´E EURO-INTERNATIONAL DU B´ETON
CH	-	Calcium Hydroxide
CS	-	Calcium silicate
CSH	-	Calcium Silicate Hydrate
CTM	-	Compression Testing Machine
E	-	Ettringite
EFNARC	-	European Federation of National Associations Representing for concrete
EDS	-	Energy Dispersive X-ray spectroscopy
FA	-	Fly Ash

FS	-	Foundry Sand
HRWRA	-	High Range Water Reducing Admixtures
ITZ	-	Inter Transition Zone
JCPDS	-	Joint Committee on Powder Diffraction Standard
MK	-	Metakaolin
OPC	-	Ordinary Portland Cement
P	-	Portlandite
PFA	-	Pulverized Fuel Ash
Q	-	Quartz
RCPT	-	Rapid Chloride Permeability Test
RHA	-	Rice Husk Ash
RH	-	Rice Husk
SCC	-	Self - Compacting concrete
SCM	-	Supplementary Cementitious Material
SEM	-	Scanning Electron Microscopy

SF	-	Silica Fume
UHP	-	Ultra High Performance
UPV	-	Ultrasonic Pulse Velocity
UTM	-	Universal Testing Machine
WFS	-	Waste Foundry Sand
w/c	-	Water to cement ratio
w/b	-	Water to binder ratio
XRD	-	X- Ray Diffraction

LIST OF UNITS

Units		Word(s)
cm	-	Centimetre
cm^2/g	-	Centimetre square per gram
C	-	Coulomb
°C	-	Degree Celsius
g	-	Gram
GPa	-	Gega Pascal
hr	-	Hour
kg	-	kilogram
kg/m^3	-	kilogram per cubic metre
kN	-	kilo Newton
kV	-	kilovolt
km/s	-	kilometre per second
l	-	Litre
m	-	Metre

mg	-	Milligram
mm	-	Millimetre
ml	-	Millilitre
µm	-	Micrometre
m/s	-	Metre per second
MPa	-	Mega Pascal
min	-	Minute
N	-	Newton
N/mm^2	-	Newton per square millimetre
lb	-	Pound
%	-	Percent
lb/yd^3	-	Pound per cubic yard
rpm	-	Revolutions per minute
sec	-	Second
θ	-	Theta
V	-	Volts
yd	-	Yard

CHAPTER- 1

INTRODUCTION

This chapter provides an overview of the physical and chemical properties of rice husk ash and waste foundry sand generation. Additionally, it covers the environmental effects of waste foundry sand and rice husk ash, as well as the purpose of the current study and its many applications.

1.1 OVERVIEW

With the development, there has been tremendous growth in the construction industry which globally makes concrete the second most consumed substance in the world, after water *(GCCA, 2019).* It leads to consumption and depletion of natural resources (fine aggregates and coarse aggregates). Due to the excessive consumption of natural resources in the construction sectors, research studies promote the use of recyclable waste products as an alternative to non-renewable materials *(Rahman et al., 2022).*The current techniques for obtaining fine aggregates include mining from river beds which has a detrimental effect on the environment. To curb the problem of diminishing natural reserves, the governments have restrained the mining of fine aggregates resulting in its scarcity. Therefore, it has become obligatory to look for some alternative strategies to reduce consumption and to protect the natural resources that should be eco-friendly and sustainable.

1.2 SELF-COMPACTING CONCRETE

The development of self-compacting concrete (SCC) is attributed to an effort in Japan in the late 1980s to improve concrete quality, where an absence of uniform and thorough compaction was recognised as the key issue causing poor concrete structure performance. Since there was no viable way to assure full compaction of concrete on a worksite, the emphasis moved towards eliminating the need to compact, whether it be by vibration or any other method. Researchers from the University of Tokyo, (*Okamura and Ouchi, 2003)*, developed the first practical SCC as a consequence of this. To obtain complete compaction, the SCC does not require vibrating. Improved concrete quality and fewer on-site repairs, shorter building periods, reduced total costs, and easier automation integration into concrete construction are just a several of the benefits. SCC mixes comprise significant amounts of fine-grained inorganic

components, allowing for the use of "dusts," that are currently waste products with no potential implementation and are expensive to manage. In addition to causing noise discomfort, vibrating concrete in congested areas may pose a risk to workers. There are usually concerns concerning the strength and durability of structures constructed in such areas. Durability is one of the crucial challenges affecting the global construction sector *(Jha et al., 2021).* As a result, if at all feasible, it is desirable to remove vibration in action and improve the durability of concrete. SCC expertise has advanced from research to implementation in nations such as Japan, Sweden, Thailand, and the United Kingdom. However, in India, this information is expected to be widely spread.

The SCC's mix proportions were designed to meet all of the concrete's performance requirements in both the fresh and hardened phases. The water-to-supplementary cementitious materials (w/cm) ratio is one of the basic mixing factors regulating the characteristics of SCC, such as rheology, strength, and durability, as it is in vibrated concrete. The w/cm is one of the primary important factors controlling properties of SCC.

Therefore, while developing SCC, a lot of parameters should be incorporated to a larger extent than when designing regular concrete. That included: (1) characteristics of naturally sourced raw materials, such as physical parameters of supplementary cementing materials (SCM) mineral additions and aggregates, (2) suitable selection of super plasticizer to achieve optimal consistency with the chosen SCM, and (3) making adjustments for the fresh properties for the casting process (pumping, etc.), shape of the cast component, and reinforcement provisions *(Gupta et al., 2021).*

The SCC mix proportion should take into account the fresh state characteristics and hardened characteristics according to the application. Criteria for the quantity of SCM and fillers, the water content (w/cm), coarse aggregate, the sand-to-aggregate ratio (S/A), and the air content for durability requirements are all taken into account. The type and quantities of chemical admixtures used in the mix design process are determined by the flow characteristics required for the desired application. SCC is type of concrete that flows under its own weight, having flowability, passing ability and resistance for segregation *(Kapoor et al., 2016).*

1.2.1 Definition of Self-Compacting Concrete

Various authors have provided a number of definitions, but they all concluded that SCC was concrete that flowed on its own i.e. under its own weight without the need for external vibrations, unlike conventional vibrated concrete.

The *EFNARC (2005)* stated that "Self-compacting concrete is an innovative concrete that does not require vibration for placing and compaction. It is able to flow under its own weight, completely filling form work and achieving full compaction, even in the presence of congested reinforcement."

The British Standard *(BS EN 206-9, 2010)* defined SCC as the "concrete that is able to flow and compact under its own weight; fill the form work with its reinforcement, ducts, box outs etc, whilst maintaining homogeneity."

1.2.2 Advantages of SCC

Structures constructed with Self compacting concrete can be built in thinner sections than conventional. SCC improves the durability, and reliability of concrete structures. It can be easily placed which results in cost savings through reduced equipment and labour requirement. Concrete may be placed even in regions where vibrators cannot be used for compaction. The quality of concrete is improved which helps in reducing onsite repairs. The construction time is faster due to which the overall construction cost decreases. The ingredients of self-compacting concrete are easily placed, which results in better surface finishes. SCC is environment friendly material. SCC can be compacted without using either internal or external vibration. Noise pollution is eliminated in SCC because vibrators are not required. Skilled worker are not required for vibration process at the time of placing concrete. Concrete structures may be built using complicated formwork shapes that were previously impossible to cast. High quality placement of concrete achieved even with unskilled workers. Automation of construction is possible with application of SCC. New types of complex structural elements can be constructed, which were not possible with normally vibrated concrete. The SCC significantly improves workability, and pumping ability in addition to stronger bonding with dense reinforcement. When using self-compacting concrete, the issues associated with pumping system choking are quite minimal. The voids in the structural members are reduced which helps in improving permeability in the concrete structures. It is possible to cast concrete in the densely reinforced structural members of the structures.

Difficulty in development of SCC was on account of contradictory factors that the concrete should be fully flow able but without bleeding or segregation. Cement mortar of the SCC should have higher viscosity to ensure flow ability while maintaining non–sedimentation of bigger aggregates. Its supply cost is two to three times higher than that of normal concrete although the use of SCC has many technical, social, and overall economic advantages, its supply cost is two to three times higher than that of normal concrete depending upon the composition of the mixture and quality control of concrete producer.

Following limitations exists while working with Self-Compacting Concrete

The selection of ingredients is stricter in case of self-compacting concrete. The cost of construction increases in comparison with regular concrete. A designed mixture is prepared after many trial batches and laboratory tests. Higher precision is required when measuring and monitoring. There is no internationally accepted test standard for self-compacting concrete mix. For formwork design, the increased flow rate of SCC compared to conventional concrete might result in a dynamic pressure in addition to the hydrostatic pressure of poured concrete.

1.2.3 Difference between Self-Compacting Concrete and Normal Vibrated Concrete

When compared to normal vibrated concrete (NVC), self-compacting concrete with a comparable water cement or cement binder ratio will usually have a little greater strength due to the lack of vibration providing a better interface between the aggregate and hardened paste. SCC concrete must be laid at a faster rate than normal concrete. Without aggregate segregation, self-compacting concrete has been used at heights more than 5 metres. It may also be utilised in regions with regular and congested reinforcement, as well as aggregates up to 2 inches in diameter. Table 1.1 demonstrates the difference between SCC and conventional concrete.

1.2.4 Applications of SCC

The SCC is a kind of concrete that is used to build structures with more complicated reinforcing. The SCC can be easily poured in drilled shafts, columns and earth retaining systems. It can reach areas with a high concentration of rebar and pipes/conduits. It is employed in restoration and redevelopment projects. SCC may be used to build highly robust and long-lasting retaining walls. It is used to build raft and

piling foundations. The SCC can be best utilised in the areas which are noise sensitive. It is extensively utilised in the precast industry.

Table 1.1 Differences between SCC and NVC

Self-Compacting Concrete	**Normal Vibrated Concrete**
Concrete has high flowability to undergo compaction by its own weight	Concrete is compacted by external means of vibration
High workability	Less workable mix
Workability gained through super plasticizers and viscosity modifying agents	Workability gained through increased moisture content
Addition of superplasticizer increase the bond between aggregate and cement matrix	The aggregate-cement matrix is weak
Water Content is Low	High Water Content
Fines Content – Cement and Fine aggregate is high	The fines content is less compared to SCC
Lower water content decreases the Bleeding	Bleeding is high
Increased fines content gives a homogeneous mix with less segregation issues	Segregation is higher
Low Viscosity due to high fines content	High Viscosity
SCC structures give good aesthetic finish	Aesthetic finish is not satisfactory
Good choice for thick reinforcement works	Normal concrete are limited in thick reinforcement areas due to external compaction difficulties.

1.3 BY-PRODUCTS FROM INDUSTRIAL AND AGRICULTURE SECTORS

1.3.1 Waste Foundry Sand

Waste Foundry Sand (WFS) is high quality silica sand that is a by-product from the production of both ferrous and nonferrous metal castings. Foundries use high quality size-specific silica sands for use in their molding and casting operations. The raw sand is normally of a higher quality than the typical bank run or natural sands used in fill construction sites. In the casting process, molding sands are recycled and reused multiple times. Eventually, however, the recycled sand degrades to the point that it can no longer be reused in the casting process. When it is not possible to further reuse in the foundry, it is removed from the foundry and is termed as waste foundry sand. The physical and chemical characteristics of foundry sand will depend in great part on the type of casting process and the industry sector from which it originates.

1.3.1.1 Types of Foundry Sands

Classification of foundry sands depends upon the type of binder systems used in metal casting. Two types of binder systems are generally used, and on the basis of that foundry sands are categorized as: clay-bonded sand (green sand) and chemically bonded sand.

Clay-bonded (Green) sand is composed of naturally occurring materials which are blended together such as high quality silica sand (85-95%), bentonite clay (4-10%) as a binder, a carbonaceous additive (2-10%) to improve the casting surface finish and water (2-5%). It is black in color due to carbon content. Green sand is the most commonly used molding media by foundries. Silica sand is the bulk medium that resists high temperatures while the coating of clay binds the sand together. The water adds plasticity.

Chemically bonded sand are used both in core making where high strength are necessary to withstand the heat of molten metal, and in mold making. Chemically bonded sand consists of 93-99% silica and 1-3% chemical binder. Silica sand is thoroughly mixed with the chemicals; a catalyst initiates the reaction that cures and hardens the mass. There are various types of chemical binder systems used in the foundry industry. The most common chemical binder systems used are phenolic-urethanes, epoxy-resins, furfyl alcohol, and sodium silicates. Chemically bonded sands are generally light in color and in texture than clay bonded sands *(Siddique, 2008).*

1.3.1.2 Waste Foundry Sand Production, Disposal and Environmental Impact

The foundry industry is of paramount importance, as it provides intermediary products to support other industries having significant growth in recent years reaching the mark of 109.8 million metric tons produced in 2017. India is the second largest casting producer (12.05 million metric tons) in the world after China according to Global Casting Production *(Census of World Casting, 2019).* The foundry units in India are above 5000 *(The Institute of Indian Foundrymen, 2019).* Foundry sand (FS) is silica-rich, uniformly sized and has a high thermal conductivity which is used in foundries for both ferrous and non-ferrous metal castings. FS is used multiple times in the casting procedure. When the FS fails to retain its characteristics and is deteriorated, it is abandoned from the metal casting process. The sand junked from the

metal casting industries is called waste foundry sand (WFS) *(Bhardwaj and Kumar, 2018)*. The shape of its particles is usually sub-angular to rounded *(Bradshaw et al., 2015).* FS being hydrophilic in nature attracts more water to its surface due to its higher silica composition. Spent foundry sand (SFS) or used foundry sand (UFS) are other assigned names to WFS *(Siddique and Singh, 2011).* The quality of WFS will depend on the casting process, the material formed in the industry and the source it is derived from *(Siddique et al., 2010).*The shape of particles is not only the fundamental shape of the aggregates but also additional characteristics like angularity, flakiness, and so on. It is a result of their formation circumstances, the mineralogical content, and particle size *(Ghasemi et al., 2018).*The metal casting industries results in the production of 0.60 ton of WFS per 1 ton of steel production and around the globe production of WFS is approximately 62.64 million metric tons *(Dyer et al., 2018).* Therefore, WFS generated from the casting industry poses serious problems. The efforts should be made to effectively recycle the waste generated so that it can reduce the consumption of raw materials, thus leading to concrete being produced that is cost-effective and environment-friendly *(Rao et al., 2007).* The use of WFS shall be beneficial from an environmental point of view and it may result in a boost to the local and global economics. Also, utilizing resources efficiently so that natural ones may be preserved is one of the key principles of the sustainable development approach *(Di Maria et al., 2020).*

Table 1.2 Typical physical properties of WFS

Property	Siddique and Noumowe (2008)	Prabhu et al. (2015)	Naik et al. (2001)	Guney et al. (2010)
Specific gravity	2.39-2.55	2.24	2.79	2.45
Moisture content (%)	0.1-10.1	-	-	3.25
Absorption (%)	0.45	1.13	5	-
Unit Weight (kg/m^3)	2589	1576	1784	-
Clay lumps and friable particles	1-144	-	0.40	-
Fineness modulus	-	-	2.32	-
Materials finer than75µm (%)	-	8	0.40	24

1.3.1.3 Physical Properties of Waste Foundry Sand

WFS exhibits sub-angular to spherical shape. Chemically bonded sands are light tan or off-white in hue compared to green sands, which are either black or grey. The distribution of grain size in waste foundry sand is homogeneous, with 85–95% of the material falling between 0.6 mm and 0.15 mm and 5–20% of the material being smaller than 0.075 mm. Table 1.2 gives the values of physical properties of WFS.

1.3.1.4 Chemical Properties

The type of metal, binder, and combustible utilised all affect the chemical composition of the WFS. The performance of the foundry sand may be determined by its chemical (elemental) composition. Waste foundry sand has a high silica concentration. It is covered in a thin layer of dust, bentonite, residual binder (sea coal, resins/chemicals), and burned carbon. Water is drawn to the surface of silica sand because it has a hydrophilic property. Chemical composition of WFS as reported by *(Arulrajah et al., 2017, Guney et al., 2010, Etxeberria et al., 2010 and Sahmaran et al., 2011)* is given in Table 1.3.

Table 1.3 Chemical Composition of Foundry Sand

Constituent	Value (%)			
	Guney *et al.* (2010)	Arurajah et al. (2017)	Etxeberria *et al.* (2010)	Sahmaran *et al.* (2011)
SiO_2	98	84.145	95.1	76
Al_2O_3	0.8	11.817	1.47	4.45
Fe_2O_3	0.25	1.533	0.49	5.06
CaO	0.035	1.507	0.19	3.56
MgO	0.023	-	0.19	1.98
SO_3	0.01	0.453	0.03	-
Na_2O	0.04	-	0.26	0.3
K_2O	0.04	0.287	0.68	1.2
TiO_2	-	0.257	0.04	0.17
Mn_2O_3	-	-		0.46
LOI	-	-	1.32	5.85

1.3.1.5 Uses and Application of Waste Foundry Sand

The waste foundry sand is mainly used for structural fill. The stratified layers of WFS can be provided as road sub-base. The WFS is used as fine aggregate in asphalt paving aggregate for flowable fill. The WFS can be used as an alternative material for fine aggregate for concrete. It is used as a raw material in cement manufacturing industry. It can also be used for soil blending, manufactured topsoil, potting soil, compost. The waste foundry sand is used in place of fine aggregate for concrete block. The waste foundry sand is too fine due to which it can be used as hydraulic barrier in landfill final cover. There is a need to concentrate on alternative construction materials since the need for construction materials in the construction industry never decreases. The waste foundry sand has also a potential to be used as fine aggregate in manufacturing normal and self-compacting concrete. The amount of disposal material may be decreased by using waste foundry sand in construction industry. Use for waste materials like foundry sand may boost the economy while lowering the amount of carbon produced and virgin materials consumed in our country.

WFS can be utilized for various applications. It can be used in asphalt concrete, as a compost additive, in concrete bricks and pavers, Portland cement, mineral wood products, structural fill, and road base/Sub-base. WFS can also be used as an alternative aggregate, as partial replacement of natural sand due to its considerably high silica content and properties of natural sand. It can be utilized as replacement of sand as filling material in embankments and structural fills, in Hot Mix Asphalt (HMA), flowable fills, concrete, as the sub -base in the construction of roads *(FIRST, 2004).Dyer et al. (2018)*carried out research and utilized WFS in HMA replacing the manufactured sand, i.e. the fine aggregates, and studied the microstructure. In another study by *Arulrajah et al. (2017)* geotechnical and environmental properties were examined and it was concluded that WFS can be utilized for road applications as subgrade fill and bedding material for pipeline construction. *Ganeshan et al. (2016)* suggested that WFS has beneficial applications in manufacturing solid masonry blocks with a substitution rate between 20% to 30% of fine aggregates. WFS after being used multiple times in the metal casting industry still has the potential to replace fine aggregates and its recycling limits the hazards which are being created by

discarding WFS. There has been a considerable endeavour for application of WFS as an alternate material, as a partial or complete replacement of fine aggregate.

There has been significant literature on WFS by partial replacement of fine aggregates, but the research regarding Self-Compacting Concrete (SCC) is very limited. The SCC is a specialized type of concrete which is formed by adopting controlled aggregate content, less water-powder ratio and treating the concrete with superplasticizer which exhibits immense deformability, balances viscosity, does not allow splitting up of aggregates (non-segregating) and flows with the force of gravity. During casting, SCC flows without being segregated, exhibits immense deformability and does not require vibrations *(ACI, 2007).* It ensures compaction especially in confined spaces and when vibrating compaction is difficult. The aggregate proportions in SCC are less than that of normal concrete but they play a major role in fresh and hardened properties *(Kapoor et al., 2016).*

Prior to the present investigation, few attempts have been made to evaluate the utilization of WFS as a partial or total replacement of fine aggregates in conventional concrete. Significant work is not available on the use of WFS in SCC. Few authors such as *Kraus et al. (2009)* produced cost-effective SCC by replacing 10%, 20% and 30% of fly ash at a 1:2 (fly ash and foundry dust) ratio with silica dust. The 20% replacement level showed better performance and was the optimum percentage. The fines in SCC increased with an increase in foundry silica dust content. Further, the requirement of water reducing admixture content becomes higher and the need for viscosity-modifying admixture was lowered. The slump-flow diameter lies between 710–725 mm and no visible bleeding was observed compared to the control mix. Minor decrement was noted in a 3-day compressive strength test and a considerable decrement in a 28-day compressive strength test. *Sahmaran et al. (2011)* studied the properties of SCC incorporating fly ash and waste foundry sand. The Portland cement was replaced with fly ash at levels of 0, 30, 50 and 70% by mass and a further 0% to 100% levels of sand were replaced with WFS through an increment of 25% by volume of each fly ash replacement. The water to binder ratio (w/b) was the same for all mixtures 0.40, and total binder content was also constant as 450 kg/m^3. Utilizing WFS in SCC was favourable as it was viable to achieve fresh properties. The compressive strengths, by using WFS and fly ash at 100% replacement of WFS were 40 MPa, 50 MPa at 28 and 90 days respectively. However, incorporating WFS and fly

ash reduces the strength at all ages with reference to the control mixture. *Pathak and Siddique (2012)* replaced fine aggregates with 10% WFS and cement partially with fly ash in SCC. It was found that the value of compressive strength of the SCC mixes was lesser at higher temperature due to the presence of fly ash and WFS. *Raju et al. (2016)* in the study replaced natural sand with WFS at differing percentages by mass 25%, 50%, 75% and 100% in SCC and concluded that as the content of WFS increases workability decreases, the maximum compressive strength was achieved at 25% replacement level which showed better performance.

In the present study, WFS as partial substitution of fine aggregates has been utilized in manufacturing green SCC. The SCC produced by utilizing industrial by-products helps to preserve natural resources which reduce the environmental impacts and may lead to economic gains.

1.3.2 Rice Husk Ash

World-wide yearly production of rice is 742 million tons, and approximately 148 million tons of rice husk is produced *(FA0, 2015).* For every ton of husk, approximately 0.19 ton of ash is generated. Rice husk ash (RHA) is produced by burning rice husk. Generally, every ton of husk produces about 0.19 ton of ash *(Bouzoubaa and Fournier, 2001; Prasad et al., 2000).* Rice husk has a high calorific value *(Bronzeoak, 2003; Asavapisit and Ruengrit, 2005).* Amorphous silica is mostly concentrated at the surfaces of the rice husk and not within the husk itself *(Jauberthie et al., 2000).*RHA is an agricultural by-product available in large quantities causing detrimental effect due to crop residue burning. By utilization of RHA in SCC greener and economical concrete is achieved. RHA an agriculture by-product being in abundance, having high surface area and pozzolanic in nature, can be effectively used as supplementary cementitious material (SCM). SCC is High Performance Concrete which saves time and energy during construction. Using RHA as SCM as partial replacement of cement helps to achieve greener and economical concrete as it reduces the cost of SCC. Further, use of RHA results in environmental benefit as lesser quantity of it would have to be land-filled, leading to reduction in environmental pollution. Carbonization and decarbonation are two different phases in the decomposition of rice husk. Silica in RHA melts around 1440ºC *(Bronzeoak, 2003).* Burning of rice husk at temperature lower than 800ºC degree produces reactive amorphous silica which contains approximately 90% silica, whereas above this

temperature some crystalline form of silica can also be obtained *(Chandrasekhar et al., 2003; Chindaprasirt et al., 2008; Reddy and Marcelina, 2006; Zhang and Malhotra, 1996)*. Silica in amorphous form is useful as a pozzolan to produce durable good quality concrete *(Chindaprasirt et al., 2008).* Crystalline and amorphous forms of silica in rice husk depend upon burning temperature and its duration. Rice husk ash should be produced with suitable specifications for a specific use as crystalline and amorphous forms of silica have different properties *(Stroven et al., 1999; Basha et al., 2005). Nair et al. (2008)* stated that the samples burnt for more than 12 h, at 500 - 700ºC produced high reactivity ashes, whereas short durations burning (15–360 min) resulted in high carbon content in RHA. *Mehta (1992)* reviewed physical and chemical properties of RHA, and its use as a supplementary cementing material. Use of RHA in cement based materials reduces heat of hydration, improves strength and durability parameters besides reduction in cement cost and other environmental benefits.

Utilization of alternate materials in construction sector boosts economy and leads to sustainable development *(Sahu et al., 2003).* The use of RHA not only produces higher quality and lower cost concrete, but also reduces carbon dioxide (CO_2) emissions from the production of cement. RHA has been used as a highly reactive pozzolanic material to improve the microstructure of the interfacial transition zone (ITZ) between the cement paste and the aggregate in self-compacting concrete (SCC). Mechanical experiments of RHA blended Portland cement concretes revealed that in addition to the pozzolanic reactivity of RHA (chemical aspect), the particle grading (physical aspect) of cement and RHA mixtures also exerted significant influences on the blending efficiency.

1.3.2.1 Physical Properties of Rice Husk Ash

The RHA is a fine material having grey to white in color due to complete burning while partially burnt RHA is blackish. Table 1.4 shows physical properties of RHA. *Della et al. (2002)* reported after burning RHA samples at 700°C for 6 h and wet-grinding (80 min), reduced particle size and grey colour was obtained because of lower carbon content depicted in Figure 1.1a. The carbon content in RHA before burning was 18.60% which was reduced to 0.14% shown in Figure1.1b. Average particle size of rice-husk ash varied between 3 and 10 mm. Before burning, RHA had a specific surface area of 177 m^2/g, which got reduced 54 m^2/g after burning, and then

increased to 81 m^2/g after wet grinding. *Habeeb and Mahmud (2010)* observed that with increasing grinding time from 90 to 360 min, size of RHA decreased from 63.8 to 11.5 mm shown in Figure1.2 with slight increase in specific surface area with time due to micro-porous and multi-layered surface of RHA. *Della et al. (2002)* reported that after burning RHA at 700ºC for 6 h, its mean particle size was 33 mm which after milling for 80 min, reduced to 0.68 mm.

Table 1.4 Physical properties of RHA

Property	Kannan & Ganesan (2015)	Le et al. (2015)	Sua-iam et al. (2013)	Safiuddin et al. (2012)	Habeeb & Mahmud (2010)
Mean particle size (µm)	6.27	5.7-15.6	39.34	6	11.5-63.8
Specific gravity	2.08	—	2.24	2.1	—
Fineness: passing 45 µm (%)	91	—	—	—	—
Specific surface area (m^2/g)	36.47	22.36-25.21	0.37	2.33	25.3-30.4

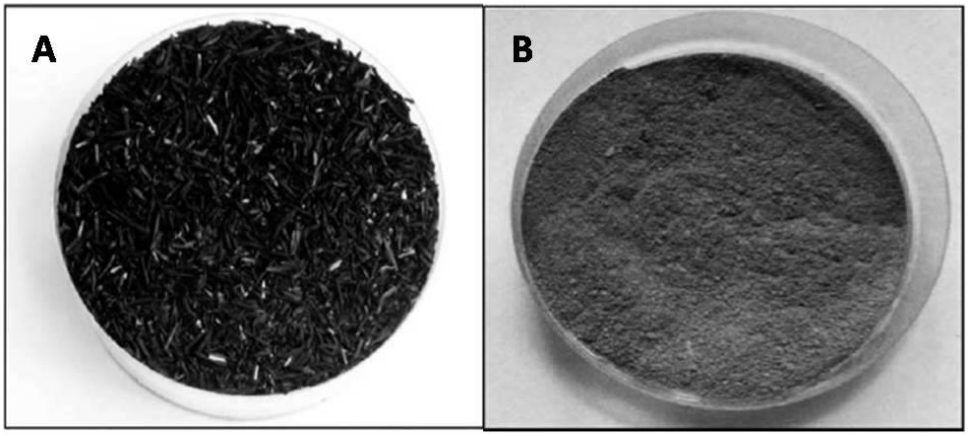

Fig.1.1 Rice husk ash, (A) as received, (B) after burning out at 700°C for 6 h (Della et al., 2002)

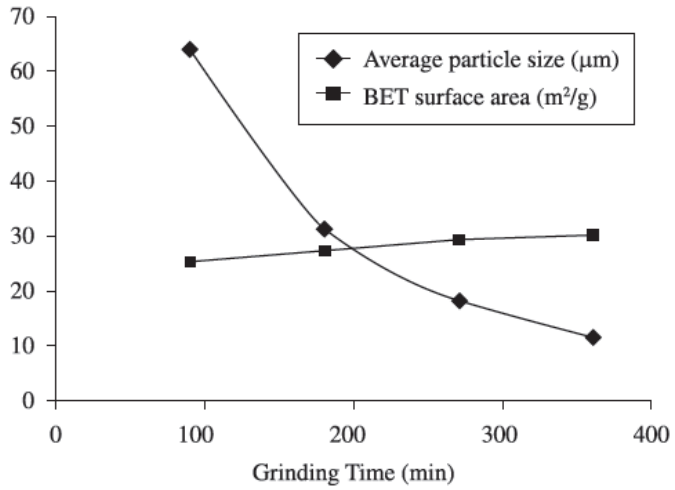

Fig.1.2 Average particle size and specific surface area of RHA against grinding time (Habeeb and Mahmud, 2010)

1.3.2.2 Chemical Properties of Rice Husk Ash

The chemical composition of rice husk varies due to variations in quality of rice, and generally contains cellulose (40–50%), lignin (25–30%), ash (15–20%) and moisture (8–15%) *(Hwang and Chandra, 1997).*Chemical properties of rice husk are tabulated in Table 1.5.

Table 1.5 Chemical properties of RHA

Constituents	Rego et al. (2015)[a]	Kannan & Ganesan (2015)	Chopra et al. (2015)	Sua-iam and Makul (2013)	Memon et al. (2011)	Della et al. (2002)[b]
Silica (SiO_2)	87.08	87.89	94.0	93.44	77.19	94.95
Aluminium oxide ($A1_2O_3$)	<0.01	0.19	1.2	0.21	6.19	0.39
Iron oxide (Fe_2O_3)	0.11	0.28	0.37	0.18	3.65	0.26
Calcium oxide (CaO)	0.70	0.73	2.93	0.76	2.88	0.54
Magnesium oxide (MgO)	0.42	0.47	0.60	0.43	1.45	0.90
Sodium oxide Na_2O)	0.18	0.66	—	0.05		0.25
Potassium oxide (K_2O)	1.40	3.43	0.50	1.98	1.82	0.94
Sulfur oxide (SO_3)	—	—	0.30	0.16		—
LOI	8.03	4.36	—	1.27	5.429	0.85

a – RHA sample grinded for 5 h b – RHA after burning out

Silica Oxide is the main component in RHA, and it varies between 77.19 and 94.95%. *Stroeven et al. (1999)* found that the silica is distributed mostly under the husk's outer surface. Silica content in RHA ranges from 85 to 95%. X-ray diffraction (XRD) analysis of RHA exhibited that it consists of amorphous materials *(Bouzoubaa and Fournier, 2001)* and shows broad peak on 2h angle of 22° 2θ depicted in Figure 1.3a *(Habeeb and Mahmud, 2010).Farooque et al. (2009)* also analyzed the XRD of RHA and indicated the presence of quartz (22.85°, 26.63°, and 42.47° 2θ), cristobalite (21.91°, 35.99°, 69.5° 2θ) and anorthite (27.91°, 29.42° 2θ) peaks shown in Figure 1.3b. Presence of cristobalite peak indicated the crystalline nature of silica in RHA produced at high temperature (above 973 K). *Cizer et al. (2006)* reported amorphous phase of RHA with a broad band between 15 and 30° 2θ shown in Figure1.3c, along with specific quantity of crystalline silica in cristobalite and tridymite form. This established that RHA was obtained by burning at 800–1000°C for crystallization of the amorphous silica takes place. SEM of rice husk ash shows silicious nature and highly porous tracery surface morphology, with a high surface area. *Farooque et al. (2009); Habeeb and Mahmud (2010)*and *Madrid et al. (2012)*analysed the RHA particles by SEM and showed multilatered, angular, microporous surface and honeycombed structure of RHA justifying its high specific surface area observed in Figure 1.4.

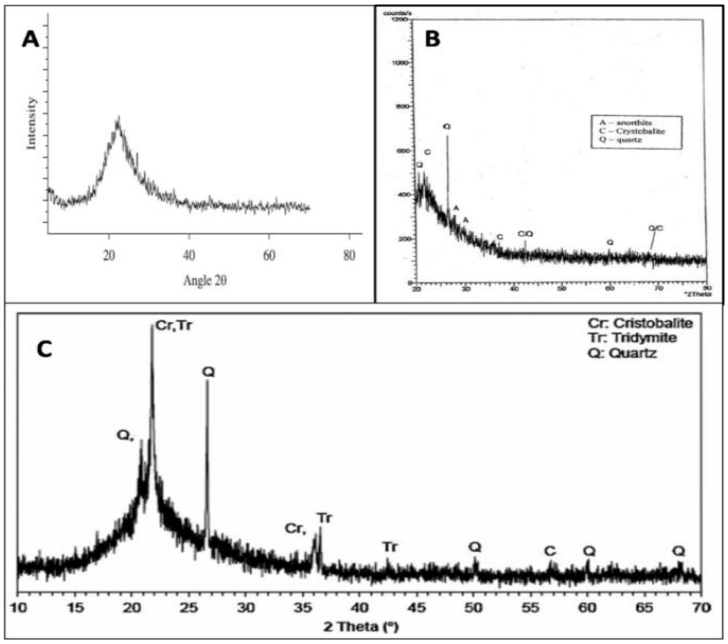

Fig.1.3 XRD of RHA
(A) Habeeb & Mahmud (2010); (B) Farooque et al. (2009); (C) Cizer et al. (2006)

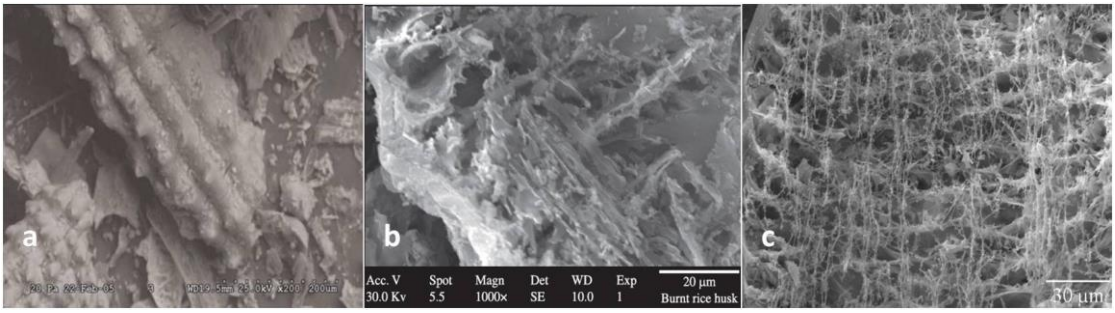

Fig.1.4 SEM of RHA
(a) Farooque et al. (2009); (b) Habeeb & Mahmud (2010); (c) Madrid et al. (2012)

Habeeb and Fayyadh (2009) revealed that the rice husk after burning at 700ºC maintains its cellular structure and after grounding, particles shapes are very irregular-with porous cellular surface. *Rego et al. (2015)* reported that RHA with higher amorphous silica formed the interstitial pores smaller than 500 nm, due to aggregation of the non-condensed SiO_2 particles inside the voids in RHA. *Xu et al. (2012)* found that interstitial pores in RHA were dependent on the calcination process and greatly influenced its specific surface area. After 5 h of grinding of RHA, its surface and morphology at different magnification levels showing macro and interstitial pores filled with finely grounded particles. At high magnification level of (20,000X) interstitial pores within of macropores was seen. *Mohseni et al. (2015)* carried out XRD analysis and showed that intensity of Alite and Belite phases decreased and new peak of portlandite achieved with the addition of nano-TiO_2 (NT). The SEM micrographs illustrated the widespread distribution of mortars containing NT with packed pore structures which resulted in promoting of strength and durability of specimens. X-ray diffraction analysis indicates that the RHA contains mainly amorphous materials with a small quantity of crystalline phases such as cristobalite (high-temperature phase of SiO_2) and sylvite (KCl), which is probably originated from the use of the fertilizers.

1.3.2.3 Uses and Application of Rice Husk Ash

Rice husk ash can is used in following applications *(Krishna, 2012; Siddique & Khan, 2011)*

The RHA is used as a pozzolan, as a filler, additive, abrasive agent, oil adsorbent, sweeping component, and as a suspending agent for porcelain enamels, among other things. RHA can be used as a partial substitute for cement in the construction industry. Each use has distinct requirements, such as reactivity for cement and

concrete, chemical purity for the synthesis of new materials, whiteness, the right particle size for filler applications, high surface area and porosity for use as an adsorbent and catalyst. Due to special physical and chemical characteristics of RH, such as its high ash and silica contents, it is well suited for use in both residential and industrial processing. Numerous studies have demonstrated that RH is utilised as fuel for a variety of purposes, including the parboiling of rice, the manufacturing of sodium silicate, and as a cleaning or polishing agent in the metal and machine industries. By directly burning and gasifying RH, heat energy is generated that can be employed in a variety of processes, such as the creation of steam during the parboiling of rice. Other uses of RHA can be in blended cements, manufacturing green concrete, high performance concrete, refractory, ceramic glaze, insulators, roofing shingles, waterproofing chemicals, oil spill absorbants, carrier for pesticides, bio-fertilizers, solar panels, plastic and rubber reinforcements, catalysts, coating, pulp and paper processing, detergents and soap, anticaking agent for packing. The high silica content of RH has made it a source for several silicon compounds, including silicon nitride, silicon tetrachloride, silicon carbide, silica, zeolite, and pure silicon.

Advantages of using RHA in cement and concrete

Rice-husk ash, a very fine pozzolanic material, when blended with cement makes it the most versatile eco-friendly supplementary cementitious material to concrete. Approximately 700 to 1000 kg of CO_2 is emitted for every tonne of clinker used in the manufacturing of Portland cement alone, which accounts for the majority of the CO_2 emissions associated with the production of concrete *(Cachim et al., 2014).* Globally, the manufacturing of cement is estimated to be responsible for 5 to 7% of all greenhouse gas emissions into the environment *(Farhan et al., 2020).*Therefore utilization of RHA in construction sector will lead towards sustainable development.

The utilization of rice husk ash as a pozzolanic material in cement and concrete provides several advantages such as:

The Rice husk ash reduces the heat of hydration in production of concrete. It helps in improving the strength of concrete when used as a partial replacement of cement. The permeability of the concrete is found to be reduced when used at higher dosages. The Rice husk ash has a potential to resist mild, chloride and sulphate acids. The cost of concrete production can also be reduced with utilisation of rice husk ash as a partial

replacement of cement. Environmental benefits related to the disposal of waste materials and to reduced carbon dioxide emissions can be achieved by utilisation of rice husk ash in construction industry. It is a suitable additional cementitious material or pozzolanic admixture because of the high silica content.

1.4 SIGNIFICANCE OF RESEARCH

With construction growing at a fast rate, it is the need of the hour to produce more sustainable concrete incorporating waste material to protect the environment and save natural resources. Use of SCC is increasing but there is a need to find alternatives for constituents so that economical SCC can be produced. Extensive research has already been done to examine the performance of conventional concrete incorporating WFS. However, required research efforts have not been made and consequently, there is a dearth of literature on the use of WFS in SCC and this requires further study. In the present research, WFS is partially replaced by fine aggregates in SCC. With this ingredient, the SCC is designed to exhibit fresh properties and give adequate strength. Fresh properties, hardened properties, and micro-structure have been examined in this research so that the possibility of using WFS in SCC can be explored. Utilizing WFS in the domain of SCC will be beneficial as it will provide cost-effective SCC manufactured from an over-utilized material.

The production of cement which is the binding component of concrete is costly, consumes high energy, depletes natural resources and emits large amounts of greenhouse gases. Consequently, environmental degradation, serious pollution and health hazards associated with cement and concrete industries, have come under intense observation from environmentalists and the governments. Use of supplementary cementitious materials in concrete as partial replacement of cement has been found to be environmentally safe, stable, durable as well as economical. Utilization of agricultural byproduct such as Rice Husk, generated in the rice milling industry, in the form of rice husk ash improves the strength and permeability of concrete. Self-compacting concrete considered costlier than normal concrete due to additional costs of higher cement content, mineral admixtures and super plasticizers but is less labour intensive and needs no vibration. The utilization of RHA in SCC helps to reduce its cost and proves economical.

Waste foundry sand, by-product of ferrous and nonferrous metal casting industries, can be used as fine aggregate replacement in cement-concrete and helps in reducing disposal problems. Several studies revealed that WFS can be successfully utilized for improving the strength and durability of concrete and helps in reducing the river and quarry mining. Keeping this in mind, the present proposal is designed to utilize RHA as partial cement replacement and WFS as fine aggregate replacement in the production of SCC.

1.5 GAP IN RESEARCH AREA

Portland cement is the most energy intensive material following aluminium and steel. The use of rice husk ash is a potential substitute for partial cement replacement in concrete and is desirable for sustainability goals in the construction industry. From last decade, several researchers have successfully used RHA in making normal and self-compacting concrete but little study has been done on durability aspect of SCC incorporating RHA.

Similarly, WFS in SCC has not been explored by many researchers. With construction growing at the fast rate we need more durable concrete. Use of self-compacting concrete is increasing but there is need to find alternatives for constituents so that economical SCC can be produced. Not much literature is reported on the use of WFS in self-compacting concrete for studying strength and durability properties. Thus, it is proposed through this research to investigate the effect of RHA and WFS on the partial replacement of cement and fine aggregate, respectively, on the strength and durability properties of SCC.

1.6 OBJECTIVES AND SCOPE OF RESEARCH WORK

- Development and characterization of SCC containing rice husk ash and waste foundry sand as partial replacements of cement and fine aggregate, respectively.
- To study the strength properties of SCC containing rice husk ash and waste foundry sand as partial replacements of cement and fine aggregate, respectively.
- To study the durability properties of SCC containing rice husk ash and waste foundry sand as partial replacements of cement and fine aggregate, respectively.
- SEM and XRD characterization of SCC mixes containing rice husk ask and waste foundry sand.

1.7 METHODOLOGY

1.7.1 Experimental Programme

SCC would be designed to have 28-day compressive strength between 20 to 50 MPa as per (EFNARC, 2005). The RHA and WFS would be used in the range 0-30% as partial replacement to cement and fine aggregate, respectively. Tests would be carried out to determine various properties of cement, fine aggregate, coarse aggregate, RHA, WFS and workability of SCC. On an average 3 specimens would be cast for each series.

1.7.2 Properties to be Investigated

Following test would be performed:

Fresh Concrete Properties (EFNARC 2005)

- Slump flow
- U- Box
- L-Box
- V-Funnel

Strength Properties

- Compressive strength (IS: 516 -1959)
- Splitting tensile strength (IS: 5816-1959)

These properties would be determined at the age of 7, 28, 91, and 365 days.

Durability Properties

- Rapid chloride permeability test (ASTM C 1202-13)
- Sulphate resistance test (ASTM C 1012)
- Water absorption (ASTM C 642-2002)
- Sorptivity (ASTM 1585C-2013)
- SEM and XRD test would be conducted for concrete specimens.

Results obtained for various properties would be statically analyzed.

The specimen properties would be determined at the age of 28, 91, and 365 days.

1.7.3 Casting of Specimen

- 150 mm cubes for compressive strength
- 150x300 mm cylinders for splitting tensile strength
- 200x100 mm cylinders for rapid chloride permeability test
- 200x100mm cylinders for sorptivity test
- 200x100mm cylinders for water absorption test
- 150mm cubes for sulphate resistance test

1.8 THESIS OVERVIEW

The thesis is organized into five chapters as described below:

Chapter-1 Presents the research's objective, rice husk ash and waste foundry sand production, issues pertaining with their disposal, environment pollution, rice husk ash and waste foundry sand application, and the research's aims and scope.

Chapter -2 Addresses the influence of rice husk ash and waste foundry sand as cementitious and fine aggregate on the fresh, strength, and durability parameters of concrete is examined in depth. This chapter also includes a quick summary of rice husk ash and waste foundry sand as potential supplementary cementitious materials and aggregate replacements in concrete, mortars, and self-compacting concrete.

Chapter-3 This section discusses the test methodology used in this study and the research techniques used to characterize materials and experiments have been used to examine the characteristics of concrete mixes.

Chapter-4 The findings of material characterization tests, fresh properties, and strength and durability parameters of SCC combinations are all presented in this chapter. This chapter also includes SEM analysis and X-Ray diffraction of various mixtures. The effects of rice husk ash and waste foundry sand on fresh concrete characteristics, as well as the strength and durability of SCC combinations, have been thoroughly examined.

Chapter-5 The major findings of this research are reported.

CHAPTER-2

LITERATURE REVIEW

This chapter gives a concise summary of the existing literature on the use of rice husk ash as an aggregate substitute or as a cement supplement material for self-compacting concrete. This chapter presents a thorough overview of the research on the effects of using waste foundry sand as a fine aggregate substitute on the characteristics of self-compacting concrete.

2.1 EFFECT OF RHA ON FRESH PROPERTIES OF SCC

2.1.1 Slump

Safiuddin et al. (2012) investigated the slump of SCC mixtures containing 5 and 10% RHA; 3.5, 4 and 4.5% super plasticizer and varied w/c ratio of 0.30, 0.35 and 0.40. All the mixes showed slump in the range of 265-280 mm and the variation in values of slump was marginal. Though the slump increased by only 5 mm in 30% RHA compared to 0% RHA (270 mm) at 0.35 w/c ratio but the deformability of concrete was significantly improved.

2.1.2 Slump Flow

Memon et al. (2008) studied the fresh SCC properties incorporating 5% and 10% RHA; and super plasticizer varied from 3.5% to 4.5% with an increment of 0.5%. It was concluded that slump flow for all the mixes except mix containing 10% RHA and 3.5% super plasticizer (595 mm) were within the EFNARC range (650-800mm) of SCC. Increase in super plasticizer content increased the flow whereas increase in RHA content decreased the flow. *Safiuddin et al. (2012)* observed slump flow of SCC mixtures in the range 665 mm to 770 mm and found relative difference in different mixtures. At w/c ratio of 0.35, 0% and 30%RHA incorporated SCC exhibited slump flow of 690 and 750 mm, respectively.

Sua-iam and Makul (2013) prepared several SCC mixtures containing RHA (0, 10, 20, 40, 60, 80 and 100%) as fine aggregate (river sand) replacement. The particle size of RHA used in the study was 84.32 µm with specific surface area of 240 m^2/kg. It was observed that slump flow increased with increasing RHA content and varied in the range of 6-15 sec, exhibiting average slump flow of 700±25 mm. The longer slump flow at higher RHA replacement levels (80 and 100%) was due to increased surface area of RHA, which increased the viscosity of the RHA-SCC paste. In another

study conducted by *Sua-iam & Makul (2014)*, slump flow time increased with increasing RHA content. Mixtures containing 0, 20, 40 and 60% coal fly ash and up to 75% RHA content showed slump flow time within 3-7 s and in the acceptable range of *EFNARC (2002).* Mixtures containing 100% RHA showed higher slump flow time as they absorbed free water due to angular shape and higher porosity of RHA. Addition of RHA (331.3 kg/m^3) as supplementary cementitious material in SCC showed slump flow of 710 mm and falls within the acceptable range of EFNARC *(Pai et al., 2014).*

Atan and Awang (2011) found that replacement of 15% ordinary Portland cement (OPC) by raw RHA (RRHA; specific gravity 2.16 and, Blaine fineness 351 m^2/kg) increased the water requirement of mix by 38%. The higher specific area (Blaine value) of RHA particles absorbed large amount of water on the surface, resulted in less water available to lubricate and reduced the flowability. Ternary mixes of SCC containing OPC, RHA (15%) and equal mass of limestone (LP), pulverized fuel ash (FA) and silica fume (SF) showed similar requirements of water at 30% replacement level as in binary mixes. In quaternary mixes (OPC+RHA+FA+LP and OPC+RHA+SF+LP), at 45% OPC replacement level, reduction in super plasticizer requirement was observed whereas mix containing OPC+RHA+SF+FA showed higher requirement for water and super plasticizer. This was due to the extreme fineness of SF particles (Blaine fineness 20,000 m^2/kg) that coupled with RHA particles resulted in high surface which increased the viscosity of the mix *(Atan and Awang, 2011; Sukumar et al., 2008).*

Kannan and Ganesan (2015) studied the slump flow values of SCC with RHA (0-30% with 5% increment) and compared with EFNARC (2005) recommended guidelines for fresh state properties of SCC. All the RHA-SCC mixes (550-740 mm) except 30% RHA-SCC mix (495 mm) falls under the categories of slump flow classes 1 (SF1) and 2 (SF2). It was observed that slump flow value decreased with increase in RHA content and this may be cause by the high reactivity and higher surface area of RHA particles. Similar findings were also observed by *Chopra et al. (2015)* where the slump flow of all the RHA-SCC mixtures ranges between 600-730 mm.

2.1.3 L-Box Test

It assesses filling and passing ability of SCC. *Memon et al. (2008)* found that majority of the SCC mixes (5 and 10% RHA; 3.5, 4 and 4.5% super plasticizer) and exhibited

the values within the range of 0.8 to 1as per EFNARC (2002). Ratio of L-Box increased with the increase in super plasticizer content; and decreased with the increase in RHA content. *Pai et al. (2014)* achieved 0.86 of L-box value for SCC mix containing RHA (331.3 kg/m^3) in addition to cement (200 kg/m^3). *Kannan and Ganesan (2014; 2015)* observed the L-box blocking ratio of different RHA-SCC mixtures according to *EFNARC (2005)* specifications. The L-box values for all the mixtures varied from 0.59-0.94, and for 15% RHA-SCC mix satisfactory blocking ratio was observed, while the L-box values were ranged between 0.8-1 in SCC mixes with up to 15% RHA content in the study conducted by *Chopra et al. (2015).* The blocking ratio for other mixes was found to be outside the EFNARC recommended values given in Table 2.1.

2.1.4 V-Funnel Test

It measures flowability and segregation resistance of SCC mixtures. Shorter flow time indicate greater flowability. According to EFNARC (2002), the V-funnel test ranges from 6-12 sec. *Memon et al. (2008)* observed that most of the results of V funnel test remained more towards minimum range (6 sec) or even lesser, and showed the filling ability of the SCC mixes but less viscous. Increase in quantity of RHA (10%) increased the viscosity of mix. At lower super plasticizer content (3.5%), 5% RHA content showed V-funnel test within the EFNARC range, while at 4 and 4.5% super plasticizer content, 10% RHA qualified the V-funnel test.

Similar findings were also observed by *Sua-iam and Makul (2013)* in SCC mixtures containing RHA as replacement to fine aggregate. Mixes containing 10 and 20% RHA showed acceptable flow time of 9 and 11 s, respectively, whereas increasing RHA content (40, 60, 80 and 100%) increased the flow time as RHA particles absorbed the water, resulted in viscous mix and reduced bleeding. Study conducted by *Sua-iam and Makul (2014)* reported that V-funnel flow time was within 8-12 s when the RHA content was 25% or less in SCC as shown in Table 2.1. With increasing RHA content the V-funnel flow time increased due to increased viscosity, and this was improved by incorporation of spherical shape and smooth surface texture of fly ash particles. *Pai et al. (2014)* reported acceptable range of V-funnel flow value (9 s) for SCC containing RHA (331.3 kg/m^3) in addition to cement (200 kg/m^3). *Kannan and Ganesan (2015)* observed the V-funnel time values for different RHA-SCC mixes varied in the range 3.9-8.4 s, and categorized under VF1 class according to *EFNARC (2005)* guidelines.

2.1.5 Orimet Test (Flow Time and Flow Spread)

According to *EFNARC (2002),* the maximum acceptable limit for orimet flow time is 9 sec. *Safiuddin et al. (2012)* reported the orimet flow time of RHA (10-30%) incorporated SCC varied from 4.8 sec to 11.5 sec. Higher the flow values higher is the viscosity of concrete. At low w/c ratio (0.30) and with increasing RHA content (25 and 30%) orimet flow time was slightly above the EFNARC limit. This suggested the viscous nature of these mixes. *Safiuddin et al. (2012)* also reported that the orimet flow spread of RHA-SCC mixes varied in the range of 690-800 mm and were greater than slump flow by 10-45 mm. This was due to greater mass of concrete and higher falling height (430 mm) of concrete used in orimet test compared to 300 mm height used in slump flow test. Table 2.1 shows the fresh properties of SCC mixes containing RHA studied by several researchers.

Table 2.1 Fresh properties of RHA-SCC mixes studied by several researchers

Study	RHA replacement (%)	w/b	Super plasticizer content (%)	Fresh concrete properties			
				Slump flow (mm)	L-box (H2/H1)	V-funnel (s)	J-ring (mm)
EFNARC (2002)	—	—	—	650-800	0.8-1	6-12	-
Chopra et al. (2015)	0	0.41	1	730	1	6	-
	10			700	0.9	8	-
	15			670	0.8	11	-
	20			600	Blocking	13	-
Kannan and Ganesan (2014)	0	0.55	2	740	0.94	3.9	-
	5			700	0.93	4.0	-
	10			670	0.87	4.0	-
	15			610	0.82	4.8	-
	20			580	0.78	6.0	-
	25			550	0.71	7.2	-
	30			495	0.62	8.0	-
Rahman et al. (2014)	0	0.38	1.8	630	-	5.9	5.2
	20	0.5	3.5	660	-	6.6	3.7
	30			670	-	6.3	3.5

	40			580	-	7.0	4.4
Sua-iam & Makul (2014)	0	0.25	1.2 (HRWRA)	720	-	10	720
	25	0.54		700	-	12	690
	50	0.90		700	-	34	660
	75	1.46		680	-	72	630
	100	1.89		680	-	-	580
Safiuddin et al. (2012)	0	0.30	0.87	710	-	-	730
	15		1.75	735	-	-	745
	20		2.10	770	-	-	765
	0	0.35	0.70	690	-	-	690
	5		0.87	700	-	-	695
	10		1.05	710	-	-	705
	15		1.40	720	-	-	720
	20		1.75	710	-	-	715
	25		2.10	740	-	-	760
	30		2.45	750	-	-	770
	0	0.40	0.60	665	-	-	675
	15		1.00	680	-	-	700
	20		1.20	675	-	-	705
Memon et al. (2011)	0	0.4	3.5	770	1	6	-
	5	0.38		650	1	6.8	-
	10	0.36		595	Blocking	29.3	-
	0	0.4	4.0	780	1	4.24	-
	5	0.38		710	1	4.26	-
	10	0.36		660	0.88	11.8	-
	0	0.4	4.5	795	1	2.18	-
	5	0.38		760	1	3.93	-
	10	0.36		700	0.94	8.62	-

2.1.6 Passing Ability of Concrete

The passing ability of SCC mixtures were obtained with respect to J-ring slump, slump cone- J ring flow spread, orimet- J ring flow spread. *Safiuddin et al. (2012)* found that the addition of adequate dose of high range water reducer (HRWR) maintained a good passing ability of SCC through the J-ring in all cases without any

blocking. The J-ring slump varied in the range of 255-270 mm for various SCC mixtures. The slump cone J-ring flow spread varied in the wide range of 650-740 mm which was lower than the slump flow by 15-30 mm. It was concluded that the reduction in slump flow in presence of J-ring should not be greater than 50 mm to maintain a good passing ability. Similarly, the orimet J-ring flow spread ranges in 675-770 mm and was decreased by 15-30 mm when compared to orimet flow spread. Incorporation of RHA in SCC as fine aggregate replacement exhibited small degree of blocking which can be improved by using finer particles such as limestone *(Sua-iam and Makul, 2013)* and fly ash *(Sua-iam and Makul, 2014).*

2.2 HARDENED CONCRETE PROPERTIES

2.2.1 Compressive Strength

Ahmadi et al. (2007) studied the compressive strength of SSC mix containing RHA (10 and 20%) in comparison to normal concrete at two different w/b ratios (0.40 and 0.35). The specimens were tested at different ages from 7 to 180 days. SCC mixes showed higher compressive strength (31-41%) than normal concrete. Mixes containing RHA up to 60 days exhibited lower compressive strength compared to SCC (0%RHA) and normal concrete (0% RHA), but after 60 days, compressive strength of composite mixes increased by increasing the rate of pozzolanic reactions of RHA (with increasing RHA content) in the matrix. Mixtures containing 20% RHA as partial replacement to OPC showed similar compressive strength compared to control mixtures up to 91 days *(Sua-iam and Makul, 2012)* due to pozzolanic reaction and denser internal structure *(Memon et al., 2011).* On the contrary, *Safiuddin et al. (2010)* reported that RHA increased the compressive strength of concrete at age of 7, 28 and 56 days due to micro filling ability and pozzolanic activity of RHA. At 28 days, the compressive strength varied from 42.7 to 94.1 MPa while at 56 days, it varied from 44.9 to 98.4 MPa for different mixes. Highest compressive strength was observed for 30% RHA content with 0.35 w/b ratio. Table 2.2 shows the compressive strength of RHA-SCC mixes reported by several researchers.

Chopra et al. (2015) achieved compressive strength in the range between 36.7-41.2 MPa at 28 days and 39.6-46.4 MPa at 56 days for SCC mixes containing RHA (10-20%) with w/b ratio of 0.41. Highest level of strength was observed in 15% RHA mix while in 20% RHA mix strength was greater than control SCC mix at 56 days of curing. The results were in concomitant with the studies reported by *Kannan and*

Ganesan (2013); and Chik et al. (2011) where SCC blended with 15% RHA attained higher 28-day strength than normal SCC. Increased strength was due to highly reactive RHA particles that react with water and calcium hydroxide to produce additional calcium silicate hydrates (CSH) resulted in reduced porosity by improving the microstructure of concrete matrix and transition zone *(Chopra et al., 2015; Sua-iam and Makul, 2012; Safiuddin et al., 2010).*Self-compacting concrete (SCC) is gaining much popularity throughout the world because of some of its interesting structural properties. However, it is not completely accepted due to higher cost (use of higher cement content) and can be reduced by using various mineral admixtures such as metakaolin, fly ash, sugarcane baggase ash, limestone, pulverized fuel ash, etc. as partial replacement of the cement. The use of mineral admixtures not only improves the structural properties of SCC but also reduce the carbon dioxide emissions.

Atan and Awang (2011) investigated the compressive strength development in SCC incorporating raw RHA (RRHA), in binary, ternary and quaternary mixes with other types of mineral additives (LP, FA, and SF), as partial cement replacement. All the mixes after 90 days of water curing exhibited lower compressive strength compared to control. In binary mix (OPC+15% RRHA), the strength development increases at high rate but less as compared to control mix due to reduced heat of hydration by replacing OPC with RRHA. It was observed that high silica content (92.99%) and specific area of RRHA contributed to the RRHA's high rate of strength development resulted in comparable 90-day compressive strength as compared with control. Inclusion of LP and FA in binary mix (OPC+RRHA+LP/FA) also produced comparable strength compared to control mix whereas mix containing SF showed reduced strength values. Similar observations were also made in quaternary mixes where mix containing OPC+RRHA+LP+FA produced lower strength values compared to other mixes and control mix. *Juma et al. (2012)* found that incorporation of RHA (0-10%) and sugarcane baggase ash (SCBA) alone and in blended with SCC significantly increased the compressive strength of concretes up to the age of 28 days. The improvement of compressive strength was due to the smaller particle size, micro filling ability and pozzolanic activity of RHA and SCBA that filled the micro-voids within the matrix. *Sua-iam and Makul (2013)* replaced the fine aggregate (river sand) with different proportions of RHA (0-100%) and observed that with increasing RHA content strength decreases. At 28 days of curing, SCC containing 100% RHA showed 3% of

the compressive strength of the control mix whereas mix containing 10% RHA showed 84% of the strength.

Table 2.2 Compressive strength of RHA-SCC mixes studied by several researchers

Study	RHA replacement (%)	w/b	Super plasticizer content (%)	Compressive strength (MPa)				
				7 d	14 d	28 d	56 d	91 d
Chopra et al. (2015)	0	0.41	1	29.0	-	36.7	39.6	-
	10			32.6	-	41.2	46.4	-
	15			36.2	-	48.8	53.7	-
	20			30.4	-	40.2	53.0	-
Pai et al. (2014)	62.35	0.31	1.8	11.3	12.9	14.1	-	-
Rahman et al. (2014)	0	0.38	1.8	32.8	-	48.5	-	-
	20	0.5	3.5	37.2	-	42.9	-	-
	30			35.1	-	40.9	-	-
	40			28.1	-	33.5	-	-
Sua-iam & Makul (2013)	0	0.22	2	55.9	-	65.0	-	82.8
	10	0.31		48.4	-	54.8	-	72.6
	20	0.46		21.2	-	28.0	-	39.6
	40	0.75		13.8	-	19.1	-	26.4
	60	1.17		8.3	-	10.4	-	14.8
	80	1.80		2.8	-	4.1	-	5.7
	100	2.18		1.5	-	2.0	-	2.6
Memon et al. (2011)	0	0.4	3.5	10.5	-	28.4	-	-
	5	0.38		25.2	-	38.0	-	-
	10	0.36		22.5	-	36.2	-	-
	0	0.4	4	6.8	-	18.3	-	-
	5	0.38		21.4	-	37.8	-	-
	10	0.36		36.8	-	41.4	-	-
	0	0.4	45	1.2	-	8.6	-	-
	5	0.38		11.9	-	22.2	-	-
	10	0.36		38.3	-	48.5	-	-
Atan & Awang (2011)	0	0.39	2.2	36.5	37.6	37.8	-	44.7
	15	0.54		22.7	29.6	39.8	-	42.5

Similar observations were also made by *Sua-iam and Makul (2014)* where increasing RHA content from 25, 50, 75 and 100% the compressive strength decreased of 31.8, 54.5, 77.1 and 87.6%, respectively. The reduction in strength was due to coarse nature of RHA that decreased the packing density of matrix and made the SCC more porous. Addition of mineral additives such as limestone powder and coal fly ash along with RHA particles improved the compressive strength due to filler effect of mineral additives by improving microstructure of the cement matrix and transition zone *(Sua-iam and Makul, 2013; 2014).*

Kannan and Ganesan (2014; 2015) investigated the compressive strength of binary blended SCC mixtures with RHA (0, 5, 10, 15, 20, 25 and 30%) and ternary blended SCC with RHA and MK in equal proportions (0, 10, 20, 30 and 40%) as partial replacement to OPC at 7, 28 and 90 days. The control SCC mix was designed with a targeted strength of 38.5 MPa (M30 grade) at 28 days with w/b ratio of 0.55 and 2% super plasticizer content. In binary blends, higher strength was observed in SCC containing 15% RHA at all ages. At 90 days, ternary blends (SCC+RHA+MK) exhibited slightly increased compressive strength than binary blends (SCC+RHA). Mixtures containing 15% RHA and 30% RHA+MK (15% RHA and 15%MK) showed maximum 28-day compressive strength values of 51.03 and 55.67 MPa, respectively, compared to control SCC (43.40 MPa). It was concluded that higher strength in RHA+MK mixes was due to the presence of high Al2O3 content in MK compared to RHA that accelerated the hardening process while presence of SiO2 in RHA reacted with CaO and supplemented the hardening process in the alkaline environment *(Carlos et al., 2006).* On the contrary, *Zhang and Malhotra (1996); and Bhanumathidas and Mehta (2004)* reported that up to 30% RHA can be used to achieve higher compressive strength in normal concrete.

Table 2.3 shows the energy dispersive X-ray (EDAX) analysis of the control SCC, SCC+15%RHA and 15%RHA+15%MK mixes carried out by *Kannan and Ganesan (2015).* It was observed that the control SCC sample consisted of porous irregular particles due to formation of gypsum and ettringite resulted in poor strength and durability performance compared to that of the blended concretes. In SCC blended with RHA and MK due to the additional hydration porosity of the blended concrete was reduced, giving a more uniform structure than is found in the unblended SCC. From the corresponding EDAX spectrum of the SCC blends given in Table 2.3,

higher silica content was observed in 10% RHA (23.23%) and 30% RHA+MK (39.84%) compared to that of unblended SCC (11.62%). The higher silica content indicated a good pozzolanic reaction and improved strength and reduced porosity in the RHA and MK blended cement.

Table 2.3 EDAX analysis of SCC, 10% RHA, and 30% RHA+MK blended SCC (Kannan and Ganesan, 2015)

Element (Mass %)	Control SCC	10% RHA	30% RHA+MK
C K	4.9	1.68	--
O K	8.63	30.56	28.65
Na K	NA	NA	1.2
Mg K	3.83	9.59	NA
Al K	1.77	6.47	15.36
Si K	11.62	23.23	39.84
Ca K	61.96	1.14	NA
Fe K	3.02	2.56	NA
Cu K	4.27	24.77	NA
K K	NA	NA	14.95

Incorporation of RHA increased the super plasticizer amount in SCC mixes due to high specific area and cellular structure of particles to maintain the flowability *(Rukzon and Chindaparasirt, 2014).* All the mixes containing grounded RHA (20, 30 and 40%) as partial replacement to cement showed reduced compressive strength values compared to control mix. The compressive strength varied from 25.5 to 27 MPa, which was higher than 20 MPa (design at the age of 28 days). Therefore, it was suggested that the use of RHA was effective in producing self-compacting concrete with 20–30% of RHBA replacement. *Pai et al. (2014)* investigated the compressive strength of SCC mix containing RHA and reported lower strength values all ages (7, 14 and 28 days) due to addition of high amount of RHA (62.35%; 331.3 kg/m^3) compared to control mix.

Memon et al. (2008; 2011) aimed at evaluating the compressive strength of SCC incorporating rice husk ash (5 and 10%) at three w/b ratios of 0.4, 0.38 and 0.36; and three percentages by weight of super plasticizer 3.5, 4 and 4.5. At 3.5% of super plasticizer content control mix developed highest compressive strength of 10.5 and 28.4 MPa at 7 and 28 days, but for control SCC and SCC with 5% RHA, strength

decreased with increase in the dosage of super plasticizer. In the mixes with 10% RHA, the strength increased with increase in super plasticizer dosage due to improved workability and sufficient self compactibility. At similar super plasticizer dosage, RHA mixes showed higher compressive strength compared to control mixes. This increase was basically due to reduced w/b ratio, dense particle packing, pore size refinement and grain size refinement.

In recent years, nanotechnology has attracted considerable scientific interest of concrete technologists due to the new potential uses of particles in nanometer scale. *Sadrmomtazi and Barzegar (2010)* studied the effect of nano silica (NS) on the compressive strength of SCC containing 20% RHA at 7, 28 and 60 days. It was observed that with addition of NS (7%), the strength increased by 86, 64 and 58% after 7, 28 and 60 days compared to control SCC (19.1, 30 and 35.4 MPa) while strength increase of 51, 34 and 15% was shown by NS-RHA-SCC mix when compared with RHA-SCC (19.9, 34.8 and 46.5 MPa) at similar curing periods. It was concluded that inclusion of NS in SCC made cement paste thicker by filling the pores lead to densification of the concrete internal structure and accelerated the cement hydration process resulted in increased compressive strength.

2.2.2 Flexural Strength

Table 2.4 shows the flexural strength of RHA-SCC mixes reported by several researchers. *Ahmadi et al. (2007)* studied the flexural strength of SSC mix containing RHA (10 and 20%) at different ages from 7 to 180 days in comparison to normal concrete at two different w/b ratios (0.40 and 0.35). It was observed that the SCC mixes exhibited flexural strength about 12% to 20% more than normal concrete. Increasing the RHA content increased the flexural strength after 60 days of curing due to increase in pozzolanic reaction of RHA in the matrix and highest flexural strength in all cases was observed in mixes containing 20% RHA.

Table 2.4 Flexural strength of RHA-SCC mixes studied by several researchers

Study	RHA replacement (%)	w/b	Super plasticizer content (%)	Flexural strength (MPa)				
				7 d	14 d	28 d	56 d	91 d
Pai et al. (2014)	62.35	0.31	1.8	2.3	3.3	3.8	-	-
Atan&Awang (2011)	0	0.39	2.2	4.5	4.7	5.7	-	5.7
	15	0.54		3.2	3.5	4.0	-	6.5

Atan and Awang (2011) reported increased flexural strength in 15% RRHA+OPC mix (6.5 MPa) compared to control mix (5.7 MPa) whereas addition of mineral additives (FA and SF) in equal mass to binary blends produced substantially lower flexural strengths but comparable to control mix. On the contrary, inclusion of LP increased the flexural strength in ternary (OPC+RRHA+LP) and quaternary (OPC+RRHA+LP+SF) blends due to pore-filling effect of LP which densifies the concrete microstructure. Pai et al. (2014) also concluded that addition of large amount of RHA (62.35%) in SCC negatively affect the strength of concrete. Incorporation of 3% nanosilica (NS) enhanced the flexural strength of RHA-SCC by 50.7, 33.6 and 15% compared to RHA alone mix at 7, 28 and 60 days, respectively *(Sadrmomtazi and Barzegar, 2010).*

2.2.3 Splitting Tensile Strength

Chopra et al. (2015) achieved compressive strengths in the range 2-2.8, 2.5-3.7 and 2.8-4 MPa at 7, 28 and 56 days, respectively, in SCC containing 10-20% RHA; and observed increase in splitting tensile strength up to 15% replacement but the strength in 20% RHA mix were still higher than control mix as shown in Table 2.5.

Table 2.5 Splitting tensile strength of RHA-SCC mixes studied by several researchers

Study	RHA replacement (%)	w/b	Super plasticizer content (%)	Splitting tensile strength (MPa)			
				7 d	14 d	28 d	56 d
Chopra et al. (2015)	0	0.41	1	2	-	2.5	2.8
	10			2.4	-	3.6	3.8
	15			2.8	-	3.7	4.0
	20			2.3	-	3.0	3.3
Rahman et al. (2014)	0	0.38	1.8	-	-	5.1	-
	20	0.5	3.5	-	-	5.1	-
	30			-	-	4.3	-
	40			-	-	2.8	-
Pai et al. (2014)	62.35	0.31	1.8	0.7	0.9	1.1	-

Rahman et al. (2014) studied the splitting tensile strength of SCC containing RHA (0, 20, 30 and 40%) as partial cement replacement. The results showed that splitting tensile strength decreased with increase in percentage of RHA. Incorporation of 20%

RHA produced acceptable strength values, as its strength was similar to the strength of control mix. It was also be observed that the splitting tensile strength of SCC are higher than the normal vibrating concrete due to uniform compaction of SCC under its own weight without any internal and external vibrator, and without segregation and bleeding.

Khadiry et al. (2014) aimed at producing and comparing SCC incorporating rice husk ash (RHA) and shell lime powder (SL), both locally available mineral admixtures as an additional cementing material. At 28 days, strength for RHA mix was higher compared to SL. Splitting tensile strength of SL-SCC was 23.98 and 5.2% higher than RHA-SCC for 7 and 14 days of curing, whereas for 28 days of curing, the strength of RHA-SCC was 0.8% higher than that of SL-SCC. The higher strength in RHA when compared to SL may be attributed to the fact that RHA contains silica contents which reacts better with cement compared to that of calcite contents of SL.

2.2.4 Modulus of Elasticity

Ahmadi et al. (2007) deliberate the flexural strength of SSC mix containing RHA in comparison to normal mix. It was observed that like compressive and flexural strength the module of elasticity increases by aging and hardening of concrete mixes. Normal concrete mixes show bigger module of elasticity around 9% to 17% more than of SCC ones. Also, by increasing the amount of rice husk ash in the matrix, module of elasticity of all mixes reduced.

2.2.5 Ultrasonic Pulse Velocity (UPV)

It is a non-destructive technique to evaluate the homogeneity of the concrete by measuring the velocity of ultrasonic pulses traveling in a solid medium depends on the density and elastic properties of the material. An UPV measurement is directly proportional to that of compressive strength, with UPV increasing with increasing compressive strength. *Sua-iam and Makul (2013)* found that UPV in SCC containing RHA (0, 10, 20, 40, 60, 80 and 100%) as replacement to fine aggregate varied in the range 0.7-4.2 km/s and 1-5 km/s at 28 and 91 days, respectively, compared to 4.4 and 5.2 km/s of control mix as depicted in Table 2.6.

Table 2.6 Ultrasonic pulse velocity of SCC mixes containing RHA (Sua-iam & Makul, 2013)

Mix	Ultrasonic pulse velocity (km/s)			
	1 d	7 d	28 d	91 d
Control (0%)	2.5	3.6	4.4	5.2
10% RHA	2.1	3.4	4.2	5.0
20% RHA	2.0	2.8	3.5	4.2
40% RHA	0.8	1.4	2.2	3.0
60% RHA	0.7	1.1	1.8	2.6
80% RHA	0.5	0.7	0.9	1.3
100% RHA	0.4	0.6	0.7	1.0

The higher velocity, indicated better quality of SCC, was achieved in control mix while 100% RHA mix achieved lowest pulse velocity. It was observed that with increasing RHA values UPV decreases. *Sua-iam and Makul (2014)* reported 7.8, 25.5, 42 and 62.8% decrease in UPV in SCC mixtures with 25, 50, 75 and 100% RHA. Addition of mineral additive such as limestone powder and fly ash increased the ultrasonic pulse velocity in SCC due to micro-filling and pozzolanic effect. Incorporation of RHA (0-30%) as partial replacement to cement with varying w/b ratio of 0.30, 0.35, 0.40 and 0.50 showed the UPV in the range 4.730-5.097 km/s and indicated the excellent condition of SCC mixtures *(Safiuddin et al., 2010).* Highest level of UPV was achieved for concretes with w/b ratio of 0.30, whereas with w/b ratio of 0.50 lowest level of UPV was obtained. Due to microfilling ability and pozzolanic effect of RHA, the pore refinement and porosity reduction lead to increase pulse velocity of SCC-RHA mixes. It was also observed that SCC-RHA mixes with air content (2%) showed higher UPV than mixes containing 6% air content. The entrained air voids and pores in the interface delayed the propagation of the ultrasonic pulse, thus reducing the UPV of concrete.

2.2.6 Rapid Chloride Permeability Test

Ramasamy (2011) reported that most of the chloride ion permeability values fall in the range of very low (100-1000 coulombs) category, and as the OPC replacement by RHA increases, the charge passed decreases and with age. The RCPT values of mixes with super plasticizer showed higher values as compared to the mixes without super plasticizer and showed low to very low rating as RHA replacement varied from higher

to lower levels. The same trend was reported by *Chopra et al. (2015)* in RHA replaced SCC where decrease in charge passed was observed in mixes containing up to 15% RHA. In 20% RHA, the charge passed increased but remained lower than control mix. *Zhang et al. (1996),* and Zhang and Malhotra (1996) reported excellent resistance to by 10% RHA concrete and the charge passed was below 1000 coulombs both at 28 and 91 days.

The incorporation of the RHA in concrete resulted in a finer pore structure in the hydrated cement paste especially at the aggregate and paste interface leading to dense structure and reduced chloride ion permeability *(Ramasamy, 2011; Chopra et al., 2015).Kannan and Ganesan (2014)* studied the chloride ion permeability in SCC mixes blended with MK, RHA and RHA+MK according to ASTM C 1202 after 28 days of curing. The minimum chloride ion permeability was observed in mixes blended with 15% RHA (306.22 coulomb), 30% MK (28.23 coulomb) and 40% RHA+MK (25.43 coulomb) compared to control SCC specimens (1486.28 coulomb). The total charge passed values of 30% MK (28.23 coulomb) and 40% RHA+MK (25.43 coulomb) SCC specimens were categorized under "very low" chloride ion permeability and this was due to fineness of MK particles, and pozzolanic reaction of MK with Portlandite (Ca(OH)2) resulted in reduced pore network and exhibited a much better resistance to chloride ion penetration depicted in Table 2.7.

Table 2.7 RCPT of SCC mixes containing RHA

Mix	RCPT (coulombs) at the age of 28 d	
	Chopra et al. (2015)	Kannan & Ganesan (2014)
Control (0%)	2830	1486
5% RHA	1970	439
10% RHA	980	389
15% RHA	1173	306
20% RHA	-	877
25% RHA	-	905
30% RHA	-	1089

2.2.7 Water Absorption and Porosity

According to *Kosmatka et al., (2002),* the water absorption of high-quality concrete should be less than 5% and this can be achieved by limited pore connectivity and reduced porosity of concrete. *Safiuddin et al. (2010)* reported that water absorption in

SCC-RHA mixtures at w/b ratio of 0.30-0.50 varied in the range 2.89-5.97%, which was relatively low. The decrease in water absorption at w/b ratio of 0.30 was about 25% compared with w/b ratio of 0.50. Inclusion of RHA reduced the water absorption and lowest level of water absorption was observed for 30% RHA concrete at 0.35 w/b ratio which was 35% less than 0% RHA concrete at similar w/b ratio. Similarly, *Safiuddin et al. (2010)* observed the total porosity in the range 6.77-13.71%. The total porosity decreased with increase in RHA content and reduction in 5-35% of total porosity was observed for various RHA contents.

Table 2.8 Water absorption and porosity of SCC mixes containing RHA at the age of 28 days

Mix	Water absorption (%)		Porosity (%)
	Rahman et al. (2014)	Kannan & Ganesan (2014)	Chopra et al. (2015)
Control (0%)	6.2	4.5	12.4
5% RHA	-	4.5	10.8
10% RHA	-	4.1	10.0
15% RHA	-	3.9	11.1
20% RHA	7.7	3.9	-
25% RHA	-	4.5	-
30% RHA	8.9	4.9	-
40% RHA	10.5	-	-

Table 2.8 shows the water absorption and porosity of SCC mixes containing RHA studied by several researchers. *Rukzon and Chindaparasirt (2014); and Chopra et al. (2015)* reported that with curing period the porosity of RHA-SCC mixes reduced due to additional hydration or pozzolanic reaction between calcium hydroxide and silica that filled the voids and increased the density of concrete. Mixtures up to 20% RHA exhibited lower porosity values than control SCC mixes at 28 days. These results can be compared with the findings of *Ramasamy (2011)* where the porosity values decreased (4.7, 4.5, 4.2, 3.9 and 3.45%) with increase in RHA content (0, 5, 10, 15 and 20%) for M30 concrete mixtures without super plasticizers. But the addition of super plasticizers showed the porosity values varied in the range 3.80 to 5.20%.

Kannan and Ganesan (2014) studied the effect of RHA and MK (5, 10, 15, 20, 25 and 30%) and RHA+MK (10, 20, 30 and 40%) as partial replacement of cement on the

water absorption (WA) of SCC at 28 days of curing. It was observed that with increasing MK and RHA+MK content the water absorption decreases except up to 15% RHA content compared to control SCC (4.54% WA). The increasing WA in SCC containing RHA (>15%) was attributed to the higher surface area of RHA and lower fineness which increased the water demand in the mix, reduced workability and consequently created the voids. *Sadrmomtazi and Barzegar (2010)* observed that incorporation of nanosilica (NS) reduced the water absorption in 20% RHA-SCC mix from 5.33 to 4.31% due to formation of nucleation sites for hydration process by NS, increased CSH, reduced porosity and by act as filler material that block the capillary pores and water channels in cement paste *(Tao, 2005; Benachour et al., 2008).*

2.2.8 Sorptivity

Kannan and Ganesan (2014) investigated the sorptivity of SCC blended with MK, RHA and RHA+MK. It was observed that with increasing RHA content up to 15% the sorptivity decreases from 3.56 (control SCC) to 3.31 x 10-6 $m/s^{1/2}$ whereas with MK and RHA+MK the minimum sorptivity (2.29 and 2.64 x 10-6 $m/s^{1/2}$, respectively) was observed for 20 and 30% replacement levels. In MK blended SCC, the minimum sorptivity was due to finer size of MK than OPC and RHA and increased formation of calcium silicate hydrate (CSH) gel leads to a reduction in pores size and ultimately the sorptivity. The increased sorptivity values in 20% (4.06 x 10-6 $m/s^{1/2}$), 25% (6.41 x 10-6 $m/s^{1/2}$) and 30% RHA (9.2 x 10-6 $m/s^{1/2}$) was due to pores developed in concrete due to reduced workability. It was also observed that SCC specimens blended with 30% MK and 40% RHA+MK showed 18.82% and 19.10% reduction in sorptivity at 28 days respectively, compared to control SCC (3.56 3.31 x 10-6 $m/s^{1/2}$).

2.2.9 Electrical Resistivity

True electrical resistivity of the concretes at 28 and 56 days varied in the range of 4.1–121.2 kΩ cm for different types of concrete *(Safiuddin et al., 2010).* Mixtures that exhibits true electrical resistivity is between 5 and 10 kΩ cm showed moderate to low corrosion rate, whereas good corrosion resistance is obtained when the true electrical resistivity is above 10 kΩ cm *(Neville, 1996).* All RHA-SCC mixtures provided a true electrical resistivity higher than 10 kΩ cm compared to non-RHA-SCC mixtures (4.1–8.9 kΩ cm). High w/b ratio of 0.50 showed lowest level of true electrical resistivity whereas w/b ratio of 0.30 showed highest level of true electrical resistivity due to the densification of the paste microstructure with a reduced porosity.

2.2.10 Acid Resistance

The acid resistance of SCC mixes blended with MK, RHA and RHA+MK was assessed by *Kannan and Ganesan (2014)* after 28 days of curing. The weight loss of blended SCC mixes was measured for 12 weeks with 1 week interval after immersed in 5% sulfuric acid (H2SO4) and hydrochloric acid (HCl) solution. It was observed that RHA and RHA+MK - SCC blends showed more resistance against sulfuric acid attack than MK-SCC blends. The lowest weight loss was observed in 25% RHA, 5% MK and 40% RHA+MK replacement levels. The maximum weight loss and deterioration was observed in MK blended SCC due to presence of high alumina content in MK. The alumina (Al2O3) reacted with silica (SiO2) to form calcium sulfoaluminate (ettringite) that leads to expansion in the concrete and disrupted the set cement paste while in RHA and RHA+MK lower alumina content was found compared to MK, thus less ettringites were formed and better resistance to sulphate attack. Similar weight loss was observed in 25% RHA, 5% MK and 40% RHA+MK replacement levels when immersed in hydrochloric acid (HCl) solution. MK blended SCC was less resistance to hydrochloric acid compared to RHA and RHA+MK blended SCC. It was also observed that the weight loss for all mixtures in the hydrochloric acid solution was lower than in the sulfuric acid solution.

2.2.11 Alkali Silica Reaction

Alkali silica reaction (ASR) is a deleterious reaction between alkali hydroxides in concrete pore solution and amorphous or poorly crystalline silica phases in SCMs or aggregates that forms alkali silica gels which absorb water and expand. *Le et al. (2015)* investigated the resistance of mortars formulated from SCC containing RHA to alkali silica reaction. The effect of RHA (particle size 5.7, 737 and 15.6 µm) at 20% replacement levels on ASR expansion of mortar bars (40×40×160 mm^3) with reactive greywacke aggregates was evaluated after 28 day immersion in 1M NaOH solution at 80°C. After 14 days of immersion, all the specimens showed expansion lower than the threshold of 0.10% whereas after 28 days, control sample and RHA (15.6 µm) sample showed increase in expansion of 0.27 and 0.46%, respectively. Several visible cracks were also appeared on the surface of RHA samples with particle size 7.7 and 15.6 µm, and the intensity of the cracks increased with increase in particle size. Mortar samples with RHA particle size 7.7 µm showed higher expansion after 56 days of immersion in 1M NaOH solution at 80°C and at later age samples with RHA particle size 5.7 µm

followed the same trend. The results indicated that this might be due to the larger particle size and porous structure of RHA. It was hypothesized that the pozzolanic reaction takes place first on the surface of the RHA particles and then inside the pore of the RHA particles. The finer RHA particles (5.7 µm) have a higher external pozzolanic reactivity due to increased surface area than the coarse ones, and refine the pore structure of mortar better than the coarse RHA (15.6µm).

2.3 EFFECT OF WFS ON FRESH PROPERTIES OF SCC

2.3.1 Workability

Sahmaran et al. (2011) explored with the different quantities of cement, fly ash and waste foundry sand, sixteen SCC combinations were created. At 0, 30, 50, and 70% by mass, fly ash (FA) was used to replace the cement in the combinations. Also, 0, 25, 50, and 100% of the fine aggregates by volume was substituted with spent foundry sand (SFS) for each FA level of replacement. The total sum of binding content (cement and fly ash) and the water to binder content (w/b) (450 kg/m3 and 0.40, respectively) were maintained constant for all combinations. The chemical characteristics of WFS might be the cause of an increase in SP dose. For fresh characteristics such as slump flow, the superplasticizer content required rises increasing SFS concentration for a given FA content. Similarly, increases SFS content is accompanied by an increase in V-funnel flow time. Additionally, the WFS contain silica sand, which is hydrophilic by nature and draws water to its surface. Another factor contributing to the reduction in mobility is the existence of a substance similar to clay in WFS, which can significantly reduce the mobility of concrete. Since that WFS has a greater bulk density than natural sand and a constant paste volume, substituting natural sand with it results in a decrease in water content and an increased solid volume. It is speculated that the ball-bearing effect is the crucial factor in achieving the flowability of WFS concrete because of the impacts listed above, though this may be another factor contributing to the decrease in WFS flowability.

Martins et al. (2022a) carried out investigation utilizing granite marble manufacturing waste (MGPW) as a mineral addition to enhance the viscosity of the concrete and waste foundry exhaust sand (WFES) as a partial replacement for natural sand in self-compacting concrete (SCC) up to 40% (10%, 20%, 30%, and 40%) at 7, 28, and 90 days. There were five different concrete combinations undertaken: WFES 0, WFES 10, WFES 20, WFES 30, and WFES 40. In place of natural sand, 0, 10, 20, 30, and

40% of WFES were used, correspondingly. The slump flow value ranged from 780 to 800 mm and the mixes lied in SF3 class according to EFNARC. The mixes were designed with constant superplasticizer content of 3.76 kg/m^3 and water to cement ratio of 0.37. The cement content was 455.20 kg/m^3.Slump flow time varied from 3 to 6 seconds. V-funnel time was 5 seconds for the control mix and with inclusion of WFES the flow time increased to 12 seconds for mix with 40% WFES.H-box values were within the range specified by EFNARC. The values varied between 0.96 and 0.97 for WFES 0% to 40%. The mixes obtained with inclusion of WFES up to 40% were deformable and workable.

Parashar et al. (2020) studied effect of WFS in SCC. The amount of fly ash FA was kept constant in all five mixtures at around 25.5% of the total weight of the powder composition. WFS was substituted for fine aggregate in the following ratios: 10%, 20%, 30%, and 40%. The slump flow values lied in the range between 633.3 to 593mm. L-box values varied from 0.78 to 0.85. V-funnel time increased with substitution rate of WFS and ranged between12.33 and 17.52. U-box values were between 0.8 and 2.2.

Makul (2019) explored certain combinations of SCC blended with rice husk ash (RHA) and foundry waste (FDW) to make high-performance SCC. The first step was to manage the water-binder materials (OPC and/or RHA) using w/b ratios of 0.35 or 0.45 using cement as ingredient of 450 and 650 kg/m^3 for each ratio, respectively. OPC was substituted by RHA at 10 and 20 weight percent, while fine aggregate was replaced by FDW at 30 and 50 weight percent. In comparison to the control SCC, the effect of FDW on the superplasticizer demand was to increase the superplasticizer requirement when fine aggregate was replaced with FDW. When compared to the specific surface area and density of the RHA particles, the FDW has a higher specific surface area and greater density, which accounts for the difference. The increase in the superplasticizer need was greatest for the samples evaluated at 50% weight FDW replacement ratio because the mix would contain a lot of FDW grains due to the higher FDW content and lower density of FDW than river sand. As a result, the SCC with FDW in its composition needs more superplasticizer than the SCC without FDW. This was so because the SCC that contained FDW had a higher proportion of finer FDW particles, requiring more water, compared to the specimens with a w/b ratio of 0.35 and the specimen with a w/b ratio of 0.45. Slump flow values lied within

the target slump flow of 700mm. Additionally, the V-funnel flow time was significantly impacted by the use of FDW in place of fine aggregate. The RHA-SCC specimen with FDW prolonged the flow duration relative to the control SCC mix by around 2.0 and 1.5 times for typical flows of 450 and 650 kg/m^3, respectively. Due to the inclusion of particles that were even finer than typical fine aggregate in the samples with RHA (50% by weight) and FDW, severe obstruction occurred at a binder content of 450 kg/m^3. This finding suggests that the fresh SCC mixture started to collapse and were significantly concentrated into agglomerates, due to SCC's low mobility. However, in spite of FDW with a considerable OPC level at 650 kg/m^3, no significant blockage happened.

Pathak and Siddique (2012) studied the effect of waste foundry sand as a partial substitute for fine aggregates and fly ash as a partial substitute for cement on the characteristics of SCC at elevated temperatures. A control mix without fly ash and three different fly ash percentages ranging from 30% to 50% were used in these mixtures. 10% used foundry sand was used to replace the fine aggregate. Slump flow values ranged from 627 to 648mm. U-box values varied from 13 to 8.

Ashish and Verma (2021) studied six different mixes with WFS up to 50% with increment of 10% and using metakaolin as a substitute for cement with fixed amount were produced in order to evaluate the impact of WFS on SCC. OPC, metakaolin, and water content remained constant in these concrete compositions, and the replacement % of metakaolin. The findings of the slump-flow test for concrete mixes with and without WFS that had various water content fluctuation were assessed in SCC. The amount of water affects how readily the SCC mixture flows; higher slump was observed as the water content increased, while a reduction in water content enhanced the SCC mixes cohesion. It was found that a modification in the water dosage of 10 L/m^3 in SCC mixes caused a 40 mm difference in slump value. The findings of the current experiment slump values experiment ranged between 676 to 746 mm, qualifying it within the SF2 category and indicating that SCC mixes should be able to withstand water content changes of between 5 and 10 L/m^3. It has been found that substituting WFS up to 50% for natural sand elevates the SP dose significantly when compared to the consumption for control and WFS concrete. According to the T500 test findings, the times vary from 8.4 seconds to 4.1 seconds, and all of the mixtures fall into the VS2 class. All mixes belong into the class VF1

according to the findings for the V-funnel flow time, which ranges from 14.9 to 8.1 seconds. The L-box test's blocking ratio, which is classified as PA2 and ranged from 0.89 to 0.97. Segregation was shown to have decreased with the rise in WFS replacement level. When compared to conventional sand, WFS's low specific density prevents particle resting downwards, which lowers segregation. All of the aggregates had similar specific gravities, which is a positive indication.

2.4 EFFECT OF WFS ON HARDENED PROPERTIES OF SCC

2.4.1 Compressive Strength

Sahmaran et al. (2011) investigated compressive strength with the different quantities of cement, fly ash and waste foundry sand, sixteen SCC combinations were created. At 0, 30, 50, and 70% by mass, fly ash (FA) was used to replace the cement in the combinations. Also, 0, 25, 50, and 100% of the fine aggregates by volume was substituted with spent foundry sand (SFS) for each FA level of replacement. The total sum of binding content (cement and fly ash) and the water to binder content (w/b) (450 kg/m^3 and 0.40, respectively) were maintained constant for all combinations. SCC exhibits compressive strengths of about 40 MPa and 50 MPa at 28 days and 90 days respectively be produced utilizing a blend of SFS and FA, despite the fact that both SFS and FA were shown to lower strengths. As in almost, all samples exhibited strengths more than 40 MPa, except for the 70% FA concrete mixtures. Regardless of the replacement level for SFS of 100%, this remains valid.

Martins et al. (2022a) investigated compressive strength utilizing granite marble manufacturing waste (MGPW) as a mineral addition to enhance the viscosity of the concrete and waste foundry exhaust sand (WFES) as a partial replacement for natural sand in self-compacting concrete (SCC) up to 40% (10%, 20%, 30%, and 40%) at 7, 28, and 90 days. There were five different concrete combinations undertaken: WFES 0, WFES 10, WFES 20, WFES 30, and WFES 40. In place of natural sand, 0, 10, 20, 30, and 40% of WFES were used, correspondingly. In comparison to the reference mix containing up to 30% waste, the compressive strength of SCC with WFES increased after 7 days. The strength of WFES40 mix, however, decreased. The control mix had a 28-day compressive strength of 72.95 MPa. In contrast to the control combination, it was found that WFES 20, WFES 30, and WFES 40 all showed increases in strength of 11.51%, 22.38%, and 2.77%, respectively (WFES 0). The control combination had a compressive strength of 80.61 MPa after 90 days. In the

WFES 20 and WFES 30 combinations, respectively, there was an increase in strength of 3.63% and 15.97%. It was also noted that the compressive strength of WFES 10 and WFES 40 was comparable to WFES 0. All SCC combinations exhibited a predictable rise in compressive strength with age. These findings demonstrated that the compressive strength of the mixes might fluctuate when natural sand is used in place of WFS in SCC, sometimes reducing it while at other times increasing it. This can be the result of variations in the waste's fineness modulus and structure. Such features affect how the particles are packaged. Compressive strength is also affected by modifications in the mixes' mineral inclusions and water/cement proportions.

Makul (2019) explored certain combinations of SCC blended with rice husk ash (RHA) and foundry waste (FDW) to make high-performance SCC. The first step was to manage the water-binder materials (OPC and/or RHA) using w/b ratios of 0.35 or 0.45 using cement as ingredient of 450 and 650 kg/m^3 for each ratio, respectively. OPC was substituted by RHA at 10 and 20 weight percent, while fine aggregate was replaced by FDW at 30 and 50 weight percent. The SCC combination with 10 wt% RHA and 30 wt% FDW obtained the highest compressive strength because to the pozzolanic activity caused by RHA and a stronger filling impact of the finer FDW grains than RHA particles. For SCC with RHA, the finer FDW particles were used as filler to densify the capillary openings inside the RHA particles. That is, too much FDW filling prevents the C-S-H gel from forming, as shown by the SCC specimen with 20 weight percent RHA and 10 weight percent FDW and the specimen with 20 weight percent RHA and 30. The SCC sample with 20 percent by weight RHA and 10 percent by weight FDW and the specimen with 20 percent by weight RHA and 30 and 50 weight percent FDW both acquired lesser compressive strength than the control SCC. This is because too much filling from FDW prevents the development of C-S-H gel. The development of SCC's compressive strength at a binder content of 650 kg/m^3 was comparable to that of SCC mixtures made with 450 kg/m^3 of binder materials.

Pathak and Siddique (2012) studied the effect of waste foundry sand as a partial substitute for fine aggregates and fly ash as a partial substitute for cement on the characteristics of SCC at elevated temperatures. A control mix without fly ash and three different fly ash percentages ranging from 30% to 50% were used in these mixtures. 10% used foundry sand was used to replace the fine aggregate. Even though

fly ash and used foundry sand lower the strength, it is still possible to produce SCC with compressive strengths up to 19.75 MPa, 29.12 MPa, and 31.95 MPa at 28, 91, and 365 days, respectively, at high temperatures.

Parashar et al. (2020) investigated compressive strength of SCC mixes. The amount of fly ash FA was kept constant in all five mixtures at around 25.5% of the total weight of the powder composition. WFS was substituted for fine aggregate in the following ratios: 10%, 20%, 30%, and 40%. SCC mixes compressive strength values were shown to decrease when WFS concentrations increased, and the results were closely correlated with the strength properties.

Ashish and Verma (2021) investigated six different mixes with WFS up to 50% with increment of 10% and using metakaolin as a substitute for cement with fixed amount were produced in order to evaluate the impact of WFS on SCC. OPC, metakaolin, and water content remained constant in these concrete compositions, and the replacement % of metakaolin. Incorporation of WFS as substitute of fine aggregates has a detrimental impact on the compressive strength behaviour of SCC mixes at 28 and 56 days of curing. Concrete with 10% WFS, showed lower compressive strength in comparison to control concrete at 28 days of curing. Compressive strength showed reduced values as the content of WFS rises. Furthermore, a rise in compressive strength can be noticed as time progressed. In the case of concrete mixes WFS0, WFS10, WFS20, WFS30, WFS40, and WFS50, wherein paste content remains constant, the compressive strengths were observed after 56 days curing ages to be 94.8 MPa, 102.5 MPa, 105.6 MPa, 108.0 MPa, 111.1 MPa, and 81.5 MPa, respectively. The aforementioned data demonstrates that concrete mixtures with a 40% WFS replacement had the highest compressive strength; above this replacement level, strength was decreased.

2.4.2 Splitting Tensile Strength

Makul (2019) explored certain combinations of SCC blended with rice husk ash (RHA) and foundry waste (FDW) to make high-performance SCC. The first step was to manage the water-binder materials (OPC and/or RHA) using w/b ratios of 0.35 or 0.45 using cement as ingredient of 450 and 650 kg/m^3 for each ratio, respectively. OPC was substituted by RHA at 10 and 20 weight percent, while fine aggregate was replaced by FDW at 30 and 50 weight percent. The 180-day curing period's splitting tensile strength development trend resembled that of the SCC made with 10 wt%

RHA and 30 wt% FDW's compressive strength development. It was observed that the splitting tensile strength somewhat decreases as FDW increases. Due to the fine particles of FDW, the formation of bond strength in the interfacial transition zone (ITZ) between the OPC paste and the aggregate is restricted. This, in turn, contributes to the increased need for superplasticizer in the SCC samples, which results in the decrease in splitting strength.

2.4.3 Capillarity

Martins et al. (2022a) studied capillarity utilizing granite marble manufacturing waste (MGPW) as a mineral addition to enhance the viscosity of the concrete and waste foundry exhaust sand (WFES) as a partial replacement for natural sand in self-compacting concrete (SCC) up to 40% (10%, 20%, 30%, and 40%) at 7, 28, and 90 days. There were five different concrete combinations undertaken: WFES 0, WFES 10, WFES 20, WFES 30, and WFES 40. In place of natural sand, 0, 10, 20, 30, and 40% of WFES were used, correspondingly. Investigations were made into how WFES affected the capillarity of SCC. After day 28 of the curing process, a capillarity test was conducted. There was no noticeable difference in the concrete's capillarity for 20, 30, and 40% of replacements. The capillarity coefficient, however, increased significantly at 10% of replacement. It was discovered that WFES contributes to capillarity reduction since WFES 30 combination displayed 38.9% lesser capillarity compared to SCC control mixture (0.14 g/cm^2).

Parashar et al. (2020) the amount of fly ash FA was kept constant in all five mixtures at around 25.5% of the total weight of the powder composition. WFS was substituted for fine aggregate in the following ratios: 10%, 20%, 30%, and 40%. In addition, it was discovered that when the replacement level increased, so did sorptivity and water permeability. Similarly, at 10% replacement level, the increase was negligible.

2.4.4 Water Absorption

Sahmaran et al. (2011) studied volume of permeable pore space (VoPP) with the different quantities of cement, fly ash and waste foundry sand, sixteen SCC combinations were created. At 0, 30, 50, and 70% by mass, fly ash (FA) was used to replace the cement in the combinations. Also, 0, 25, 50, and 100% of the fine aggregates by volume was substituted with spent foundry sand (SFS) for each FA level of replacement. The total sum of binding content (cement and fly ash) and the water to binder content (w/b) (450 kg/m^3 and 0.40, respectively) were maintained

constant for all combinations. VoPP is considerably increased by substituting SFS at 100%. Furthermore, VoPP does not vary considerably with SFS quantity when the SFS replacement level is 50% or below.

Martins et al. (2022b) explored the use of waste foundry sand in SCC. In place of natural sand, 0, 10, 20, 30, and 40% of WFES were used, correspondingly. Water absorption was shown to vary between 1% and 3%. As indicated by ASTM C 642, all mixes showed extremely low absorption characteristics, i.e., less than 5%. Concrete water absorption and concrete quality may be connected, states the (CEB). Absorption values under 3.0% signify high-quality material with low absorption rates. Absorption rates between 3.0 and 5.0% are categorised as concrete possessing medium absorption and medium quality. According to the CEB's recommended classifications, mixes SCCW0, SCC-W20, and SCC-W30 be categorised as low-absorption, good-quality concrete, whereas mixes SCC-W10 and SCC-W40 be categorised as medium-absorption, medium-quality concrete.

2.4.5 Sulphate Resistance

Martins et al. (2022a) investigated compressive strength utilizing granite marble manufacturing waste (MGPW) as a mineral addition to enhance the viscosity of the concrete and waste foundry exhaust sand (WFES) as a partial replacement for natural sand in self-compacting concrete (SCC) up to 40% (10%, 20%, 30%, and 40%) at 7, 28, and 90 days. There were five different concrete combinations undertaken: WFES 0, WFES 10, WFES 20, WFES 30, and WFES 40. In place of natural sand, 0, 10, 20, 30, and 40% of WFES were used, correspondingly. During the test period, no SCC samples had any fractures that may have been induced by the production of expansive compounds such calcium sulphate (Gypsite) and calcium sulfoaluminate (ettringite). The compressive strength of the specimens kept in sulphate compared to those kept in water was lower for SCC mixes, as was to be predicted. For the samples held in the sulphate solution and the samples retained in water, the compressive strength in the control mixture was 84.81 MPa and 91.29 MPa, respectively. Comparing the samples WFES 0, WFES 10, WFES 20, WFES 30, and WFES 40 to the samples stored in sulphate and evaluated for compressive strength, there was an increase of 7.63%, 1.99%, 12.73%, 5.95%, and 4.01% in each case. Additionally, for samples stored in sulphate and water, respectively, there was an increase in compressive strength of 12.50% and 10.74% when compared to the control combination (WFES 0). Both the

samples maintained in sulphate and those in water had a change (rise) in mass. For samples stored in sulphate, the increase in mass of the control mix was 1.08%; for samples stored in water, it was 1.47%. The WFES40 combination had the largest mass fluctuation, although it did not go over 2%. The WFES 30 combination, on the other hand, showed the least variance, with 0.84 and 0.99% for the samples held in the sulphate solution and water, respectively.

2.4.6 Chloride Permeability

Sahmaran et al. (2011) investigated chloride permeability with the different quantities of cement, fly ash and waste foundry sand, sixteen SCC combinations were created. At 0, 30, 50, and 70% by mass, fly ash (FA) was used to replace the cement in the combinations. Also, 0, 25, 50, and 100% of the fine aggregates by volume was substituted with spent foundry sand (SFS) for each FA level of replacement. The total sum of binding content (cement and fly ash) and the water to binder content (w/b) (450 kg/m^3 and 0.40, respectively) were maintained constant for all combinations. Despite the fact that SFS reduces chloride permeability, the impact is very negligible as long as the mixes also contain FA (particularly for SFS quantity is 50% less than 50%). At 90 days, the overall charge in these kinds of mixes has been below 900 coulombs.

Martins et al. (2022b) studied the utilization of waste foundry exhaust sand in SCC. In place of natural sand, 0, 10, 20, 30, and 40% of WFES were used, correspondingly. Comparing SCC-W30 to the control mixture, there was a 24.7% drop in electrical charge, which shows that SCC-W30 gets denser. All samples had an electrical charge of less than 1000 Coulombs, which shows that the probability of corrosion for all mixes is extremely low. The effective lifespan can be extended by adding WFES since the corrosion start time is correlated with the amount of chloride ions that enter the structure.

Makul (2019) explored certain combinations of SCC blended with rice husk ash (RHA) and foundry waste (FDW) to make high-performance SCC. The first step was to manage the water-binder materials (OPC and/or RHA) using w/b ratios of 0.35 or 0.45 using cement as ingredient of 450 and 650 kg/m^3 for each ratio, respectively. OPC was substituted by RHA at 10 and 20 weight percent, while fine aggregate was replaced by FDW at 30 and 50 weight percent. SCC specimen with 10 wt% RHA, the FDW reduced the chloride permeability, which was a result of the finer FDW grains

packing the microstructure and generating an SCC sample with an extremely robust structure.

2.4.7 Water Permeability

Makul (2019) investigated certain combinations of SCC blended with rice husk ash (RHA) and foundry waste (FDW) to make high-performance SCC. The first step was to manage the water-binder materials (OPC and/or RHA) using w/b ratios of 0.35 or 0.45 using cement as ingredient of 450 and 650 kg/m^3 for each ratio, respectively. OPC was substituted by RHA at 10 and 20 weight percent, while fine aggregate was replaced by FDW at 30 and 50 weight percent. Water permeability for 28 and 180 days was observed in this study. Water permeability coefficient (k) values for SCC samples with fine aggregate substituted with 10% and 20% FDW reduced moderately.

2.5 SUMMARY

In this chapter, detailed literature has been reviewed on utilization of RHA in SCC as partial replacement of cement and WFS as partial replacement of fine aggregates in SCC. Previous studies showed dearth of literature on durability properties and also there was limited study with utilization of RHA and WFS together as partial replacement of cement and fine aggregates in SCC. Therefore, detailed study has been conducted to utilize RHA, WFS and combination of RHA and WFS to develop SCC and investigate fresh, strength and durability properties.

CHAPTER- 3

MATERIALS AND METHODOLOGY

This chapter describes the materials used and its characterization which were utilized in this research study for the preparation of Self-Compacting Concrete and test methods used to study the influence of rice husk ash and waste foundry sand as replacement of cement and fine aggregates on properties of Self-Compacting Concrete.

3.1 INTRODUCTION

The experimental investigation included casting, curing, and testing of specimens to determine the impact of rice husk ash as a substitute for cement and waste foundry sand as a partial replacement of fine aggregates on the characteristics of self-compacting concrete. Figure 3.1 is an illustration of the experimental programme.

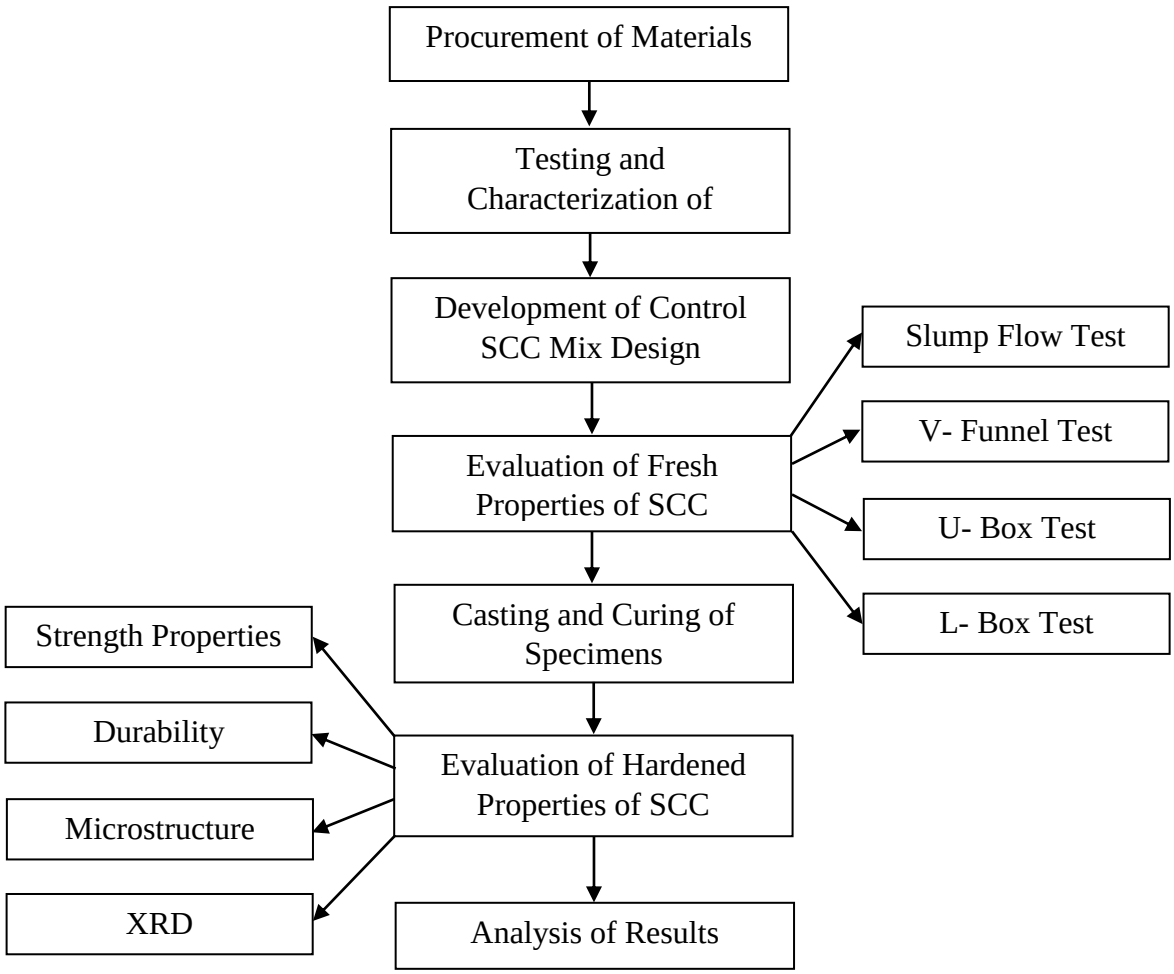

Fig.3.1 Schematic diagram for orientation of the experimental investigation

3.2 MATERIALS USED

3.2.1 Cement

Ordinary Portland cement of grade 43 (OPC 43) was utilized in this research study, conforming to BIS 8112:2013 (BIS 2013) equivalent ASTM C150M (ASTM 2016). The BIS: 4031-1989 (BIS 1989) standard was used to determine the consistency and setting time of cement. Table 3.1 shows the basic tests conducted on OPC.

a) Consistency

Cement consistency may be described as the least amount of water added to cement in order to achieve a homogenous paste with suitable viscosity and strength for various types of structural work as required. The consistency of the cement was determined using a procedure which conformed BIS: 4031 (BIS 1989). Initially, a 500g cement paste was prepared and placed in the mould (Vicat mould). The top surface of the mould was levelled, and any undesired air was expelled by shaking it. The Vicat apparatus' rod bearing plunger was used to keep the mould in place. The plunger was made to touch the top surface of the mould by lowering it. Trial mixes of pastes containing various amounts of water were used to determine the exact amount of water needed to obtain the desired consistency.

b) Setting time

The BIS: 4031 (Part 5)-1988 procedures were used to determine the setting time of cement. The paste was made by mixing 0.85 times the amount of water needed to get the desired consistency in the cement. The entire mixture was poured into the mould, then levelled with a trowel. The rod bearing needle was kept under the mould. By lowering the needle, it was able to penetrate the top surface of the mould. The procedure was repeated until the needle could not penetrate the mould any further than 5.0 mm from the bottom. The initial setting time is determined from the point where water is added to the cement to the point where the needle fails to penetrate beyond 5.0 mm when measured from the bottom.

A needle with an annular collar is used to determine the final setting time. When an impression on the surface of the specimen is formed following a gentle contact by the needle on the surface, the cement is considered fully set. The final setting time is calculated from the time water is added to the cement until the time an impression on the surface of the test sample is obtained.

Table 3.1 Test conducted on Ordinary Portland Cement (OPC) Grade 43

Tests	Results	Standard results as per IS: 8112-2013
Specific Gravity	3.15	-
Compressive Strength (N/mm^2)		
3 days	23.40	23
7 days	34.70	33
28 days	45.30	43
Normal Consistency (%)	30	-
Fineness (m^2/kg)	274	≥225
Initial Setting time (min)	41	≥30
Final Setting time (min)	312	≤600

3.2.2 Fine Aggregates

These are aggregates with a diameter of 4.75 mm or less. Particles pass through a sieve with a size of 4.75 mm and are retained on a sieve with a size of 0.075 mm. These are necessary to regulate essential cement qualities such as workability. The experiment was carried out using fine aggregates from two different sources. Locally available river sand was used conforming provisions of BIS: 383-1970 (BIS 1970) equivalent to ASTM C33/ C33M (ASTM 2018). Fine aggregates were bought from two different quarries in Punjab which were used in different ratios. Both fine aggregates were mixed in the ratios of 65: 35 to achieve the grading requirements of Self Compacting Concrete (SCC). Fine aggregates which were collected from Pathankot, Punjab, India was first source. The fine aggregates collected had a specific gravity of 2.63, a fineness modulus of 3.10, and 0.63 % water absorption. Anandpur Sahib, Punjab, India was the second source. It had a specific gravity of 2.61, a fineness modulus of 2.17, and 0.40 % water absorption. The combined specific gravity was 2.72 and the fineness modulus was 2.93 after mixing in 65:35 proportions. Water absorption was 0.71 %.FA_{35} represents 35% sand which was obtained from Anandpur Sahib, Punjab, India, and FA_{65} represents 65% sand obtained from second source Pathankot, Punjab, India. The particle grading was achieved by blending these two different types of fine aggregates. These proportions of different fine aggregates were selected after repeated trials with various percentages of fine

aggregates to obtain fresh properties and strength requirements of the designed SCC mix.

3.2.3 Coarse Aggregates

Aggregates with size greater than 4.75 mm constitute the coarse aggregates. They govern the strength properties of concrete. Coarse aggregates with the specific gravity of 2.70 were used and the water absorption of aggregates was 0.40%. The coarse aggregates of 10mm size were sourced from quarries around Pathankot, Punjab, India.

3.2.4 Fly Ash

Fly ash is commonly used as a cementitious material in manufacturing concrete. It possesses pozzolanic characteristics, which aid in the lime reaction. It is a by-product in coal-fired power plants in the form of a grey powdered form. As an extra substance, fly ash was employed. It fulfilled the requirements of BIS 3812:2013 (BIS 2013), which is equivalent to ASTM C618-05 (ASTM 2005). The fly ash was obtained from a thermal power plant in Rajpura, Punjab, India. The Blaine's fineness was 330 m^2/kg, and the specific gravity was 2.27. Fly ash serves as a mineral admixture, contributing fluidity and a finer overall grain structure to the mix.

3.2.5 Waste Foundry Sand

WFS was collected from a local foundry (Mahadev Foundry) at Mandi Gobindgarh, Punjab, India where annual production of WFS was approximately 120 to 150 tons. Morphology of WFS is shown with the help of the SEM image in Figure 3.2. It depicts particles of WFS are spherical, rough textured and angular in nature. Figure 3.3 depicts the morphology and chemical constituents of WFS through Scanning electron micrograph (SEM) image and Energy dispersive spectroscopy (EDS). It shows that WFS particles are rough-textured, and angular. EDS indicates that it has a higher silica concentration.WFS was carbon black in color. The basic properties of the fine aggregates, coarse aggregates, fly ash and waste foundry sand used for experimentation are given in Table 3.2 and the chemical composition of WFS is tabulated in Table 3.3. Particle size distribution curve of fine aggregates and waste foundry sand are demonstrated in Figure 3.4. The 50% of average size particles of WFS and normal sand were found to be passing from sizes 0.443mm and 0.811mm in diameter respectively. It can be concluded here that the WFS particles were finer than fine aggregate particles. Figure 3.4 also shows the particle size distribution curve

representing 75.90% of WFS particles are finer compared to 41.10% particles of blended sand at 0.60 mm size sieve.

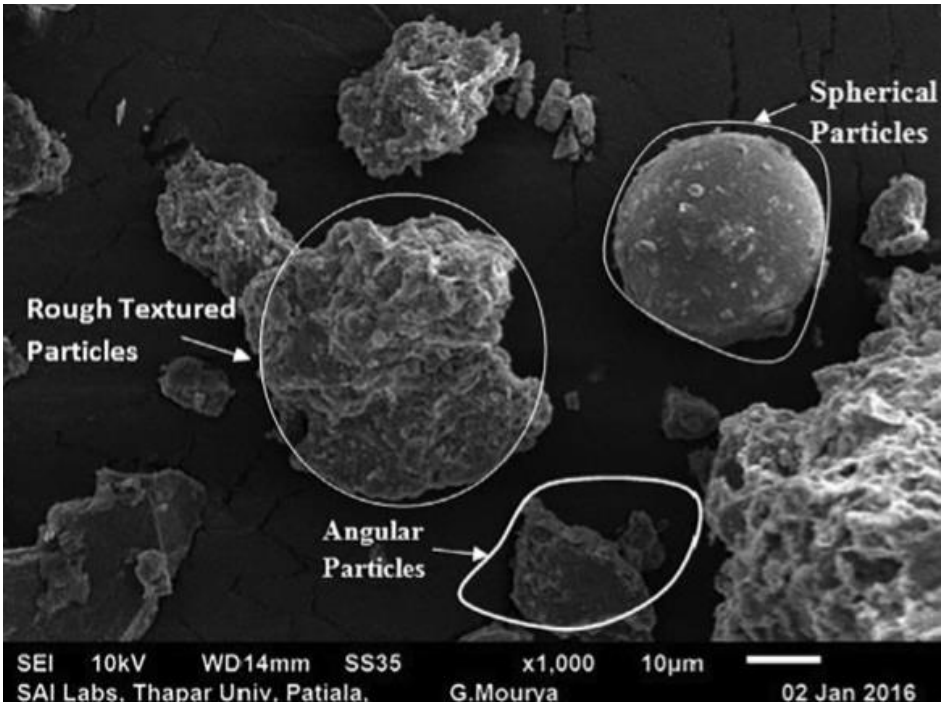

Fig.3.2 Scanning electron microscope (SEM) image of WFS

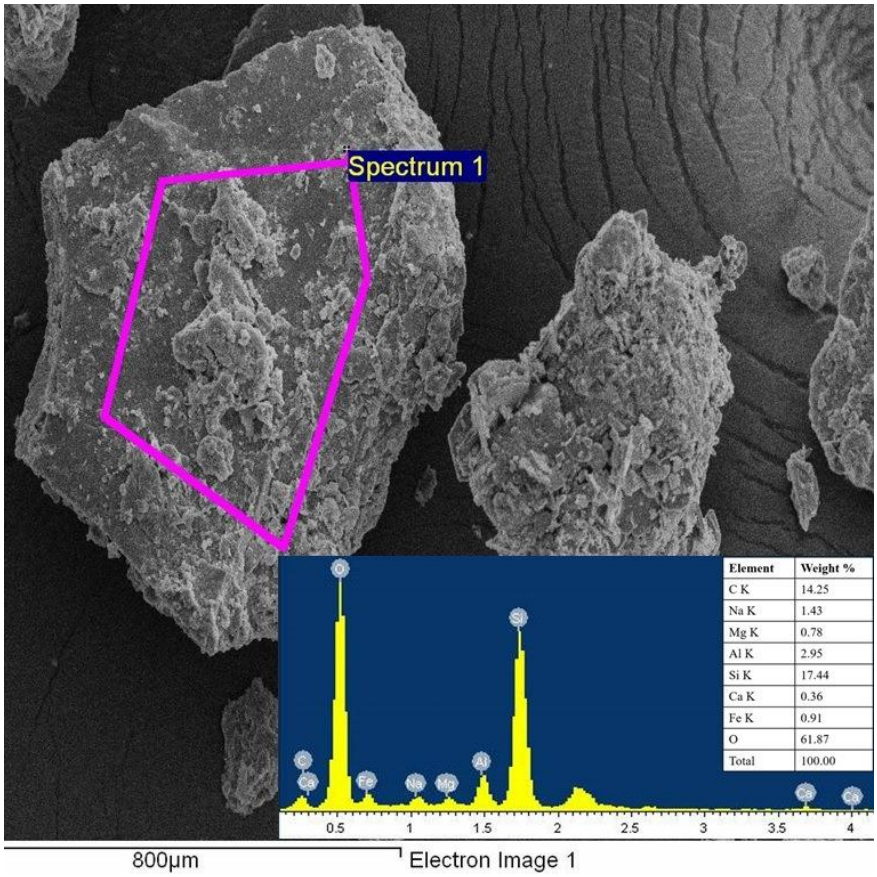

Fig.3.3 SEM and EDS image of WFS

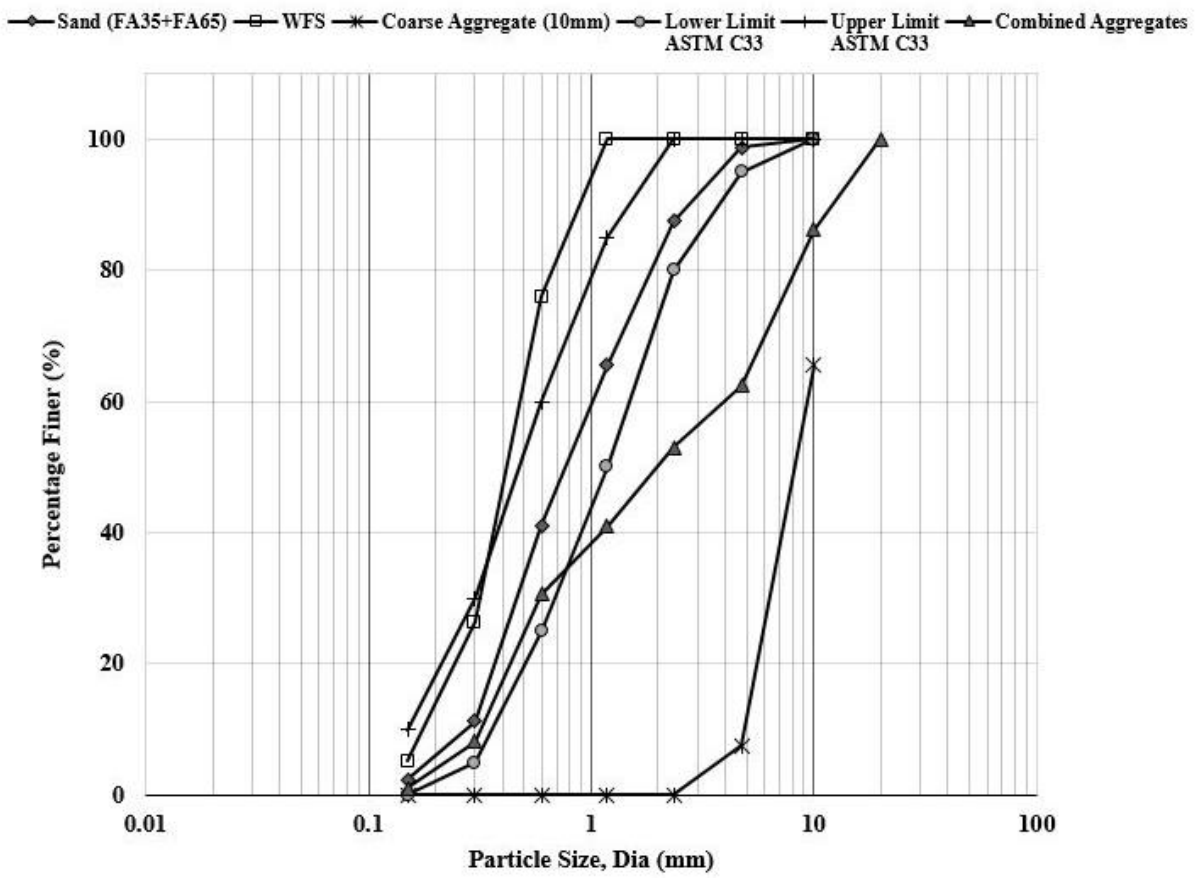

Fig.3.4 Particle size distribution

Table 3.2 Basic properties of materials

Aggregates	Sieve Size (mm)								Fineness Modulus	Specific Gravity	Absorption (%)
	20.0	10.00	4.75	2.36	1.18	0.60	0.30	0.15			
	Percentage Passing (%)										
Coarse Aggregates (CA)	100	65.44	7.57	0.01	0.00	0.00	0.00	0.00	-	2.70	0.40
Fine Aggregates (FA_{35})	100	100	98.30	93.30	90.20	82.30	17.30	0.80	2.17	2.61	0.60
Fine Aggregates (FA_{65})	100	100	99.40	85.50	56.40	34.10	11.60	2.30	3.10	2.63	0.63
Fine Aggregates (FA_{35}+FA_{65})	100	100	98.70	87.50	65.50	41.10	11.30	2.40	2.93	2.72	0.71
Waste Foundry Sand (WFS)	100	100	100	100	100	75.90	26.40	5.20	1.93	2.65	0.62
ASTM C33/ AASTHO M6 Upper Limit	100	100	100	100	85	60	30	10	-	-	-
ASTM C33/ AASTHO M6 Lower Limit	100	100	95	80	50	25	5	0	-	-	-

Table 3.3 Chemical composition of WFS

Constituents	Formula	Values %
Silica	SiO_2	86.44
Alumina	Al_2O_3	4.31
Iron Oxide	Fe_2O_3	2.74
Calcium Oxide	CaO	0.98
Magnesium Oxide	MgO	0.88
Sulfur Trioxide	SO_3	0.19
Sodium Oxide	Na_2O	0.39
Potassium Oxide	K_2O	0.28
Titanium Dioxide	TiO_2	0.17
Phosphorus Pentaoxide	P_2O_5	0.00
Manganese Oxide	Mn_2O_3	0.04
Strontium oxide	SrO	0.03
Loss on Ignition	LOI	3.55

3.2.5.1 Types of Waste Foundry Sand

Waste foundry sand is classified according to the binder systems which are used in metal casting. The types of waste foundry sand are categorized into two main types of binder systems. Clay-bonded systems (green sand) and chemical-bonded systems are the different sorts.

1. Green Sand

   Green sand is composed of a combination of naturally occurring materials. High-quality silica sand (85-95 %), bentonite clay as a binder (4-10 %), water (2-5 %) and a carbonaceous additive (2-10 percent) to enhance the casting surface finish. It is black in colour due to the presence of carbon content.

2. Chemically-Bonded Sand

   Such type of sands are used both in core making process where there is a requirement of high-strength and in mould making. Most of the chemical binder systems comprise of an organic binder which is activated by means of a catalyst. However, there are some systems that make of inorganic binders as well. Such sands are light in colour in comparison to the clay-bonded sands.

3.2.5.2 Properties of Foundry Sand

1. Physical Properties

Foundry sand is often sub-angular to spherical in shape. Green sand is typically black or grey in colour, whereas chemically bonded sands are off-white. The grain size distribution of spent foundry sand is uniform. It is non-plastic and has low absorption capacity. Foundry sand has a specific gravity ranging from 2.39 to 2.55.

2. Chemical Properties

The metal moulded at the foundry determines the chemical composition of foundry sand. Type of binder and combustible used also play a major role. The chemical composition of foundry sand varies from foundry to foundry. Foundry sand's chemical composition can have a significant impact on its performance.

3.2.6 Rice Husk Ash

The pozzolanic natured agricultural by-product RHA was used as a replacement of cement in this study. Its Blaine fineness evaluated was 698m^2/kg, specific gravity 2.47. It has very fine angular and porous particles of large surface area as can be seen in scanning electron microscopy (SEM) image in Figure 3.5. Figure 3.6 shows the X-ray diffraction (XRD) pattern of RHA that revealed the presence of silica in crystalline as well as amorphous phase. Sharp intense peaks of cristobalite (00-039-1425) and silica (00-0330-1161) depicting the crystalline form of silica in RHA was observed in diffraction graph. The broad humps depicted silica in the amorphous phase. Table 3.4 displays the chemical composition of RHA, which also indicates that silica it its main constituent.

3.2.6.1 Properties of RHA

1. Physical Properties

Rice husk which has been completely burned is grey to white in colour, whereas rice husk that has not been completely burned is black. Rice husk is an extremely fine material found in nature. The average particle size of rice husk ash was 3 to 10 microns.

2. Chemical Properties

Rice husk ash has a high silica concentration of more than 80%. The total amount of silicon dioxide (SiO_2), aluminium oxide (Al_2O_3), and iron oxide (Fe_2O_3) in a mixture should not be less than 70%.

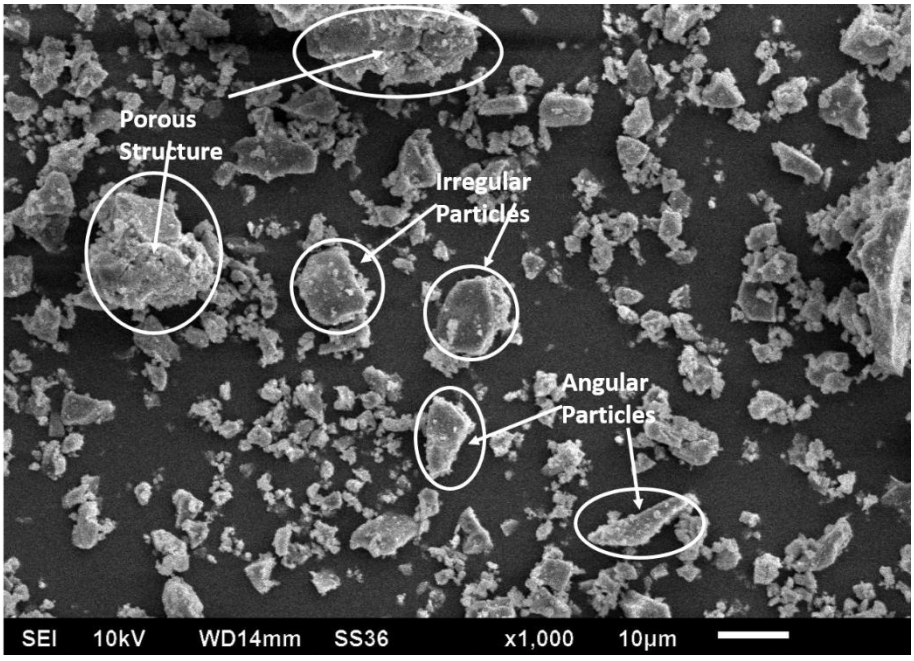

Fig.3.5 SEM image of RHA

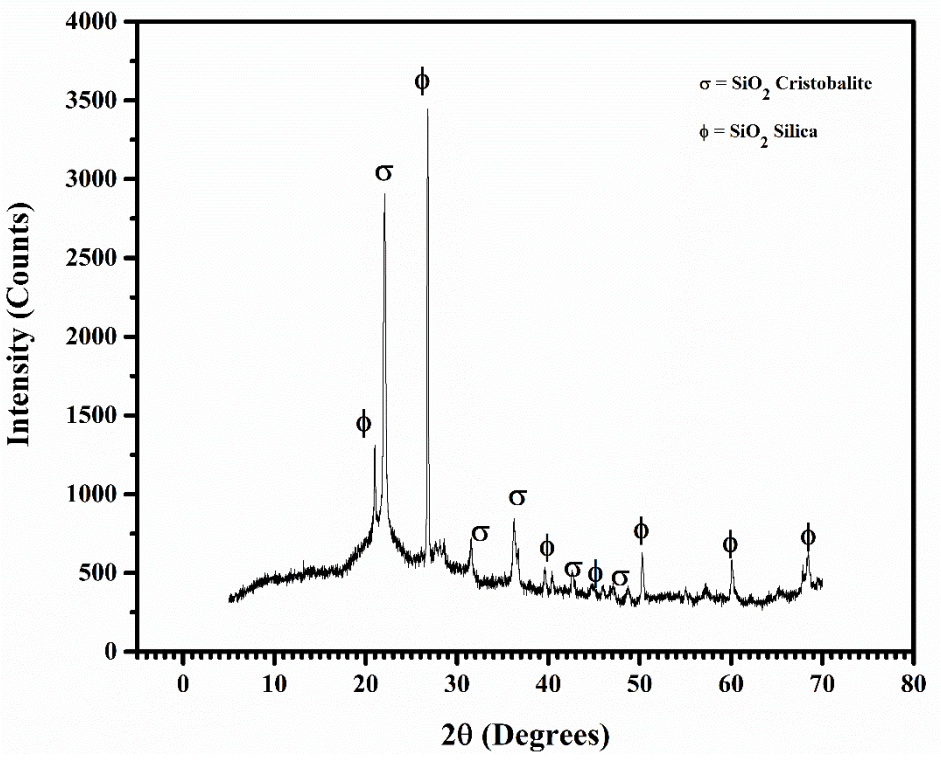

Fig.3.6 XRD pattern of RHA

Table 3.4 Chemical composition of RHA

Constituents	SiO_2	Fe_2O_3	Al_2O_3	CaO	Na_2O	K_2O	TiO_2	SO_3	Mgo	LOI
Percentage (%)	87.90	0.79	1.28	1.69	0.33	2.20	0.01	0.42	0.63	4.26

3.2.7 Water

In the concrete production process all the ingredients of SCC were mixed with potable water i.e. ordinary tap water with a pH of 6.5-8.5 is used.

3.2.8 Super Plasticizer

Polycarboxylate Ether (PCE) based superplasticizer was used in the experimental program as a water-reducing admixture. The cementitious material had a superplasticizer content of 1.17 % by weight. Auramix 400 of FOSROC with specific gravity of 1.09 was used in the development of SCC, which is polycarboxylic ether polymer, low viscosity high-performance superplasticizer. It is a light yellow colored viscous liquid. It lowers the water demand and helps to maintain the fluidity in self-compacting concrete by creating electrostatic scattering at the time of mixing, which greatly improves cement dispersion. Normally, the dosage of admixture ranges between 0.5 to 3.0 litres for 100 kg of cementitious material but its optimum dosage is calculated by trials considering the specification of material and the conditions prevailing.

Fig.3.7 Magnesium Sulphate Solution

3.2.9 Magnesium Sulphate

The sulphate resistance of mixes was investigated using magnesium sulphate. Magnesium sulphate was used for this investigation because it had a more aggressive effect on the concrete than sodium sulphate solution when exposed to it. *(Mostofinejad et al., 2020).*

3.3 MIX DESIGN

3.3.1 EFNARC (2005) Guidelines

General

The performance criteria for concrete should be satisfied by the mix composition in both the fresh as well as hardened stages.

Initial Mix Composition

Volume should be given preference over mass while estimating the relative proportions of the major components in the process of designing a mix.

The general material ratios and quantities required to achieve self-compactability are mentioned below. These values may change in the future to fulfil performance and strength requirements.

- Water/powder ratio of 0.80 to 1.10. This ratio is by volume.
- 160 to 240 litres; that is, (400-600 kg) per cubic metre of total powder content.
- The content of coarse aggregates generally 28 to 35 per cent of the mix by volume.
- Generally the water content value should not increase over 200 litre/m^3
- The volume of the other components is balanced by the sand content.

In order to make sure that concrete shows its fresh properties, it is suggested that the design should be conservative in nature. Certain amount of variation in the moisture content of aggregates is allowed as well as expected to occur in the stage of mix designing. Generally, viscosity modifying admixtures are considered to be quite effective in order to compensate for any kind of alterations due to changes in the grading of sand and the moisture content of aggregates.

Adjustment of mix

Trials in the laboratory should be conducted in order to check the required properties of the initial composition of the mix. The composition of the mix should be adjusted if it is necessary. The complete testing of the mix should be conducted in situ or at the plant once the requirements have been fulfilled. When no satisfaction in the performance is obtained, fundamental redesigning of the mix should be done in that case. On the basis of the problem, the following actions could be the appropriate:

- Usage of extra or different types of filler, (if available);
- varying the ratios of the sand or the coarse aggregate;
- Usage of a viscosity modifying agent, if not already added in the mix;
- modifying the dose of the superplasticizer and/or the viscosity modifying agent;
- using substitute types of superplasticizer (and/or VMA), more agreeable with local materials;
- Varying the dosage of admixture to change the water content, and hence the water/powder ratio.

3.3.2 Mixture Proportions

3.3.2.1 Using Rice Husk Ash

EFNARC (2005) was used in the designing process of SCC in order to achieve the desirable properties in both the hardened and fresh stages. The composition of the ingredients is the deciding factor in attaining the deciding properties in SCC. The quality of concrete is controlled by choosing the appropriate amount of materials and ensuring that they are of standard quality. The composition of seven mixes were developed by substituting cement with RHA by weight up to 30% in 5% increments are given in chapter 4. Cement content of 500kg/cum was first incorporated in the control mix (RHA). All of the planned mixes fulfilled the requirements of ACI 318. The maximum SCM was 50% of the total cementitious content *(ACI 318).* There was a change in the proportions in the cement content in the mixes produced in the further stages. On the other hand, the quantities of fly ash, w/b ratio and superplasticizer remained constant. They were 40 kg, 0.36 and 1.17% respectively. In order to obtain better workability and to optimize the grading limits. In order to study the effect of RHA on fresh, strength and durability properties for SCC mixes, tests were conducted. The SCC mixes were assigned as RHA0, RHA10, RHA15, RHA20,

RHA25 and RHA30. Here, 0 to 30 represents the percentage of cement replaced while RHA is the SCC mix.

3.3.2.2 Using Waste Foundry Sand

The proportions of several Self Compacting Concrete (SCC) ingredients such as cement, coarse aggregates, fine aggregates, fly ash, waste foundry sand, water, and superplasticiser have been determined by laboratory experiments. The compressive strength achieved by the control mix (WFS0 with 0% WFS) at 28 days of curing was 58.25 MPa. Cement content and fly ash as a mineral admixture were used with constant values of 500kg/cum and 40kg/cum respectively. Fine aggregates, i.e. natural sand, which were collected from two different sources, were in 35% and 65% proportions to achieve the requirements associated with grading and workability in SCC. The superplasticiser content of 1.17% of cementitious material in terms of weight was used and a constant value of water-binder ratio of 0.36 was maintained. The Self-Compacting Concrete mixes are assigned as WFS5, WFS10, WFS15, WFS20, WFS25, WFS30 in which there is a replacement of fine aggregates with waste foundry sand in terms of volume at 5%, 10%, 15%, 20%, 25% and 30% levels respectively. The compositions of the various mixes prepared by utilizing WFS in SCC are given in chapter 4.

3.3.2.3 Using Rice Husk Ash and Waste Foundry Sand

The SCC mixes were designed to achieve the fresh state properties using EFNARC (2005) guidelines with characteristic strength of 50 MPa at 28 days of curing. The compressive strength achieved by the control mix at 28 days of curing was 58.44 MPa. Cement content of 500kg/cum was used for the control mix. Fly ash as a mineral admixture was used with constant value of 40kg/cum in the SCC mixes. Seven SCC mixes were prepared with a superplasticizer content of 1.17% by weight of cementitious materials and a constant water-powder ratio of 0.36. All these mixes were prepared to evaluate the fresh, compressive strength and durability properties of SCC. The composition of seven mixes of SCC were prepared by replacing cement with RHA (by weight) up to 30% at an increment of 5% and fine aggregates were partially replaced with WFS (0-30%) by volume in the design mix. The mixes were titled as R0WFS0, R5WFS5, R10WFS10, R15WFS15, R20WFS20, R25WFS25, and R30WFS30 for 0 to 30% of RHA and WFS substitution, respectively.

3.4 PREPARATION, CASTING AND TESTING PROCEDURE OF SPECIMEN

The physical properties of the constituents were evaluated prior to the casting process. It was ensured that the aggregates were soaked and dried on the surface. A pan mixer was used to blend the fine and coarse aggregates in dry condition. The cement was mixed with fly ash until the dry mixture had a uniform colour. Precautions were made while adding water and superplasticizer to prevent any form of loss in the mix. In order to design SCC mixes, with RHA, WFS and both with RHA and WFS the calculations were done according to replacement percentage. Further these materials were substituted at the time of mixing procedure.

Fig.3.8 Preparation of SCC

Fig.3.9 Casting of specimens

Cubical and cylindrical molds were cleaned, tightened, and oiled properly before casting. All the dry state ingredients were mixed in pan mixer, thereafter water along with admixture was added to form cohesive and non-segregating concrete.

Fig.3.10 Curing of specimens

EFNARC (2005) was used in order to estimate the fresh properties of SCC mixes. Compressive strength was calculated till the age of 365days by making use of 150mm cubes according to BIS 516:1959 equivalent to ASTM C39-18. Splitting tensile strength was evaluated till a time span of 365days by conforming to the regulations of BIS 5816:1999 (BIS 1999) equivalent to ASTM C496/C496M-17 (ASTM 2017). For evaluating properties such as water absorption and porosity, cylinders were casted with length 200mm and diameter 100 mm. Further, these cylinders were shaped into circular disks having length of 50mm for the purpose of evaluation of water absorption till the age of 365days as per the code ASTM C642-13 (ASTM 2013). Sorptivity was calculated up to the testing time span of 365 days by making use of ASTM C1585-13 (ASTM 2013). In SCC mixes, rapid chloride permeability was estimated at 28, 90, and 365days as per the regulations of ASTM C1202-10 (ASTM 2010). Alike samples having a circular shape with dimensions of 100mm diameter and 50mm length were made use of for RCPT. After a 28-day curing period, 150mm cubes were used for the sulphate attack test. These cubes were soaked in sulphate solution (Magnesium sulphate) for a time of 28, 90, and 365days. Loss of mass and the compressive strength of samples attacked by sulphate were evaluated as per the

technical regulations of ASTMC1012/C1012M-10 (ASTM 2010). Further, microstructure of SCC was analyzed using SEM. Fragments of broken compressive strength samples were taken from inner core of the cubes. It was then coated with a gold film and tested by using electron microscope. The Jeol electron scanning electron microscope was used for SEM analysis.

3.5 FRESH STATE PROPERTIES

3.5.1 Slump Flow Test

This is a workability test with the main objective of measuring SCC flow. There are no obstacles in the way of the flow, which is measured horizontally. The test is conducted using a standard sized slump cone, with the exception that SCC is not rodded as in the standard test. After the cone is lifted, SCC begins to spread. The horizontal direction is used to determine the spread diameter. This test is used to evaluate concrete's consistency, workability, and flowability. According to EFNARC standards, SCC should have a diameter of 650mm to 800mm.

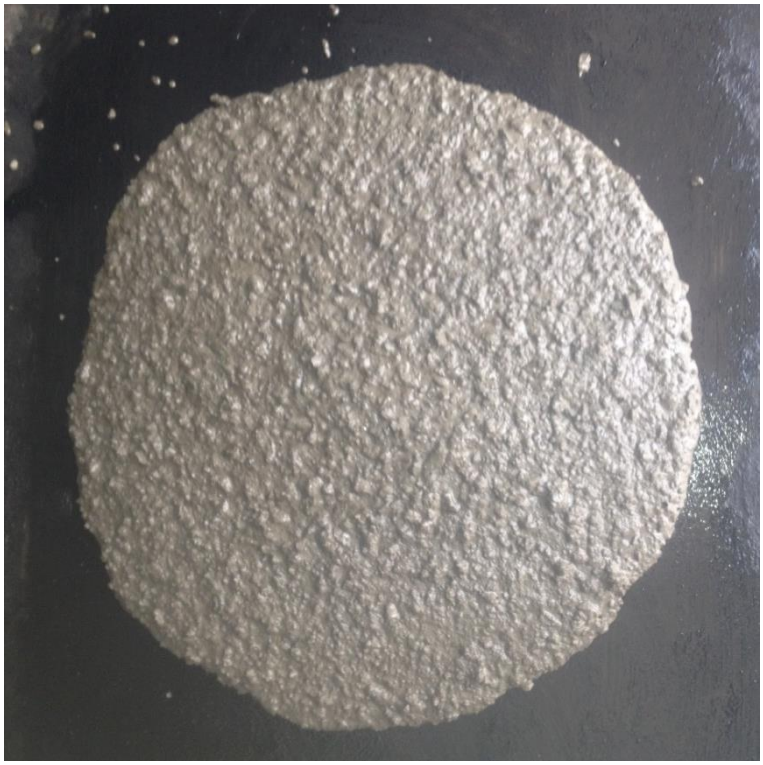

Fig.3.11 Slump flow test for SCC

Due to its relatively simple method of application and equipment it is the most commonly used method. The equipment to be used for this test should coincide with EN 12350-2. The base at the bed should have a minimum size of 900 x 900 mm. The

minimum thickness should be 2 mm. The material used should be sturdy and waterproof. The Abram's cone to be used should have dimensions complying with ISO 4190.

3.5.2 L-Box Test

This test was originally designed to determine the underwater casting properties of concrete. But this test came out to be appropriate for concretes which have a high flow rates such as the case of SCC. This test is used to access properties such as flow rate and the ability to undergo through congested spaces. Two chambers are kept perpendicular to each other in order to set up the arrangement. Portioning of these chambers is done by making use of 3 reinforcing bars which are of standard size. The vertical chamber is filled with SCC and there is passage of concrete through these bars. The height of concrete in both chambers (H1 and H2) is measured once the flowing concrete has stopped flowing.

Fig.3.12 L-box test for SCC

3.5.3 U-Box Test

Two upright chambers in the shape of U letter comprise of the equipment for this type of test. Partitioning of both these chambers is done by using 3 reinforcing bars at a gap of 50 mm. SCC filling takes place in the first chamber and the flow of concrete through the reinforcing bars is initiated by opening the gate between the two chambers. When the concrete passage comes to a standstill, the height of the concrete in both chambers (H1 and H2) is measured, and the difference between the heights is calculated. The entire procedure should take less than 5 minutes to finish. The difference in heights has a direct relationship with the efficiency of the outcome; the lower the height, the more positive the result. As a result, an H1-H2 value approaching 0 indicates that the concrete is excellent at passing and filling EFNARC (2005).

Fig.3.13 U-box test SCC

3.5.4 V-Funnel Test

This test determines the filling ability and viscosity of SCC. It also gives information regarding static segregation resistance by lengthening the time between concrete filling in the container and the test's actual start time. The apparatus is shaped like the letter V. The primary objective of the test is to complete a concrete passage through an orifice in a certain period of time. The V shaped chamber which holds the capacity of around 12 litres is filled with concrete. After the chamber is filled entirely with concrete, the lid provided at the bottom of the equipment is opened and the time taken for the concrete to pass through the orifice is noted.

3.6 HARDENED STATE PROPERTIES

3.6.1 Strength Properties

3.6.1.1 Compressive Strength Test

This is the fundamental test in order to evaluate the strength of concrete in the hardened state. Cubes are used as samples and their testing is conducted at various time spans.

Fig.3.14 Compressive strength

Procedure

This test is performed with a Universal Testing Machine (UTM) or a Compressive Strength Testing Machine. The machine should apply load at a rate of 5.148 KN/sec, which is the test's specified load. Cured cube specimens are placed between the plates of the testing machine, then a load is applied at a predefined rate. The specimen is placed in the middle of the plates to ensure uniform load application. The particular load at which the specimen cracks or fractures is noted down. The compressive strength is calculated by dividing the load by the sample area. Digital equipment, on the other hand, may now be used to immediately determine the strength of a sample.

Testing age

Testing is generally done at particular ages of curing in accordance with the Indian Standards. This test is generally preferred at 7 days and 28 days ages respectively. Testing age of 56 days can also be considered for performing the test. For strength at later ages, 90 days and 365 days is a good alternative as well.

Number of Samples

At least 3 samples should be testing for evaluating the compressive strength per mix. The final strength would be the average of the strengths obtained in case of all these 3 samples at that specified age. The dimensions of the specimens to be used should be taken nearest to 0.2 mm.

3.6.1.2 Splitting Tensile Strength Test

Cylinder shaped specimens of diameter 150 mm and 300 mm in length are used for this test. Strength could be found at various ages. Universal Compression Testing Machine is made use of for completing the test procedure. The specimens are cured in water for a period of about 24 hours before testing and the surface water and grit should be wiped off with a clean cloth. There should be proper calculation of the mass and dimensions of the test specimen before the experiment starts. The test sample is placed in between the two steel plates of the machine. The upper and bottom platens of the machine should be parallel to each other. Typically, cylindrical shaped specimens are made use of for the test, so plywood strips are made use of. Both faces of the specimen are covered with plywood strips having length greater than that of the specimen. This is done to ensure uniform application of load. Load application is done

at a fixed rate of 1.4 KN/min. The load application should be done without any kind of shock. The splitting tensile strength should be measured to the nearest of 0.05 N/mm^2.

Fig.3.15 Splitting tensile strength test

Procedure

- Initially, aligning of the ends of the specimen is done in same axial plane by making lines along the diameter at both the ends.
- Then one plywood strip is placed at the bottom platen/ bearing block, such that their centres coincide.
- After proper alignment, the cylindrical specimen is kept on the plywood strip. The specimen should be placed in such a manner that it is exactly in the middle of plywood strip.
- The other plywood strip is placed on the top of specimen. It should be placed along the length on specimen and should be in the centre.

- Once proper placing and aligning are complete, load application is done at the specified rate as per Indian standards.
- Load application is continued until the specimen breaks or cracks.
- After the specimen cracks or breaks, that load is substituted in given equation (3.1),

$$f_{st}^{'} = \frac{2P}{\pi\ ld} \qquad (3.1)$$

Where,

P = Load at which specimen breaks or cracks

l = Length of specimen

d = Diameter of specimen

3.6.2 Durability Characteristics

3.6.2.1 Water Absorption

It is a very important property to assess the durability of concrete. Test took place as per the regulations in ASTM C 642-13 (ASTM 2013). Initially the mass of the specimen is measured and further the specimen is oven dried at a temperature of 115^{o}C for not less than 24 hours. The test specimens are then air dried, preferably in desiccators at temperatures ranging from 20-25^{o}Cfor mass determination. The difference between the initial mass and mass found after oven drying should not be more than 0.5%. If this condition is satisfied then the sample could be considered as dry. However, if this value is exceeded then the sample is termed as a wet one. In this case, the specimen is kept in oven again for another 24 hours and the mass is measured. The difference between the mass of the specimen before placing into the oven and after oven drying should not exceed 0.5%. Once this value comes under 0.5%, the value should be noted as A.

The specimen is then immersed in water for at least a period of 48 hours at a temperature of about 21^{o}C. It is cleaned with a cloth in order to eliminate the excessive moisture from the surface. This process is termed as surface drying of specimen. Once the surface has been dried, the mass is measured. This surface dry mass is assigned as B. The specimen is then kept in boiling water for a time span of 5

hours at least. The specimen is then given a minimum time period of 14 hours to cool to a final temperature of 20-25^{o}C. The specimen is then cleaned with a towel. This soaked and boiled surface-dry mass is assigned as C. The apparent mass is measured after suspending the specimen in the bucket at a fixed water level by means of a wire. The specimen is taken out from water and its surface is cleaned with a damp cloth. Term this mass as D after it has been cleaned. Water absorption is calculated after recording all the masses using equations (3.2) to (3.7).

Absorption after immersion (%) = [(B – A)/ A] X 100 (3.2)

Absorption after immersion and boiling (%) = [(C – A)/ A] X 100 (3.3)

Bulk density, dry = [A / (C – D)] . p = g1 (3.4)

Bulk density after immersion = [B / (C – D)] . p (3.5)

Bulk density after immersion and boiling = [C / (C – D)] . p (3.6)

Apparent density = [A / (A – D)] . p = g2 (3.7)

Where;

A = Mass of oven dried specimen

B = Mass of surface dry specimen after immersion

C = Mass of surface dry specimen after immersion and boiling

D = Apparent mass of specimen in water after immersion and boiling

g 1 = Bulk density, dry

g 2 = Apparent density

p = Density of water

Fig.3.16 Water absorption test

3.6.2.2 Sorptivity

This test is used to find the rate of absorption of water by SCC. The test procedure is followed as per the regulations of ASTM C 1585-13 (ASTM 2013). The specimen used in this case is disc shaped and has dimensions of about 100 mm diameter and length near 50 mm. At least 2 specimens are required to conduct the test.

Conditioning of the sample

The specimens are condition as per the vacuum-saturation procedure but the side surfaces of the specimen should not be coated. The mass of each specimen is measured after saturation and is rounded to 0.01 g. The test specimens are then placed in an environmental chamber at a temperature of around 50^{o}C for a span of 3 days. A desiccator can be used alternatively for this process as well. After 3 days, the specimens are placed in a sealable container which has a provision of free flow. The specimens are stored at 23^{o}C for at least 15 days before the absorption procedure is initiated.

Fig.3.17 Sorptivity test

Procedure

- The mass of the specimen is recorded nearest to 0.01g after removing the specimen.
- At the surface which is exposed to water, at least 4 diameters are to be measured nearest to 0.1 mm and their average is taken.
- The side surfaces of the specimen are to be sealed with a proper sealing material. In order to avoid contact with water the ends are also sealed with plastic coating.

Water Absorption Procedure

- The mass of the specimen is measured to nearest 0.01g and is recorded as the initial mass.
- A support device is placed under the pan and the pan is filled with tap water in order to ensure that water level is 1 to 3mm above the bottom of the support device.
- The test surface of the specimen is immediately placed above the support device and the timing device is started to record the time.
- The mass is recorded at regular intervals after initial contact with water. This is done at particular intervals. The first point of measurement is at around 60 seconds while the other at 2 minutes. Further measurements would be made at 2 minute increments of 10, 20, 30, 40, 50 and 60 minutes respectively. Continue the measurements for every hour till the overall time period of 6 hours is reached. After 6 hours, take the measure once a day for 3 days. During days 4 and 7 there should be measurements taken with at least a gap of 24 hours. The final measurement is taken 24 hours after the day 7. There will be 7 data points for contact time.
- The test specimens are removed from the pan for mass determination and the excess water is bloated. After 15 seconds of removal from the pan the mass is recorded nearest to 0.01g.

The absorption is calculated using the equation (3.8)

$$I = mt/ a*d \quad (3.8)$$

where: I = the absorption,

mt = the change in specimen mass in grams, at the time t,

a = the exposed area of the specimen, in mm^2,

and d = the density of the water in g/mm^3.

3.6.2.3 Sulphate Resistance Test

Test takes place as per the regulations of ASTM C 1012 – 10 (ASTM 2010). A magnesium sulphate solution was used for this test. This solution had strength of 5%. SCC specimens are submerged in this solution and these are tested in future at their respective ages. Universal Compression Testing Machine is used to find the compressive strength of specimens and these are checked relative to the compressive strengths of the specimens cured in ordinary water.

The difference between both of them is calculated using equation (3.9):

Loss in compressive strength (%) = [(S1 – S2)/ S1] X 100 (3.9)

Where,

S1 = Compressive strength of specimen cured in water

S2 = Compressive strength of specimen immersed in magnesium sulphate solution at same age.

Fig.3.18 Sulphate resistance test

3.6.2.4 Rapid Chloride Permeability Test

The test took place as per the regulations of ASTM C 1202-10 (ASTM 2010). Cylindrical specimens were taken for this test. The dimensions of the specimen are 50 mm length and 100 mm diameter respectively. The testing apparatus is used and the specimens are fitted into it. Passage of electric charge is done through the specimens. This is done for a time span of 6 hours. A difference of 60 V Direct Current is kept between the terminals of the specimen. One end uses sodium chloride solution while the other is made prone to sodium hydroxide solution. The charge passing through the solution is inversely proportional to the resistance offered to the chloride ion penetration. Table 3.5 demonstrates the values of charge passed with RCPT values.

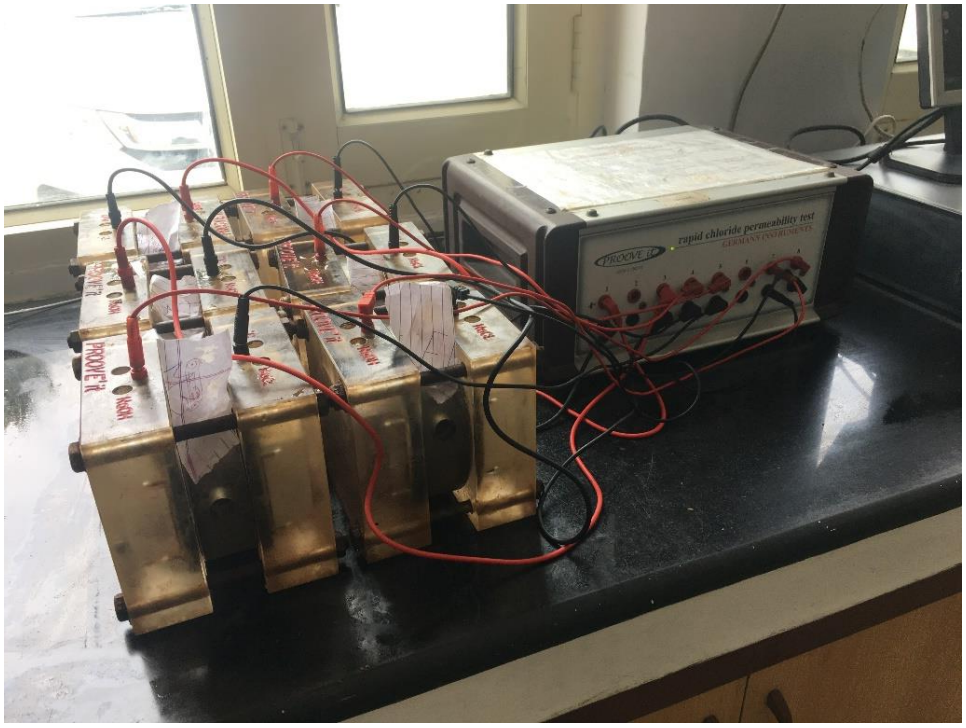

Fig.3.19 Rapid chloride penetration test

Table 3.5 Chloride ion penetration based on charge passed (ASTM C 1202-10)

Charge passed (Coulombs)	Chloride ion penetration
>4000	High
2000 - 4000	Moderate
1000 - 2000	Low
100 – 1000	Very low
<100	Negligible

3.7 MICROSCOPY (SCANNING ELECTRON MICROSCOPY-SEM)

SEM has a significant role in giving information related to the morphology of the particles. It also tells us about the texture, agglomeration and porosity of sample. Conducive substrate such as aluminium stub and gold plated in vacuum are used for mounting the SEM analysis sample. The samples which are coated are placed on the sample stage of the microscope. The samples can show movement in all the three dimensions. They can be rotated as well as tilted. The interactivity between the atoms and electrons of the specimens release the data signals. These data signals are caused due to elastic and inelastic interactivity of atoms of the specimens and the beam electrons. Back scattered electrons (BSE) are produced by elastic collisions while secondary electrons are produced by inelastic collisions. Information about the composition of the specimen as well as the topographical properties can be found out using back scattered electrons (BSE). Samples used in this study are broken concrete fragments.

Fig.3.20 Coating of sample before SEM

3.8 X-RAY DIFFRACTION

XRD is a very important test in order to evaluate the crystalline phases and compositions. There is an analysis of the diffraction peaks which are under the observation. The analysis is in terms of the intensity and position. A comparison is made with the crystalline phases which are already known. These phases help in the identification of the target material. It was done using a PanalyticalX'Pert pro, with Cu Kα radiations. The X'Pert high score plus software was used to identify the phases.

Fig.3.21 X'Pert PRO

3.9 PROPERTIES INVESTIGATED

The following properties were investigated in the research program. The tests were conducted for all the three approaches used in the study i.e. SCC mixes incorporating RHA, SCC mixes incorporating WFS, SCC mixes incorporating RHA and WFS respectively. Fresh properties, strength and durability properties for all the approached were studied and results were analysed. Table 3.6 shows the properties to be investigated, age and size of specimens.

Table 3.6 Properties to be investigated, age and size of specimens

Fresh Properties				
Property	Reference Code		Testing Age	Number of Samples
Slump Flow	EFNARC (2005)	ASTM C1610/ C1610M ASTM C1611/ C1611M ASTM C1621/ C1621M ASTM C1712 –C17	Before Casting	Each Batch
T_{500} slump flow			Before Casting	
V-funnel			Before Casting	
L-box			Before Casting	
U-box	EFNARC (2002)		Before Casting	

Strength Properties				
Property	Reference Code	Testing Age (days)	Number of Samples	Sample Details
Compressive Strength	BIS 516:1959 equivalent to ASTM C39/C39M	7, 28, 90 and 365 days of water curing	336	150 mm Cubes
Splitting Tensile Strength	BIS : 5816:1999 equivalent to ASTM C496/ C496M		336	150 mm diameter and 300 mm length cylinder
Microstructure (SEM, EDS)	-	28, 90 and 365 days of water curing	63	Broken pieces retrieved from SCC samples
XRD phase identification			63	Powdered sample retrieved from SCC samples

Durability Properties				
Property	Reference Code	Testing Age (days)	Number of Samples	Sample Details
Water absorption and Volume of permeable voids	ASTM C642-13	28, 90 and 365 days of water curing	189	100 mm diameter and 50 mm length cylinder
Sorptivity	ASTM C1585-13		189	
Rapid Chloride Permeability	ASTM C 1202		189	
Sulphate resistance compressive strength	ASTM C 1012	28 days water curing& 28,90 & 365 days sulphate immersion	189	150 mm Cubes

3.10 SUMMARY

The methodology used in the research study is described in this chapter. There is a brief explanation of the various experiments performed, the materials utilised, and the experimentation process followed. The basic tests were performed for coarse aggregates, fine aggregates, cement, RHA and WFS. These materials were utilized to develop SCC mix and further tests were performed which will be discussed in next chapter. Material characterisation of RHA and WFS was also carried out that explained silica rich angular particles of RHA.WFS particles were irregular and rough textured. Fresh properties of SCC mixes were investigated using EFNARC. In the next chapter, results of the various mix proportions of RHA in SCC, WFS in SCC and combined RHA and WFS in SCC are studied. Fresh, strength and durability properties at different curing age are investigated for all the mix proportions.

CHAPTER- 4

RESULTS AND DISCUSSION

The test findings for the fresh, strength and durability properties of hardened SCC mixes are presented in this chapter. It also covers X-Ray diffraction phase identification and microstructural analysis of scanning electron micrographs. First, the effects of using RHA as partial cement substitute in SCC are reported. Second, test findings using WFS as partial replacement of fine aggregates in SCC are discussed. At last, test results of using RHA as partial cement substitute and WFS as partial replacement for fine aggregate in SCC are discussed.

4.1 INCORPORATING RHA AS CEMENT REPLACEMENT IN SCC

4.1.1 Development of SCC (Objective 1)

SCC was designed using *EFNARC (2005)* guidelines to achieve the required fresh and hardened properties. The composition of ingredients is the key to achieve the properties of SCC. The careful selection of quality and quantity of materials plays a vital role in the fresh properties and performance of SCC. Table 4.1 demonstrates the composition of seven mixes of SCC by replacing cement with RHA (by weight) up to 30% at an increment of 5%. The cement content in the control mix i.e. RHA0 was 500 kg/cum initially. All the designed mixes satisfied the ACI 318 requirements of a maximum of 50 percent SCM of the total cementitious content *(ACI 318).* The cement content changed in succeeding mixes whereas, a fixed quantity of fly ash, w/b ratio, and superplasticizer content at all replacement levels were 40kg, 0.36, and 1.17% respectively. The admixture was used for water reduction and to maintain dispersion. The viscosity of paste was adjusted by proper selection of cement and water/binder ratio. Blended sand was used to have an optimization of the grading limits and to meet the workability properties. The experiment was conducted with sands of two types from different sources. Specific gravity, fineness modulus, and water absorption of the natural sand collected from the first source i.e. Pathankot, Punjab, India were 2.63, 3.10, and 0.63% respectively. Whereas, sand collected from the second source i.e. Anandpur sahib, Punjab, India had values of specific gravity, fineness modulus, and water absorption as 2.61, 2.17, and 0.40% respectively. These two types of fine aggregates were used in a ratio of 65% and 35% to achieve the grading requirements of SCC in the design mix. The combined specific gravity and

fineness modulus of sand mixed in the 65:35 ratios were 2.72 and 2.93 respectively with water absorption of 0.71%. Coarse aggregates with specific gravity 2.70 were used. Its water absorption was 0.40%. Coarse aggregates of 10mm size were collected from quarries in Pathankot, Punjab, India. Various tests were conducted to analyze the effect of RHA on the strength and durability properties of SCC mixes. The mix id for the SCC mixes was RHA0, RHA5, RHA10, RHA15, RHA20, RHA25, and RHA30 where RHA stands for SCC mix while 0 to 30 stands for the percentage of cement replaced.

Table 4.1 Mixture constituents of SCC

Mix	Cement (OPC) (kg/m³)	Fly ash (kg/m³)	RHA (kg/m³)	Water[a] (kg/m³)	10mm Aggregate SSD (kg/m³)	Fine Aggregate[b] (FA_{35}+FA_{65}) (kg/m³)	Admixture (kg/m³)	Density (kg/m³)
RHA 0	500	40	0	196	672	1015	6.32	2429
RHA 5	475	40	25	196	669	1011	6.32	2423
RHA 10	450	40	50	196	667	1008	6.32	2417
RHA 15	425	40	75	196	665	1004	6.32	2411
RHA 20	400	40	100	196	662	1001	6.32	2405
RHA 25	375	40	125	196	660	997	6.32	2399
RHA 30	350	40	150	196	658	994	6.32	2393

Note: The coarse and fine aggregates used in concrete mixes are SSD condition.

a: The water content described in the table is free water content used in the mix.

b: The fine aggregate used in the mix is composed of 35% of fine sand and 65% of coarse sand.

4.1.2 Fresh Properties (Objective 1)

4.1.2.1. Slump Flow

Fresh properties of the mixes are presented in Table 4.2. Fresh properties of SCC are essential attributes that differentiate SCC from conventional concrete. It is a prerequisite to observe the calculations of moisture content, water absorption, grading, and total fine content to produce good quality SCC. The w/b ratio and superplasticizer content were constant in the experimental program which influences the fresh properties of SCC.

The workability of SCC decreases with the replacement of cement with RHA. Paste volume plays an important role in SCC, apart from filling the voids between aggregates it aids the movement of aggregates by lubricating them properly. The paste volume increased from 37.81% to 39.12% thereby reducing aggregate content in the SCC mixes. The reduced coarse and fine aggregate content decreases their internal friction and enhances the passing ability by reducing the interlocking action of aggregate particles. It also provides momentum to the mix so that it can pass through restricted openings with increased fluidity *(EFNARC, 2005; Ling and Kwan, 2016).*The percentage paste volume in the mix increased up to 3.37% due to the higher Blaine's fineness and specific surface area of RHA compared to cement. Consequently, it increased the water demand by lowering the free content of water and increased the quantity of water adsorbed in the SCC mixes. However, the decrease in the value of workability was marginal.

Table 4.2 Fresh Properties of RHA-SCC mixes

Mix Id	Slump Flow		V-Funnel Time (Sec)			L-Box		U-Box
	Diameter (mm)	T_{500} mm (Sec)	T_{10S} (Sec)	T_{5min} (Sec)	h_2/h_1	T_{200mm} (Sec)	T_{400mm} (Sec)	h_2-h_1 (mm)
RHA 0	750 (SF2)	2.3 (VS2)	5.6 (VF1)	6.5 (VF1)	0.95 (PA2)	1.54	1.83	0.00
RHA 5	750 (SF2)	2.9 (VS2)	6.2 (VF1)	6.9 (VF1)	0.92 (PA2)	1.76	2.06	7.00
RHA 10	720 (SF2)	3.3 (VS2)	7.2 (VF1)	8.4 (VF2)	0.88 (PA2)	2.19	2.65	13.00
RHA 15	710 (SF2)	3.5 (VS2)	8.0 (VF1)	8.9 (VF2)	0.83 (PA2)	2.50	2.88	18.00
RHA 20	700 (SF2)	4.3 (VS2)	8.5 (VF2)	10.5 (VF2)	0.81 (PA2)	2.84	3.38	22.00
RHA 25	690 (SF2)	4.5 (VS2)	9.7 (VF2)	11.3 (VF2)	0.8 (PA2)	3.02	3.50	26.00
RHA 30	680 (SF2)	5.7 (VS2)	10.3 (VF2)	13.6 (VF2)	0.76 (PA2)	3.30	3.66	31.00

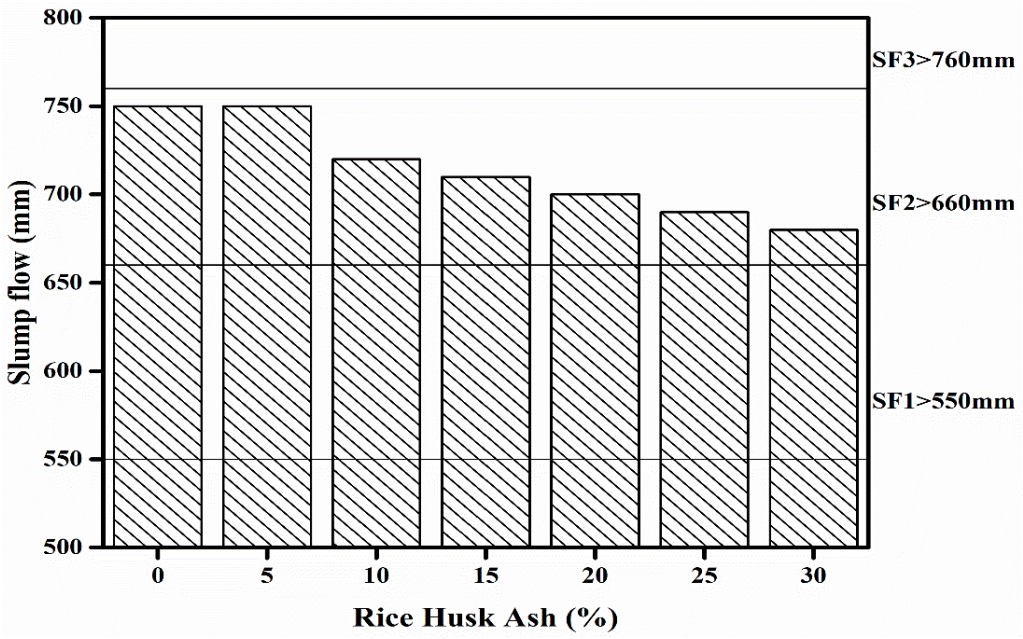

Fig.4.1. Slump flow results of SCC mixes with RHA

All the mixes obtained by the utilization of RHA in SCC mixes were self-compacting and were fulfilling the requirements to be categorized as SCC *(Molaei Raisi et al., 2018).* There were no visible signs of segregation or bleeding of the SCC mixes that ensured homogeneous, cohesive blends, and good surface finish. All the mixes ranging from 750 to 680 mm lied in SF2 class and confirmed to *EFNARC (2005)* criteria as shown in Figure 4.1.

4.1.2.2 L-Box Test

The term "passing ability" refers to the fresh concrete capacity to flow through constricted places and small openings, such as dense reinforced areas, without causing blockage, segregation, or loss of homogeneity. The maximum aggregate size, the flowability/filling ability, the shape and density of the reinforcement, and the passage ability must all be properly considered. L-box ratio or blocking ratio (H2/H1) portrays the passing ability of SCC without segregation through dense locations. The results of the L-box ratio mentioned in Table 4.2 range from 0.95 to 0.76. Figure 4.2 represents the variation of L-box ratio with an increase in the content of RHA.

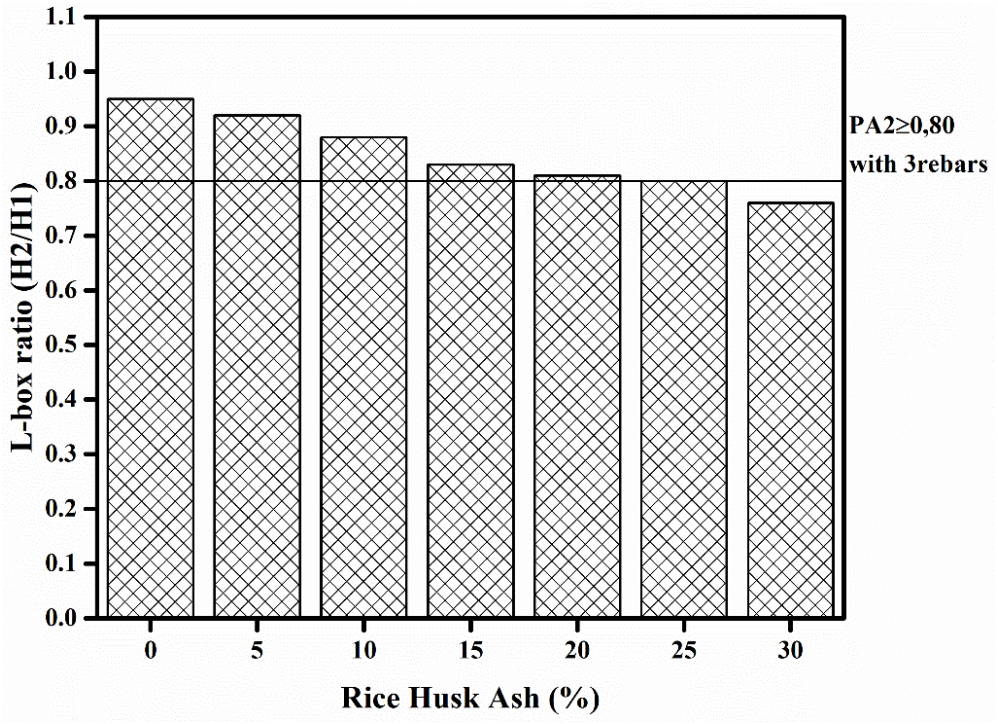

Fig.4.2. L-box results of SCC mixes with RHA

All the SCC mixes exhibited passing ability and characterization according to EFNARC. Hence, RHA incorporated as a substitution of cement can be effectively utilized to prepare SCC for all civil engineering structures. In RHA0, and RHA5, the values of blocking ratio were greater than 0.9 that indicated mixes prepared with RHA up to 5% replacement have higher fluidity. Further, T_{200} (sec) and T_{400} (sec) flow time along the horizontal section of L-box were observed. These values represent that increase in RHA content increase the value of T_{200} and T_{400} flow time thereby decreasing the workability. Figures 4.3 and 4.4, which illustrate the T_{200} and T_{400} values, respectively, provides some insight into the concrete mixtures' ability of flow. L-box values for T200 and T400 of the RHA0 mix takes around 1.54 and 1.83 seconds to complete. It was observed increase in rice husk ash content increased the T_{200} and T_{400} values to 3.30 and 3.66 seconds for RHA30 mixes.

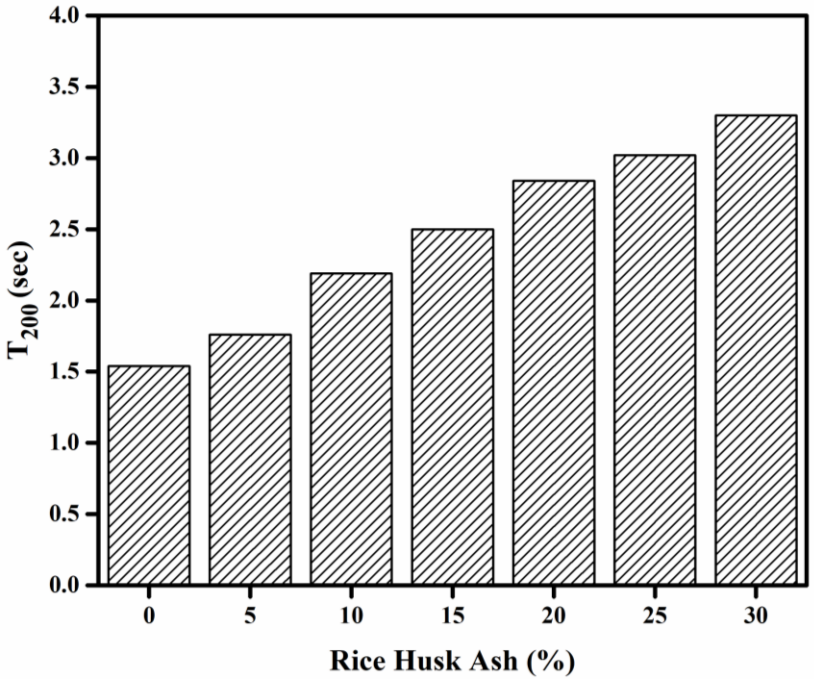

Fig.4.3. T_{200} results of SCC mixes with RHA

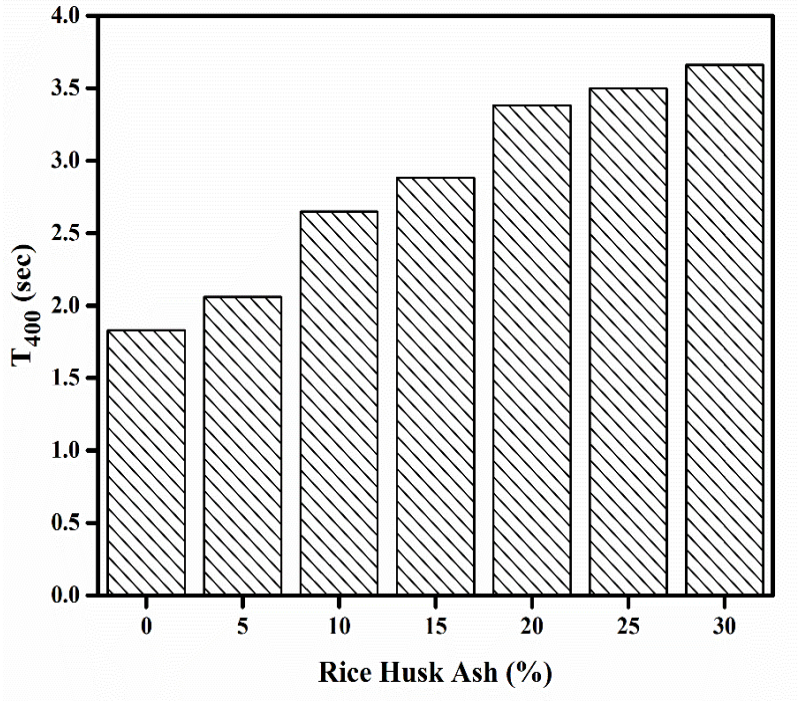

Fig.4.4. T_{400} results of SCC mixes with RHA

4.1.2.3 V-Funnel Test

Viscosity can be measured using the T_{500} time during the slump-flow test or the V-funnel flow. The time measured value represents the rate of flow instead of assessing the viscosity of SCC. Low viscosity concrete will flow quickly in the beginning and eventually halt. High viscosity concrete may continue to advance gradually over time. The rate of flow of various SCC mixes is illustrated in Figure 4.5, 4.6 and 4.7. As illustrated in Figure 4.5, the values of T_{500} flow time varying from 2.30 to 5.70 sec lies in the category of VS2 class as per EFNARC. The minimum value of T_{500} flow time at RHA0 depicts the highest workability of all the mixes. The maximum slump flow time at RHA30 demonstrates the reduction in workability with higher RHA concentration. V-funnel time illustrated in Figure 4.6 and 4.7 shows the same trend as that of T_{500} slump flow time i.e. increased content of RHA increases the V-funnel flow time. The T_{10} sec values varied from 5.60 sec to 10.30 sec and were classified in VF1 and VF2 class. RHA0, RHA5, RHA10, and RHA15 lie in VF1 class while RHA20, RHA25, and RHA30 lie in VF2 class. The VF1 class is suitable for dense reinforcement which can level itself while for VF2 class if flow time increases, adverse effects such as stoppages, blockages or rough finished surface can be observed. V-funnel flow time T_{5min} sec varies from 6.50 to 13.60 sec. The increased values of T_{5min} sec represent the abruption in the smooth flow of SCC.

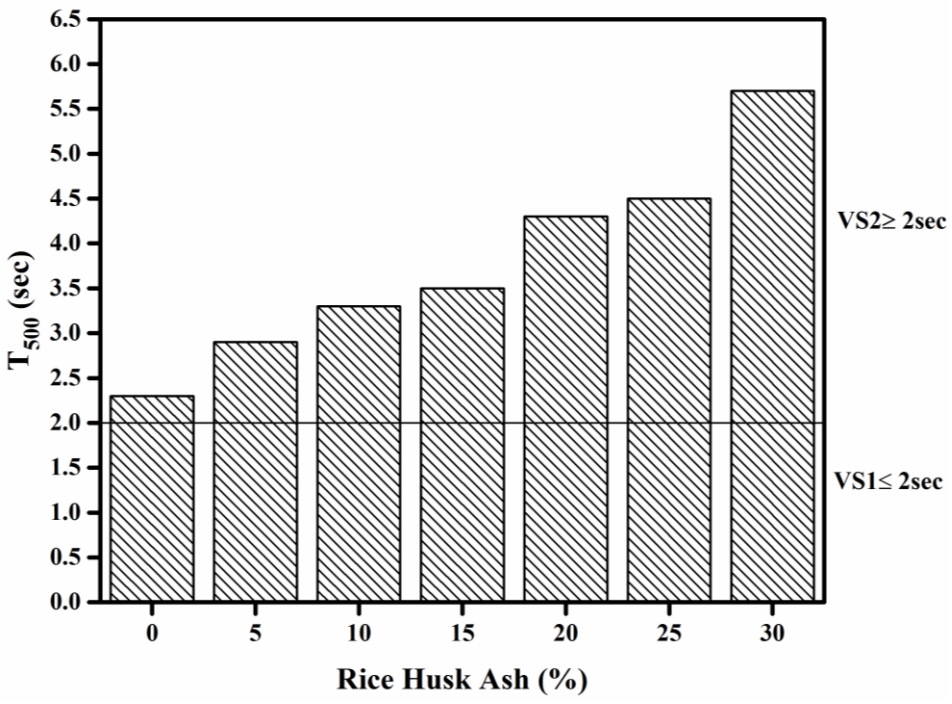

Fig.4.5. T_{500} results of SCC mixes with RHA

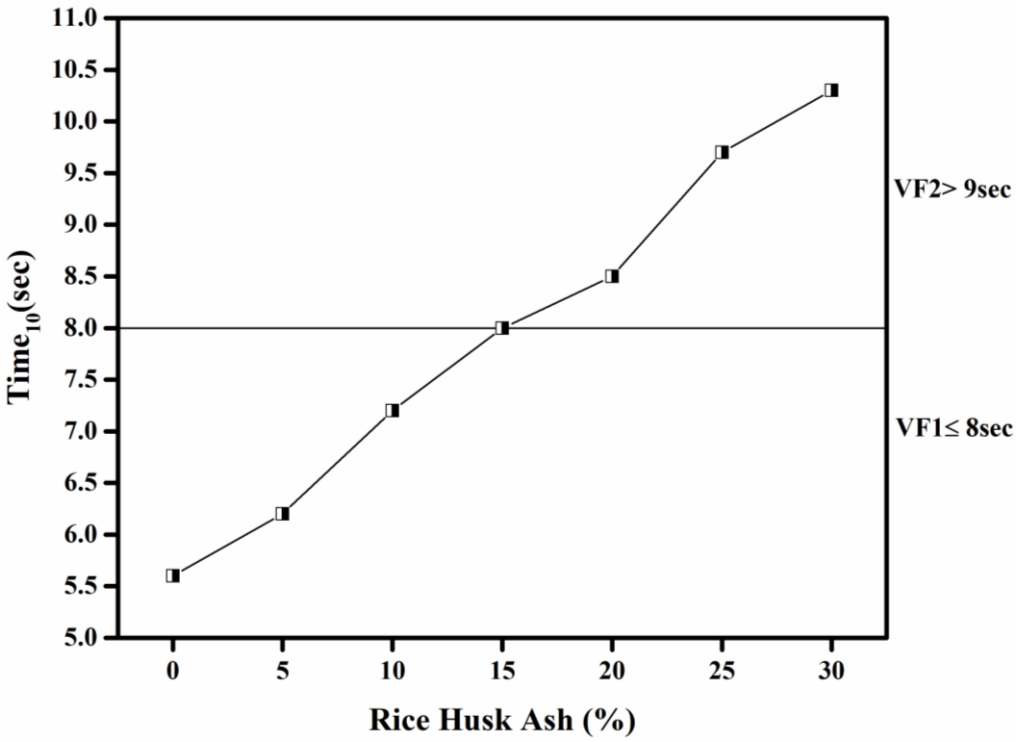

Fig.4.6.T_{10} (sec) result of SCC mixes with RHA

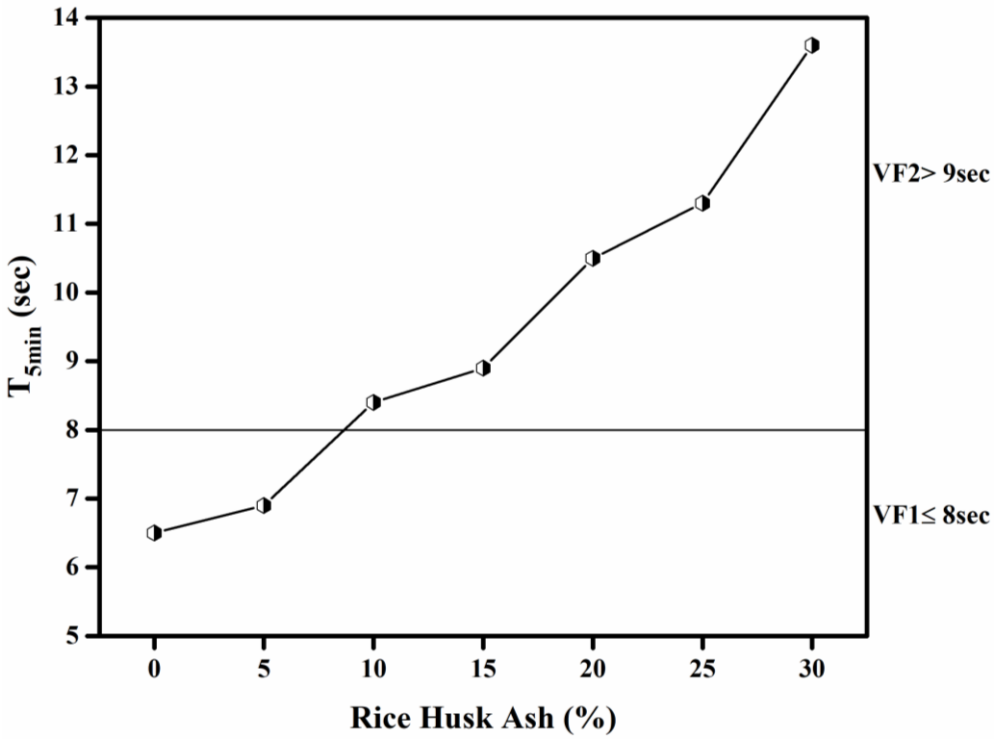

Fig.4.7.T_{5min} results of SCC mixes with RHA

4.1.2.4 Passing Ability of Concrete

U-box describes the passing and filling ability of SCC mixes. RHA0 showed H2-H1=0 i.e. concrete flows freely as water. All SCC mixes in U-Box test results were within the limits of EFNARC. Values of U-box vary between 0 and 31 and are presented in Figure 4.8. There is a negative correlation between workability and utilization of RHA on fresh properties of SCC. There is a gradual fall in workability with increased RHA content.

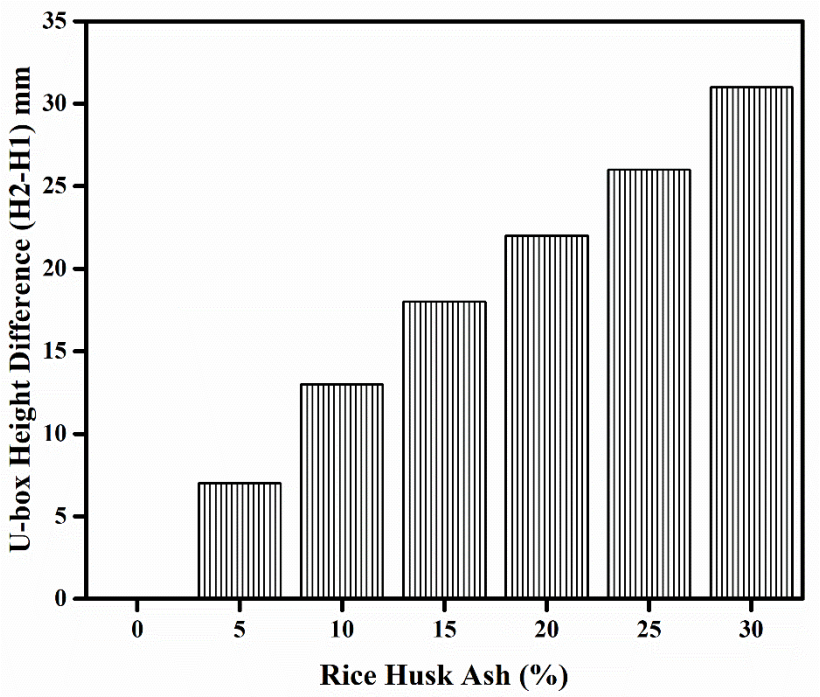

Fig.4.8. U-Box results of SCC mixes with RHA

4.1.3 Strength Properties of SCC (Objective 2)

4.1.3.1 Compressive Strength

Figure 4.9 shows the variation of compressive strength with RHA at 7, 28, 90, and 365 days. At 28 days, the control mix attained a compressive strength of 59.16 MPa. However, with the inclusion of 5%, 10%, 15%, 20%, 25% and 30% RHA the percentage change in compressive strength was 3.06%, 7.20%, 1.64%, -5.17%, -6.69% and -12.31% respectively. It was observed that SCC with 10% RHA achieved maximum compressive strength. Thereafter, strength values started decreasing but

remained higher than the control mix up to RHA15. The reason for increased strength was due to RHA properties. RHA, a pozzolanic material with higher silica content, finer structure and a more focused surface area, increases the strength of concrete when added to the SCC mix. In this process, cement during its hydration reaction produces Calcium silicate hydrates (CSH) and calcium hydroxide (CH) also known as Portlandite. When RHA, being pozzolanic, is added it consumes Portlandite produced during hydration reaction of cement that forms additional C-S-H gel thereby increasing the packing and strength of the SCC mix *(Molaei Raisi et al., 2018).*

Another reason for increased strength is the volume of paste that comprises cement, fly ash, RHA, and water. The volume of paste in the mix increases with the increase of RHA resulting in a reduction in aggregate quantities. It improves the pore structure by a reduction in the volume of pores contributing to a dense matrix. However, a marginal reduction of 5 to 6% in compressive strength was noted at RHA20 and RHA25. Further, the strength reduced up to 12% in RHA30. It was concluded from these observations that the maximum increase in strength up to 7% can be attained with the replacement of 10% cement with RHA. Initially, the compressive strength of the mixes increased due to high paste content but subsequently reduced with an increased level of RHA.

This decrease in strength was due to the reduced w/b ratio. The free water in the mix was reduced as the content of RHA increased in the mix at constant w/b ratio resulting in a water deficit mixture and inadequate hydration. In the present study, Blaine's fineness of cement and RHA was 305 kg/m^2 and 698 kg/m^2 respectively (more than twice as that of cement) because of which RHA will be more reactive and provides greater surface area for reaction. Hence, this increased surface area absorbs more water thereby reducing workability and hydration reaction. Another aspect of compressive strength reduction was silica-rich RHA. It replaced cement particles and became the source of excess unreacted silica in SCC that did not contribute to the improvement of compressive strength *(Molaei Raisi et al., 2018; Rahman et al., 2014).*

Also, all the mixes had enhanced compressive strength at 90 and 365 days of curing. The compressive strength of all the mixes at 90 and 365 days was greater than RHA0 at 28 days. There was an increasing trend of compressive strength due to the pozzolanic nature of RHA and continuous hydration reaction with an increase in age

(Sua-iam et al., 2019). Slow pozzolanic reaction of RHA makes concrete achieve later compressive strength and such mixes have high later age strength as compared to early-age strength *(Park et al., 2016).* This may be due to the reason that RHA absorbs free water from the mix because of its porous nature (Park et al., 2016). This excessive absorbed free water is released for prolonged hydration reaction of pozzolanic material contributing to the greater strength of SCC. These results are in harmony with previous studies *(Molaei Raisi et al., 2018; Sua-iam et al., 2016)* on the contrary *(Rahman et al., 2014)* reported decreased compressive strength with RHA.

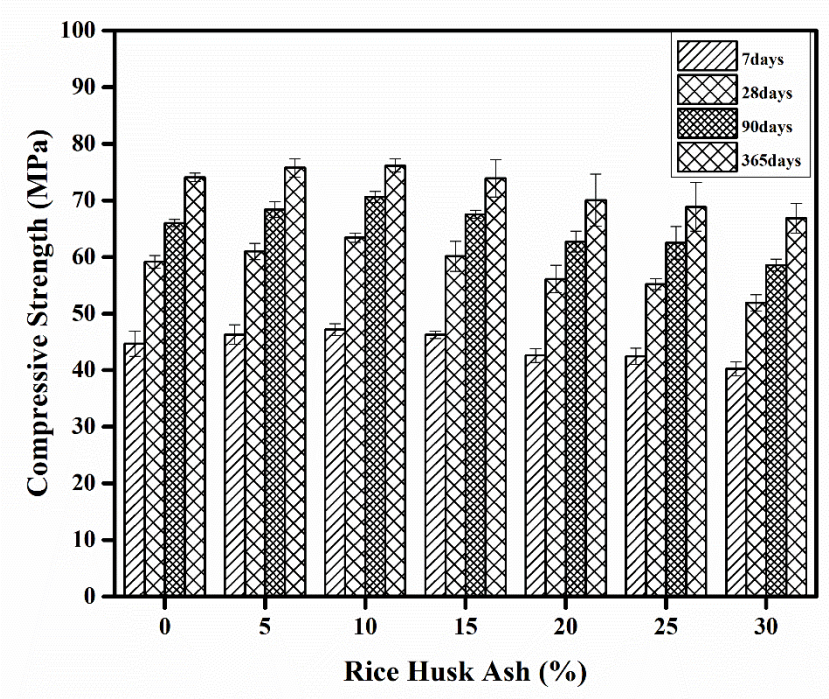

Fig.4.9.Compressive strength (MPa) results of SCC mixes with RHA at different testing ages

4.1.3.2 Splitting Tensile Strength

Splitting tensile strength was evaluated at 7, 28, 90, and 365 days and the results are shown in Figure 4.10. At 7 days the percentage change in the splitting tensile strength at 5%, 10%, 15%, 20%, 25% and 30% RHA were 7.71%, 8.46%, 1.00%, -3.23%, -8.71% and -13.43% respectively. At 28 days, the values were 5.11%, 10.02%, -1.23%, -2.25%, -4.09% and -7.57% at 5 to 30% of RHA respectively. As time advanced splitting tensile strength also progressed in the same manner that of compressive strength. Further, at 90 days these values were 3.49%, 13.57%, 3.68%, 2.13%, -2.91% and -5.43% at 5 to 30% of RHA respectively. Furthermore, at 365 days the values were 6.50%, 12.81%, 3.44%, 1.53%, -2.87% and -4.97% at 5 to 30%

of RHA respectively. The results illustrate that the presence of RHA in mixes improved the splitting tensile strength. Initially, the splitting tensile strength results increased with the inclusion of RHA up to 10%, but there was a decrease in value at 15% RHA. Whereas, results surpassed the control mix values up to 15% of partial replacement of cement with RHA. Further, there was a decreasing trend of tensile strength with the replacement of cement beyond RHA15. The factors responsible for reduced strength of splitting tensile strength were the same as that of compressive strength. Previous literature showed a similar trend of splitting tensile strength and compressive strength variation (*Molaei Raisi et al., 2018; Rahman et al., 2014).*

The strength of the splitting tensile is needed to withstand fatigue cracking while compressive strength is often used as a function to assess the quality of the concrete *(Chhorn et al., 2018).* Therefore, the relation between the tensile and compressive strengths of the SCC must be analyzed. SCC manufactured with RHA displayed a ratio of splitting tensile strength to compressive strength of 8.97, 8.42, 8.09, and 7.37 at 7, 28, 90, and 365 days, respectively. This ratio of splitting tensile strength to compressive strength decreased with age which inferred that the compressive strength increased at a faster rate in comparison to splitting tensile strength.

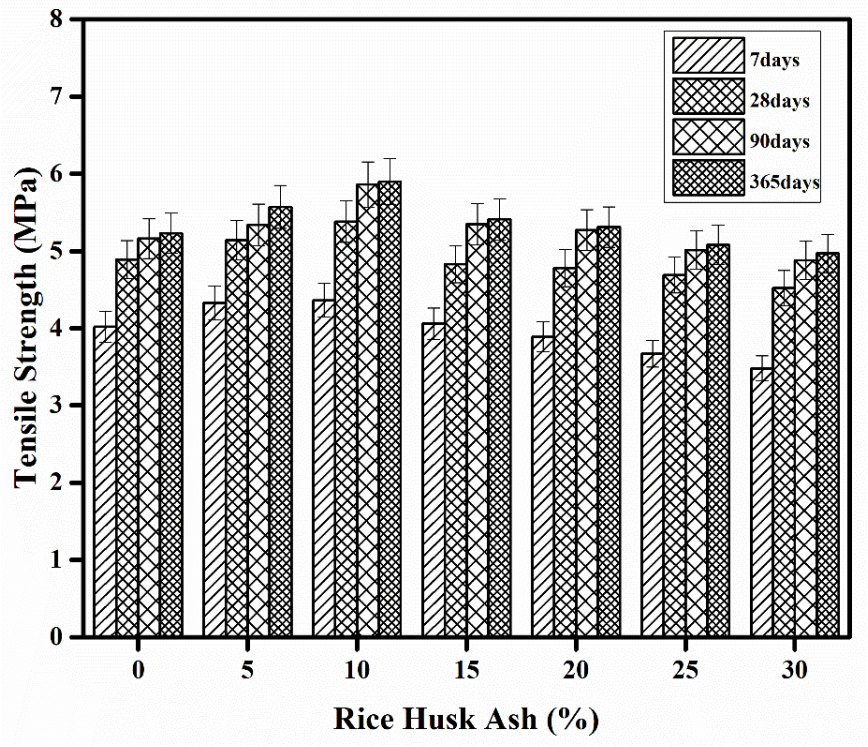

Fig.4.10. Splitting Tensile strength (MPa) results of SCC mixes with RHA at different testing ages

4.1.4 Durability Properties of SCC (Objective 3)

4.1.4.1 Rapid Chloride Permeability Test

Figure 4.11 shows the RCPT results of various mixes containing different proportions of RHA at 28, 90, and 365 days of curing. RCPT values showed a decreasing trend in comparison to control mix with an increase in the content of RHA. The decrease in the results of RCPT was attributed to the voids that get filled with finer solid RHA particles during the replacement of cement. It resulted in lower density due to the reduction of coarse and fine aggregates. The specific gravity of RHA was less therefore the theoretical density of the SCC mixes reduced with an increase in replacement level of RHA by weight. On the other hand, RHA increased the volume of fines and had higher values of Blaine's fineness relative to cement, because of which it filled the matrix's voids with solid material. Consequently, RCPT results showed a decreasing trend. Furthermore, RHA being rich in silica content forms additional CSH gel that increased the strength, improved pore structure thus contributing to dense microstructure and improved packing of SCC mixes. With age, the effect of RHA was more predominant. For instance, the charge passed ranged from ‘moderate’ for RHA0 to ‘low’ for RHA5-RHA10 and ‘very low’ for the rest of the mixes at 28 days. RHA0 lied in the category of ‘low’ and from RHA5 to RHA 30 the SCC mixes lied in ‘very low’ category at 90 days. All the values lied in the range of ‘very low’ category of chloride ion penetration rate as per ASTM 1202 at the age of 365 days.

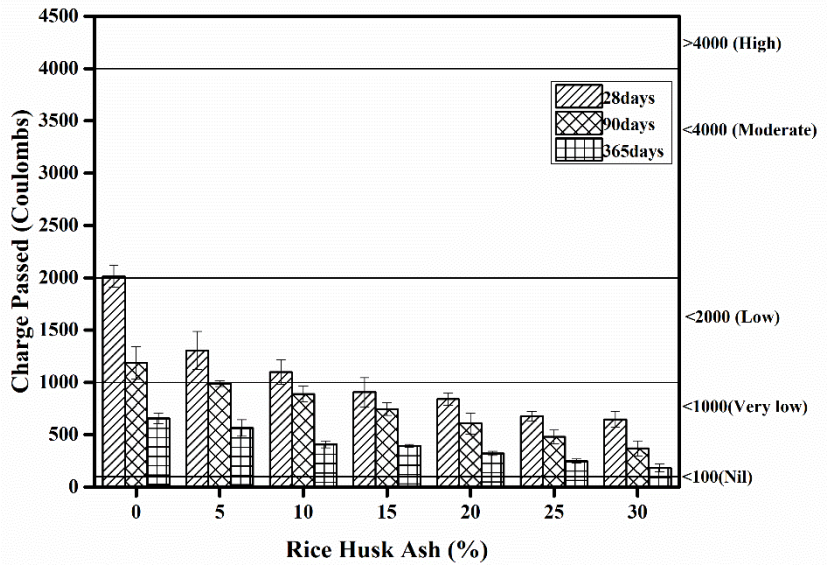

Fig.4.11. RCPT results of SCC mixes with RHA

The path for the diffusion of charge into the SCC mixes was blocked by a dense matrix formed with the inclusion of RHA. The pore enhancement occurred with the inclusion of RHA and the matrix became dense, showing significantly improved durability after 28 days curing. Improvement of pore structure is essential in reducing concrete diffusion. Total pore volume and size reduce with RHA resulting in decreased diffusivity as RHA increases the density of the particle packing. Hence, RHA enhances the pore structure contributing to a decreased charge passed and diffusion *(Zhu and Bartos 2003).* The value of charge passed decreased drastically at 90 and 365 days of curing depicting a very dense matrix. RHA30 shows a significant reduction of 67.86%, 68.77%, and 72.04% with reference to RHA0 at 28 days, 90 days, and 365 days respectively. RHA proved to be beneficial in reducing chloride ion penetration when compared with the control mix. Similar findings were observed by *(Zareei et al., 2017)*in the study incorporating RHA.

4.1.4.2 Water Absorption and Porosity

Table 4.3 illustrates the water absorption at 28, 90, and 365 days of curing. At 28 days of curing, the values of water absorption decreased continuously when cement was substituted with RHA at all replacement levels (5 to 30 %) and ranged from 5.71 to 5.52 %. The value of water absorption perpetually decreased with substitution level of up to 15% which depicted a positive effect of RHA on porosity thereafter the values began to increase with an increase in RHA level. RHA made the matrix denser, improved its compactness, and helped in filling the voids.

A similar trend was observed at curing ages of 90 and 365 days where durability increased with an increase in the percentage of RHA. The water absorption varied from 5.26% to 5.13% at 90 days and from 1.46% to 1.42% at 365 days. The pozzolanic activity of RHA comes into action with age. At a later age, additional CSH gel formation leads to matrix densification. A reduction in water absorption up to RHA15 was observed, after which the values were higher but remained lower than RHA0 representing an enhanced performance compared with the control mix. When the cement was replaced with lower specific gravity RHA by weight, the addition of finer particles resulted in matrix densification and the filling of the voids. The matrix thus became denser reducing porosity and water absorption of SCC. Hence, RHA

proves to be beneficial for manufacturing economical SCC satisfying both strength and durability criteria.

The volume of permeable pore (VoPP) space shows a similar variation with the inclusion of RHA. Table 4.3 shows the variation of VoPP at a different level of RHA in SCC. The mixes exhibited VoPP values at 28 days in the range from 13.11 to 12.60%. Further, at 90 days these values ranged from 12.12 to 11.65% and at 365 days from 3.53 to 3.20%. At 365 days, the matrix was densest. To achieve sustainability, the prime requirement is to produce durable SCC using a by-product. Lower w/b ratio and utilization of SCM in SCC helps to reduce porosity by reducing the pore space through the blockage. Therefore, it can be inferred that RHA has an approving effect on durability. These results are in line with previous studies on SCC utilizing RHA *(Ameri et al., 2019; Ali et al., 2011; Rukzon and Chindaprasit, 2014).*

Table 4.3 Water absorption and porosity of RHA-SCC mixes

Mix Id	28 Days			90 Days			365 Days		
	Absorption after immersion %	Absorption after immersion and boiling %	VoPP (%)	Absorption after immersion %	Absorption after immersion and boiling %	VoPP (%)	Absorption after immersion %	Absorption after immersion and boiling %	VoPP (%)
RHA0	4.57	5.71	13.11	4.34	5.26	12.12	1.19	1.46	3.53
RHA5	4.06	5.63	12.88	3.91	5.07	12.03	1.12	1.33	3.17
RHA10	3.65	5.19	12.08	3.53	4.84	11.65	1.10	1.21	3.11
RHA15	3.26	4.84	11.45	3.05	4.58	11.15	1.04	1.05	2.75
RHA20	3.48	5.05	12.08	3.27	4.83	11.45	1.09	1.22	3.19
RHA25	3.56	5.24	12.17	3.41	5.02	11.63	1.13	1.32	3.21
RHA30	3.78	5.52	12.60	3.53	5.13	11.65	1.17	1.42	3.20

4.1.4.3 Sorptivity

Sorptivity also follows a similar trend as that of porosity and water absorption. The values of capillary water absorption i.e. sorptivity were evaluated from 60sec,5min,10min,20min, 30min, 60min, every hour up to 6 hours, and then up to 7 days with the square root of time in sec. Capillary absorption is a function of connected pores and volume of permeable pore space i.e. porosity. The results are presented for the initial rate of absorption and secondary rate of absorption in Figures 4.12 and 4.13. It was found that the sorptivity (Initial and Secondary) had decreasing variation when the content of RHA was up to 15% beyond which the sorptivity started

increasing. The values decreased drastically and showed a very dense matrix having very low values of sorptivity with an increase in the testing age. The initial rate of absorption for RHA0 was 0.068, 0.0076, 0.0038 at 28, 90, and 365 days respectively while, the secondary rate of absorption was 0.0016, 0.0013, and 0.0005 at 28, 90 and 365 days respectively. It is visible from Figure 4.12 that sorptivity (initial) decreases with an increase in the content of RHA. The value of secondary absorption was almost constant for 28 days varying from 0.0016 to 0.0018 and 0.0013 to 0.0011 for 90 days and 0.0005 to 0.0002 at 365 days.

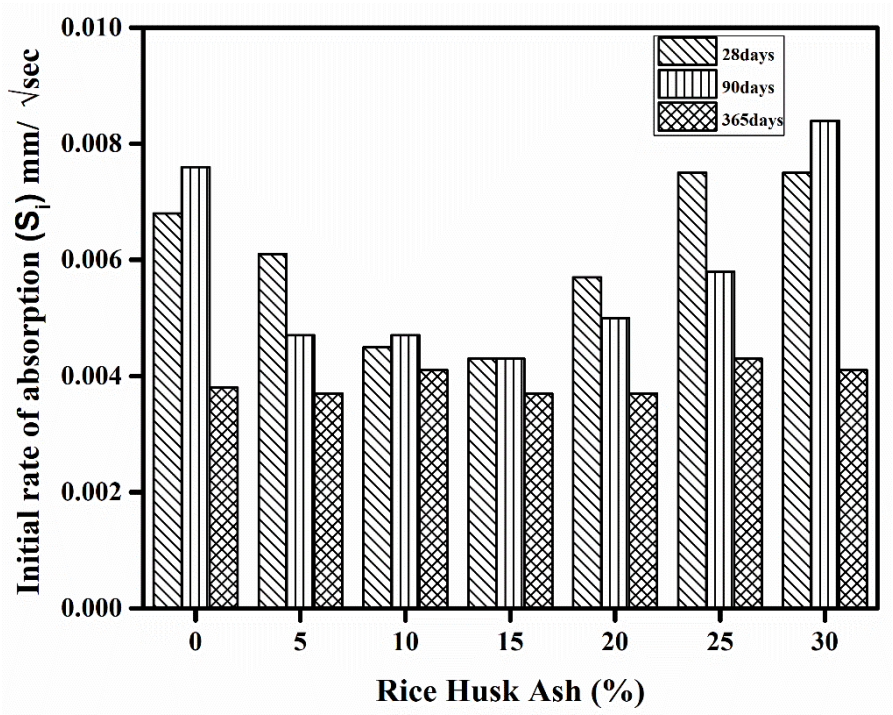

Fig.4.12. Initial rate of absorption results of SCC mixes with RHA

Figure 4.14 shows the variation of absorption per unit area with time versus substitution level of RHA. Cumulative water absorbed is reduced up to RHA15. This reduction can be seen at 90 and 365 days as well. RHA leads to pore refinement, denser matrix, and increased paste volume. These results depicted that maximum water was absorbed by the control mix i.e. RHA0. A greater reduction in absorption was observed as hydration of pozzolanic material increases with age at 365 days. The results showed that the maximum amount of water was absorbed by the control mix at all curing times. It can be inferred from the results that improved pore structure and durability was observed with RHA.

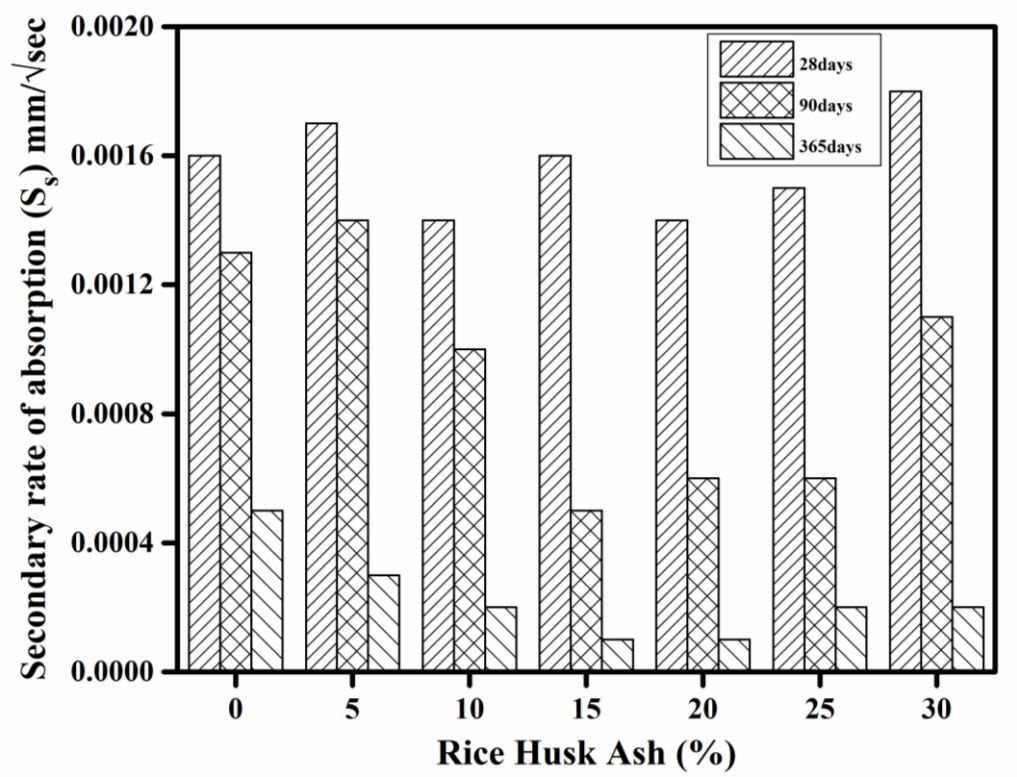

Fig.4.13. Secondary rate of absorption results of SCC mixes with RHA

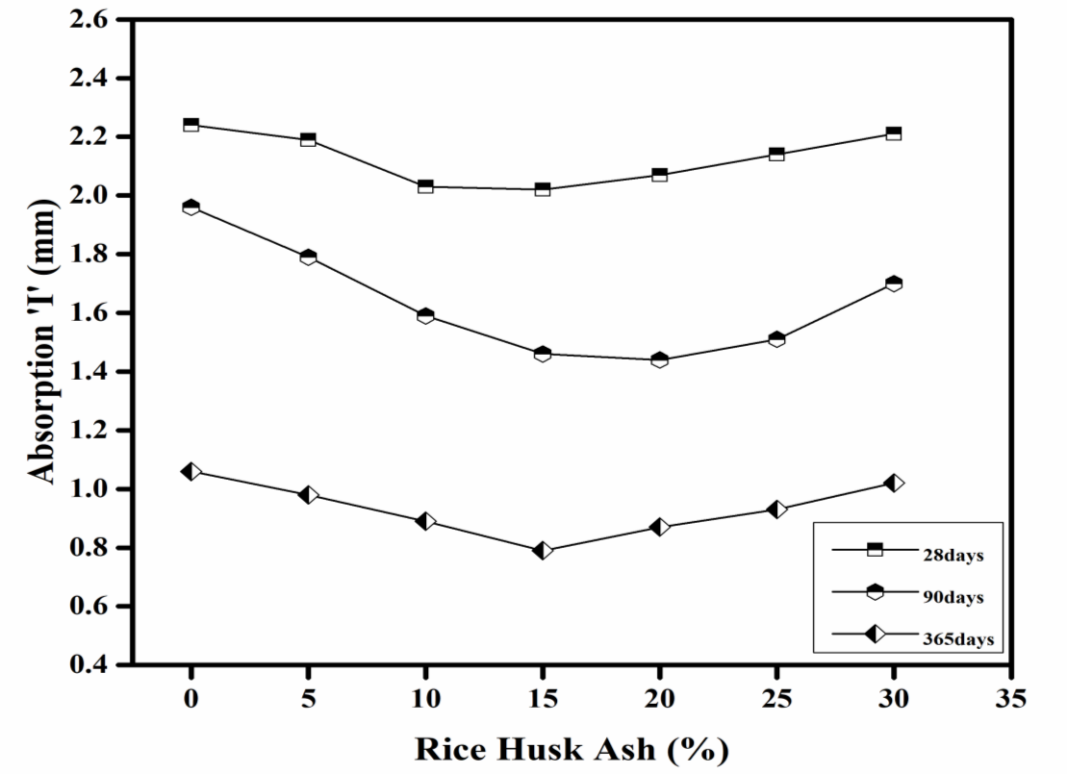

Fig.4.14. Absorption after 7 days of SCC mixes with RHA

4.1.4.4 Sulphate Attack

Concrete specimens subjected to magnesium sulphate attack were tested for mass variation, visual observation, and change in compressive strength parameters. The concrete samples were examined visually, and it was noticed that there was no deterioration, cracking, or spalling of concrete cubes by immersion in a sulphate solution. It was also observed that there was no variation in the mass of concrete samples on its exposure to magnesium sulphate solution. The mass measurements before and after exposure to sulphate solution were not considerably different.

The 28 days water cured concrete cubes of all the SCC mixes were used to assess sulphate resistance. These cubes were further immersed in magnesium sulphate solution for 28 days, 90, and 365 days. Thereafter, the 28 days sulphate exposed cubes were exhibiting 4 to 8 percent increased strength in comparison to the water cured samples for all the mixes. Sulphate solution ingression decreased due to reduced porosity and absorption, making it less vulnerable to damage from the sulphate. The 90 days sulphate exposed cubes of all the mixes subsequently showed an enhanced strength relative to the 90 days water cured samples. The percentage rise was lower than the 28 days increase and ranged between 0.3 to 3 percent. Whereas, sulphate attacked compressive strength values of 365 days were found to be lower than water cured compressive strength of 365 days. This may be attributed to the severity of age-related sulphate damage on cubes. Sulphate attack mainly leads to deterioration of hydration products formed in concrete. The existing hydration products are disintegrated and new harmful products are formed during sulphate reaction*(Xu et al., 1998).* Therefore, it is important to examine the impact of aggressive environments on concrete while designing with agro-waste (RHA) to verify the material's practicality. Damage from sulphate attacks depends on various factors, such as the Interfacial Transition Zone (ITZ)*(He et al., 2020),* porosity, diffusion, permeability, pozzolanic mineral admixtures *(Burgos et al,. 2019),* w/b ratio, exposure time *(Mostofinejad et al., 2020),* pH of the solution, sulphate concentration and concrete microstructure *(CCAA, 2011).* ITZ becomes weaker due to higher porosity, lesser cement paste at the interface for the ingress of sulphate ions, and causing damage to the inner matrix than the bulk paste *(He et al., 2020).*

Compressive strength values of sulphate immersed samples at different ages, i.e. 28, 90, and 365 days, were identified to be higher compared to water-cured samples of 28

days. These values are shown in Figure 15. RHA being pozzolanic helps to increase strength with age while the SCC samples tend to deteriorate with a solution of sulphate. It can be inferred from the results that age-related sulphate attack did not yield devastating impact. Sulphate attack mainly involves the reaction of calcium aluminate present in cement to form ettringite (calcium sulpho aluminate), which leads to cracking and expansion, with sulphate*(Barger et al., 2001; CCAA, 2011; Mostofinjenad et al., 2020).*Gypsum is a product after sulphate exposure on reaction with Portlandite *(Mostofinejad et al., 2020).*Sulphate attack also leads to the production of brucite and Magnesium silicate hydrates (MSH) which are non-binding in nature and reason for strength loss. The Magnesium sulphate reacts with Portlandite to form gypsum, brucite (magnesium hydroxide), and silica gel. MSH and brucite formation results in loss of strength as it decomposes the binding material *(Burgos et al., 2019; Xu et al., 1998; CCAA, 2011).*Specimens were less susceptible to sulphate attack because porosity and diffusion were low that reduced penetration of sulphate ions in SCC mixes. Also, RHA being pozzolanic utilizes portlandite and does not react to the ettringite and gypsum produced by sulphates.

It was found after analysis of samples immersed in sulphate for 28 days that initially, compressive strength values increased up to RHA10 relative to RHA0. These values further significantly reduced up to RHA30. A similar pattern was observed at 90 & 365 days. The test results of the 365 days sulphate attacked cubes were even lower than the results of 365 days water-cured samples. This may be because up to this age concrete is more prone to the sulphate attack. Loss of strength was observed at later ages primarily as a result of the loss of adhesion and disintegration of hydration products by ingress sulphates in the pore solution *(Xu et al., 1998).* During sulphate exposure formation of gypsum, ettringite, brucite, MSH leads to reduced strength and adhesion due to the reaction of magnesium and sulphate present in the solution with hydration products *(Mostofinejad et al., 2020).*

The pores of the mixes reduced due to the fineness of RHA as compared to cement by filling the voids and blocking the capillary action which can be verified from other durability properties. As a result, sulphate solution penetration into the samples reduced to some extent which helped in resisting the sulphate attack.

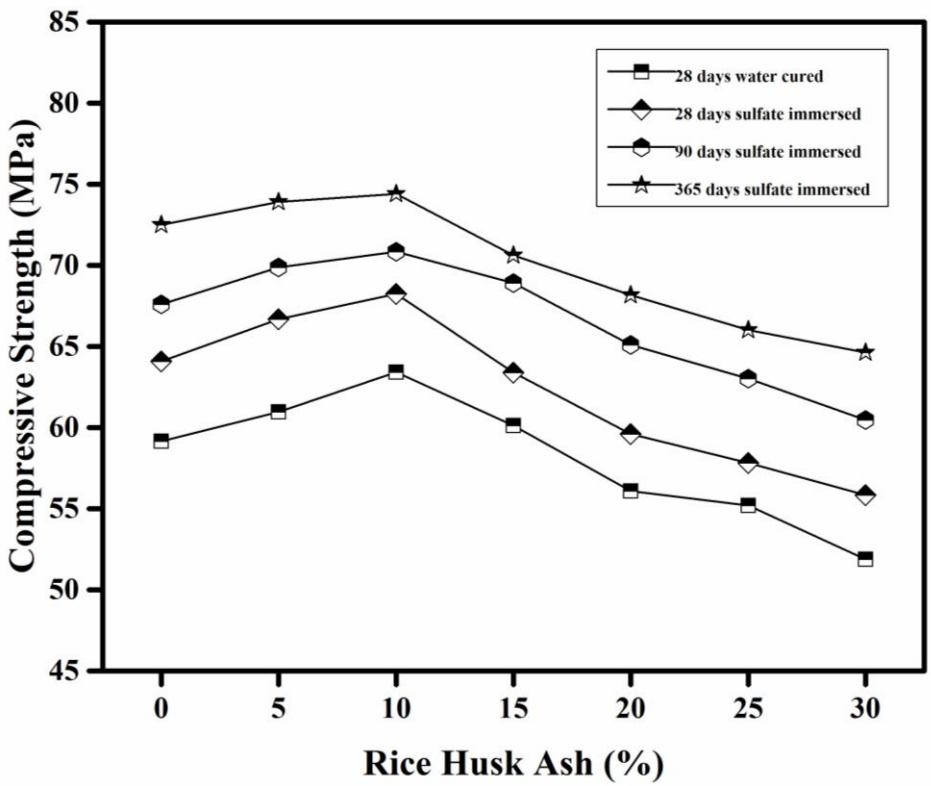

Fig.4.15. Compressive strength of SCC mixes with RHA after exposure to sulphate solution

4.1.5 Microstructural Analysis and Phase Identification (Objective 4)

4.1.5.1 Microstructure

Microstructure analysis of SCC mixes was performed to investigate the morphology through SEM together with Energy Dispersive X-Ray Spectroscopy (EDS) of the micrographs to provide insight into hydration products formed at 28 and 365 days of curing time. The SEM image of RHA0 in Figure 4.16 depicts a plated structure representing mainly calcium hydroxide that indicates Portlandite in SCC after 28 days of concrete cube curing. Also, the pores and voids were seen in this image along with calcium silicate hydrates (C-S-H) in the form of a fibrous gel. In Figure 4.18 (a) of RHA10, a dense and compact microstructure showing pore refinement and better response compared to RHA0 was noted. Figure 4.18 (a) also represents calcium aluminum silicate hydrates which explain the increased strength of the mix. The EDS analysis displaying the presence of calcium and silica at spectrum 1 and 2 are shown in Figure 4.18 (b) and 4.18 (c). RHA plays a key role in increasing the volume of the paste, improving particle packing, reducing porosity, and permeability of concrete contributing to the dense homogeneous matrix. This may be due to the filler effect or

its pozzolanic reaction, which consumes CH and forms additional CSH gel thus contributing to improved microstructure and pore refinement of the porous concrete. In the present context, the porosity decreases at RHA10, and diffusivity decreases depicting compact and pore refining of concrete microstructure. In Figure 4.19, micro-cracks and voids reflecting porosity and increased permeability of RHA30 were observed as compared to RHA10.

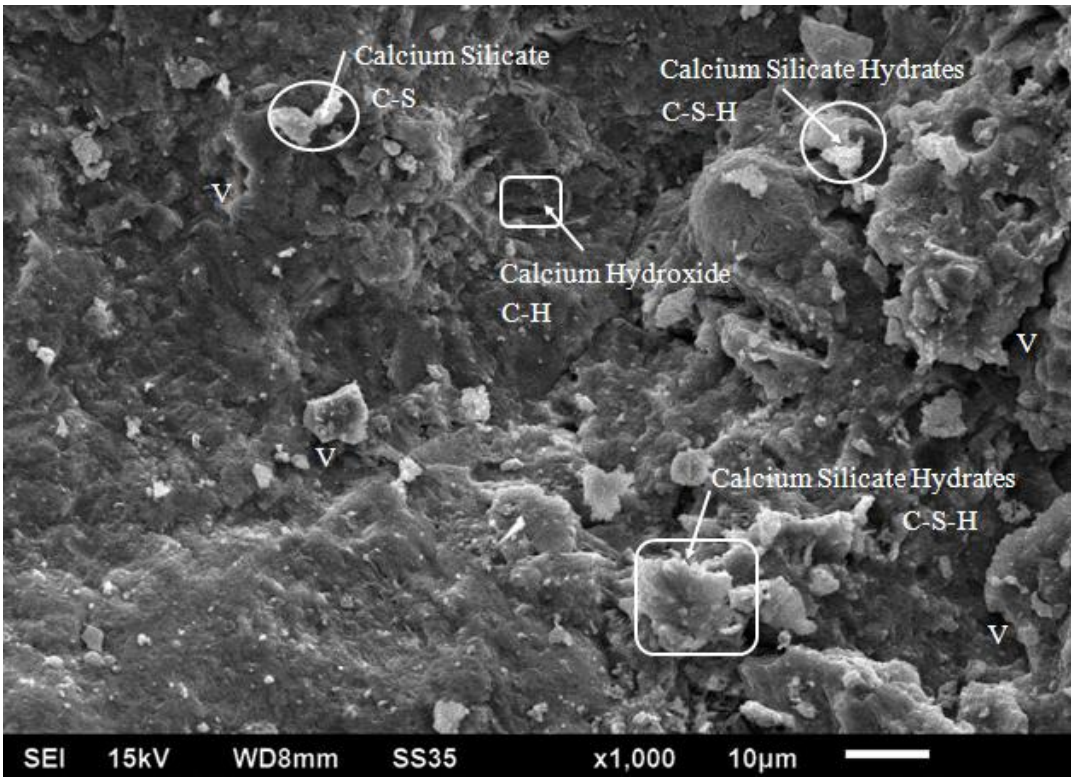

Fig.4.16.SEM image of RHA0 after 28 days

The SEM images of mixes after 365 days of curing are shown in Figures 4.17, 4.20, and 4.21. The SEM image of RHA0 shown in Figure 4.17 mainly consisted of C-S-H gel, calcium silicate, and calcium hydroxide depicting dense structure after 365 days of curing which is possibly due to decreased porosity and water permeability. Figure 4.17 shows RHA0 with light gray hydration product C-S-H gel which forms the paste of the matrix. Since RHA is pozzolanic material, concrete develops later strength in comparison with early concrete strength. Figure 4.17 shows the compact, solid, homogeneous morphology after 365 days of curing. It was noted that there was more C-S-H gel present in the cement phase depicting the consumption of CH at a later age due to the pozzolanic nature of RHA. All 365 days micrographs did not reveal voids, cracks, confirming the pozzolanic action of RHA at a later age. It can be verified from the compressive strength results showing strength gain at a later age. Figure 4.20

represents the SEM micrograph of RHA10 after 365 days of curing. The silica formation was confirmed in Figure 4.20 (a) of EDS showing the presence of silica in the RHA matrix. The presence of C-S-H was confirmed through EDS in Figure 4.20 (b). These results can be validated with results of compressive strength and permeability which show higher strength of RHA10 compared to RHA0. The results of durability also show a more compact structure reducing porosity as well as permeability that can be verified by RHA30 micrographs in Figure 4.21.

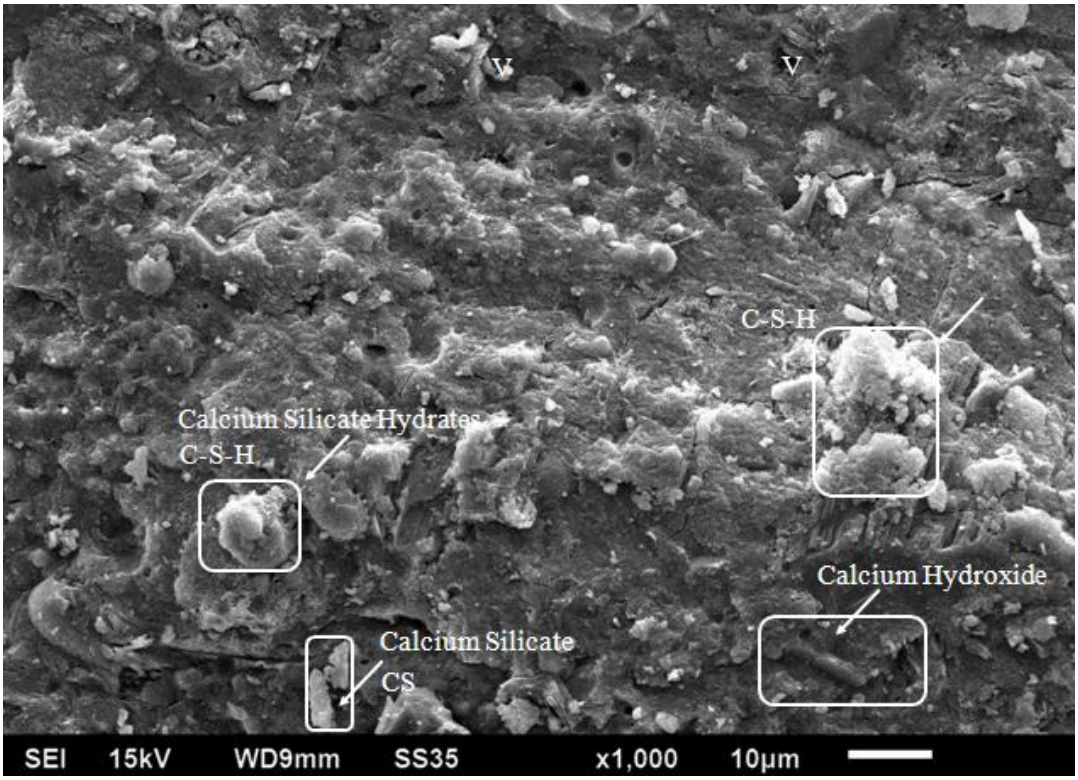

Fig.4.17.SEM image of RHA0 after 365 days

The microstructure of the specimens varies due to the hydration reaction of cement in concrete with age. RHA being an SCM when added in concrete alters the microstructure due to change in the strength, and durability properties of SCC as in the present case. SCM causes changes in the hardened properties and the microstructure of SCC, which is being monitored in the present study as well. For instance, Figures 4.16 and 4.17 represent RHA0 at 28 and 365 days showing an increase in the hydration process with the age of curing and dense matrix with an increased ratio of hydration products in the mix. Figure 4.16 showed deposits of CH hexagonal crystals representing un-hydrated CH at 28 days. RHA30 in Figure 4.19 represents the larger porosity and presence of voids in comparison to RHA30 in Figure 14. VOPP and water absorption are associated with pores. Pore refinement of

cement paste due to SCM, fill the pores with hydration product making it less porous and out of reach of the water. It can be verified from the microstructure images that RHA contributed positively to strength and durability and made the matrix denser. As observed in compressive strength there was high strength due to RHA which produces additional C-S-H in the mixes *(Molaei Raisi et al., 2018).*

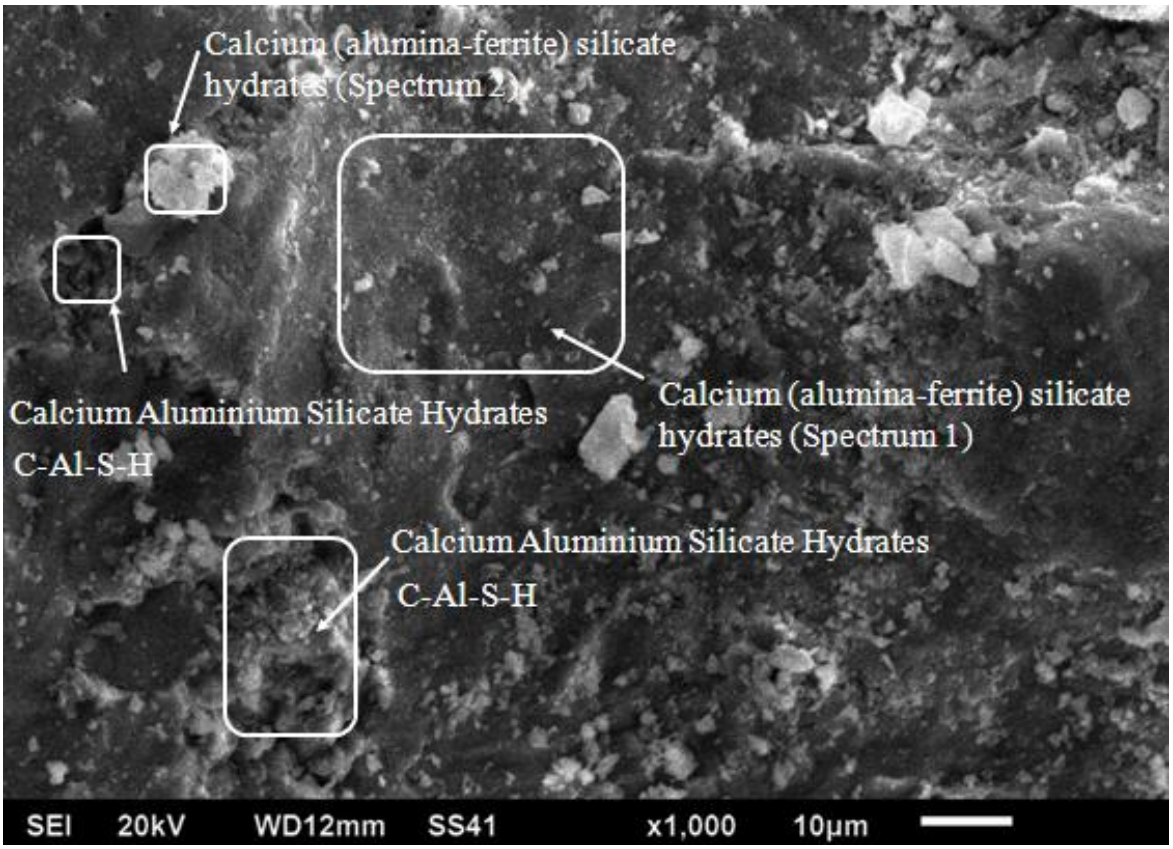

a) RHA10 at 28 days

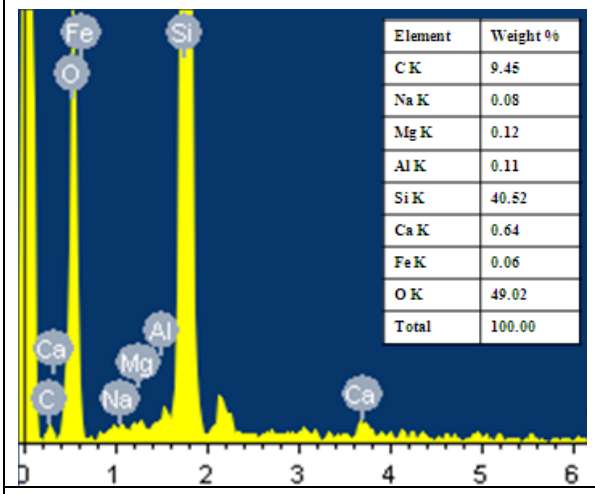

Element	Weight %
C K	9.45
Na K	0.08
Mg K	0.12
Al K	0.11
Si K	40.52
Ca K	0.64
Fe K	0.06
O K	49.02
Total	100.00

b) Spectrum1

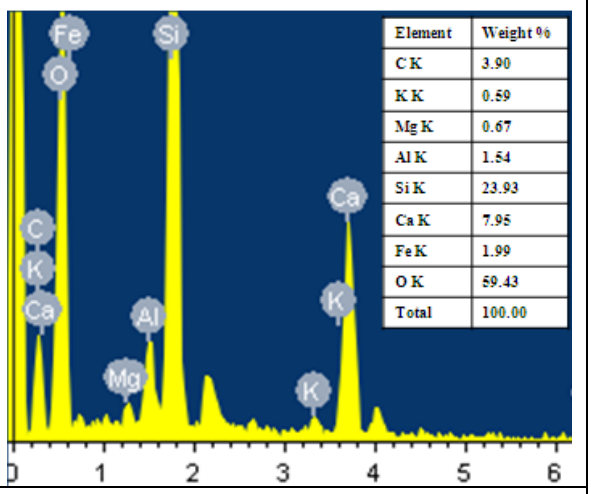

Element	Weight %
C K	3.90
K K	0.59
Mg K	0.67
Al K	1.54
Si K	23.93
Ca K	7.95
Fe K	1.99
O K	59.43
Total	100.00

c) Spectrum2

Fig.4.18.SEM image of RHA10 after 28 days and EDS of spectrum 1 and 2

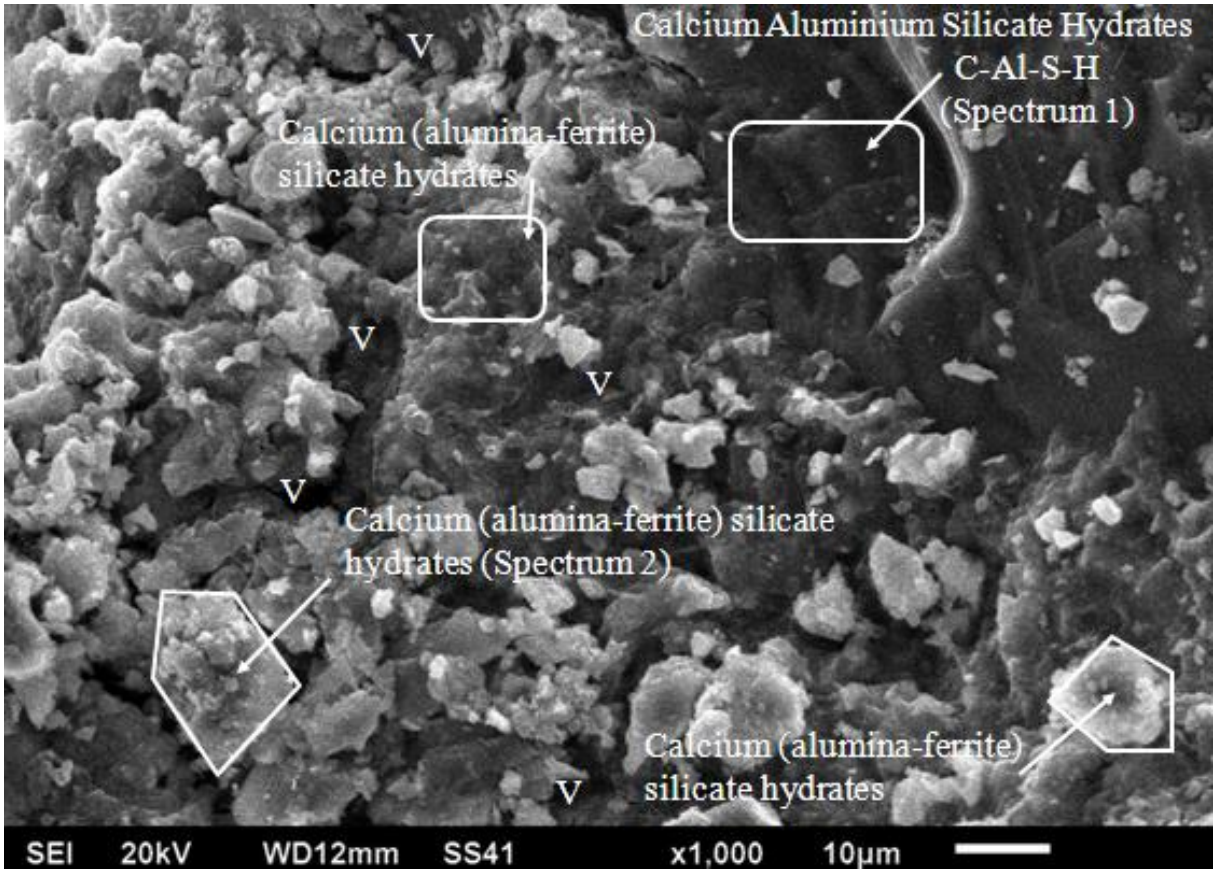

a) RHA30 at 28 days

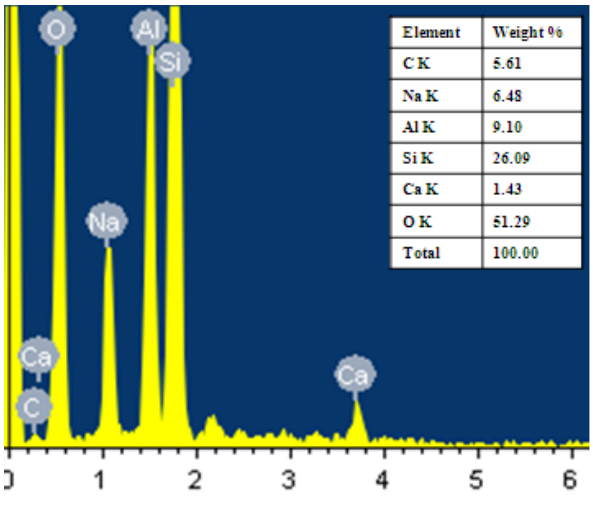

b) Spectrum1

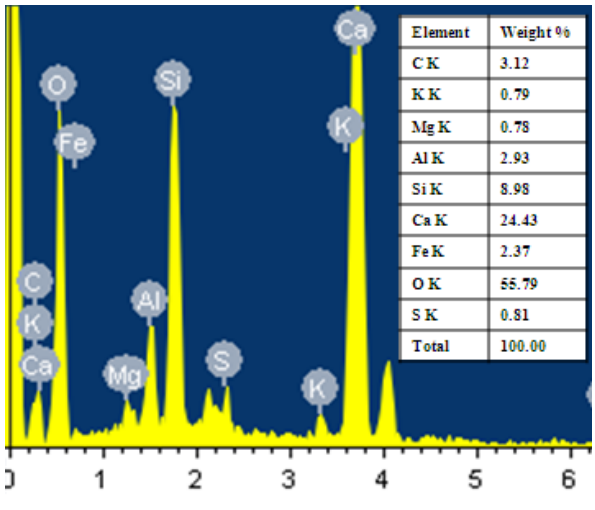

c) Spectrum2

Fig.4.19.SEM image of RHA30 after 28 days and EDS of spectrum 1 and 2

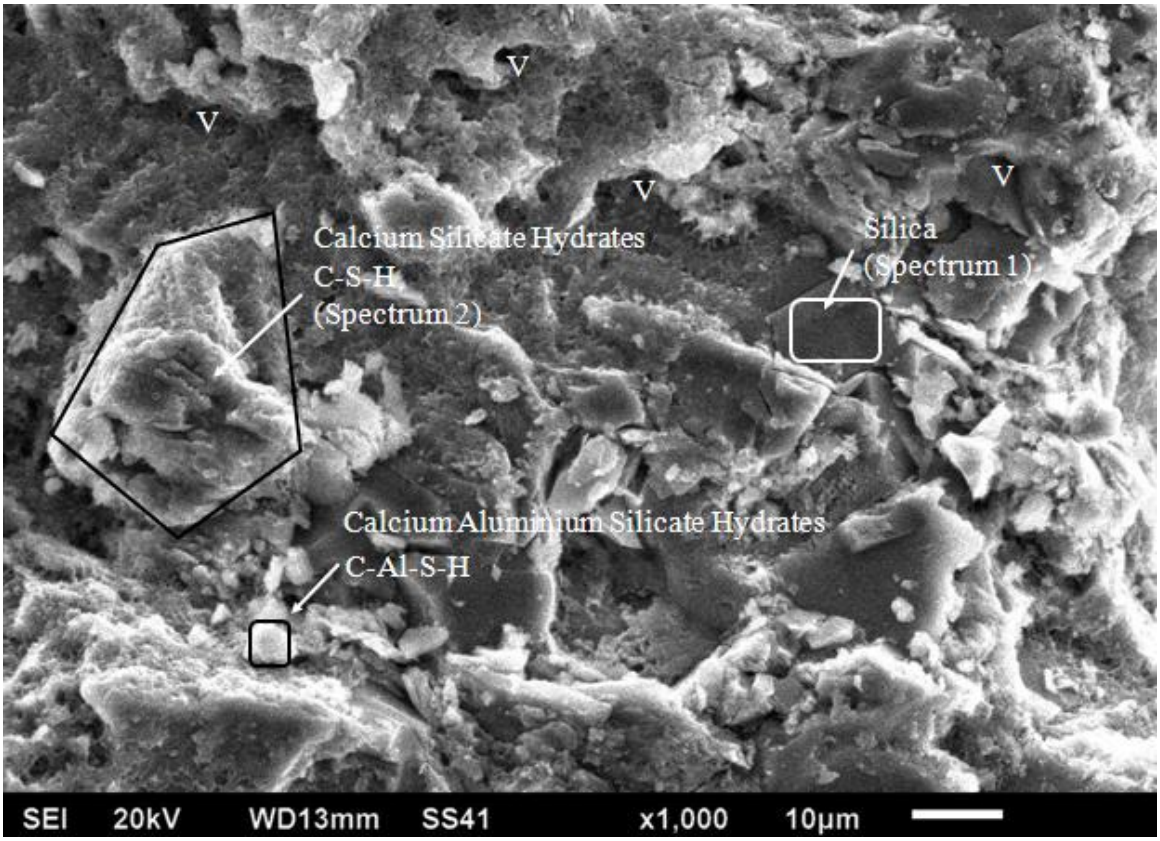

a) RHA10 at 365 days

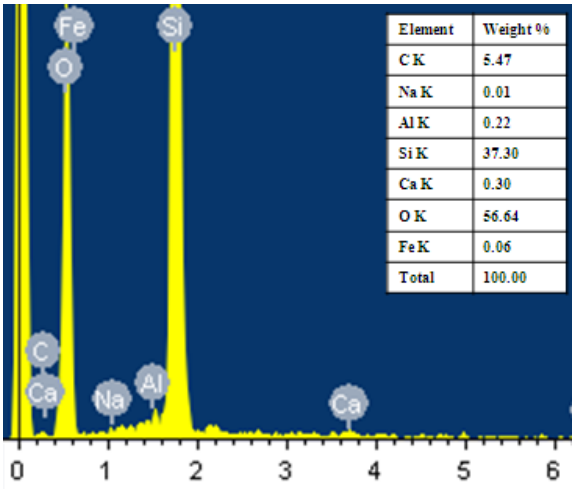

Element	Weight %
C K	5.47
Na K	0.01
Al K	0.22
Si K	37.30
Ca K	0.30
O K	56.64
Fe K	0.06
Total	100.00

b) Spectrum1

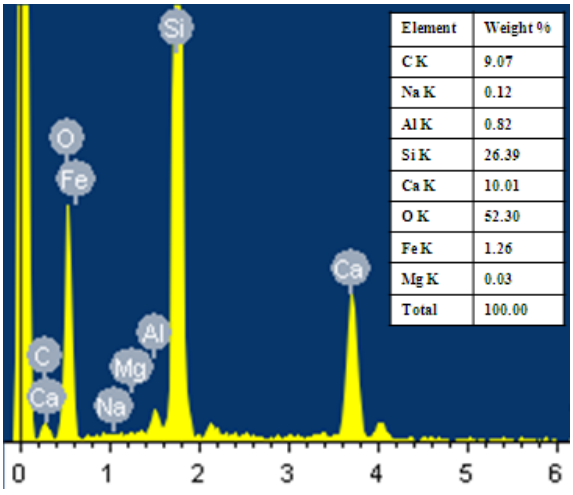

Element	Weight %
C K	9.07
Na K	0.12
Al K	0.82
Si K	26.39
Ca K	10.01
O K	52.30
Fe K	1.26
Mg K	0.03
Total	100.00

c) Spectrum2

Fig.4.20.SEM image of RHA10 after 365 days and EDS of spectrum 1 and 2

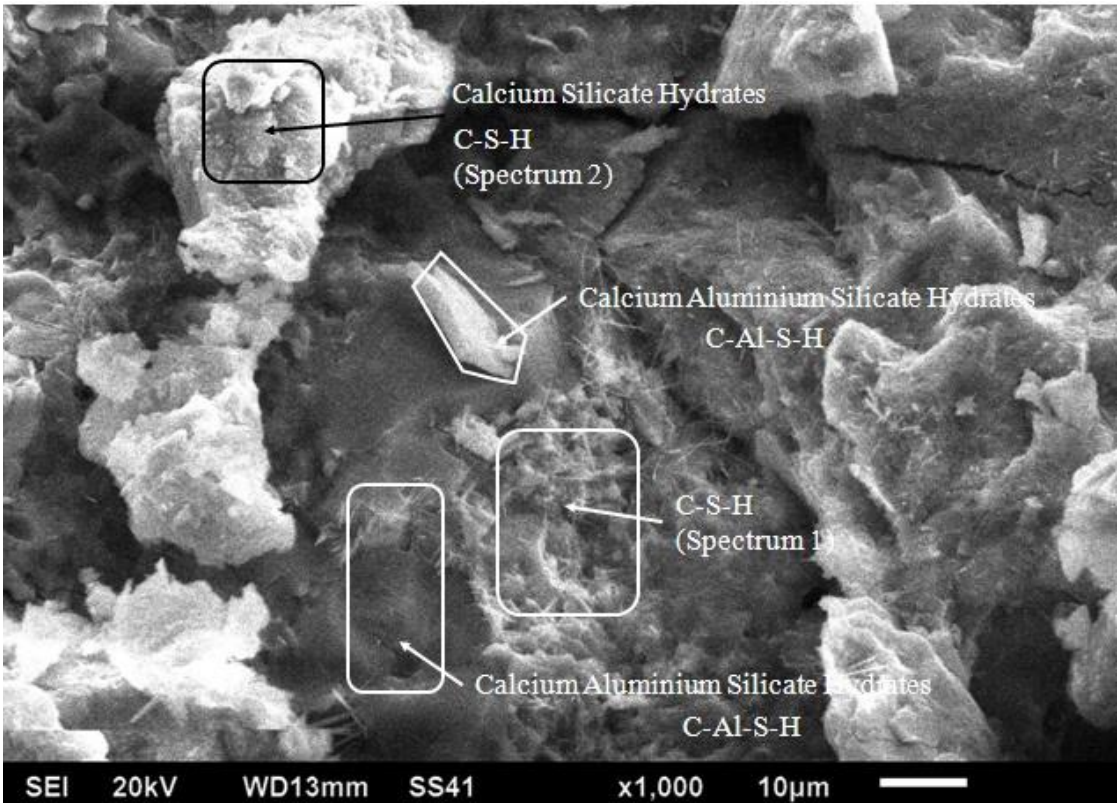

a) RHA30 at 365 days

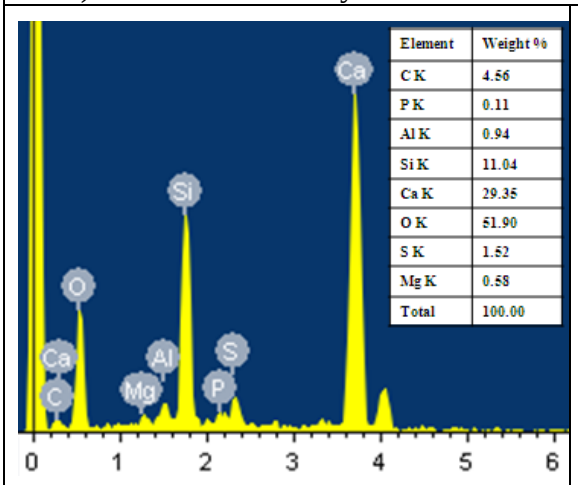

b) Spectrum1

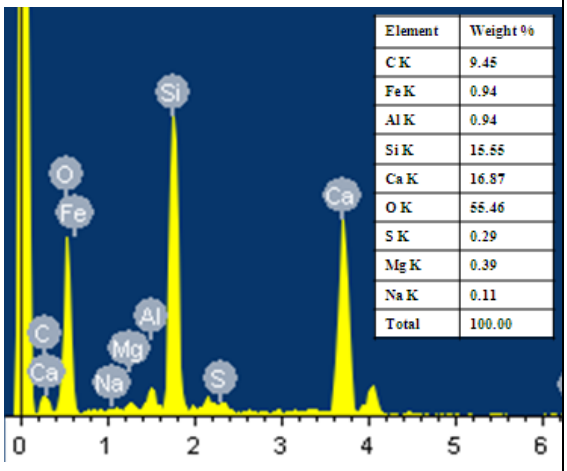

c) Spectrum2

Fig.4.21.SEM image of RHA30 after 365 days and EDS of spectrum 1 and 2

4.1.5.2 XRD

The use of X-ray diffraction (XRD) analysis is one technique for determining the mineral composition of concrete, such as presence of Silica (SiO_2), Calcite ($CaCO_3$), Calcium Silicate Hydrate (C-S-H), portlandite ($Ca(OH)_2$), and ettringite. An XRD test

was performed on the powdered samples of various hardened SCC mix proportions. The samples were collected from the inner core of the concrete structure. XRD diffraction patterns of RHA0, RHA15, and RHA30 mixes at 28 and 365 days of curing are shown in Figures 4.22 to 4.27. Silica (SiO_2) showed multiple sharp peaks in the XRD study of RHA0, while calcite ($CaCO_3$) showed a major peak at 29° in Figure 4.22. Figure 4.23 presented that the partial replacement of cement with 15% RHA causes the broad phase of the SCC mix to develop weak peaks of amorphous calcium silicate hydrates in addition to Silica and Calcite peaks. The amorphous phase present in the SCC mixes did not show any clear peaks. Figure 4.24 represented that additional compounds of Tobermorite ($Ca_5Si_6O_{16}(OH)4H_2O$) were formed in RHA30 at 28 days of curing along with sharp peaks of Silica (SiO2) and Calcium Silicate Hydrate (C-S-H). It was found that the peak levels of cement hydration product i.e. portlandite were increased. The less prominent peaks of silica (SiO_2), calcite ($CaCO_3$), and calcium silicate hydrate (C-S-H) were shown in Figure 4.25. It was observed in Figure 4.27 that additional compounds of Portlandite ($CaOH_2$) and Aluminium Oxide (Al_2O_3) were formed in RHA30 at 28 days of curing. Portlandite is a less desirable, weaker product that leaches out over time resulting in loss of concrete strength. These results are in line with values for compressive strength.

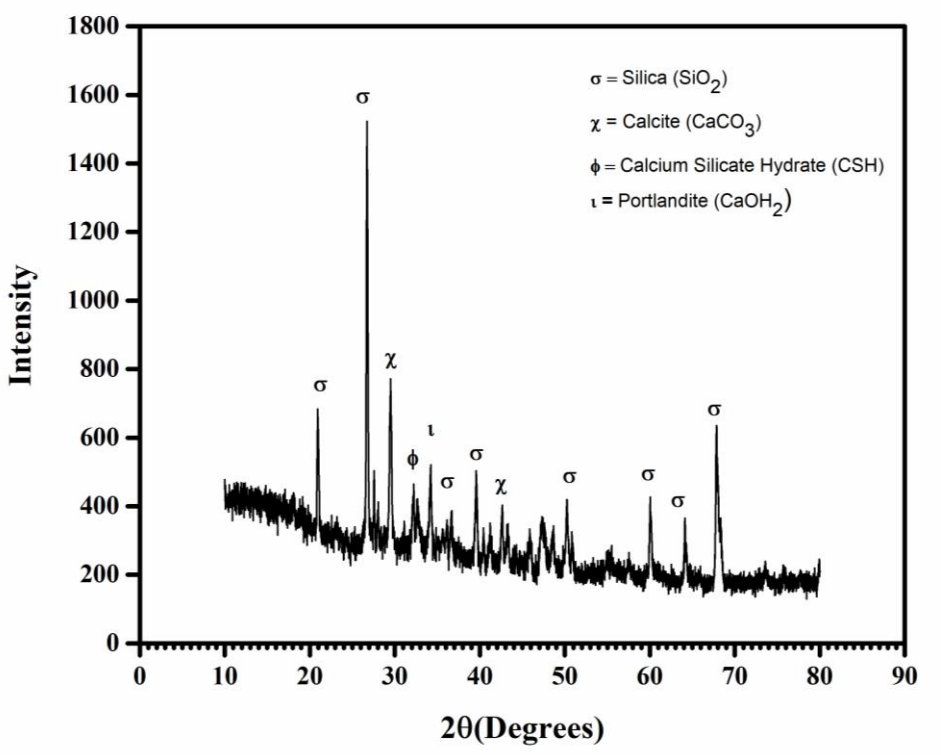

Fig.4.22. XRD pattern of RHA0 at 28 days

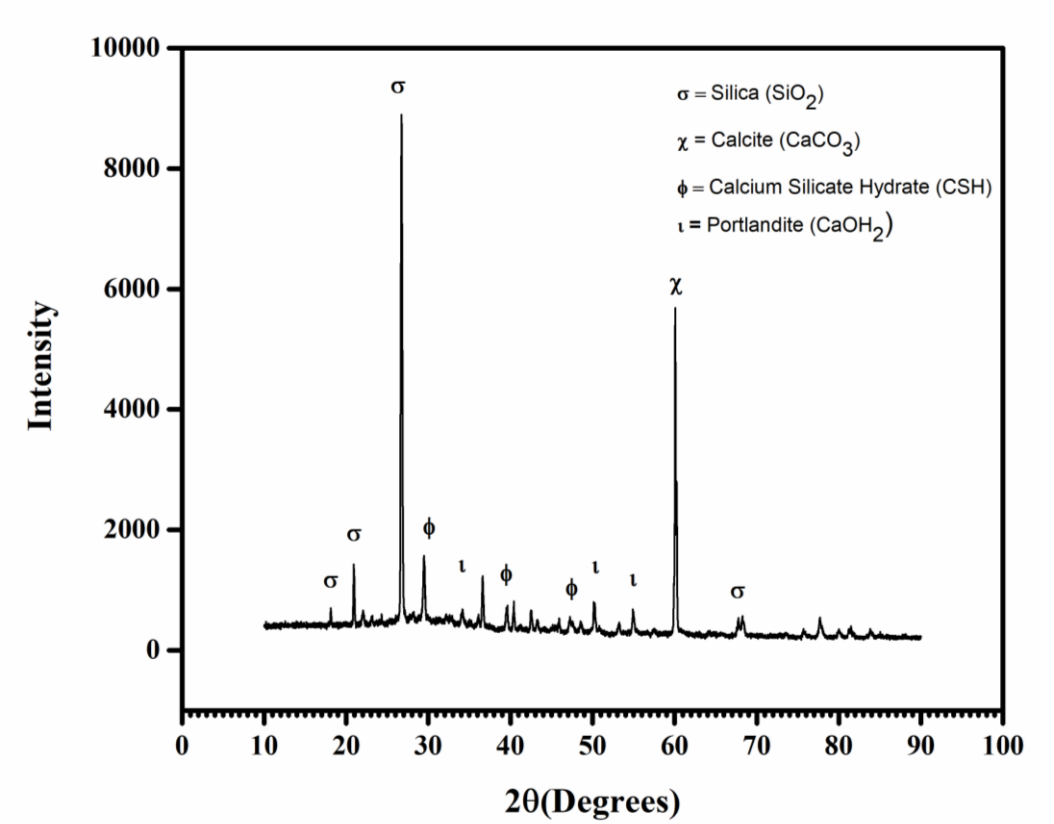

Fig.4.23. XRD pattern of RHA15 at 28 days

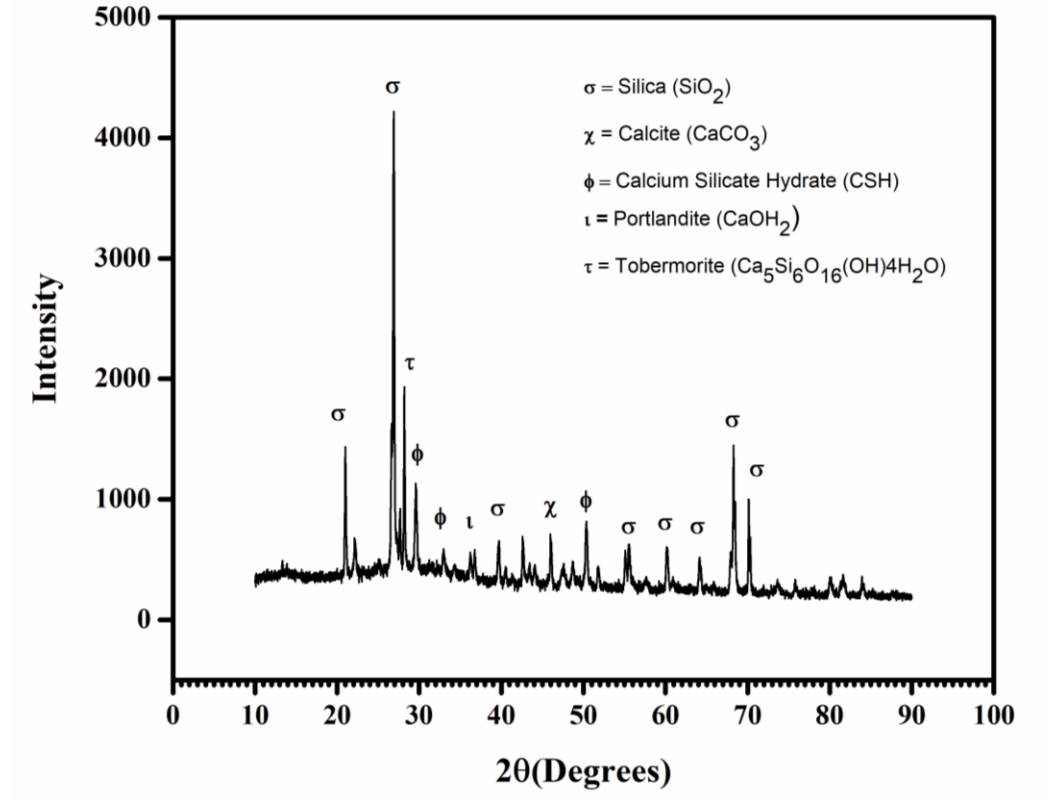

Fig.4.24. XRD pattern of RHA30 at 28 days

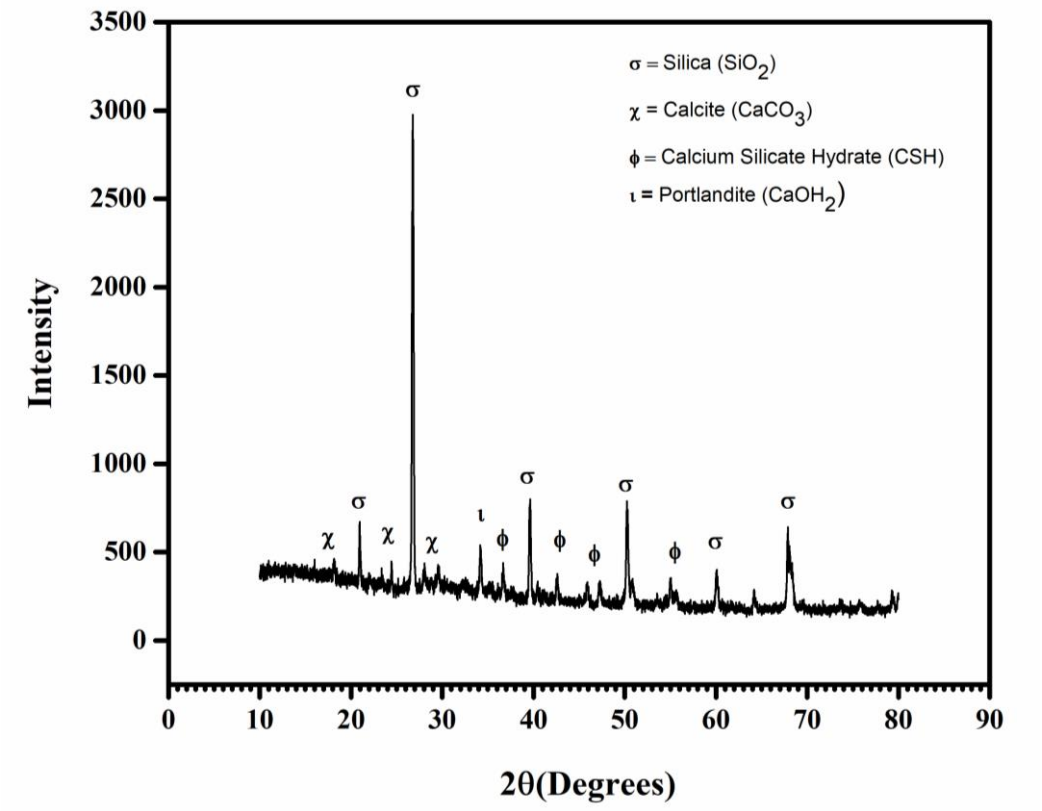

Fig.4.25. XRD pattern of RHA0 at 365 days

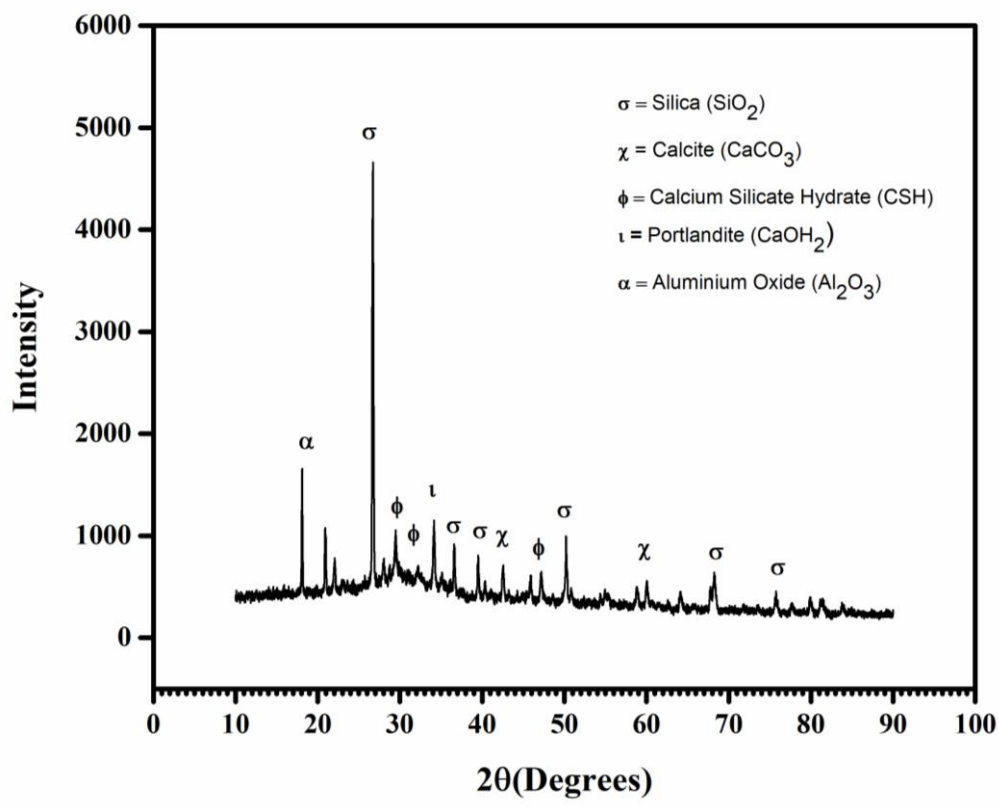

Fig.4.26. XRD pattern of RHA15 at 365 days

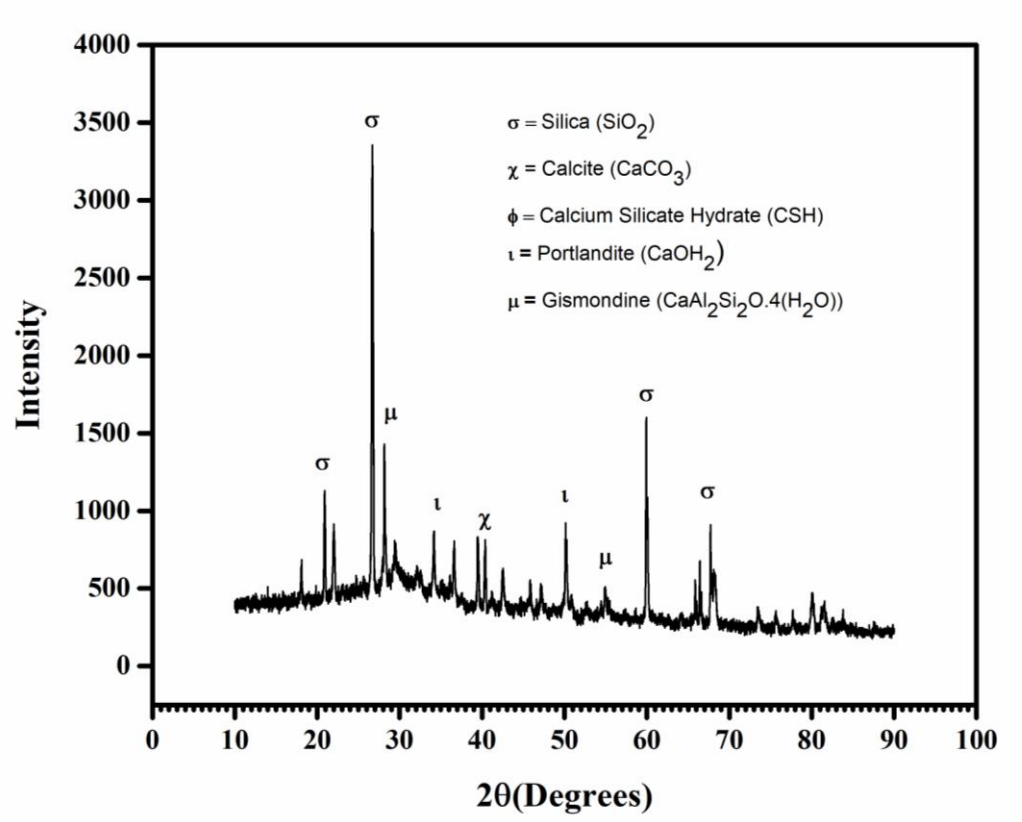

Fig.4.27. XRD pattern of RHA30 at 365 days

4.1.6 Statistical Analysis

Regression analysis is an application of statistical procedures which is used to model associations between a response variable and one or more predictor variables. It determines the significance of relationship between variables, and to model their possible relationship. In the present study, association between dependent parameters i.e. compressive strength, tensile strength, RCPT, and sorptivity and independent parameters i.e. curing age and percentage of RHA was established using Multiple Linear Regression (MLR). MLR is a statistical approach for the formulation of a linear equation between dependent variables and multiple independent variables for prediction of the output.

MLR mathematical equation (4.1) is given by;

$$Y = A_0 + A_1 (AGE) + A_2 (PERCENTAGE) \pm \varepsilon \quad (4.1)$$

Where Y is the value of dependent variable

A_0 is y-intercept or constant in the equation

A_1 and A_2 are the regression coefficients for independent variables

ε is the error associated with the equation

Each value of the independent variables (age and percentage) is associated with dependent variable (Y). In the regression modelling, 84 observations for each of compressive strength and tensile strength were calculated and MLR model was applied for the prediction. Similarly, for durability properties 63 number of observations for both RCPT and sorptivity at different curing ages and percentages of RHA content. Table 4.4 shows the standard errors and p-values for intercept and regression coefficients. It was observed that p values were significant i.e. $p<0.05$ for the regression coefficients and the intercept consequently, important for the formulation of the MLR equation. Further, correlation coefficient (R) measures the relationship between the actual and predicted values of a dependent variable derived from MLR. The correlation coefficient values mentioned in the equation indicated a very good relation between observed and predicted values which depicted the accuracy of the model. Hence, it can be inferred that compressive strength, tensile strength, RCPT, and sorptivity were affected by curing age and percentages of RHA in the SCC mixes.

Y=42.545 + 9.099 (Age) - 1.337 (Percentage) R= 0.96 for Compressive Strength (4.2)

Y= 4.117 + 0.452 (Age) - 0.093 (Percentage) R= 0.86 for Tensile Strength (4.3)

Y= 1960.698 – 336.714 (Age) – 136.905 (Percentage) R= 0.92 for RCPT (4.4)

Y= 2.85 - 0.597 (Age) – 0.0223 (Percentage) R= 0.97 for Sorptivity (4.5)

Table 4.4 Regression model results for strength and durability properties of RHA-SCC mixes

	Compressive Strength		Tensile Strength		RCPT		Sorptivity	
	Standard Error	P-value	Standard Error	P-value	Standard Error	P-value	Standard Error	P-value
Intercept	1.124	0.000	0.112	0.000	69.979	0.000	0.055	0.000
Age	0.318	0.000	0.032	0.000	25.841	0.000	0.020	0.000
Percentage	0.178	0.000	0.018	0.000	10.550	0.000	0.008	0.009

4.2 INCORPORATING WFS AS FINE AGGREGATE IN SCC

4.2.1 Development of SCC (Objective 1)

The various proportions of SCC ingredients i.e. cement, fly ash, coarse aggregates, fine aggregates, waste foundry sand, water, and superplasticizer were decided after performing laboratory experiments. The control mix i.e. WFS0 with 0% WFS attained a compressive strength of 58.25 MPa at 28 days of curing. The constant value of 500 kg/cum cement content and 40 kg/cum of fly ash as mineral admixture was used. Fine aggregates (natural sand) collected from two distinctive sources were used in proportions of 35% and 65% respectively to achieve workability criteria and grading requirements of SCC. A fixed water-binder ratio of 0.36 was maintained and superplasticizer content of 1.17% of cementitious material by weight was used. SCC mixes are designated as WFS5, WFS10, WFS15, WFS20, WFS25 and WFS30 in which fine aggregates are replaced by volume with WFS at 5, 10, 15, 20, 25 and 30% levels respectively. The compositions of seven different SCC mixes prepared are given in Table 4.5.

Table 4.5 Mix proportion of WFS mixes

Mix	Cement (OPC) (kg/m^3)	Fly Ash (kg/m^3)	$Water_a$ (kg/m^3)	Coarse Aggregate (10mm) (kg/m^3)	$Fine\ Aggregate_b$ ($FA_{35}+FA_{65}$) (kg/m^3)	WFS (kg/m^3)	Admixture (kg/m^3)	Density (kg/m^3)
WFS0	500	40	196	672	1015	0	6.32	2429
WFS5	500	40	196	672	964	49	6.32	2428
WFS10	500	40	196	672	913	99	6.32	2427
WFS15	500	40	196	672	863	148	6.32	2425
WFS20	500	40	196	672	812	198	6.32	2424
WFS25	500	40	196	672	761	247	6.32	2423
WFS30	500	40	196	672	710	297	6.32	2421

Note: The coarse and fine aggregates used in concrete mixes are SSD condition.

a: The water content described in the table is free water content used in the mix.

b: The fine aggregate used in the mix is composed of 35% of fine sand and 65% of coarse sand.

The basic physical properties of ingredients of SCC were evaluated before casting of concrete. All the aggregates used in the SCC were in saturated surface dry condition. The pan mixer was used for mixing of coarse and fine aggregates thoroughly in a dry

state. Thereafter, the cement along with fly ash was added until the dry mixture attains a uniform color. Precautions were taken while adding water and superplasticizer into the mix to avoid any spillage and loss of the same. The workability properties were checked with the experiments such as Slump test, V-Funnel, L-Box, and U-Box.

4.2.2 Fresh Properties (Objective 1)

The fresh state behavior of SCC mixes was evaluated as per *EFNARC (2005).* European procedure (EFNARC) depicts the key characteristics i.e. flow-ability by slump flow, viscosity (measured by the rate of flow) by T_{500} slump flow or V-funnel, passing ability by L-box, U-box and resistance to segregation of fresh state concrete. The requirements of SCC in the fresh state varies and are classified into various classes depending upon its type of application.

Table 4.6 Fresh properties of the WFS mixes

Mix ID	Flowability Test					Passing Ability		
	Slump Flow		V-Funnel Time (Sec)			L-Box		U-Box
	Diameter (mm)	T_{500} mm (Sec)	T_{10S} (Sec)	T_{5min} (Sec)	h_2/h_1	T_{200mm} (Sec)	T_{400mm} (Sec)	h_2-h_1 (mm)
WFS0	774 (SF3)	2.14 (VS2)	4.56 (VF1)	6.84 (VF1)	0.96 (PA2)	0.98	1.43	0
WFS5	762 (SF3)	2.38 (VS2)	4.84 (VF1)	7.33 (VF1)	0.92 (PA2)	1.46	2.32	0
WFS10	747 (SF2)	2.73 (VS2)	5.12 (VF1)	8.27 (VF2)	0.93 (PA2)	1.26	2.56	5
WFS15	665 (SF2)	3.25 (VS2)	7.36 (VF1)	9.12 (VF2)	0.87 (PA2)	1.53	3.17	12
WFS20	640 (SF1)	3.46 (VS2)	8.45 (VF2)	12.29 (VF2)	0.89 (PA2)	1.84	3.62	15
WFS25	623 (SF1)	3.69 (VS2)	9.6 (VF2)	11.96 (VF2)	0.81 (PA2)	1.97	3.21	20
WFS30	608 (SF1)	3.98 (VS2)	10.72 (VF2)	14.15 (VF2)	0.85 (PA2)	2.06	3.55	27

The influence of WFS at various substitution levels (0-30%) in SCC mixes was studied by maintaining the constant water-powder ratio of 0.36 and superplasticizer content of 1.17% by weight of cementitious material. In the present study, all the mixes were free from bleeding, visible segregation or honeycombing representing fresh state properties as per EFNARC. However, there was a decreasing trend of

workability in SCC mixes by substitution of fine aggregates with WFS. The values of the fresh properties of SCC obtained from the experimental program are given in Table 4.6.

4.2.2.1 Slump Flow

The slump flow diameter values shown in Figure 4.28 of the current research were varying between 774 mm to 608 mm and lies within the prescribed limits of *EFNARC (2005).* The slump flow results revealed that incorporating WFS in SCC decreases the workability. Shape and texture of particles is an important parameter of workability. Morphology of WFS in Figure 3.2 indicates rough, angular and spherical particles which create hindrance in flow ability and interrupt the smooth flow due to internal friction leading to decreased workability. In Figure 3.4, it is clear from the particle size distribution curve that 75.90% of WFS particle size lies between 600 microns to 150 microns sieves whereas in fine aggregates the value is 41.10%. This increases the content of fines with an increase in substitution rate of WFS thereby increasing the water demand. Also, decreased workability might be due to the fact that the value of fineness modulus of WFS is lower than fine aggregates increasing specific surface area, therefore the water required to lubricate the particles increases. In the present study, the water absorption of WFS (0.62%) is less than the water absorption of fine aggregates (0.71%). The lesser water absorption value of WFS does not affect the workability much because its substitution in the SCC mixes is up to 30% which makes a marginal difference (0.013%) in total volumetric content of mix design. The loss in workability of the mixes was probably due to the finer grains of WFS which replaced the coarser grains of fine aggregates. WFS has impurities which make it more hydrophilic and attracts more water to its surface. Depending upon the type of SCC application requirements, it is categorized into various classes in its fresh state. WFS0 and WFS5 fall under SF3 class, which can be utilized in densely reinforced structures and complicated forms while WFS10, WFS15 lies in SF2 class which is appropriate for purposes like walls and columns. Further WFS20, WFS25, and WFS30 mixes lie in SF1 category which is suitable for housing, tunnel, pile and deep foundation construction works. Flowability of SCC mixes reduced with an increase in the content of WFS. As the content of water- powder ratio and superplasticizer were constant, the decreasing trend can be seen from the spread flows as WFS is rich in silica which is hydrophilic and imbibes more water to its surface *(Sahmaran et al.,*

2011). Spread (diameter) is highest for control mix i.e. 774mm than all other mixes with the inclusion of WFS. Up to 10% substitution of WFS with fine aggregates, the loss in workability is insignificant and maintains workability of 747 mm. Further increase in WFS content decreases the workability drastically. The effect is more prominent beyond 10% replacement level. However, it was possible to achieve fresh properties for all the mixes as per *EFNARC (2005).*

However, in conventional concrete similar results were reported by *(Prabhu et al., 2014)* where the influence of WFS on workability is not noticeable with the replacement level up to 10%. These results are in harmony with that of conventional concrete which illustrated reduced slump with the inclusion of WFS. Few researchers reported a loss in workability of conventional concrete with the inclusion of waste foundry sand at constant w/c ratio and superplasticizer content as in the present study *(Prabhu et al., 2014; Prabhu et al., 2015; Gurumoorthy et al., 2016; Torres et al., 2017).*

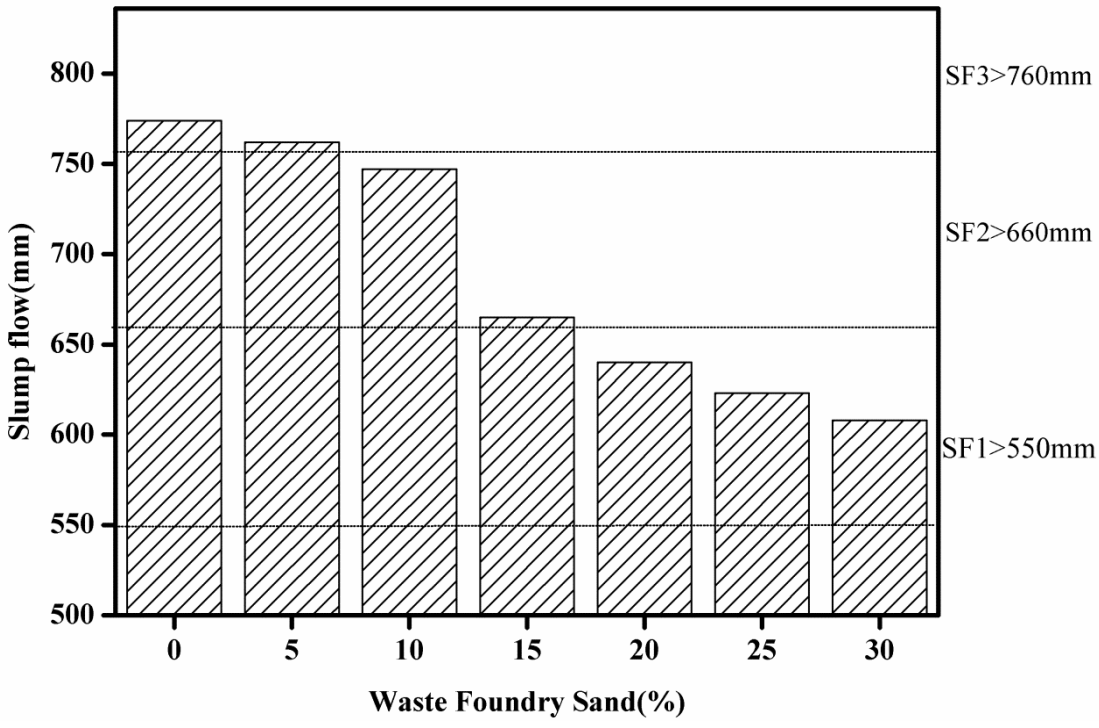

Fig. 4.28 Slump flow results of SCC mixes

4.2.2.2 L-Box Test

The fresh state property of SCC mix which allows it to flow through the compact and restricted zone is known as passing ability. Within allowable limits, the SCC can pass through gridlocked reinforced locations avoiding blockage and hindrance to the flow. L-box ratio or blocking ratio (H2/H1) portrays the passing ability of SCC without segregation through dense locations. The results of the L-box ratio mentioned in Table 4.6 range from 0.96 to 0.85. Figure 4.29 represents the variation of L-box ratio with an increase in the content of WFS. All the SCC mixes exhibited passing ability and characterization according to EFNARC i.e. within permissible limits (0.80 to 1.00). Hence, WFS incorporated as a substitution of fine aggregates can be effectively utilized to prepare SCC for all civil engineering structures. In WFS0, WFS5, and WFS10, the values of blocking ratio were greater than 0.9 that indicated mixes prepared with WFS up to 10% replacement have higher fluidity. Further, T_{200} (sec) and T_{400} (sec) flow time along the horizontal section of L-box were observed. These values represent that increase in WFS content increase the value of T_{200} and T_{400} flow time thereby decreasing the workability.

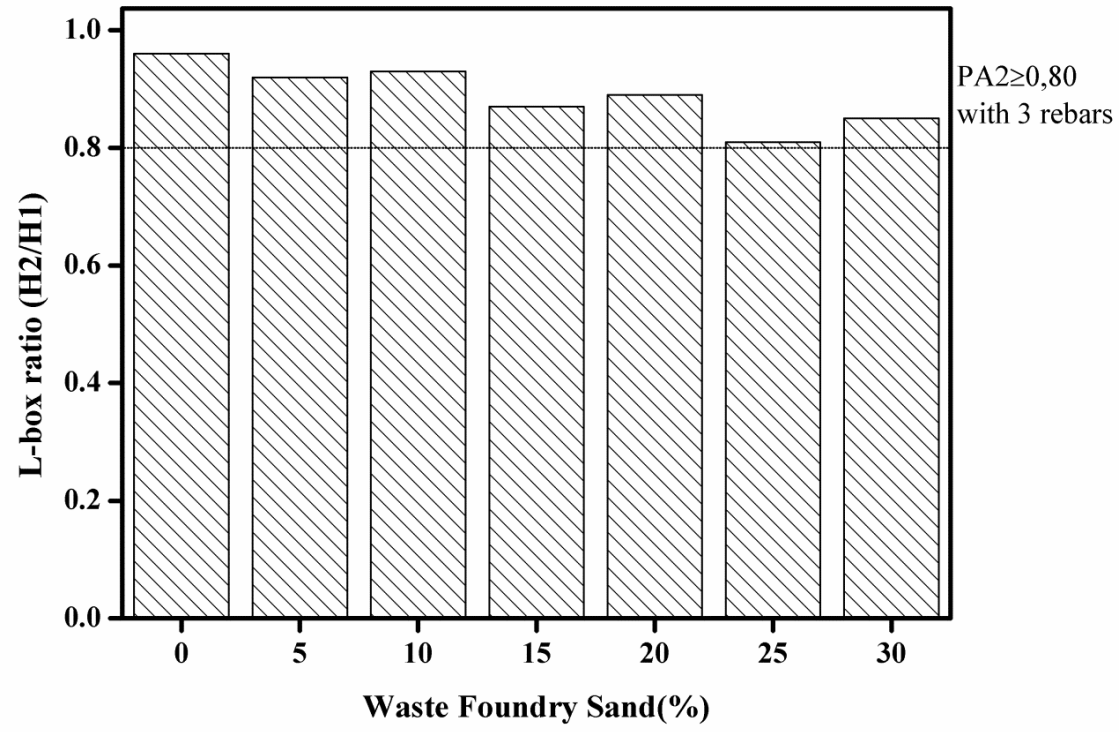

Fig. 4.29 L-Box results of SCC mixes

4.2.2.3 T_{500} and V-Funnel Flow Time

Viscosity of SCC can be accessed by T_{500} or V-funnel flow time with measurement of the rate of flow. If the viscosity is too low, then there will be quick initial flow. The rate of flow of various SCC mixes is illustrated in Figure 4.30, 4.31 and 4.32. As illustrated in Figure 4.30, the values of T_{500} flow time varying from 2.14 to 3.98 sec lies in the category of VS2 class as per EFNARC. The minimum value of T_{500} flow time at WFS0 depicts the highest workability of all the mixes. The maximum value of slump flow time at WFS30 shows the negative effect of WFS in SCC.

V-funnel time illustrated in Figure 4.31 and 4.32 shows the same trend as that of T_{500} slump flow time i.e. increased content of WFS increases the V-funnel flow time. The T_{10} sec values varied from 4.56 sec to 10.72 sec and were classified in VF1 and VF2 class. WFS0, WFS5, WFS10, and WFS15 lie in VF1 class while WFS20, WFS25, and WFS30 lie in VF2 class. The VF1 class is suitable for dense reinforcement which can level itself while for VF2 class if flow time increases, adverse effects such as stoppages, blockages or rough finished surface can be observed. V-funnel flow time T_{5min} sec varies from 6.84 to 14.15 sec. The increased values of T_{5min} sec represents the abruption in the smooth flow of SCC.

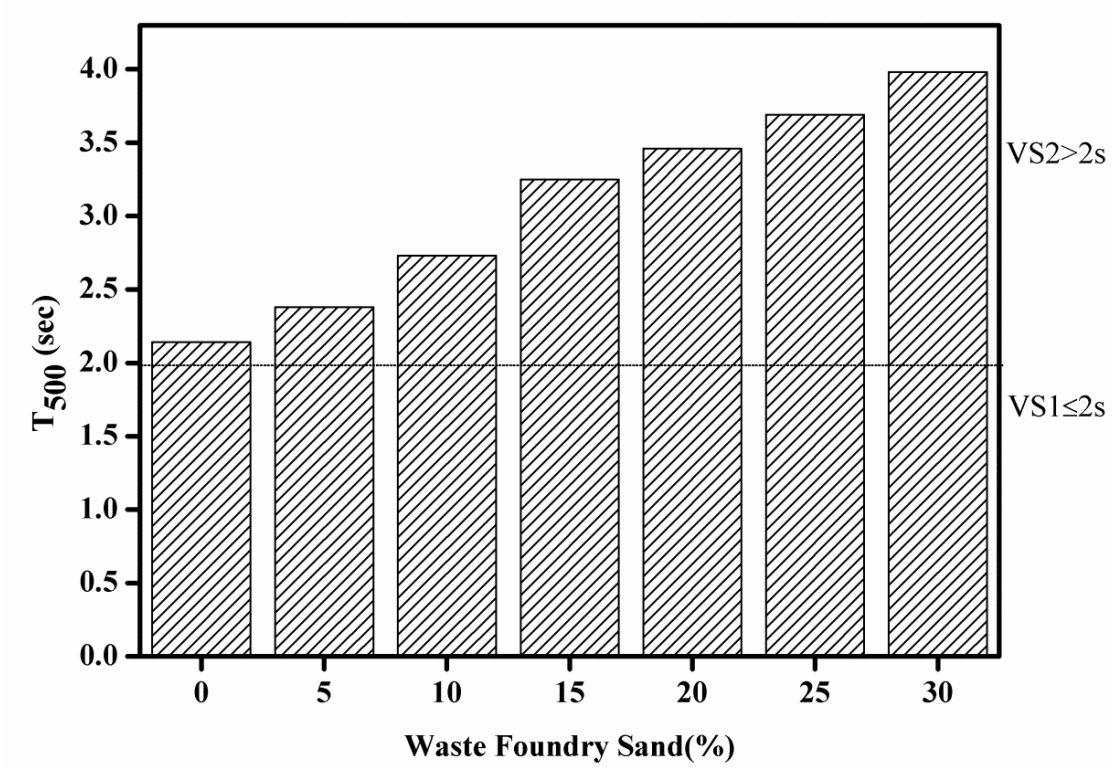

Fig. 4.30 T_{500} results of SCC mixes

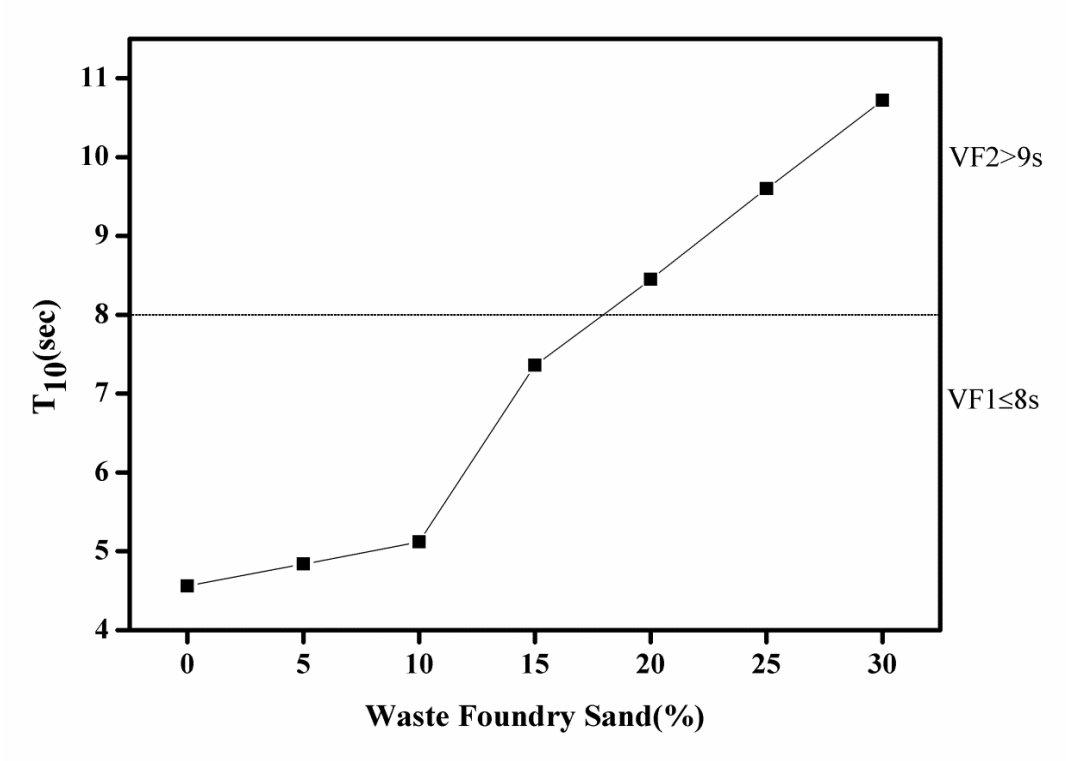

Fig.4.31 T_{10} (sec) results of SCC mixes

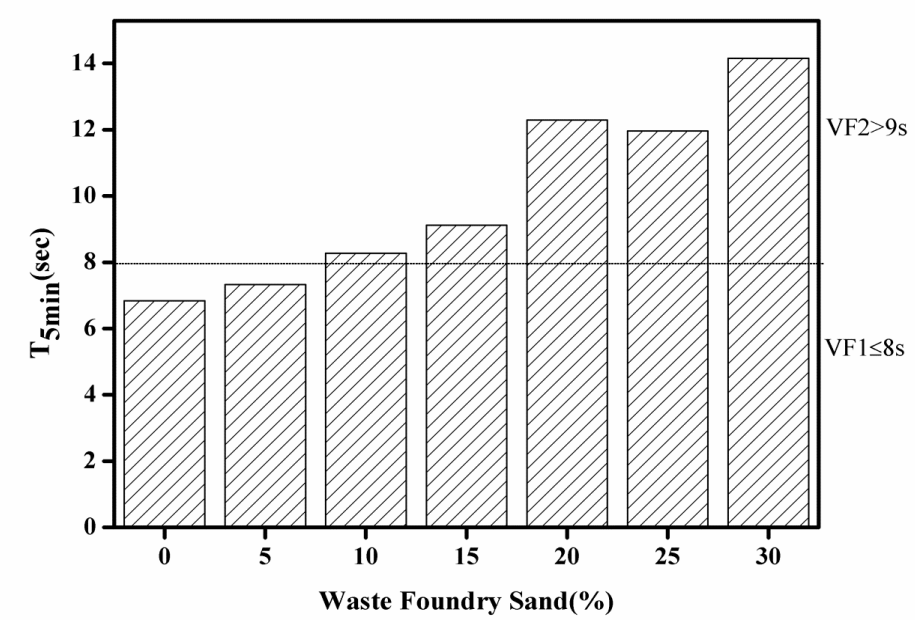

Fig.4.32 T_{5min} results of SCC mixes

4.2.2.4 Passing Ability of Concrete

U-box describes the passing ability of SCC mixes. WFS0, WFS5 have H2-H1=0 i.e. concrete flows freely as water. All SCC mixes in U-Box test results were within the

limits of EFNARC. Values of U-box vary between 0 and 27 and are presented in Figure 4.33. There is a negative correlation between workability and utilization of WFS on fresh properties of SCC. There is a gradual fall in workability with increased WFS content.

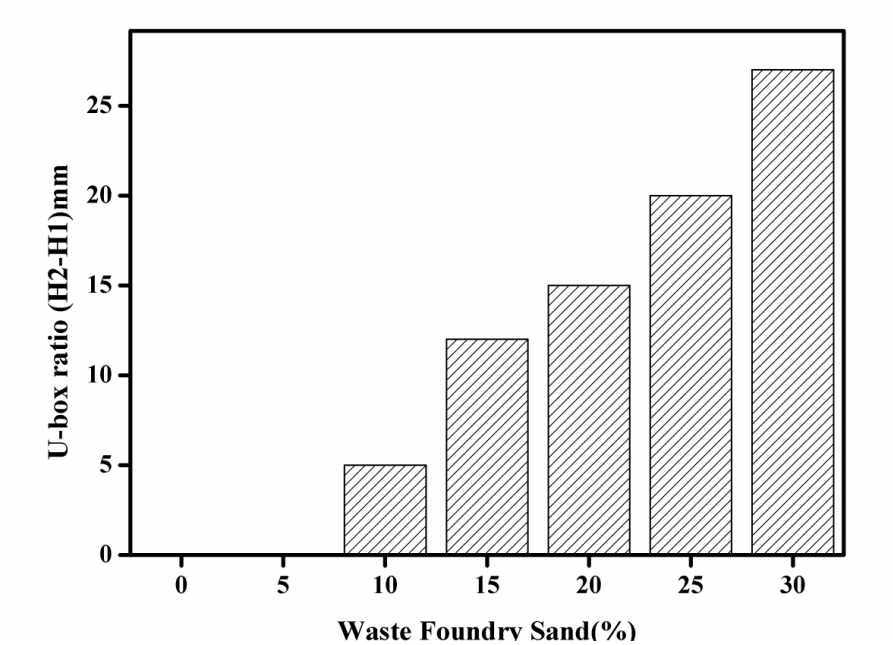

Fig.4.33 U-Box results of SCC mixes

4.2.3 Strength Properties of SCC (Objective 2)

4.2.3.1 Compressive Strength

Figure 4.34 shows the reduction in the compressive strength at all testing ages with the incorporation of WFS in SCC. For WFS0, the compressive strength is 44.61 MPa, 58.25 MPa, 63.67 MPa, and 75.56 MPa at 7, 28, 91 and 365 days, respectively. SCC mixes with substitution of 5%, 10%, 15%, 20%, 25% and 30% of WFS have negative effect on compressive strength and suffers a strength loss of 6.38%, 8.19%, 11.18%, 14.25%, 16.05% and 18.76% respectively, as compared to control mix at the testing age of 28 days. The WFS is recycled silica sand which has poor properties as compared to natural sand. In this research study, the coarser natural sand was replaced with finer WFS keeping the volume of mix constant, as a result, the specific surface area of inert particles increased in the SCC mix. Thereby, increasing the water demand which further reduces the amount of free water available for hydration reaction. Due to improper hydration and insufficient binding of inert particles, the compressive strength reduces significantly. The density of the mixes decreased when

the substitution of fine aggregates was carried out with WFS by volume. At 90 days, percentage reduction in compressive strength is 6.23%, 9.69%, 12.89%, 16.40%, 18.37% and 22.66% with respect to control mix. Further, the strength of other SCC mixes in comparison to control mixes reduces to 5.79%, 13.71%, 15.14%, 18.89%, 25.15% and 29.89% at the testing age of 365 days. It was observed that at all curing ages, the SCC produced with WFS had lower values of compressive strength as compared to the control mix.

WFS0 achieved the strength of 58.25 MPa at 28 days, whereas with the increase in age (curing time) at 90 and 365 days the percentage increase was 9.30% and 29.72%, respectively. There was an increasing trend of compressive strength with curing time of concrete. The supplementary cementitious material i.e. fly ash was one of the components in mix design, contributing to the future strength of SCC. The mechanical properties of SCC with fly ash essentially develop after 90 days of curing as per American Concrete Institute (*ACI 237).* At the substitution level of 5% WFS, the rate of increase in strength with age was found to be higher i.e. 9.48%, 30.54% for 90 days, 365 days, respectively at 28 days. While at 30% replacement level of WFS, an increase in the percentages was found to be 4.06% and 11.95%. It was observed that the strength values of all SCC mix at various replacement levels of WFS increased significantly with an increase in curing time of concrete.

Sahmaran et al. (2011) investigated the properties of SCC incorporating fly ash & WFS and discovered incorporation of these reduces the strength at all ages with reference to the control mixture. However, in conventional concrete, some authors *(Siddique et al., 2011 ;Singh and Siddique, 2012; Basar and Deveci, 2012)* reported an increase in compressive strength. Also, (*Prabhu et al., 2014; Siddique et al., 2009; Torres et al., 2017)*concluded that the inclusion of WFS provides satisfactory results and hence can be effectively utilized in manufacturing concrete. While similar results were reported in conventional concrete by *Siddique and Kadri(2011) and Khatib et al. (2010)* where results showed that there is a declining trend in compressive strength with the inclusion of foundry sand in concrete. This may be attributed by the unimodal particle size distribution of WFS, finer particles which contribute to weaker interfacial transition zone between cement paste and fine aggregates, improper compaction which leads to enlargement of pores. The authors revealed that

satisfactory strength can be achieved at an apt replacement level of WFS with natural sand.

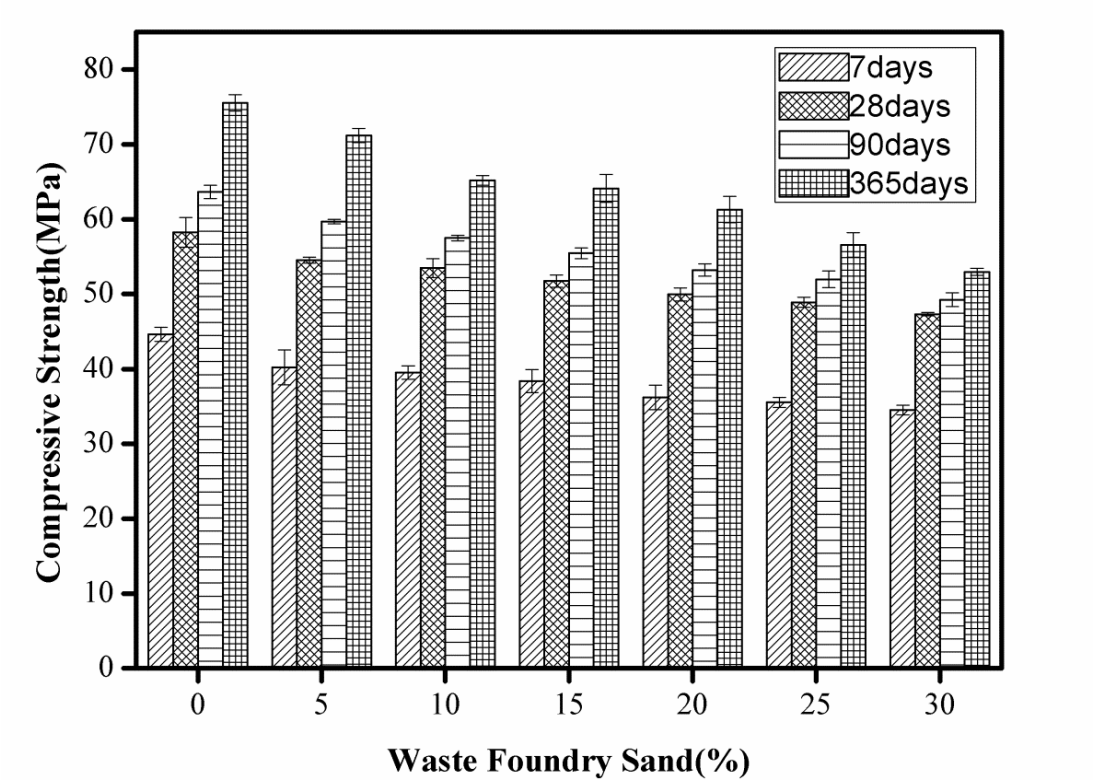

Fig. 4.34 Compressive Strength of SCC mixes

4.2.3.2 Splitting Tensile Strength

Figure 4.35 illustrates the effect of WFS as substitution of fine aggregates on splitting tensile strength of SCC. Splitting tensile strength values of WFS0 were 4.19 MPa, 4.56 MPa, 5.27 MPa, and 5.41 MPa at 7, 28, 90 and 365 days of curing respectively. At 28 days of curing, the splitting tensile strength of WFS5 to WFS30 shows decreasing trend i.e. 3.63%, 4.69%, 6.44%, 8.28%, 9.36%, and 11.03% respectively. Control mixes exhibit maximum values of splitting tensile strength at all ages of curing. At 90 days of curing, percentage decrease in values of splitting tensile strength was 6.08%, 9.15%, 10.73%, 11.52%, 15.67% and 19.03% at various replacement levels. At 365 days, the percentage decrease of splitting tensile strength as compared to the control mix was 6.67%, 6.97%, 11.05%, 16.81%, 17.24%, and 19.85%. Splitting tensile strength showed a similar trend as that of compressive strength. Tensile strength declines with an increase in the percentage of WFS. The tensile strength has an increasing trend like compressive strength with age. The maximum values for the rate of increase of tensile strength with age were 12.78% & 15.07% at

90 and 365 days in WFS5. Whereas the minimum values were observed at WFS30 i.e. 5.31 % & 7.03% at 90 and 365 days. At all replacement levels of WFS with fine aggregates, the value of the percentage of splitting tensile to compressive strength reduces with age whereas the values of splitting tensile strength and compressive strength increase individually. It shows that the rate of increase of compressive strength is higher than the rate of increase of splitting tensile strength at all replacement levels and with age. The values are depicted in Table 4.7.

Pathak and Siddique (2012) provided similar results in SCC mixes where splitting tensile strength declines with the utilization of foundry sand. *Prabhu et al. (2014); Siddique et al. (2011) and Smarzewski et al. (2016)* provided the comparable results in conventional concrete i.e. splitting tensile strength follows the declining trend in compressive strength with an increasing replacement of WFS. Contradicting to present research, *Siddique et al.(2009)*showed increased splitting tensile strength with increased WFS content.

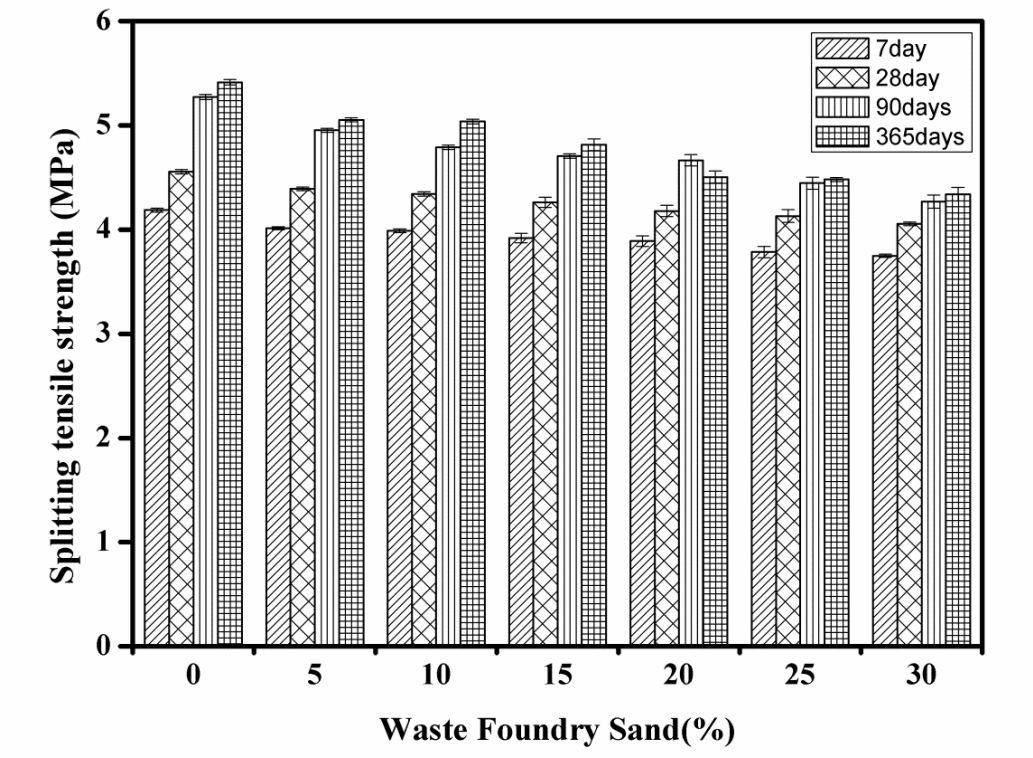

Fig. 4.35 Splitting tensile strength of SCC mixes

Table 4.7 Splitting tensile to compressive strength ratio percentage

Mix	Percentage of Splitting Tensile to Compressive Strength (%)			
	7 Days	28 Days	90 Days	365 Days
WFS0	9.39	7.82	8.28	7.17
WFS5	9.99	8.05	8.30	7.10
WFS10	10.10	8.12	8.33	7.73
WFS15	10.21	8.24	8.49	7.51
WFS20	10.74	8.37	8.77	7.35
WFS25	10.65	8.45	8.56	7.92
WFS30	10.87	8.57	8.67	8.19

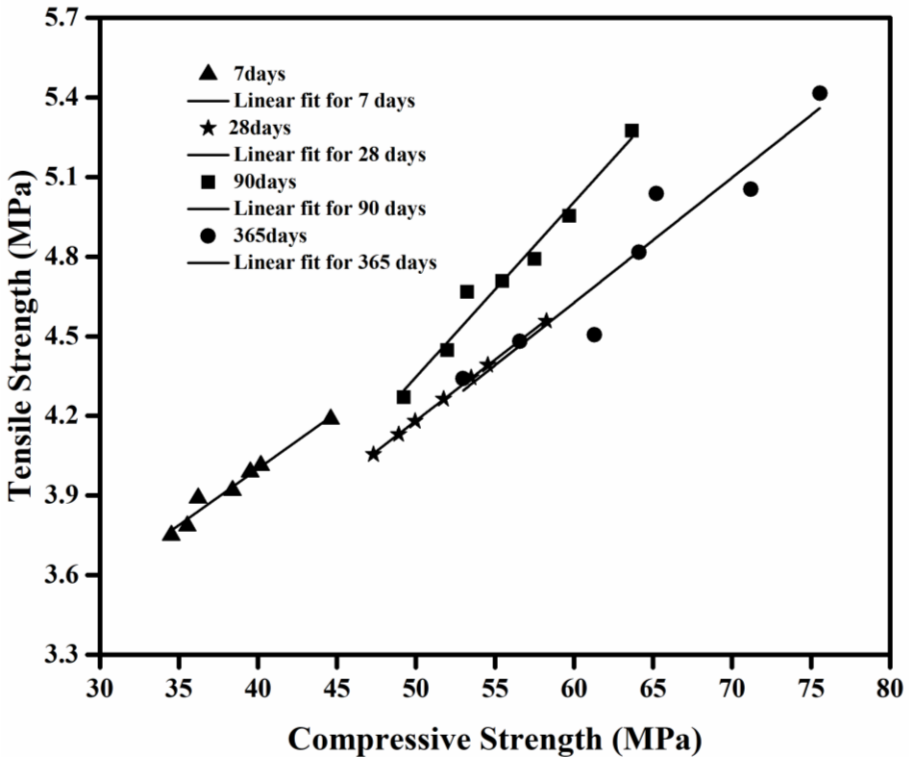

Fig. 4.36 Relation between compressive strength and splitting tensile strength of SCC mixes

4.2.4 Durability properties of SCC (Objective 3)

4.2.4.1 Rapid Chloride Permeability Test

Concrete starts to deteriorate in two different stages through external weathering action. Initially, water or chloride ingression and movement take place through concrete media. Further, these external agents lead to deterioration mechanisms.

Therefore, it is notable that concrete with low permeability is the key to durable concrete *(Kosmatka et al., 2011).* Usually, SCC has better durability as compared to conventional concrete because of the greater quantity of fines, pore refinement, improved pore structure, and dense microstructure *(Booya et al., 2015).*

The penetrability of chloride increases with an increase in WFS against river sand at all replacement levels. Figure 4.37 displays the increase in the value of charge passed through concrete at all ages. Charge passed at 28 days were 2119, 2451, 2847, 3127, 3263, 3452 and 3533 Coulombs at 0, 5, 10, 15, 20, 25 and 30% replacement levels of WFS respectively. The test values were 1249, 1303, 1384, 1436, 1481, 1784, and 2038 Coulombs at 90 days respectively at various replacement levels of WFS. The charge passed value at 365 days were 648, 680, 710, 712, 746, 774, and 832 Coulombs i.e. 'very low' at different replacement levels. All these values of charge passed decreased with the passage of curing time. The values of charged passed at WFS30 were 3533, 2038, and 832 coulombs at 28, 90 days, and 365 days of curing respectively. All the SCC mixes fall under the category of 'moderate' according to ASTMC 1202 at 28 days, whereas mixes lied in the range of 'low' category except the SCC mix with 30% replacement level at 90 days and all mixes at 365 days of curing fall under the category of 'very low' permeability.

RCPT results can be verified with compressive strength, where the adhesion of particles in the matrix did not occur properly due to deficient cement gel, which increased the pores and formed permeable concrete. Figure 4.38 shows a good correlation between RCPT and compressive strength. *Sahmaran et al.(2011)* reported an increase in the value of charge passed which implies penetrability increases with the substitution of natural aggregates with WFS at all ages for SCC mixes. The chloride penetrability decreased with age where all mixes lie in the category of 'moderate' permeability at 28 days and fall under the range of 'low' & 'moderate' at the age of 90 days. Hence, it can be inferred from the results that the chloride permeability of SCC does not improve with the utilization of WFS in comparison to natural river sand. Moreover, chloride permeability results of WFS mixes were comparable with the control mix at all ages which were lying in the same range according to ASTM C 1202 and all the RCPT values improve with curing age.

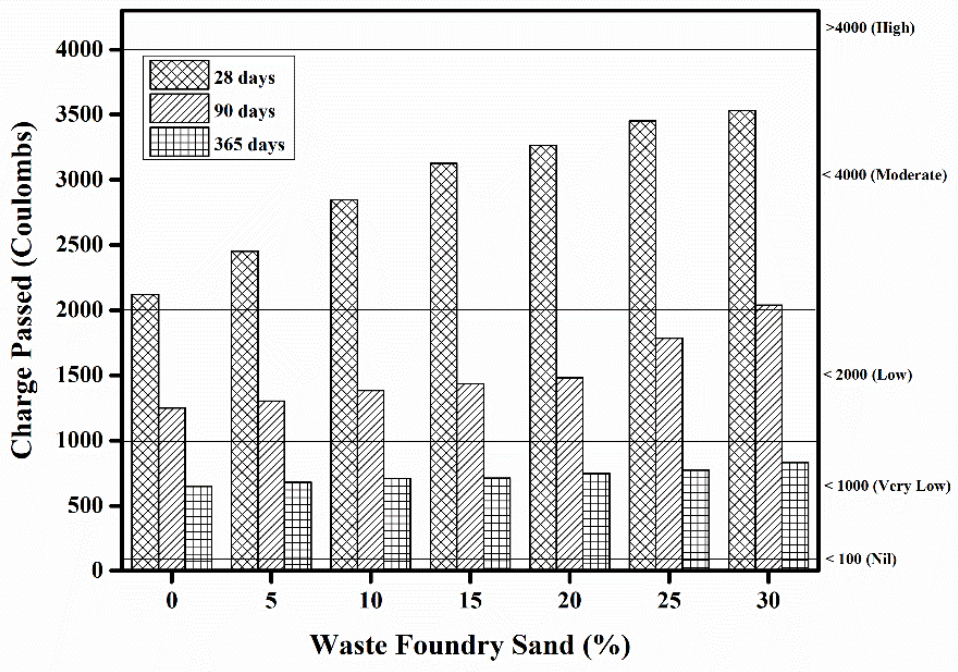

Fig. 4.37 Charge passed (Coulombs) of SCC mixes

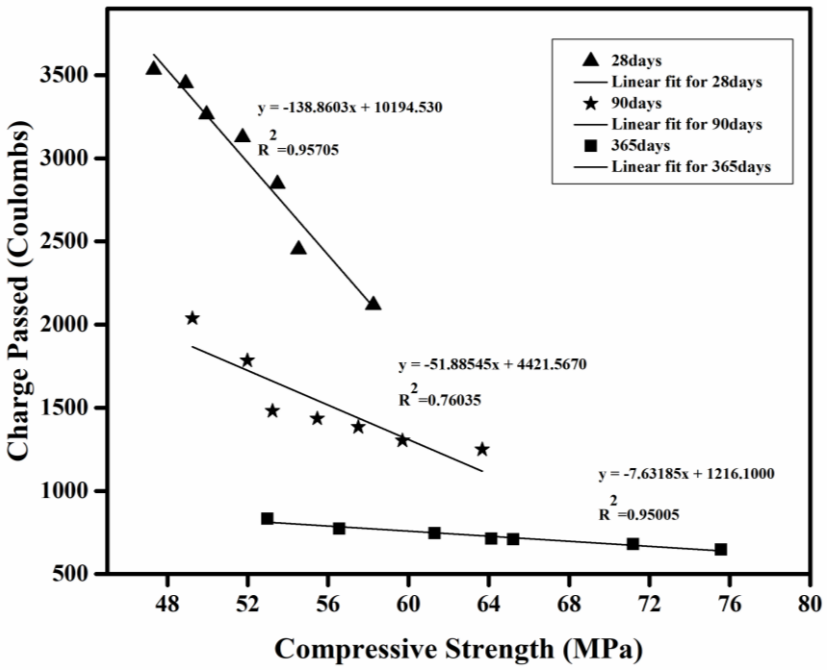

Fig. 4.38 Relation between RCPT & Compressive strength of SCC mixes at 28, 90 and 365 days

4.2.4.2 Water Absorption and Porosity

Durability of concrete is greatly affected by porosity and water absorption *(Kolias and Georgiou 2005).* Concrete loses its serviceability due to its porous structure and movement of fluids. Hence, it is important to study the pore structure and permeation property of concrete. Porosity of concrete is empty space inside its

structure which defines characteristic properties of entire concrete material. Porosity is calculated by the percentage of water stored within these empty spaces *(Kosmatka et al., 2011).* Water absorption and porosity of SCC specimens were evaluated using ASTMC 642-13, as illustrated in Table 4.8.

Water absorption values for WFS0 were 5.77%, 5.38%, and 1.54% at 28, 90, and 365 days respectively. The increasing trend in water absorption after immersion was observed and the values varied from 4.75 to 6.29 at 28 days, 4.47 to 5.80 at 90 days, and 1.28 to 1.70 at 365 days of curing after inclusion of WFS up to 30%. The reduction in values of water absorption after immersion at WFS30 dropped from 6.29 % at 28 days to 1.70% at 365 days of curing. Water absorption of SCC mixes also increased on boiling the concrete samples. These findings were in coherence with compressive strength test results, which may be attributed to the constant pozzolanic behavior of cementitious materials in the SCC mixes with age. The continuous hydration reaction densifies the concrete's internal structure with an increase in the curing period. Consequently, decreasing the water absorption of SCC mixes with age at all replacement levels of WFS. In the present research, WFS did not help in the formation of new hydration products during hydration reactions, as it acted as inert material in concrete mixes *(Burgos et al., 2017).* However, WFS being finer and of higher specific surface area than river sand resulted in reduced density, created voids and increased water absorption with WFS substitution level (0 to 30%) at the constant water-binder ratio in present SCC mixes.

From Table 4.8, it can be observed that the permeable pore space values increase with the inclusion of WFS in SCC mixes. The value of permeable pore space ranged from 13.39% to 16.37% with an increase in WFS from 0 to 30% at 28 days of curing. Further, values of permeable pore space ranged from 12.71 to 15.84% at 90 days of curing and the significant drop was observed at 365 days of curing, where values ranged from 3.65 to 6.47%. The results indicated an increase in porosity of SCC as both water absorption and volume of permeable pores (VoPP) displayed an increasing trend at all curing ages with an increase in the WFS substitution rate. It was also found that VoPP values decrease with an increase in curing age at different percentage rates of WFS. Figure 4.39 demonstrates the important linear association between water absorption and VoPP. It depicts strong positive correlation between VoPP and

water absorption at 28, 90, and 365 days i.e. if VoPP increases water absorption also increases and vice-versa.

Table 4.8 Water absorption and Porosity of SCC mixes

Mix	28 Days			90 Days			365 Days		
	Absorption after immersion %	Absorption after immersion and boiling %	VoPP (%)	Absorption after immersion %	Absorption after immersion and boiling %	VoPP (%)	Absorption after immersion %	Absorption after immersion and boiling %	VoPP (%)
WFS0	4.75	5.77	13.43	4.47	5.38	12.26	1.28	1.54	3.66
WFS5	4.78	6.06	13.81	4.67	5.46	12.61	1.33	1.92	4.47
WFS10	4.94	6.14	13.91	4.78	5.57	12.64	1.36	1.99	4.49
WFS15	5.15	6.66	14.56	4.83	5.69	12.79	1.38	2.16	5.28
WFS20	5.23	7.16	15.78	5.21	5.72	12.89	1.41	2.22	5.31
WFS25	5.36	7.26	15.83	5.20	6.01	13.04	1.45	2.42	5.74
WFS30	6.29	7.74	16.67	5.80	6.48	13.89	1.70	2.85	6.20

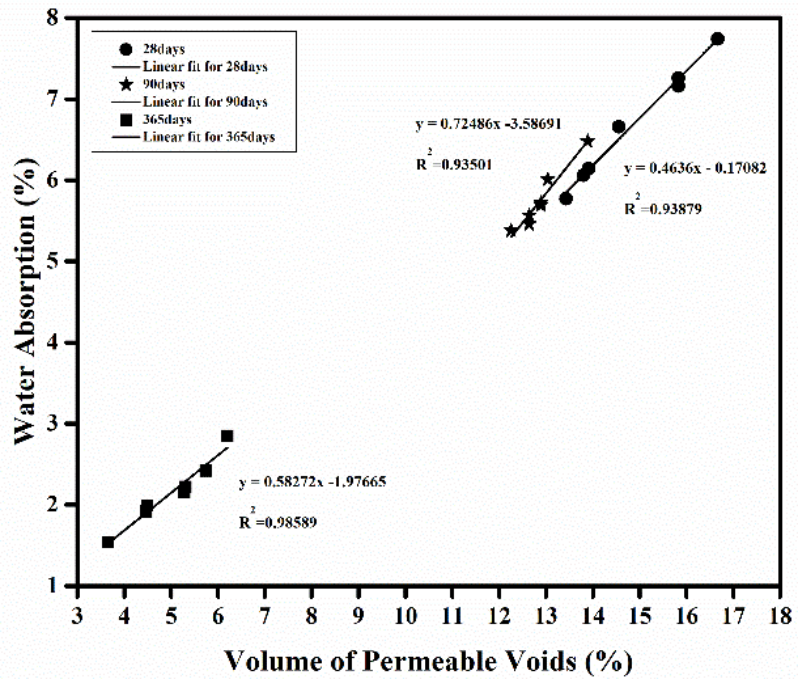

Fig. 4.39 Relationship between water absorption and volume of permeable voids of SCC mixes at 28, 90 and 365 days

4.2.4.3 Sorptivity

Sorptivity as a transport property refers to the volume of liquid absorbed through capillary action by unsaturated concrete pore space. Sorptivity depends on workability, compaction, interconnected capillary pores, cementitious content, mix proportion, supplementary cementitious material, and curing *(Güneyisi et al., 2014).*

The higher porosity represents more porous concrete and consequently affects the capillarity *(Aïssoun et al., 2016).* Sorptivity related to the presence of cavities and capillaries in the SCC specimens was evaluated in the present research. The sorptivity test was conducted as per ASTMC 1585-13. Figures 4.40-4.42 illustrate the variation in absorption of WFS0 to WFS30 after 8 days of sorptivity experiment with the square root of time at 28, 90, and 365 days. The value of absorption increased from 2.11 mm to 3.07 mm with increment in WFS content up to 30% at 28 days. Further, the values of absorption ranged from 1.83 mm to 2.48 mm and 0.92 mm to 1.29 mm at 90 and 365 days respectively. These results depicted that the absorption with time increases with an increase in the percentage of WFS. It is evident that absorption values decrease with curing age, which can be confirmed from the results of compressive strength and porosity of mixes with age. Reduction is noteworthy at testing age of 365 days where the water absorption values decreased significantly compared with all the mixes at 28 days of curing. Durability increases with curing age as the permeability of mixes decrease with curing period. The explanation for increased durability with age was probably due to hydration of cement and another cementitious component of mixes like fly ash in this case which, being one of the components of design mix, lead to increased compressive strength, decreased porosity and absorption at a later age. On the contrary, it is worth noting that WFS being non-pozzolanic does not contribute to hydration reaction, whereas it only fill voids, and makes the matrix dense. However, on replacement of the river sand with WFS by volume, the water molecules got absorbed and adsorbed by the larger surface area of finer WFS particles. It also resulted in reduced density and effective water-binder ratio making it less workable, causing inadequate hydration with increased porosity. Subsequently, the increased pores developed due to lesser paste formation in the hardened stage increased the permeability and capillary action during water travel *(Dinakar et al., 2008).*

The sorptivity increases when the pores align themselves to form capillary tubes *(Booya et al., 2015).* Minimizing sorptivity is of utmost importance for concrete transport properties and mechanisms. Sorptivity at various ages i.e. 28, 90, and 365 days showed an initial rate of absorption and secondary rate of absorption. Figures 4.43 and 4.44 shows the initial rate of absorption (S_i) i.e. rate of capillarity of water was observed at 6 hours and the secondary rate of absorption (S_s) was observed up to

8 days of testing at 28, 90 and 365 days of curing. The initial rate of absorption varies with WFS inclusion, but the secondary rate of absorption is almost constant. The secondary rate of absorption calculations indicated an increasing trend with the inclusion of WFS at 28 days, while there was no significant change in the values at 90 and 365 days. The possible explanation for this may be that the larger pores in concrete are initially saturated faster and the smaller pores are gradually filled with time *(Aïssoun et al., 2016).* At 28 days, the calculated values of S_i for WFS0 and WFS5 were 0.0039 and 0.0035 respectively. Further, an increasing trend with values 0.0041, 0.0043, 0.0046, 0.0048, and 0.0052 was observed for WFS10 to WFS30 respectively. In general value of sorptivity increases except for WFS5 (0.0035) at 28days where S_i had the lowest values. In case of S_S, the sorptivity coefficient is almost same for WFS0, WFS5 and WFS10 i.e. 0.0017, then for WFS15, WFS20, WFS25 and WFS30 its 0.0022, 0.0022, 0.0023 and 0.0025 respectively. Further, the values of S_i ranged from 0.0033 to 0.0067 and 0.0015 to 0.0035 on extended exposure to water at 90 and 365 days respectively. These results of S_i showed that utilizing WFS leads to porous SCC and eventually reduced durability at 28 days. The finer WFS particles disrupt the overall grading of mixes which can be seen in Figure 3.4. The majority of WFS particles fall within the same size range contributing to inadequate grading, increased capillary pores and sorptivity. It can be inferred from the results that higher the values of sorptivity, the higher will be the rate of absorption, the volume of capillaries, and consequently more deterioration of concrete.

The results of sorptivity represented that there was no substantial change in the values of sorptivity at 28 and 90 days of curing. However, sorptivity values decreased considerably at testing age of 365 days. This may be attributed to its pore size refinement which decreased sorptivity coefficient values. In the present scenario, improvement of durability with curing age is measured by the study of pore connectivity. The probable reasons for improved durability due to a decrease in sorptivity with age are modified pore structure and reduced size of capillary pores *(Dinakar et al., 2008).* Sorptivity results depict these results are consistent with water absorption and VoPP results tabulated in Table 4.8. It was found that the sorptivity (initial rate of absorption and secondary rate of absorption) follows the increasing trend with inclusion of WFS (0-30%) in SCC mixes. Whereas, the values of sorptivity

showed a decreasing trend at 365 days due to long term hydration reactions of cementitious materials, making the specimen denser.

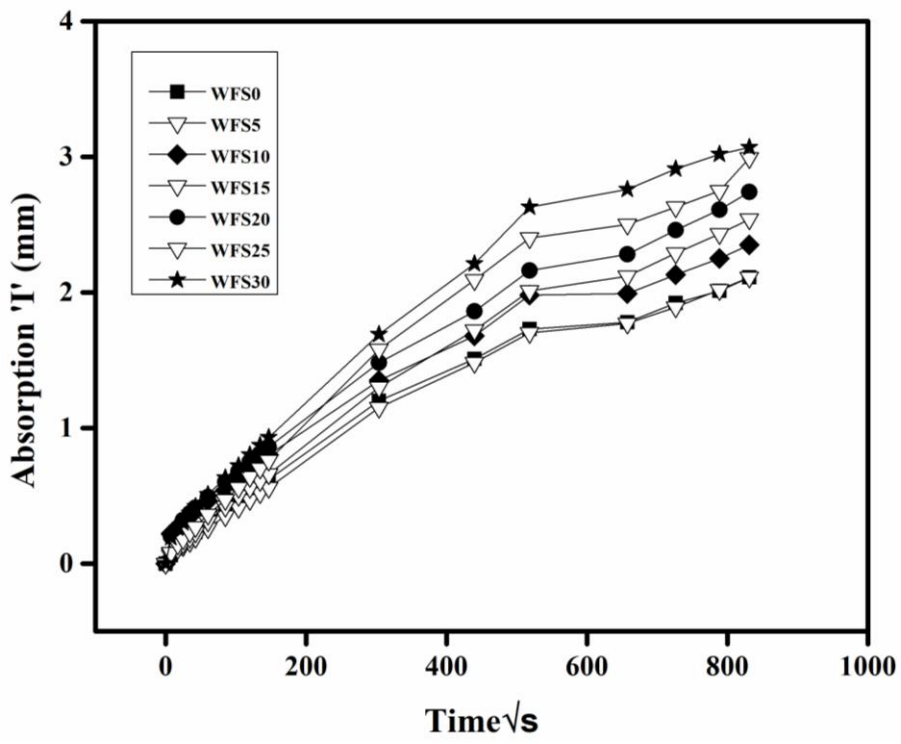

Fig. 4.40 Water absorption (by capillarity) of SCC mixes at 28 days

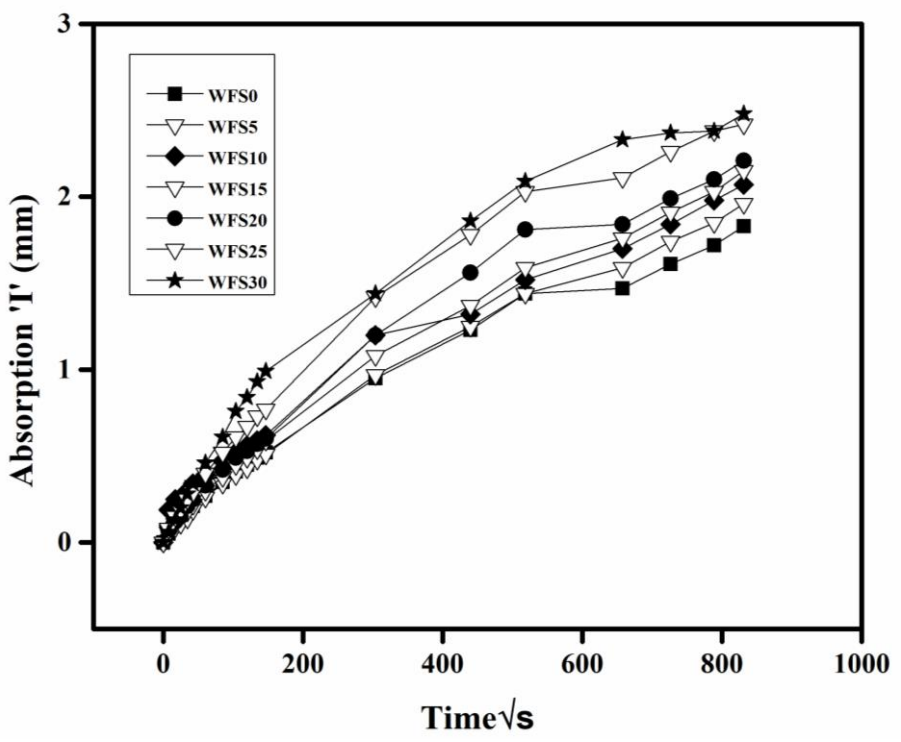

Fig. 4.41 Water absorption (by capillarity) of SCC mixes at 90 days

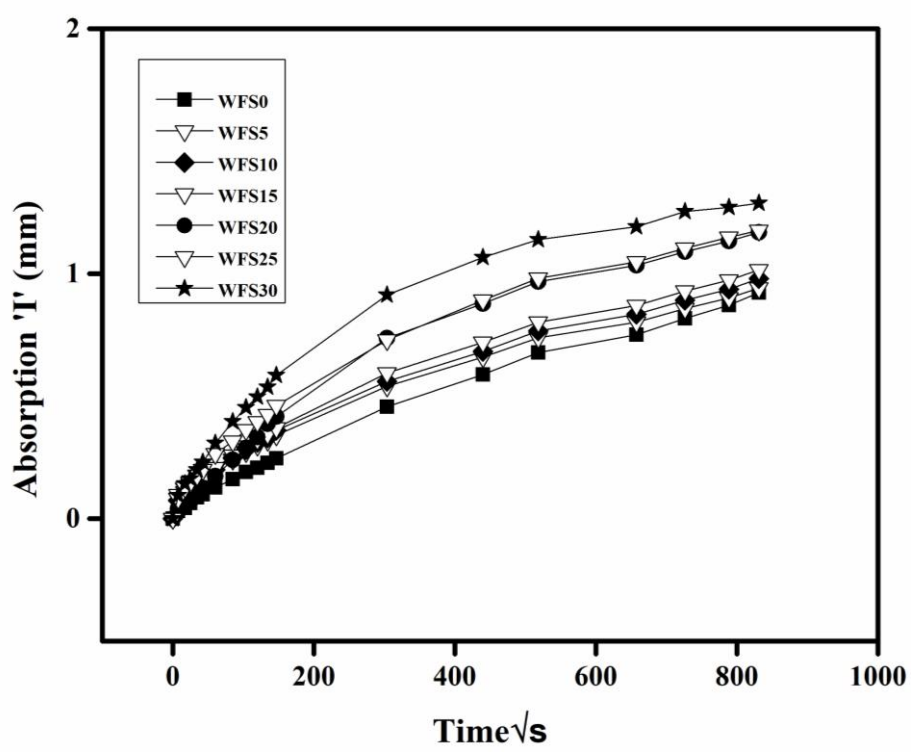

Fig. 4.42 Water absorption (by capillarity) of SCC mixes at 365 days

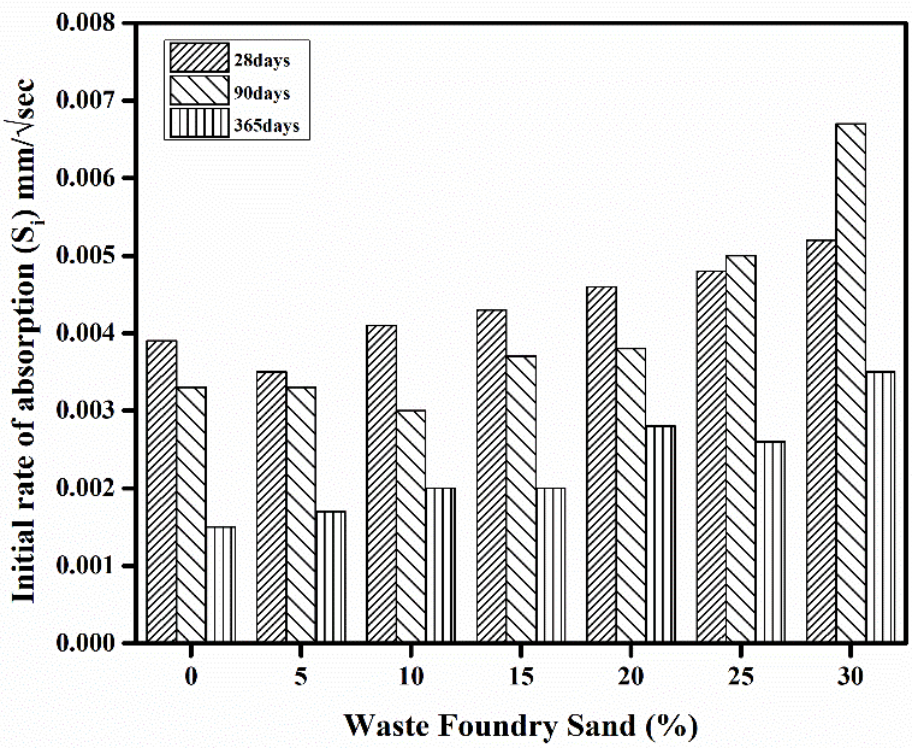

Fig. 4.43 Initial rate of absorption of SCC mixes

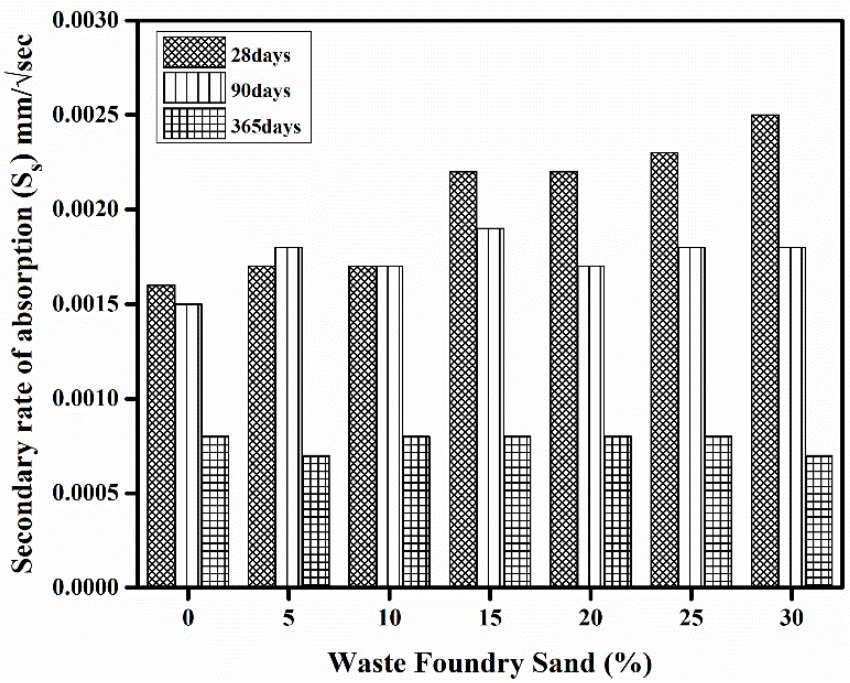

Fig. 4.44 Secondary rate of absorption of SCC mixes

4.2.4.4 Sulphate Attack

The major factors for sulphate attacked concrete are porosity and permeability of concrete along with the chemical resistance of cementitious materials in the mix *(CCAA, 2011).* Sulphate attack is a chemical breakdown in which the compounds (sulphate ions) percolates into the concrete surface and travel through its pores. These chemicals react slowly with chemically active components to deteriorate the concrete structure by formation of ettringite (calcium sulphate hydrate), gypsum (calcium sulphate dehydrate), and brucite. Further, leading to spalling, cracking, mass variation, and strength loss. Thereafter, the durability of concrete is affected due to changes in the mechanical properties of the concrete.

Visual Examination

The 28 days water cured SCC samples were immersed in magnesium sulphate solution for studying the effect of sulphate attack. Further, the SCC mixes were visually examined carefully at all testing ages i.e. 28, 90, and 365 days after immersing them into sulphate environment. It was observed that no spalling, cracking, or breaking of edges of the samples occurred at any testing age, which can be verified from Figure 4.45. There were no visible effects after 28 and 90 days of sulphate attack. However, at 365 days of exposure to sulphate environment white precipitates were observed on the SCC samples.

Mass variations

The change in mass of various SCC samples immersed in sulphate solution with and without WFS was evaluated. It was observed that there was no mass change up to the age of 90 days. At the age of 365 days, the mass gain was observed in concrete samples. Also, the pores of SCC samples got filled due to the ingress of sulphate solution leading to mass gain at higher replacement levels of WFS. Although, the mass change was not significant the percentage mass gain in SCC samples ranged from 0.09 to 0.45% at 365 days of curing.

Compressive Strength

The compressive strength results of concrete samples after immersion for 28, 90, and 365 days in sulphate solution are presented in Figure 4.46. When these results were compared with water cured samples, the strength loss was observed in sulphate cured samples and are shown in Figure 4.47. For instance, the compressive strength at 28 days of sulphate cured samples reduced nearly 5% in comparison to water cured samples.

The loss in compressive strength of SCC mixes at 28 days in the sulphate environment with WFS replacement levels up to 30% varied from 6.51 to 18.29%. The sulphate environment started its action vigorously at the age of 90 days resulting in loss of 8.30 to 23.10% compressive strength. Further, an even more, prominent impact on SCC mixes was observed at 365 days of sulphate attack causing the loss in strength of 6.34 to 28.28%. The inclusion of WFS reduced the compressive strength of the mixes at all ages by the reason of sulphate environment. Magnesium sulphate attack contributes to the formation of brucite, i.e. $Mg(OH)_2$ which is less soluble precipitates calcium hydroxide and other calcium phases. Also, Mg^{2+} decreases the pH of pore solution to acidic causing dissociation of calcium ions to form gypsum. Furthermore, it transforms C-S-H into non-cementitious and non-pozzolanic M-S-H of a non-binding type which contributes to a loss of concrete strength *(Piasta et al., 1985; Santhanam et al., 2001).* However, all the SCC samples showed good strength in comparison to control mix strength. These results depicted that the concrete in the sulphate solution immersion condition shows satisfactory performance by maintaining the minimum desired strength. The mixes continued to achieve higher strength than the 28-day water cured SCC samples even after immersion of these samples in

sulphate bearing solution. However, there was a reduction in the compressive strength of the mixes with an increase in the percentage of WFS.

The compressive strength of 50.74 N/mm^2 was observed in WFS30 on exposure conditions of sulphate solution for 365 days. However, with age the SCC mixes gained higher strength than 28-day water cured samples, there was an increase in compressive strength due to continued hydration reaction. All the mixes maintained design compressive strength probably due to continuous hydration process even after the attack of sulphate solution. The overall performance of WFS in SCC mixes was satisfactory due to two simultaneous processes of softening and hardening *(Boudali et al., 2016).* The higher cementitious material (cement and fly ash) content and low water-binder ratio in all SCC design mix resulted in increased strength with age even in sulphate environment because of continuous hydration reaction *(CCAA, 2011)*. The results at 90 days and 365 days showed that WFS incorporated SCC to have acceptable resistance to sulphate attack at all replacement levels of WFS. However, compared with water cured concrete samples at the testing age of 90 and 365 days, there was a reduction in compressive strength.

In conventional concrete, resistance to sulphate attack decreased with an increase in the substitution rate of WFS probably due to sulfur present in WFS. The sulfur reacted with sodium sulphate and magnesium sulphate to form ettringite which resulted in decreased strength *(Ikumi et al., 2019; Prabhu et al., 2015).*

Fig. 4.45 SCC specimens after 365 days of sulphate attack

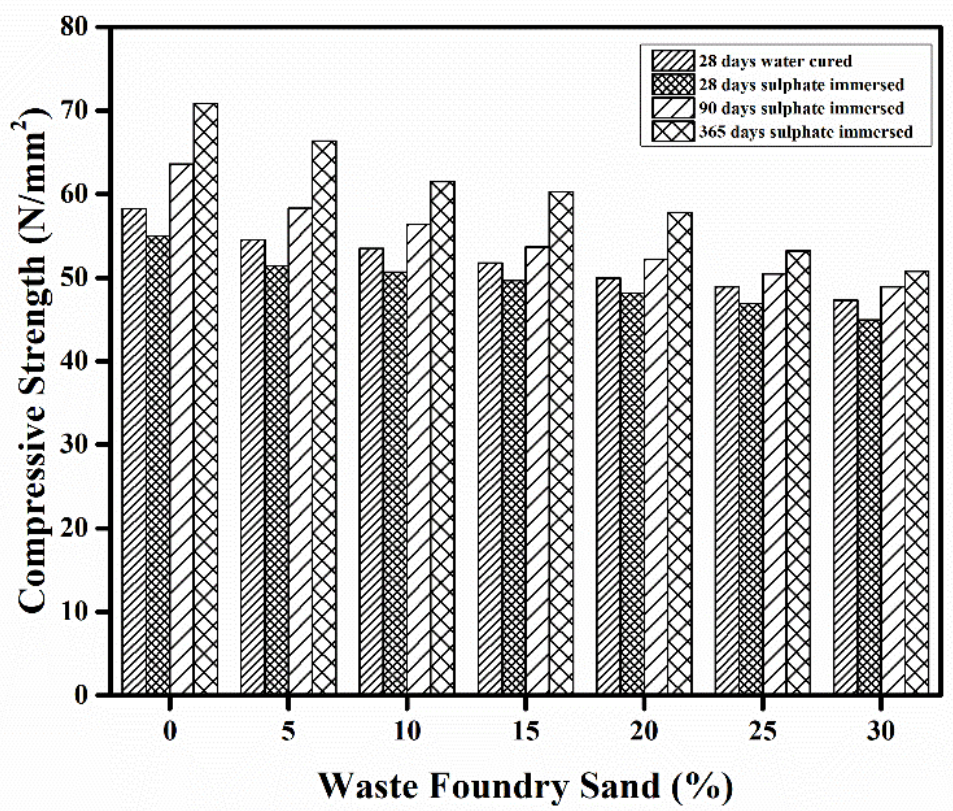

Fig. 4.46 Compressive strength of sulphate attacked and water cured SCC mixes

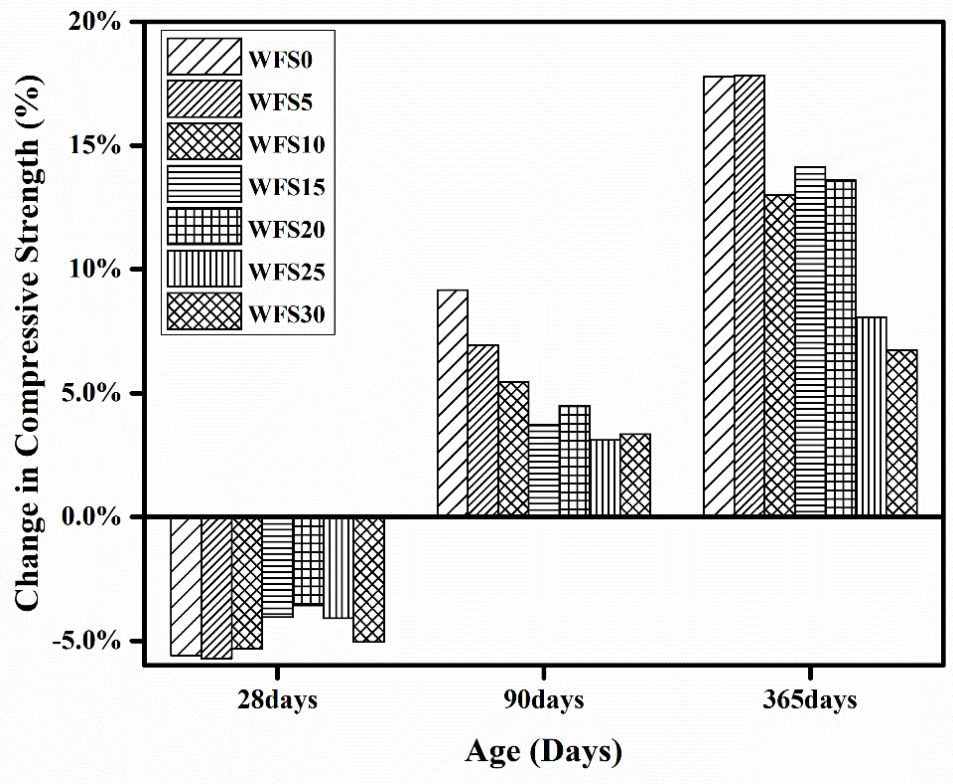

Fig. 4.47 Percentage variation in compressive strength of sulphate attacked SCC mixes w.r.t water cured samples at different curing age

4.2.5 Microstructural Analysis and Phase Identification (Objective 4)

4.2.5.1 Microstructure

The performance of each ingredient of concrete can be linked to its microstructure. Microstructure analysis of SCC mixes with and without WFS was performed by means of scanning electron microscope (SEM) images. SEM images were obtained using secondary electron (SE) image mode for representing the structure of SCC samples. SEM images of SCC include all significant information of particles shape, texture, interfacial phase, voids, and cracks. The formation of different phases such as portlandite (P), calcite, ettringite (E) and calcium silicate hydrate (CSH) developed in the concrete are marked on the SEM images of various SCC mixes at 28, 90 and 365 days and are shown in Figures 4.48, 4.49 and 4.50, respectively. SCC has a composite structure consisting of the solid phase, voids, and water.

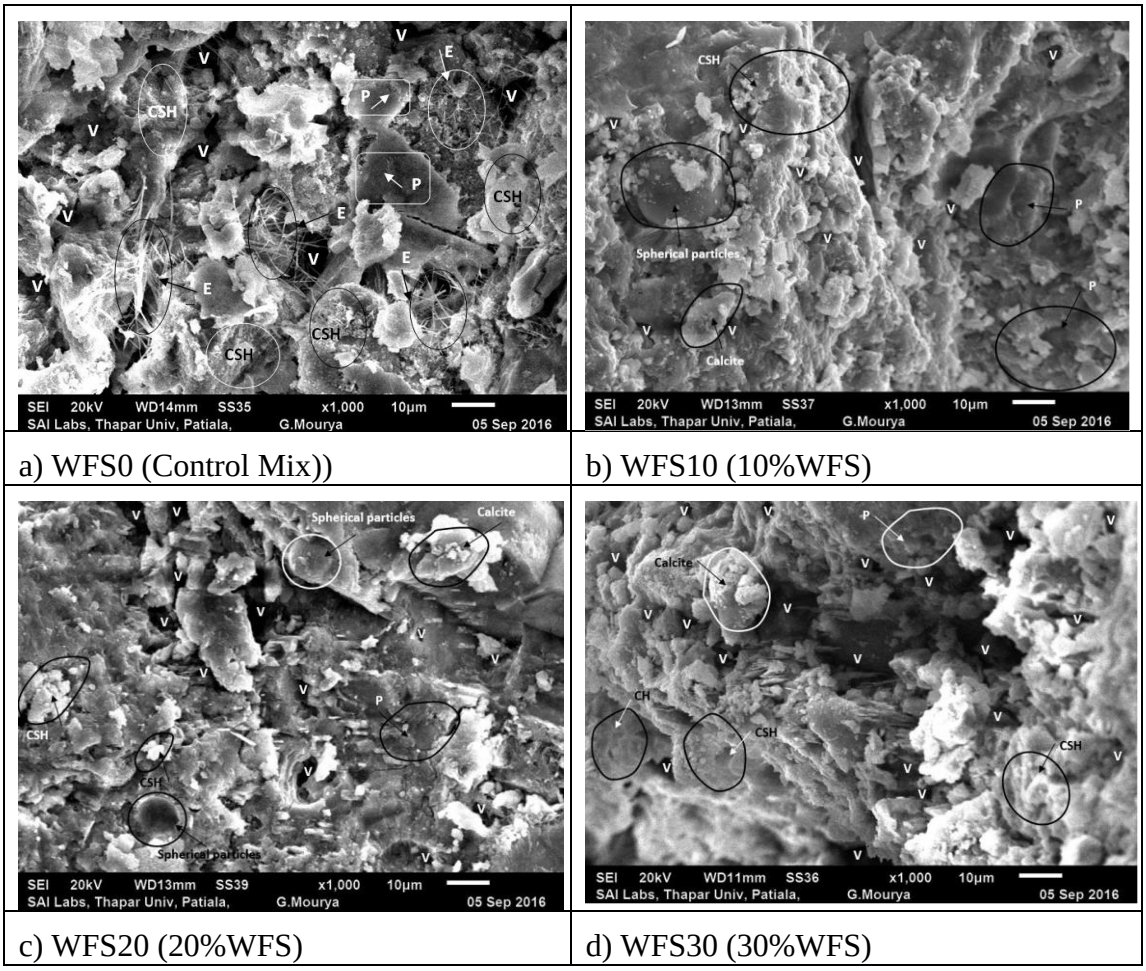

a) WFS0 (Control Mix)) b) WFS10 (10%WFS)

c) WFS20 (20%WFS) d) WFS30 (30%WFS)

Fig. 4.48 SEM micrograph of SCC mixes (a), (b), (c), (d) at 28 days of curing period

The long needle crystal kind micromorphology of ettringite in the voids of aggregate interfaces and plated morphology in the solid phase of paste i.e. calcium hydroxide is

clear in SEM image of control mix. The ettringite found in the early age of WFS0 at 28 days is marked in Figure 4.48 (a) that controls the stiffening of concrete. It spreads in the empty space of the interfacial transition zone (ITZ) in concrete by providing hexagonal rod shape filler effect. In the initial stage, micro cracks emerge in the interfacial transition zone which is weakest part of the concrete *(Smarzewski et al., 2018).*

The presence of spherical shaped particles in WFS10, WFS20 at 28 days is due to the increased content of WFS shown in Figure 4.48 (b) & (c) respectively. In Figure 4.48 (d), the formation of large voids and portlandite is clearly visualized in WFS30 at 28 days which may probably be the reason of reduced strength of SCC that validates the compressive strength results.

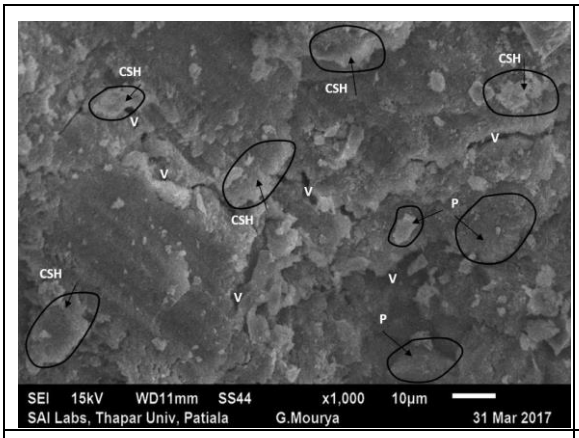

a) WFS0 (Control Mix)

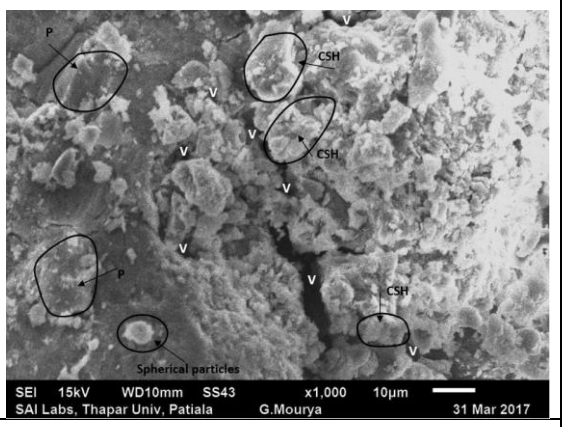

b) WFS10 (10% WFS)

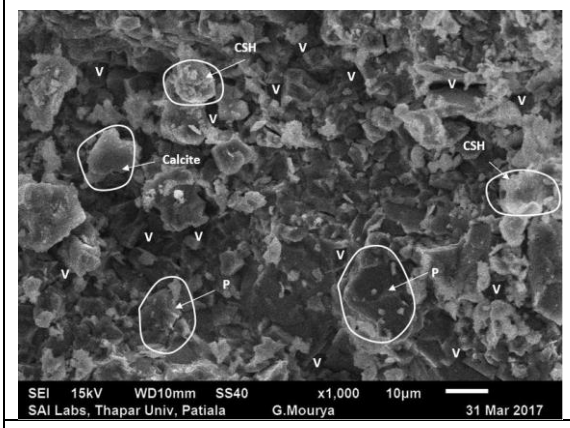

c) WFS20 (20% WFS)

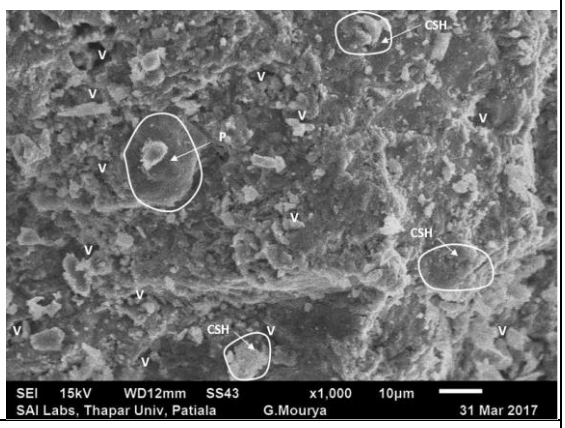

d) WFS30 (30% WFS)

Fig. 4.49 SEM micrograph of SCC mixes (a), (b), (c), (d) at 90 days of curing period

At 90 days of curing period, the homogeneous structure can be observed in SEM images of SCC mixes at various levels of WFS replacements with fine aggregates in Figures 4.49(a), (b), (c) and (d). In the present study, the additional supplementary

cementitious material i.e. fly ash was used in SCC which reacts with calcium hydroxide to form additional CSH gel as filler product and improves the impervious property of structure resulting in improved strength. The fly ash helps the SCC to gain later age strength which can be validated by compressive strength results at curing age of 90 days.

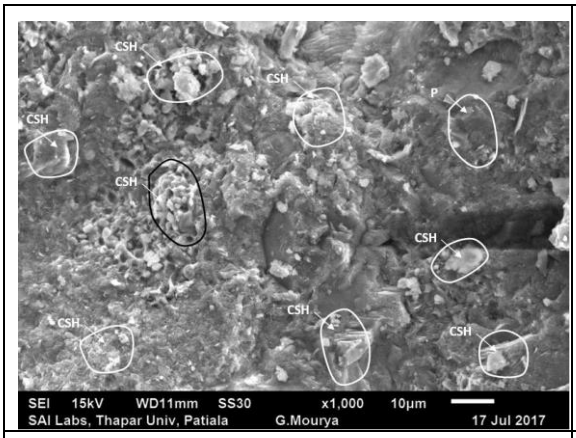

a) WFS0 (Control Mix)

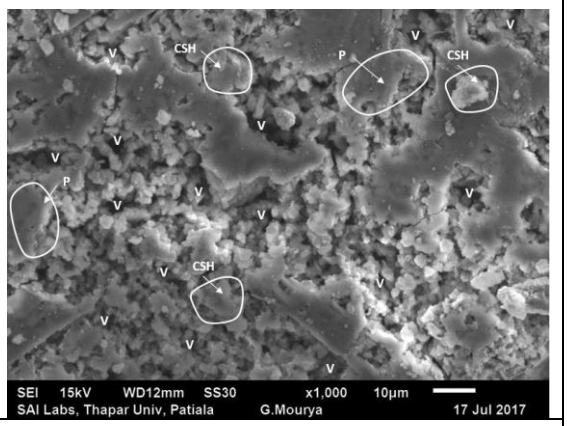

b) WFS10 (10% WFS)

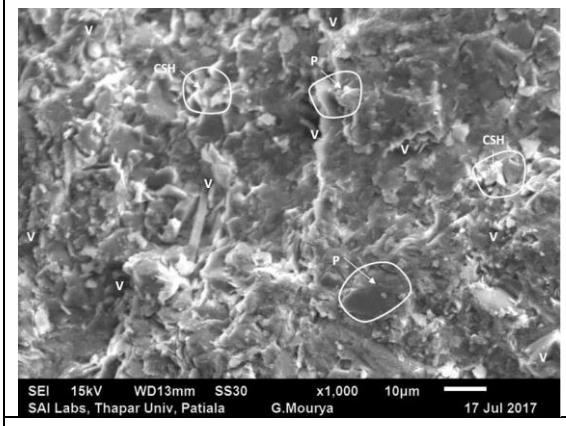

c) WFS20 (20%WFS)

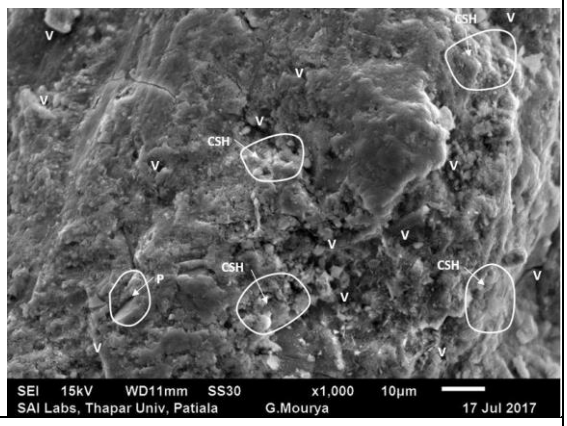

d) WFS30 (30%WFS)

Fig. 4.50 SEM micrograph of SCC mixes (a), (b), (c), (d) at 365 days of curing period

Whereas, the SEM image of WFS0 at 365 days in Figure 4.50 (a) depicts a compact and crystal phase of the concrete structure. The reduction in voids with age can be observed in the SEM images. CSH is more evenly distributed over the entire image as compared to the control mix at the age of 28 days. The same trend is also observed in compressive strength where WFS0 at the age of 365 days achieved the strength of 75.56MPa. The microstructure of WFS0 at 365 days leads to the densification of pore structure and reduced porosity. Also, it is clear from the SEM images that SCC mixes at 365 days have evenly distributed CSH gel resulting in the compact and homogeneous structure as compared to the SCC mix at 28 days. At 365 days of curing WFS30, Figure 4.50 (d) showed denser morphology and a smaller number of voids in

comparison to WFS30 at 28 days as shown in Figure.48 (d). On the contrary, at the age of 365 days, WFS30 depicted less formation of CSH gel and a larger number of small voids in comparison to WFS0 (365 days). Therefore, it can be concluded that the SCC mixes showed denser morphology and enhancement of strength with curing age. Whereas with an increase in substitution rate of WFS, the voids and pores were observed prominently, contributing to a reduction in compressive strength.

4.2.5.2 XRD

XRD test was conducted on the powdered samples of different proportions of hardened SCC mixes. Figures 4.51 to 4.56 shows XRD diffraction pattern of WFS0, WFS15 and WFS30 mixes at 28 and 90 days of curing. XRD analysis indicates the presence of silica, calcite, calcium silicate, calcium silicate hydrates and portlandite at 2theta angles 26.69°, 29.45°, 28.12°, 32.07°and 34.10°, respectively. In WFS0 and WFS15 hump was formed due to amorphous calcium silicate hydrates between 31° to 33°whereas in SCC 30 there was hump from 30° to 33°. No sharp peaks were observed for the amorphous phase present in the SCC mixes. From the results, it was found that no additional compounds were formed in SCC mixes with the substitution of WFS.

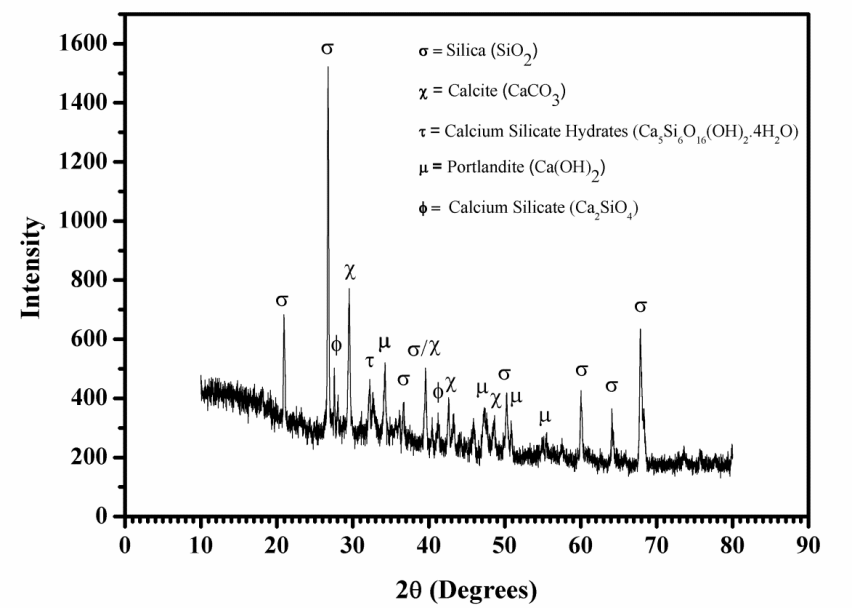

Fig.4.51 XRD of WFS0 at 28 days

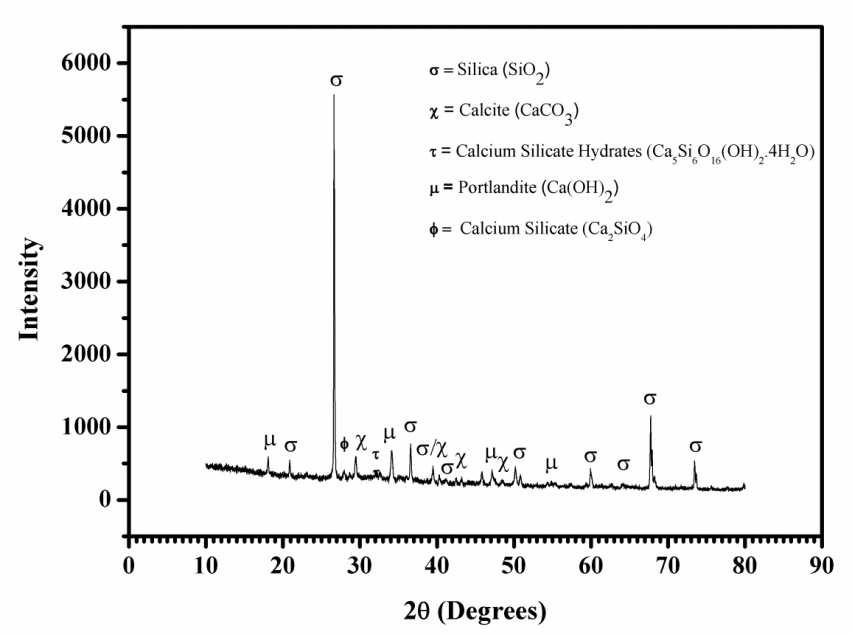

Fig.4.52 XRD of WFS15 at 28days

There were no qualitative changes found in the chemical composition of SCC mixes. It was observed that portlandite (cement hydration product) peaks were increased which an undesirable weaker product that leaches out with time is resulting in decreased strength. The major peaks of calcite at 29° were decreasing and additional silica peaks were seen with increased replacement level of WFS. It decreases the gel matrix formation and increases the inert filler content which leads to reduced strength. These results are in harmony with compressive strength values.

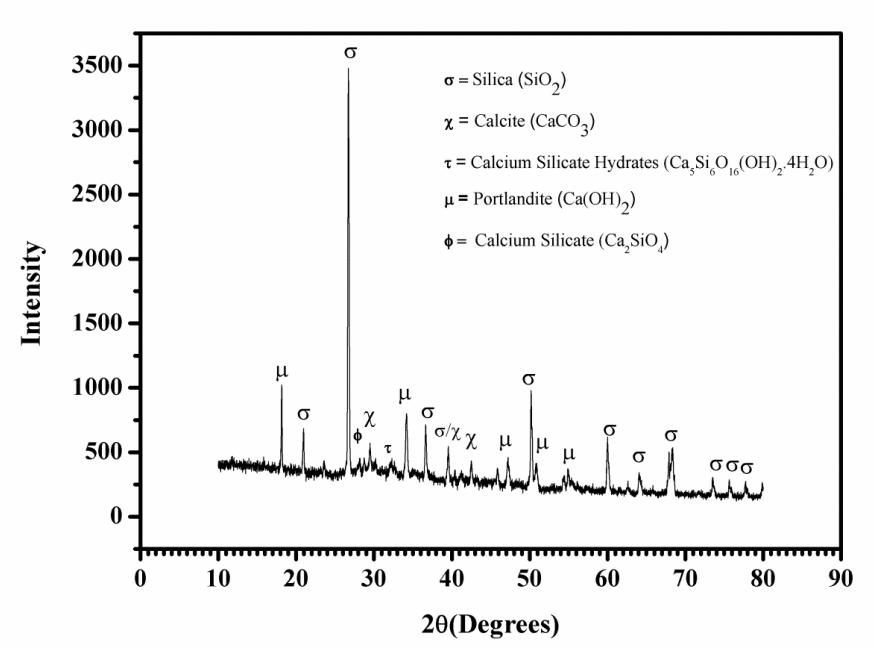

Fig.4.53 XRD of WFS30 at 28 days

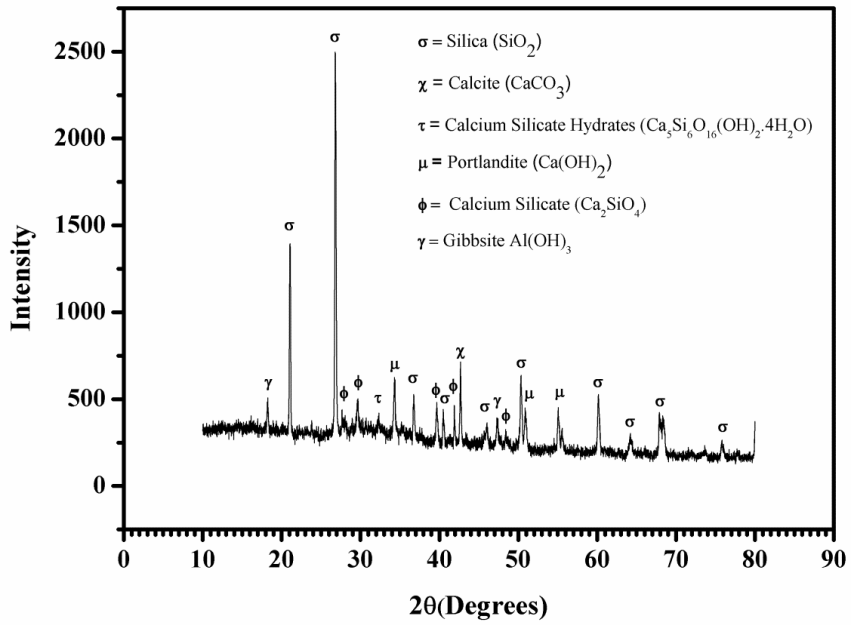

Fig. 4.54 XRD of WFS0 at 90 days

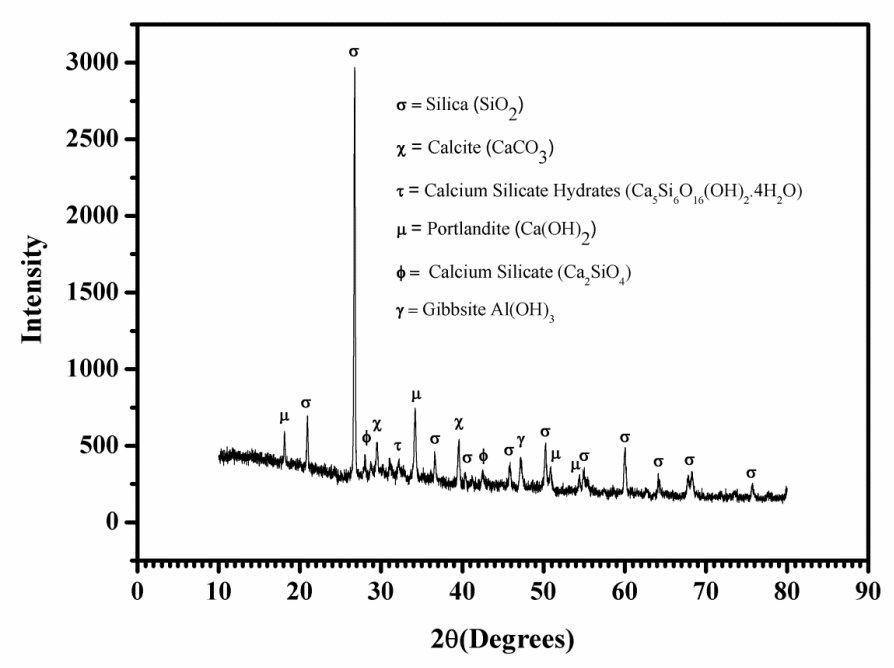

Fig. 4.55 XRD of WFS15 at 90 days

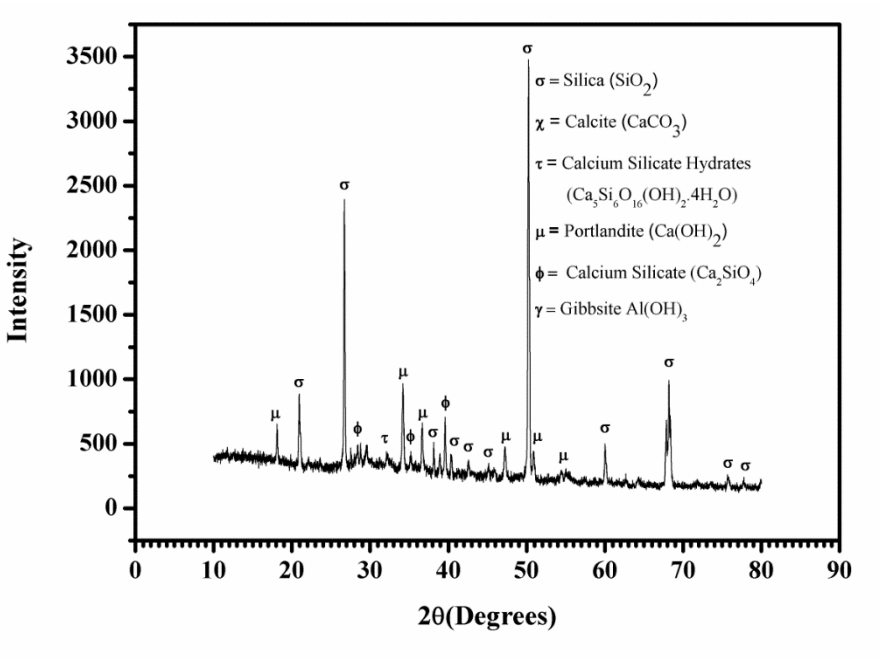

Fig. 4.56 XRD of WFS30 at 90 days

4.2.6 Statistical Analysis

The splitting tensile strength is not directly evaluated from the tensile load, hence the relation between compressive strength and tensile strength can be used for prediction of mechanical properties of SCC with WFS. The correlation between compressive strength and tensile strength of SCC mixes at the testing age of 7, 28, 90 and 365 days was evaluated. The value of R at 7, 28, 90 and 365 days were 0.99, 1, 0.99 and 0.96, respectively. A positive value of R reveals that there is a perfect positive correlation between compressive strength and splitting tensile strength i.e. if compressive strength value decreases, tensile strength decreases subsequently. The slope of the regression line is positive, which proves a positive correlation between the compressive and splitting tensile strength.

Statistical investigation was carried out on RCPT, VoPP and sorptivity using two-way ANOVA. The dependent variables were the durability parameters such as RCPT and VoPP, total water absorption and fixed factors were curing age (days) and varying percentage of WFS. It was determined whether the data was statistically significant. It was observed that values are highly significant with curing age and percentage of WFS (%) for RCPT, VoPP and total water absorption given in Table 4.9.

RCPT test results were analysed and it was observed that the results were statistically significant for all ages i.e. the p value (0.0000) was less than 0.05 (5% significance level) therefore the values of RCPT were significant at all ages. It can be interpreted

from the results that with age there was significant difference in the values of charge passed (RCPT) values. Pairwise comparison results also signified the relevance of curing age on RCPT. The effect of WFS content on RCPT values were also statistically significant and values were found to greater than 0.05. Further Post hoc tests was conducted on various percentages of WFS at 28, 90 and 365 days. At 28 days increase the Post hoc values reveal that the change is significant when WFS content varies from (0-30%), at 90 days inclusion of WFS is insignificant up to 10% replacement of WFS, beyond which the change is significant with p value of 0.011, 0.003, 0.000 and 0.000 at 15, 20 ,25 and 30% respectively (level of significance 0.05) . At 365 days, the p value is greater than (0.05) signifying insignificant difference up to 15% replacement level. Further at 20% the values start to have significant difference. It can be concluded with age, durability is not negatively affected with inclusion of WFS up to 15% replacement level of WFS.

When Post hoc Tukey HSD was conducted on VoPP the results were insignificant up to 15% WFS at 28 days, at 90 days insignificant up to 25% concluding WFS did not had detrimental effect on durability of SCC up to 25% .Further at 365 days, all results with WFS content up to 30% were statistically insignificant signifying that WFS does not have negative impact on durability.

Table 4.9 Tests of between subjects effects using two-way ANOVA

Dependent Variable: Charge Passed (Coulombs)		
Parameter	F value	Significance
Age (Days)	4756.93	0.00
WFS (%)	124.14	0.00
Age * WFS (%)	33.41	0.00
R Squared = .996 (Adjusted R Squared = .994)		
Dependent Variable: VOPP (%)		
Parameter	F value	Significance
Age (Days)	3581.958	0.00
WFS (%)	40.895	0.00
Age * WFS (%)	3.673	0.00
R Squared = .994 (Adjusted R Squared = .992)		
Dependent Variable: Rate of water absorption (mm)		
Parameter	F value	Significance
Age (Days)	1153.7	0.00
WFS (%)	53.427	0.00
Age * WFS (%)	5.094	0.00
R Squared = .985 (Adjusted R Squared = .977)		

*. The mean difference is significant at the .05 level.

4.3 INCORPORATING RHA AND WFS AS CEMENT AND FINE AGGREGATES REPLACEMENT IN SCC

4.3.1 Development of SCC (Objective 1)

The SCC mixes were designed to achieve the fresh state properties using EFNARC (2005) guidelines with characteristic strength of 50 MPa at 28 days of curing. The compressive strength achieved by the control mix at 28 days of curing was 58.44 MPa. Cement content of 500kg/cum was used for the control mix. Fly ash as a mineral admixture was used with constant value of 40kg/cum in the SCC mixes. Seven SCC mixes were prepared with a superplasticizer content of 1.17% by weight of cementitious materials and a constant water-powder ratio of 0.36. All these mixes were prepared to evaluate the fresh, compressive strength and durability properties of SCC. The composition of seven mixes of SCC were prepared by replacing cement with RHA (by weight) up to 30% at an increment of 5% and fine aggregates were partially replaced with WFS (0-30%) by volume in the design mix. The mixes were titled as R0WFS0, R5WFS5, R10WFS10, R15WFS15, R20WFS20, R25WFS25, and R30WFS30 for 0 to 30% of RHA and WFS substitution, respectively. Mixture proportions are given in Table 4.10.

Table 4.10 Mix Proportions of SCC with RHA and WFS

Mix	Cement (OPC) (kg/m³)	Fly Ash (kg/m³)	RHA (kg/m³)	Coarse Aggregate 10mm (kg/m³)	Fine Aggregate$_b$ (FA_{35}+FA_{65}) (kg/m³)	WFS (kg/m³)	Water$_a$ (kg/m³)	Admixture (kg/m³)	Density (kg/m³)
R0WFS0	500	40	0	672	1015	0	196	6.32	2429
R5WFS5	475	40	25	669	961	49	196	6.32	2422
R10WFS10	450	40	50	667	907	98	196	6.32	2414
R15WFS15	425	40	75	665	854	147	196	6.32	2407
R20WFS20	400	40	100	662	801	195	196	6.32	2400
R25WFS25	375	40	125	660	748	243	196	6.32	2393
R30WFS30	350	40	150	658	695	290	196	6.32	2386

Note: The coarse and fine aggregates used in concrete mixes are SSD condition.

a: The water content described in the table is free water content used in the mix.

b: The fine aggregate used in the mix is composed of 35% of fine sand and 65% of coarse sand.

4.3.2 Fresh Properties (Objective 2)

Fresh properties (passing ability, flow ability, filling ability, viscosity, and segregation resistance) directly affect the in-situ properties of hardened concrete. Slump flow

measures flow ability. V-funnel, T_{500} measures viscosity which is essential for good surface finish. VS1/VF1 are good with filling capacity of concrete even with congested reinforcement, self-levelling, better surface finished and may have more bleeding and segregation. VS2/VF2 may have problem in surface finish and have thixotropic effects. Passing ability is the ability of fresh concrete to flow through narrow opening such as between steel reinforcement bars without segregation or blocking. L-box and U-box measures passing ability. Addition of RHA and WFS leads to robust concrete. All mixes lie in classification conforming PA2 (structure with gap of 60 to 80 mm and good for all civil engineering structures). Fresh properties of SCC mixes with RHA and WFS are tabulated in Table 4.11

Table 4.11 Fresh properties of SCC with RHA and WFS

Mix ID	Flowability Test				Passing Ability			
	Slump Flow		V-Funnel Time (Sec)		L-Box			U-Box
	Diameter (mm)	T_{500} mm (Sec)	T_{10S} (Sec)	T_{5min} (Sec)	h_2/h_1	T_{200mm} (Sec)	T_{400mm} (Sec)	h_2-h_1 (mm)
R0WFS0	730 (SF2)	2.26 (VS2)	5.30 (VF1)	6.96 (VF1)	0.98 (PA2)	1.32	1.70	0
R5WFS5	730 (SF2)	2.76 (VS2)	5.76 (VF1)	7.43 (VF1)	0.96 (PA2)	1.68	2.29	4
R10WFS10	700 (SF2)	3.15 (VS2)	6.44 (VF1)	8.71 (VF2)	0.95 (PA2)	1.80	2.72	9
R15WFS15	680 (SF2)	3.52 (VS2)	8.02 (VF2)	9.40 (VF2)	0.89 (PA2)	2.10	3.16	16
R20WFS20	640 (SF1)	4.05 (VS2)	8.85 (VF2)	11.90 (VF2)	0.89 (PA2)	2.44	3.66	19
R25WFS25	600 (SF1)	4.28 (VS2)	10.08 (VF2)	12.15 (VF2)	0.84 (PA2)	2.61	3.51	24
R30WFS30	570 (SF1)	5.88 (VS2)	10.99 (VF2)	14.51 (VF2)	0.81 (PA2)	2.80	3.77	33

4.3.2.1 Slump flow

Slump flow is the vital fresh property to describe SCC. The slump flow diameter of R0WFS0 (control mix) was 730 mm. There were no visible changes observed in R5WFS5 and its slump flow value remained the same. The value of slump flow for R10WFS10 was found to be 700 mm which decreased by 30 mm from R0WFS0. Further, a reduction of 20mm in the slump flow diameter was observed for

R15WFS15 and value of slump flow was 680 mm. Furthermore, 640 mm, 600 mm and 570 mm slump flow values were observed for 20%, 25% and 30% replacements of RHA and WFS, respectively. The total loss of 160 mm was observed in slump flow values due to the inclusion of 30% RHA and 30% WFS in SCC mixes. All the SCC mixes ranging from 730 to 570 mm lied in SF2 and SF1 classes and were meeting the main criteria of classifying the concrete as SCC as per EFNARC. These mixes were ideally suitable for normal applications like the construction of walls and columns, slabs and tunnel linings. The slump flow diameter of R0WFS0 (control mix) was 730 mm. There were no visible changes observed in R5WFS5 and its slump flow value remained the same.

4.3.2.2 T_{500} (sec)

Slump flow and T_{500} both depict the flow-ability of SCC, which depends on the viscosity of the mixes. Therefore, it is important to ensure that all the mixes are flow-able to be termed as SCC. The time taken was 2.26 sec and 5.88 sec for R0WFS0 and R30WFS30 respectively. Even though all the mixes were flowing well and maintained fluidity. The time taken to reach the target slump flow of 500 mm increased as the flow-ability of mixes decreased due to an increase in viscosity. The water available for other ingredients in the matrix reduced due to increased adsorption of free water by finer and porous RHA. The paste maintained adequate viscosity with an increased number of fines, henceforth there was no honeycombing, bleeding, and segregation on visual observation.

4.3.2.3 V-funnel time (sec)

V-Funnel time was measured for all the SCC mixes. It is also a measure of obtaining the flow-ability of SCC. It gives a prediction of the performance of SCC in heavily reinforced sections and its final finish after concreting. The V-funnel experiment was carried out twice, once just after the mix had been made, and the second time after 5 minutes of rest. The results ranged from 5.30 sec to 10.99 sec immediately after mixes were prepared which showed that the time increased with an increase in RHA and WFS. Thereafter an increase from 6.96 to 14.51 sec was observed after letting it rest for 5 minutes. It signified that the flow-ability reduced in both cases with the addition of RHA and WFS. All of these test values were within the approved range by EFNARC. Moreover, the mixtures were found to be compact and viscous.

4.3.2.4 L-box

L-Box test was conducted to verify its practical applications in the heavily reinforced sections by evaluating the passing ability of SCC. This kind of assessment is important because it indicates the performance of SCC. In the present research, R0WFS0 exhibited the desired properties of SCC with a passing ratio (H2/H1) of 0.98. The results of H2/H1 indicating the passing ratio lied in the range of 0.98 to 0.81 showing a decreasing trend of workability. It was interpreted from the test values that the mixes lied in PA2 classification as per EFNARC. Smooth uninterrupted flow without blocking, honeycombing, segregation, and bleeding was observed in the mixes. However, the colour of the mixes was slightly blackish with the inclusion of RHA and WFS.

4.3.2.5 U-box

U-box test was conducted to evaluate the passing ability with the height difference values i.e. H2-H1 ranging between 0-33mm. These values were within the range of EFNARC. The values in this test also depicted the decreasing trend like other workability tests. The passing ability decreased with an increase in the percentage level of RHA and WFS in SCC. The results ranged from 0 to 24 up to R25WFS25 while for R30WFS30 the 33 mm height difference was marginally greater than EFNARC's recommended 30 mm value.

4.3.3 Strength Properties of SCC (Objective 2)

4.3.3.1 Compressive Strength

Table 4.12 shows the values of compressive strength of SCC mixes with RHA and WFS. At 7, 28, 90, and 365 days, the compressive strength of control mix specimens was 42.51, 58.44, 65.77, and 74.10 MPa, respectively. The percentage increase in compressive strength for the mixes R0WFS0, R5WFS5, R10WFS10, R15WFS15, R20WFS20, R25WFS25, and R30WFS30 was observed as 26.80%, 24.97%, 23.68%, 25.28%, 23.97%, 27.71%, and 28.87%, respectively, with age increasing from 28 to 365 days. At all ages, the blend R10WFS10 showed the development of highest strength, whereas R30WFS30 showed the lowest strength development. It is evident that mixes with replacement levels as high as 10% developed significant strengths.

Table 4.12 Compressive strength of RHA & WFS blended SCC mixes

Mix ID	7 Days		28 Days		90 Days		365 Days	
	fc (N/mm²)	SD	fc (N/mm²)	SD	fc (N/mm²)	SD	fc (N/mm²)	SD
R0WFS0	42.51	0.89	58.44	0.49	65.77	0.36	74.10	1.23
R5WFS5	44.35	0.64	61.11	0.29	68.43	0.89	76.37	0.33
R10WFS10	45.24	0.37	62.32	0.30	69.23	0.70	77.08	0.55
R15WFS15	43.16	0.51	59.66	0.47	66.69	0.16	74.74	0.58
R20WFS20	40.18	1.09	55.10	0.52	61.51	0.29	68.31	0.17
R25WFS25	37.68	0.71	51.21	1.31	59.31	0.84	65.40	0.60
R30WFS30	34.77	0.46	48.95	0.66	56.79	1.86	63.08	0.58

Note: f_c denotes compressive strength in N/mm^2, SD represents standard deviation

Compressive strength normally grows with curing age. For instance, the compressive strengths of blends R0WFS0 and R30WFS30 at curing age 28 days were around 58.44 MPa and 48.95 MPa, which is increased nearly 40% than strength at age 7 days. The quick pozzolanic reaction of the cementitious characteristics of RHA may be the cause of the higher early strength of RHA and WFS blended SCC. This pozzolanic reactivity can enhance the C-S-H gel in concrete production and can have an impact on the characteristics of hardened concrete. All mixtures outperformed the control mix in terms of strength up to 15% replacement level. It should be noted that the RHA and WFS blend SCC has a higher compressive strength which may be because by-product particles have higher fineness than OPC. Further replacing cement and fine aggregates with waste materials causes a considerable reduction in SCC strength while maintaining a consistent amount of binder content. The decrease in strength can be attributed to the demand in cement paste volume which is contributed to the poor interlocking between the aggregate and cement paste. The porosity of the mixture is increased, and its compressive strength is decreased with the addition of finer particles. It can be concluded from the results that compressive strength of the blended SCC, which included 10% RHA and 10% WFS, was 62.32 MPa at 28 days, 69.23 MPa at 90 days, and 77.08 MPa at 365 days. These values are 6.64%, 5.26%, and 4.02% greater than the control SCC at the corresponding ages, respectively. WFS is an inert material, whereas RHA has pozzolanic properties. These waste materials increase the fineness of the mix after 15% of partial replacement while decreasing the total quantity of cement and aggregates. As a result, the volume of the paste increases

while the volume of the solid aggregate decreases, which may be one of the reasons of the decrease in compressive strength after 15% of partial replacements.

4.3.3.2 Splitting Tensile Strength

Tensile strength as shown in Table 4.13 showed a substantial improvement in the SCC mixes for RHA and WFS blending up to 10%, and after that stage it declined significantly. At ages 7, 28, 90, and 365 days, the mix R10WFS10 exhibited maximum tensile strengths of 4.21 MPa, 5.09 MPa, 5.40 MPa, and 5.72 MPa, that were 3.80%, 4.52%, 5.37%, and 7.34% more than the control mix at those ages. This may be primarily attributable to the pozzolanic reaction and the capacity of RHA and WFS particles to fill small voids, both of which contributed to the enhancement of strength.

Table 4.13 Splitting Tensile Strength of SCC mixes with RHA and WFS

Mix ID	7 Days	28 Days	90 Days	365 Days
	fc (N/mm²)	fc (N/mm²)	fc (N/mm²)	fc (N/mm²)
R0WFS0	4.05	4.86	5.11	5.30
R5WFS5	4.11	4.93	5.36	5.57
R10WFS10	4.21	5.09	5.40	5.72
R15WFS15	4.04	4.77	5.15	5.47
R20WFS20	3.72	4.68	4.86	4.97
R25WFS25	3.57	4.44	4.62	4.71
R30WFS30	3.06	4.30	4.47	4.59

Note: f_c denotes compressive strength in N/mm^2

At 28 days, tensile strength variation in SCC using RHA and WFS replacement at 5%, 10%, 15%, 20%, 25%, and 30% was 1.44%, 4.73%, -1.85%, -3.70%, -8.64%, and -11.52%, respectively. Investigations have also been conducted on the relationships between the compressive and tensile strengths of all blends which have been cured for 7, 28, 90 and 365 days. At 28 days of curing, the SCC mixes containing 0% to 30% RHA and WFS have a splitting tensile strength to compressive strength ratio of between 8.07% and 8.78% as shown in Table 4.14. The ratio of tensile strength to

compressive strength is influenced by the amount of fine particles because they impact the quality of the paste and interfacial transition zone in the concrete. At 28, 90, and 365 days of curing, it was discovered that the splitting tensile strength of the SCC mixes with 30% RHA and 30% WFS blends was 11.52%, 12.52%, and 13.40% lower than control mix respectively. The quantity of fine particles in the mix is greater than the amount required to combine with the cementitious particles during the process of hydration, resulting in excess improper mixing and causing a deficiency in strength as it replaces most of the cementitious material but does not contribute to strength, which may account for the reduced tensile strength for replacement levels of RHA and WFS blends more than 10%.

Table 4.14 Splitting tensile strength to compressive strength ratio of RHA and WFS mixes

Mix ID	7days		28 days		90 days		365 days	
	Ratio C/T	Percentage of Tensile to Comp	Ratio C/T	Percentage of Tensile to Comp	Ratio C/T	Percentage of Tensile to Comp	Ratio C/T	Percentage of Tensile to Comp
R0WFS0	10.50	9.53%	12.02	8.32%	12.87	7.77%	13.98	7.15%
R5WFS5	10.79	9.27%	12.40	8.07%	12.77	7.83%	13.71	7.29%
R10WFS10	10.75	9.31%	12.24	8.17%	12.82	7.80%	13.48	7.42%
R15WFS15	10.68	9.36%	12.51	8.00%	12.95	7.72%	13.66	7.32%
R20WFS20	10.80	9.26%	11.77	8.49%	12.66	7.90%	13.74	7.28%
R25WFS25	10.55	9.47%	11.53	8.67%	12.84	7.79%	13.89	7.20%
R30WFS30	11.36	8.80%	11.38	8.78%	12.70	7.87%	13.74	7.28%

4.3.4 Durability Properties of SCC (Objective 3)

4.3.4.1 Rapid Chloride Permeability Test (RCPT)

The rapid chloride permeability test (RCPT) examines concrete's electrical conductivity to provide an immediate evaluation of its resistance to chloride ion penetration. Table 4.15 represents RCPT values for SCC mixes with RHA and WFS.

Table 4.15 RCPT of SCC mixes with RHA and WFS

Mix ID	28 Days		90 Days		365 Days	
	Charge Passed (Coulombs)	Result	Charge Passed (Coulombs)	Result	Charge Passed (Coulombs)	Result
R0WFS0	2167	Moderate	1213	Low	627	Very Low
R5WFS5	1338	Low	1012	Low	589	Very Low
R10WFS10	1173	Low	983	Very Low	473	Very Low
R15WFS15	1038	Low	896	Very Low	418	Very Low
R20WFS20	1263	Low	988	Very Low	445	Very Low
R25WFS25	1477	Low	1112	Low	501	Very Low
R30WFS30	1776	Low	1342	Low	526	Very Low

At the end of the experiment, the conductivity of saturated specimens was measured. The rapid chloride permeability test results of SCC control mix were 2167 Coulombs, 1213 Coulombs and 627 Coulombs after 28, 90 and 365 days of curing, respectively. The permeability of the specimen increases with the amount of charge passed during the test. Total charge passed through the control mix R0WFS0 was 2167 coulombs, whereas 1338, 1173, 1038, 1263, 1477, and 1776 coulombs were passed through the RHA and WFS blended SCC mixes R0WFS0, R5WFS5, R10WFS10, R15WFS15, R20WFS20, R25WFS25, and R30WFS30 respectively. It was observed that the permeability of RHA and WFS blended SCC mixes was reduced at all ages, up to 20% replacement levels. Thereafter, the permeability marginally increased. It may be due to the reason that the pore structure of SCC mixes refined with physically packed finer pozzolanic particles. RHA and WFS blended SCC mixes were found to be under the category of "low chloride permeability" after 28 days of curing. Whereas, low and very low permeability was observed at 90 and 365 days. It indicates that as the curing time for RHA and WFS blended SCC specimens increases, the penetration of chlorides decreases.

4.3.4.2 Water Absorption and Permeable Pore Space

The capacity to absorb water by capillary suction is referred to as absorption. A water absorption test was conducted to evaluate the resistance to water penetration. At ages 28, 90, and 365 days, the water absorption of control mix was 4.64%, 4.23%, and 1.40%, respectively, whereas the water absorption of mix R30WFS30 was 5.07%,

4.47%, and 1.59%. The volume of permeable pore space (VoPP) of the RHA and WFS blended SCC mixes was 13.24%, 12.98%, 13.03%, 13.62%, 14.03%, and 14.68% for R5WFS5, R10WFS10, R15WFS15, R20WFS20, R25WFS25, and R30WFS30, respectively, as compared to 13.29% of the control mix R0WFS0 after 28 days of curing. Specimens with 5%, 10%, and 15% RHA and WFS mixes showed a reduction in water absorption. The trends typically reveal a positive effect of RHA as a pozzolan on the water absorption properties of SCC specimens. The filling effects of fine RHA and WFS particles may be responsible for this trend. The observations are represented in Table 4.16, which shows that volume of permeable spaces clearly affects the absorption.

Table 4.16 Water Absorption and VoPP of SCC mixes with RHA and WFS

Mix ID	28 Days			90 Days			365 Days		
	Absorption after immersion %	Absorption after immersion and boiling %	VoPP (%)	Absorption after immersion %	Absorption after immersion and boiling %	VoPP (%)	Absorption after immersion %	Absorption after immersion and boiling %	VoPP (%)
R0WFS0	4.64	5.74	13.29	4.23	5.42	12.38	1.40	1.48	3.64
R5WFS5	4.53	5.77	13.24	4.05	5.31	12.25	1.36	1.46	3.56
R10WFS10	4.36	5.63	12.98	3.95	5.28	12.18	1.31	1.43	3.54
R15WFS15	4.48	5.72	13.03	4.03	5.28	12.31	1.38	1.47	3.61
R20WFS20	4.71	5.96	13.62	4.16	5.65	12.76	1.46	1.61	3.88
R25WFS25	4.87	6.21	14.03	4.25	5.93	13.12	1.52	1.66	3.97
R30WFS30	5.07	6.56	14.68	4.47	6.14	13.33	1.59	1.76	4.22

The observations show that higher replacement quantities lead to lower water absorption values because rice husk is finer than cement. The paste volume of the SCC has a significant impact on the influence of fine particles on the characteristics of the material. Thereafter, for all sample ages, an increase in the water absorption for SCC specimens with RHA and WFS blends was observed in comparison to the control SCC specimens. For a constant water binder ratio, concrete mixes with high paste volumes are often expected to have higher absorption values than concrete with lower paste contents. The SCC became more porous as a result of the inclusion of finer RHA and WFS particles because the SCC required more water to achieve the appropriate workability. The key factors affecting water absorption of SCC mixes are

its porosity, pore size, and pore inter-connectivity. The absorption will increase as the permeable voids increase.

4.3.4.3 Sorptivity

The sorptivity test was conducted as per ASTMC 1585-13. The tendency of a porous material to absorb and transfer water by capillary action is known as sorptivity. When the sorptivity value is lower, the concrete is considered to as water resistant. The measurements used to determine the initial and final sorptivity were made every 1 minute, 5 minutes, 10 minutes, 20 minutes, 30 minutes, 1 hour, 2 hours, 3 hours, 4 hours, 5 hours, 6 hours, 1 day, 2 days, 3 days, 5 days, 6 days, 7 days, and 8 days. After 1, 20, 60, 120, 180, 240, and 360 minutes of observation at the age of 28 days in the control mix, the ingress of water was found to be 0.05, 0.14, 0.28, 0.38, 0.48, 0.55, and 0.68 mm. The same values were recorded for R5WFS5 at 0.06-0.63 mm, R10WFS10 at 0.06-0.74 mm, R15WFS15 at 0.07- 0.71 mm, R20WFS20 at 0.12-0.81 mm, R25WFS25 at 0.13-0.90 mm, and R30WFS30 at 0.14-1.02 mm. At the age of 90 days, it was noted that 0.06, 0.20, 0.32, 0.39, 0.46, 0.51, and 0.63 mm of water had infiltrated after 1, 20, 60, 120, 180, 240, and 360 minutes of observation in R0WFS0. Further, for RHA and WFS mixes the ingression observed varied from 0.06-0.61 mm, 0.07-0.67 mm, 0.06-0.66 mm, 0.07-0.81 mm, 0.10-0.83 mm, and 0.12-0.96 mm for the concrete mixes R5WFS5, R10WFS10, R15WFS15, R20WFS20, R25WFS25, and R30WFS30. The amount of water that entered R0WFS0 after 1, 20, 60, 120, 180, 240, and 360 minutes of observation ranged from 0.06-0.45 mm at 365 days. Similarly, for mixes R5WFS5, R10WFS10, R15WFS15, R20WFS20, R25WFS25, and R30WFS30, which were recorded between 0.06-0.50, 0.08-0.51, 0.10-0.50, 0.10-0.52, 0.11-0.59, and 0.11-0.68 respectively.

The variation in absorption of R0WFS0 to R30WFS30 after 8 days of sorptivity experiment with the square root of time at 28, 90, and 365 days was also noted. The value of absorption increased from 2.10 to 2.60 with increment in RHA and WFS content up to 30% at 28 days. Further, the values of absorption ranged from 1.78 to 2.07 and 0.98 to 1.17 mm at 90 and 365 days respectively. It is evident that absorption values decrease with curing age, which can be confirmed from the results of compressive strength and porosity of mixes with age. The computed values for the initial sorptivity (Si) and final sorptivity (Ss) coefficients have all been shown in

Table 4.17. At all ages, there was marginal decrease in sorptivity value up to 10% of replacement level. The sorptivity value is decreased due to filling effect of finer pores and diminishing interconnected capillaries in the SCC specimens. Enhanced homogeneity and compact microstructure of SCC incorporating RHA and WFS are the cause of the sorptivity reduction. At 15% to 30% partial replacement levels of RHA and WFS in SCC blends, it was discovered that the sorptivity values significantly increased. The increased paste volume and decreased aggregate content may have contributed to the decreased permeability in this scenario.

Table 4.17 Sorptivity of SCC mixes with RHA and WFS

Mix ID	28 Days		90 Days		365 Days	
	Si (mm/√sec)	Ss (mm/√sec)	Si (mm/√sec)	Ss (mm/√sec)	Si (mm/√sec)	Ss (mm/√sec)
R0WFS0	0.0046	0.0017	0.0039	0.0014	0.0027	0.0006
R5WFS5	0.0041	0.0016	0.0038	0.0013	0.0032	0.0006
R10WFS10	0.0049	0.0015	0.0042	0.0013	0.003	0.0006
R15WFS15	0.0045	0.0018	0.0043	0.0013	0.0028	0.0006
R20WFS20	0.0049	0.0017	0.005	0.0012	0.0029	0.0005
R25WFS25	0.0056	0.0018	0.0051	0.0012	0.0034	0.0005
R30WFS30	0.0062	0.0021	0.0058	0.0014	0.0039	0.0004

4.3.4.4 Sulphate Resistance

Sulphate is one of the core aspects affecting SCC durability. After 90 and 365 days of immersion in the sulphate solution, there were no signs of spalling or other surface damage in any SCC specimens during visual inspection. The surface of the test specimens had developed a white film of precipitation. It was observed that there was no noteworthy variation in the final mass of specimens. The compressive strengths of SCC specimens that had been cured in a sulphate solution were comparable to control mix up to 10% replacement levels of RHA and WFS blends at all ages. The pozzolanic characteristics of RHA and the filling effect of WFS in the SCC mixes may be to responsible for the increase in the strength of the concrete soaked in sulphate solution because of hydration and pozzolanic reactions. According to test results, tabulated in Table 4.18 the introduction of RHA and WFS reduced the resistance to sulphate attack at 90 days and 365 days. The declining strength is a sign of matrix weakening because of the reduction in cement particles in the SCC mixes.

Table 4.18 Sulphate immersed compressive strength of SCC mixes with RHA and WFS

Mix ID	28 + 28 Days		28 + 90 Days		28 + 365 Days	
	fc (N/mm²)	SD	fc (N/mm²)	SD	fc (N/mm²)	SD
R0WFS0	59.42	0.59	66.60	1.50	72.56	0.73
R5WFS5	60.80	0.50	65.72	0.88	72.88	0.51
R10WFS10	60.48	0.60	66.07	0.76	72.69	1.00
R15WFS15	58.03	0.75	63.53	1.26	69.26	1.41
R20WFS20	55.59	0.49	60.34	1.54	65.51	1.08
R25WFS25	51.57	0.66	58.12	0.62	62.93	0.49
R30WFS30	49.24	0.47	55.38	1.32	59.45	0.97

Note: f_c denotes compressive strength in N/mm^2; SD represents standard deviation

The ongoing hydration and the development of expansive reaction products, such as ettringite, might explain this behaviour by densifying the matrix and making it more difficult for the sulphate ions to infiltrate. As a result, the matrix's densification has a significant impact than the penetration of sulphates. It was discovered that the strength had significantly dropped for RHA and WFS blended SCC mixes with replacement levels more than 10% at all curing ages.

4.3.5 Microstructure Analysis and Phase Identification (Objective 4)

4.3.5.1 Microstructure

In the present study, magnification of 1000x was used to identify all the phases present in the microstructure. Morphology of each hydrated and un-hydrated phase helps to differentiate the product formation in the mix which can be validated with strength and durability results for better understanding and interpretation. SEM images of the SCC mixes with RHA and WFS were obtained to investigate the microstructure aspects in the transition zone and paste around the aggregates. Energy Dispersive X-Ray Spectroscopy of the micrographs as also been used at various spectrums in the SEM images. When concrete hydrates, C-S-H gel, crystals, and other mineral compounds are formed which affect the unique characteristics of concrete. After 28 days of curing, the SEM image of R0WFS0 in Figure 4.57 shows a plated structure that mostly consists of calcium hydroxide in SCC blended with RHA and WFS. In comparison to the control mix and the RHA and WFS blended SCC specimen, it can be seen in Figure 4.58 that there is improved consistency in the interaction between the phases of the materials up to 10% replacement levels. The

improved structure of RHA and WFS blended SCC may be due to enhanced fineness of the mix, which activates the pozzolanic property and improves the interfacial zone between the aggregates and cement paste. The hardened properties and microstructure of SCC are altered by SCM, and these changes are being studied in the present study.The XRD pattern also revealed that mixing RHA and WFS to SCC transformed portlandite into C-S-H gel, changing the basic properties of the concrete. The self-compacting behaviour of the SCC changes considerably as fineness of filler increases. Therefore, the microstructure will become denser with the addition of finer particles by improving particle packing, which will reduce the amount of space that must be occupied by hydration products. However, these particles serve as points of interaction with hydration products, which leads to the hardening of the microstructure. It was observed from Figure 4.59 that micrographs of 20% RHA and 20% WFS blended SCC mixes showed both the partly and fully un-reacted particles. Whereas, Figure 4.60 shows the SCC specimens with 30% RHA and 30% WFS replacement levels i.e. R30WFS30 exhibited the large size fractures, interstices, and pores. It may be because the surplus water that remains after the hydration reaction evaporates, causing pores and cracks to form in the SCC specimens. The RHA in the blend appeared to increase the formation of ettringite and create a weaker structure, resulting in decreased calcium silicate hydrate homogeneity and internal structural strength. Some characteristics of the hydrated concrete structure, such as pore spaces (dark spots), aggregate particles, and the hydrated cement binder, may be seen on Figure 4.61.The amount of water absorbed and how that water absorbed is adjusted can both have a significant impact on the microstructure of the SCC. The behaviour of the SCC may be considerably influenced by such porosity. Figures 4.62 and 4.64 also displayed an improved ITZ with denser packing, improved compressive and tensile strengths, and better workability. After 365 days of curing, Figure 4.65 indicates the dense, solid, homogenous structure. The absence of voids or fissures in all micrographs of 365 days cured samples confirms the pozzolanic activity of RHA at a later age. The durability results also reveal a more compact structure that decreases permeability and porosity, which is supported by R10WFS10 micrographs in Figure 4.66.According to Figures 4.67 and 4.68, the ageing and microstructure of R20WFS20 and R30WFS30 are identical based on the mineralogical data retrieved from the microstructural analysis. Using SEM and EDS, it was discovered that the inclusion of RHA and WFS in SCC led to the production of crystalline structures.

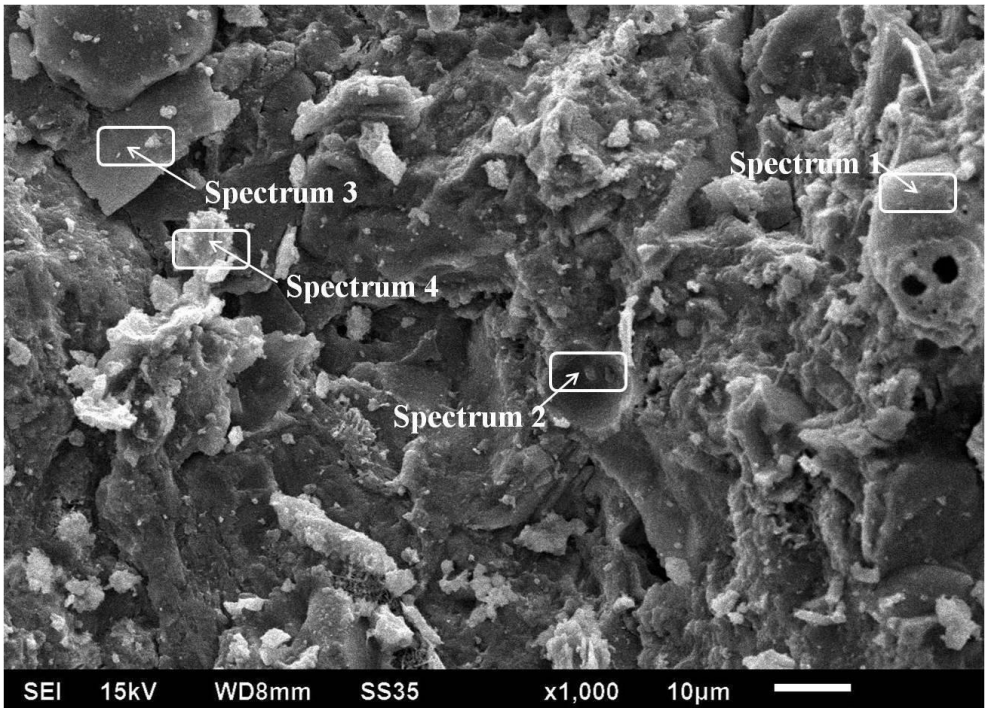

a) R0WFS0 at 28 days

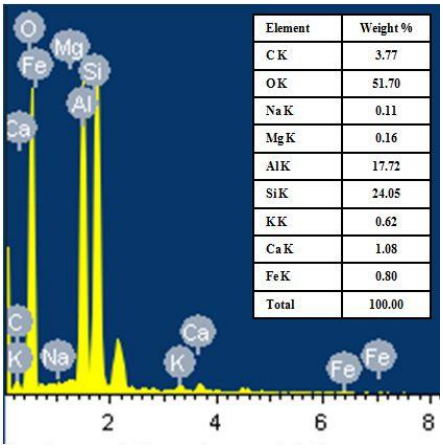

b) Spectrum1

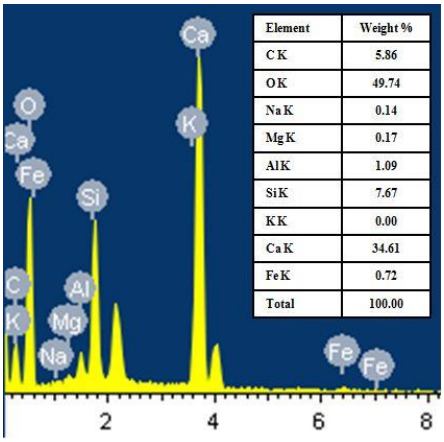

c) Spectrum2

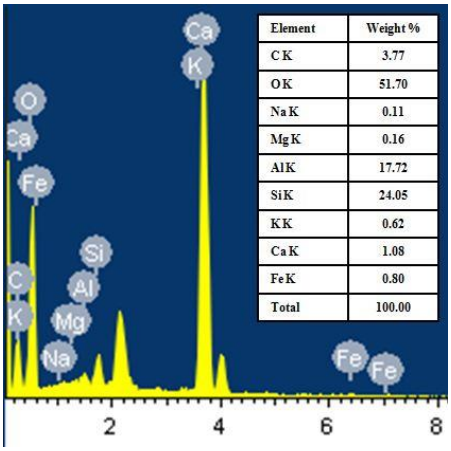

d) Spectrum3

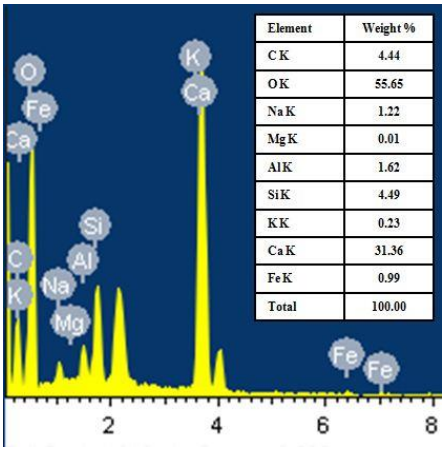

e) Spectrum4

Fig.4.57.SEM image of R0WFS0 after 28 days and EDS of spectrum 1 to 4

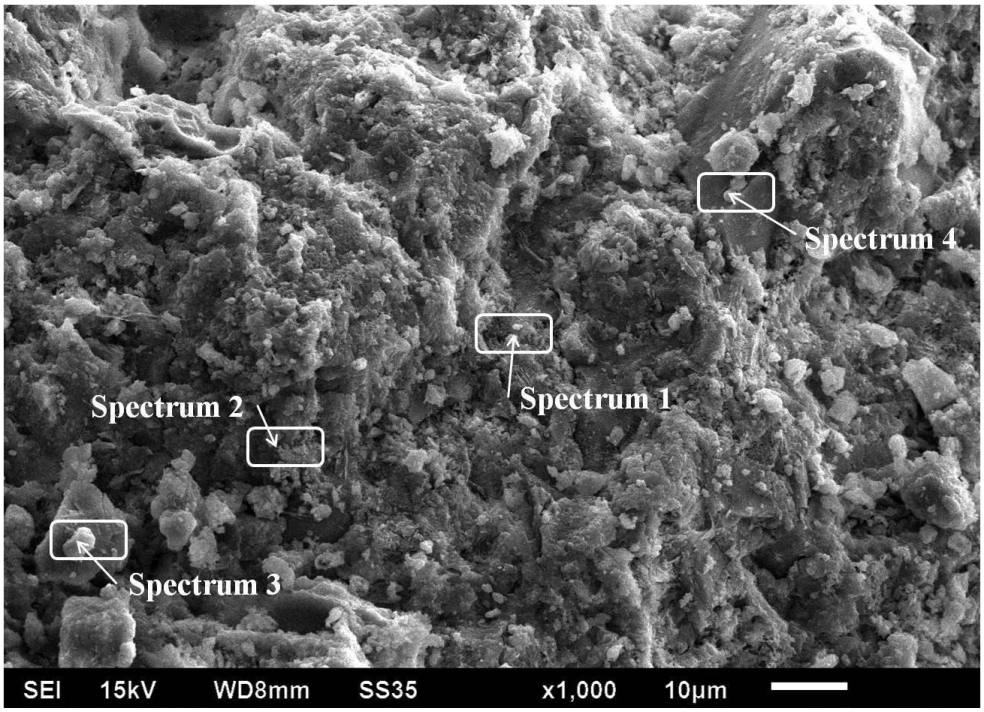

a) R10WFS10 at 28 days

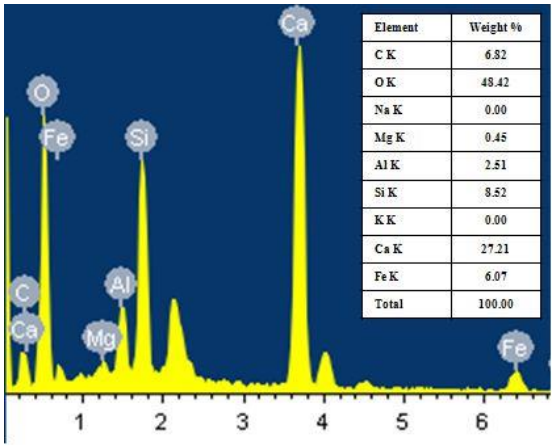

b) Spectrum1

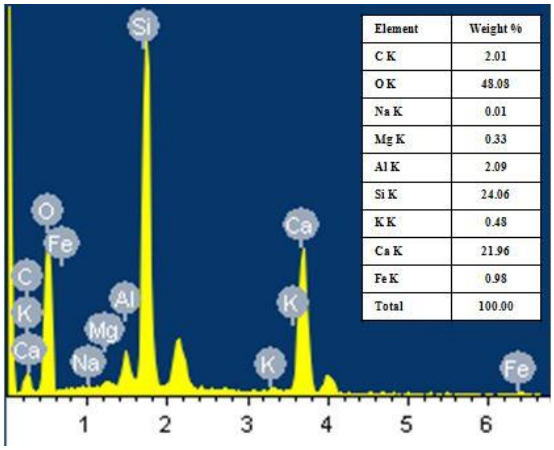

c) Spectrum2

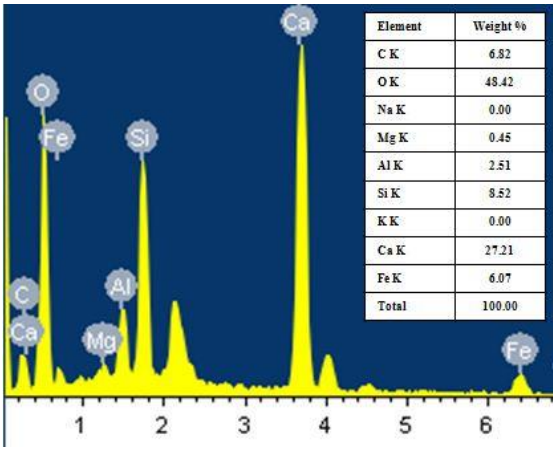

d) Spectrum3

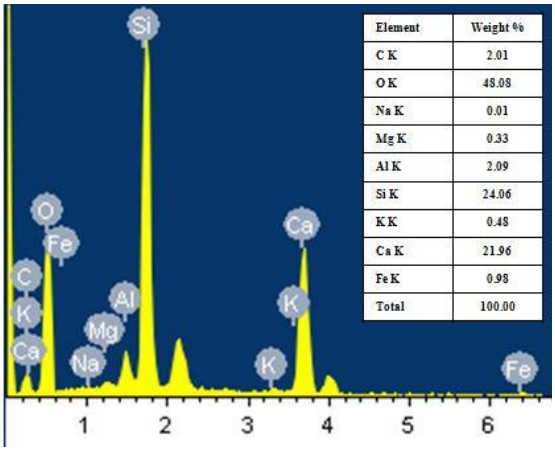

e) Spectrum4

Fig.4.58.SEM image of R10WFS10 after 28 days and EDS of spectrum 1 to 4

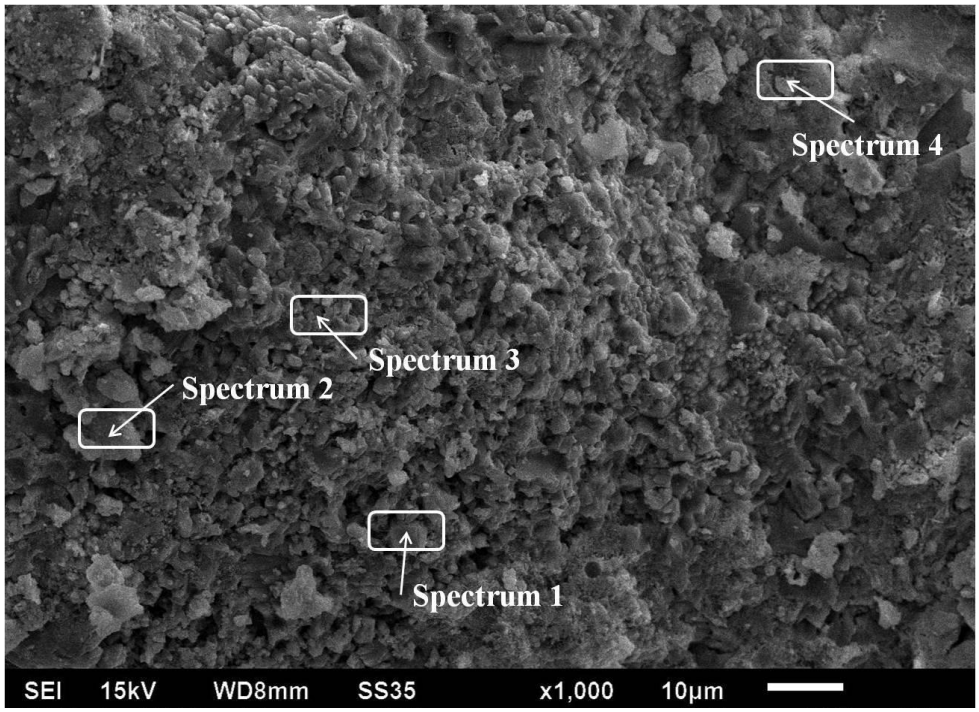

a) R20WFS20 at 28 days

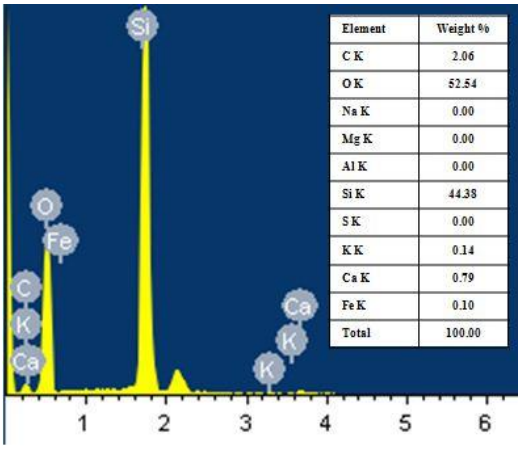

b) Spectrum1

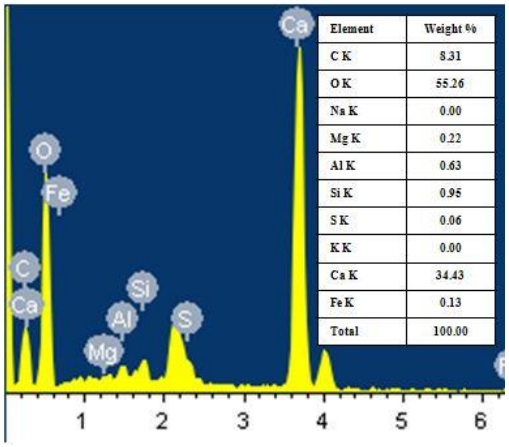

c) Spectrum2

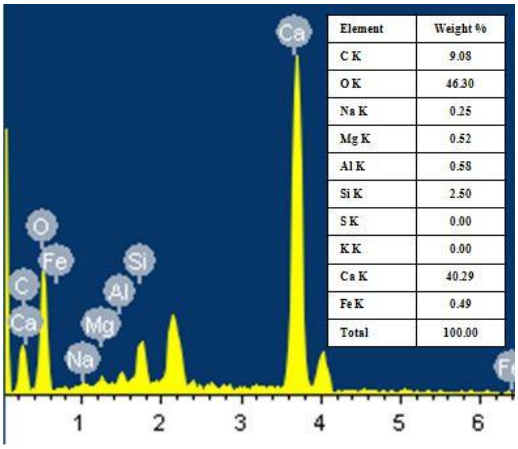

d) Spectrum3

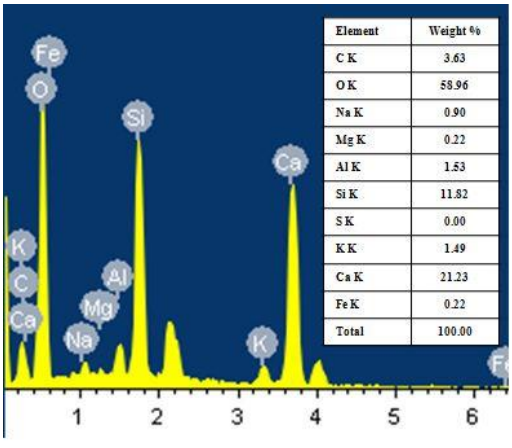

e) Spectrum4

Fig.4.59.SEM image of R20WFS20 after 28 days and EDS of spectrum 1 to 4

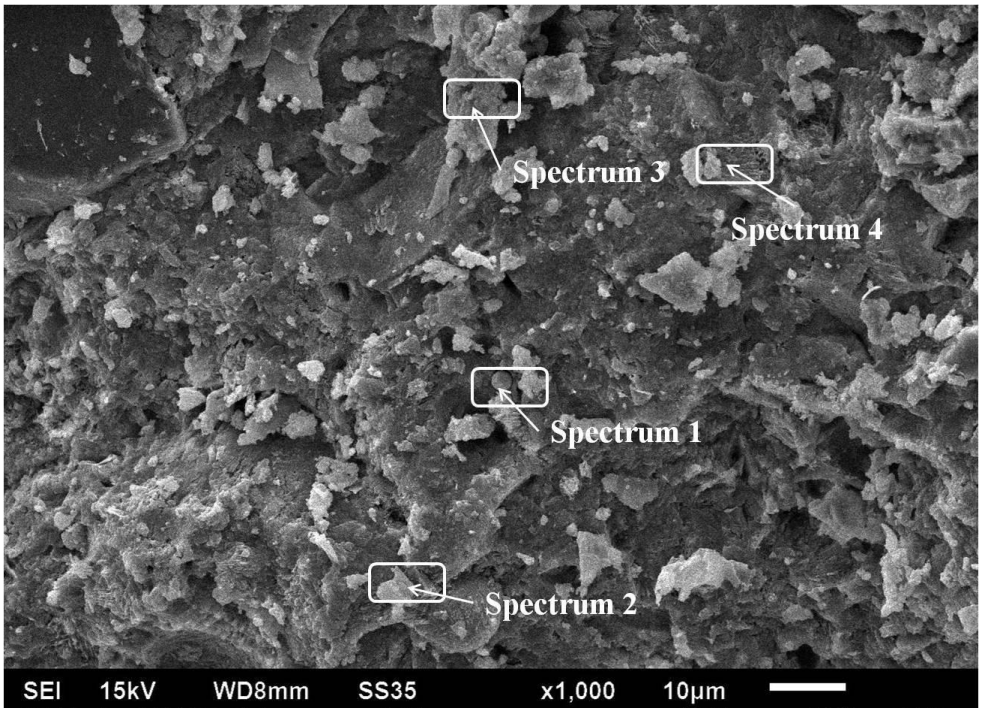

a) R30WFS30 at 28 days

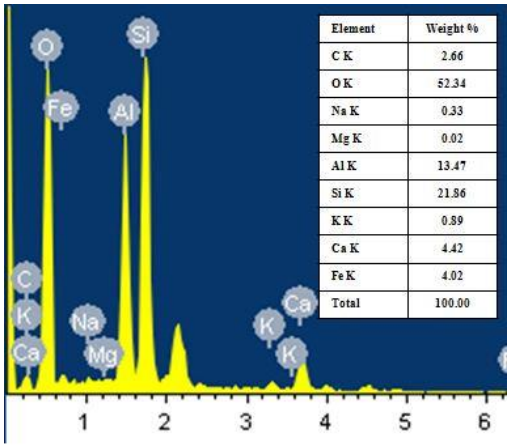

b) Spectrum1

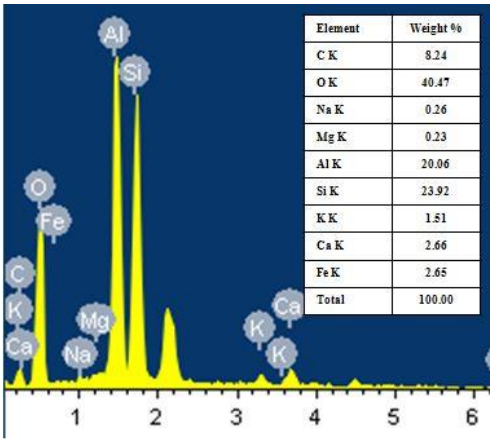

c) Spectrum2

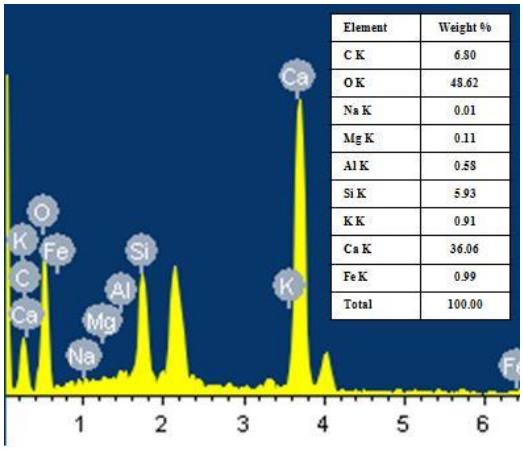

d) Spectrum3

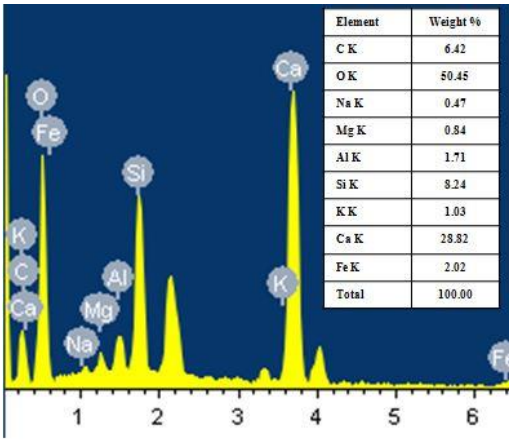

e) Spectrum4

Fig.4.60.SEM image of R30WFS30 after 28 days and EDS of spectrum 1 to 4

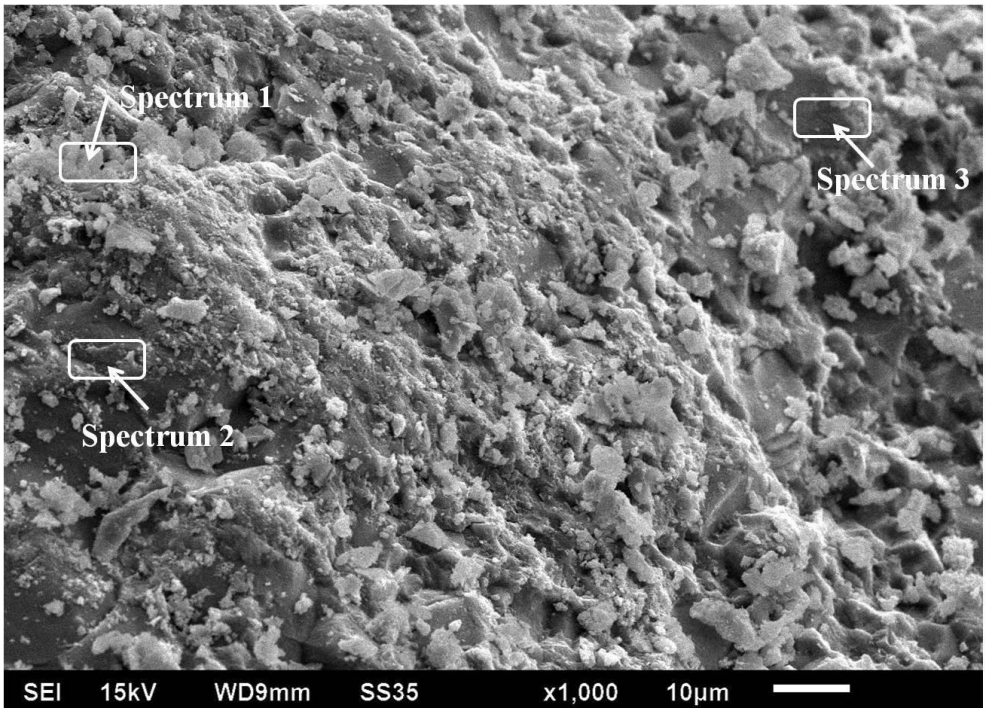

a) R0WFS0 at 90 days

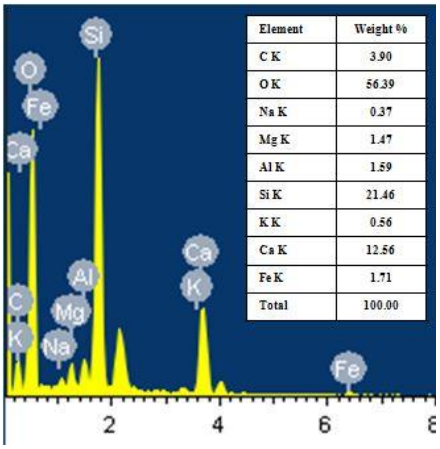

b) Spectrum1

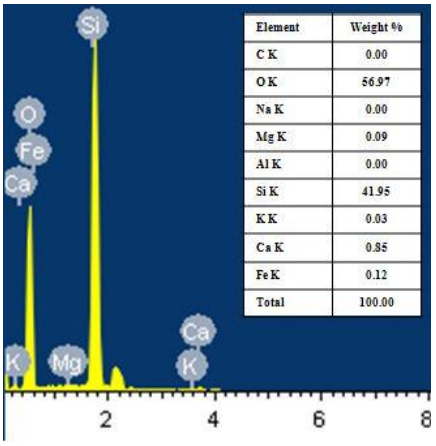

c) Spectrum2

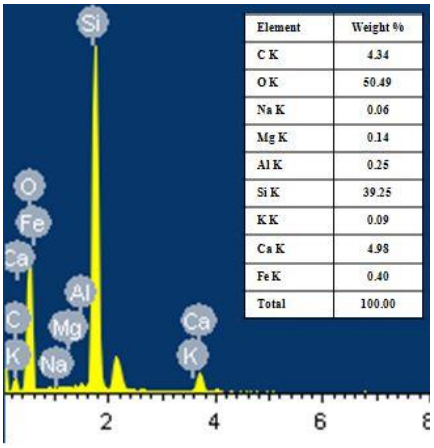

d) Spectrum3

Fig.4.61.SEM image of R0WFS0 after 90 days and EDS of spectrum 1 to 3

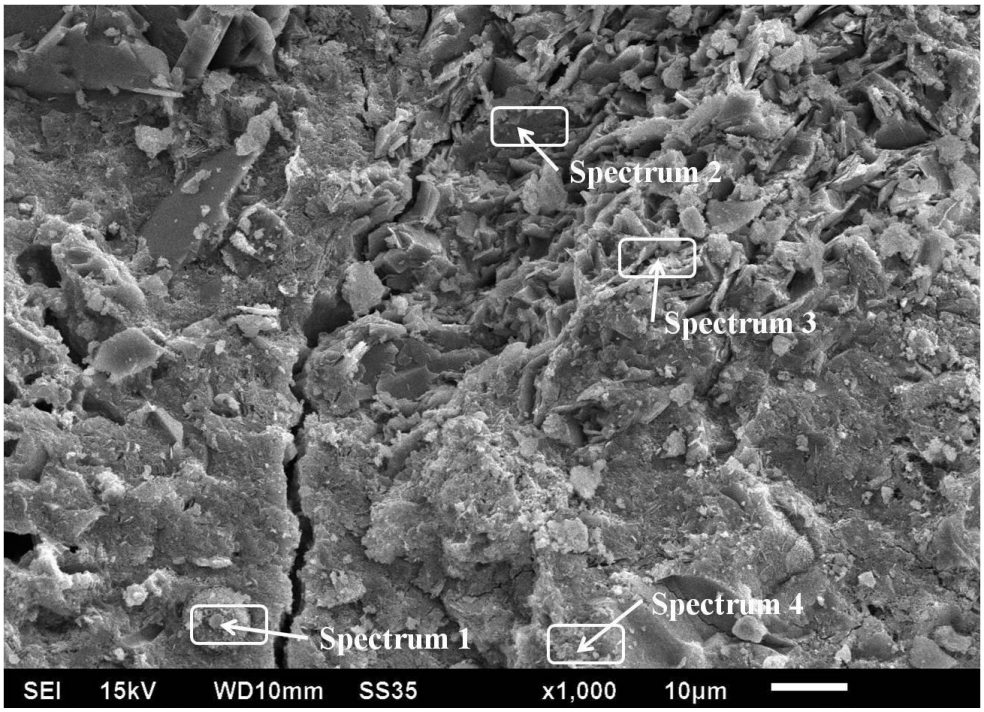

a) R10WFS10 at 90 days

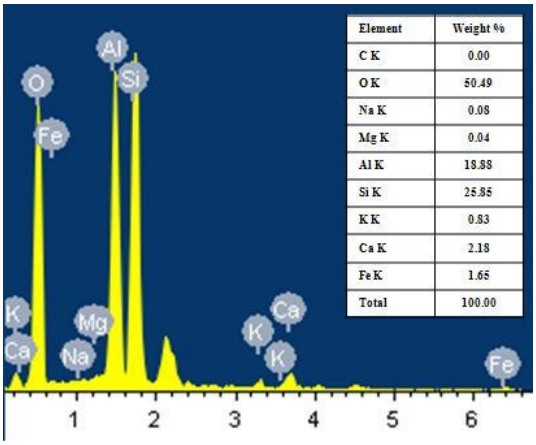

b) Spectrum1

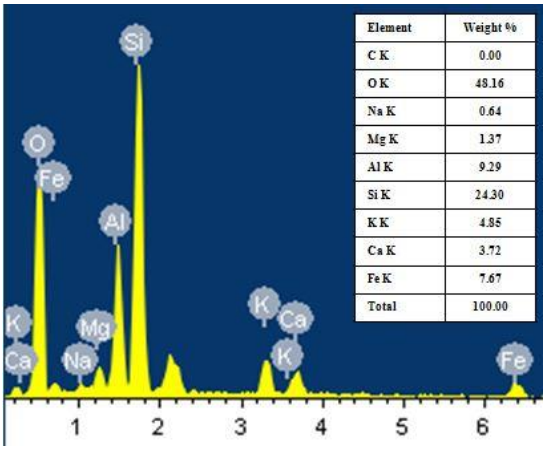

c) Spectrum2

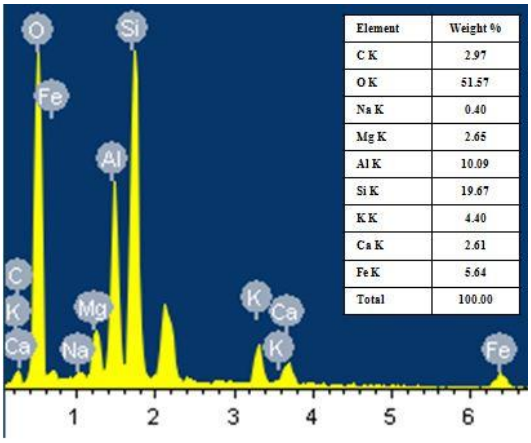

d) Spectrum3

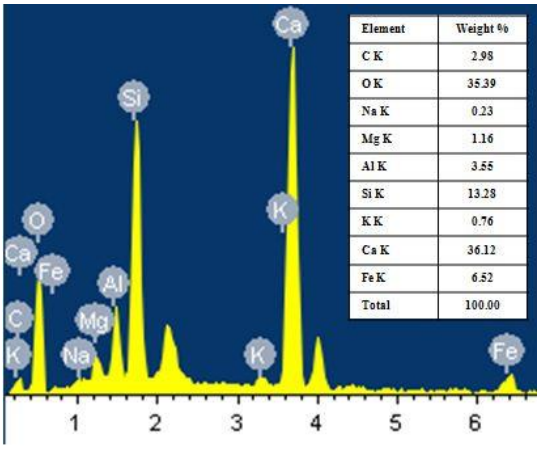

e) Spectrum4

Fig.4.62.SEM image of R10WFS10 after 90 days and EDS of spectrum 1 to 4

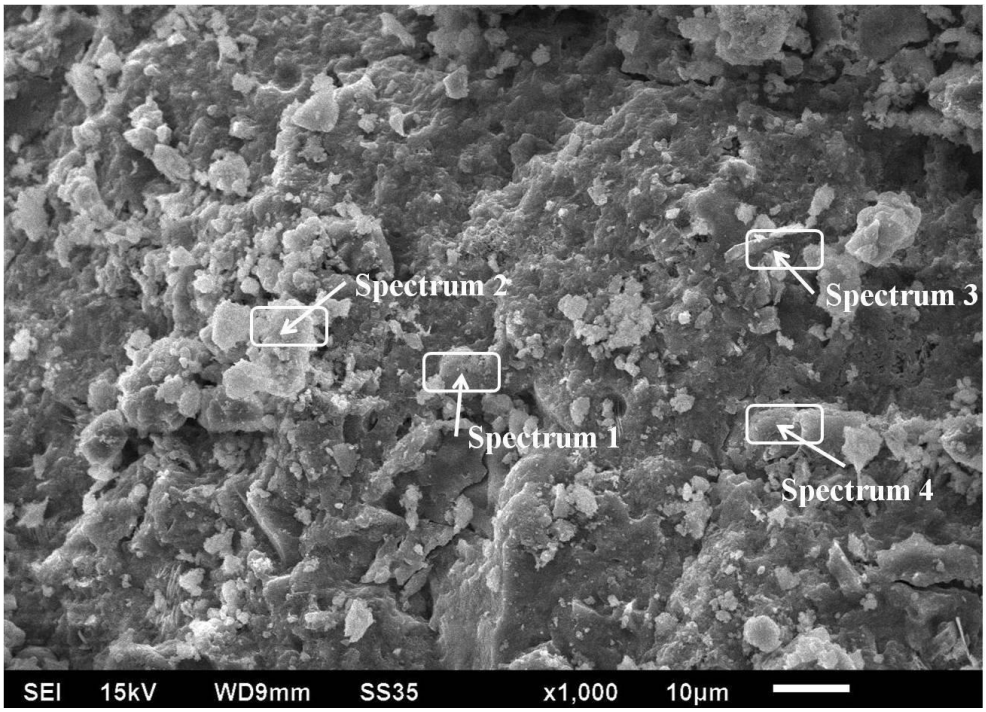

a) R20WFS20 at 90 days

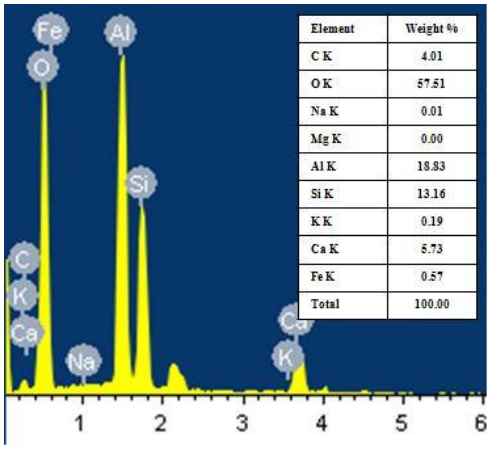

b) Spectrum1

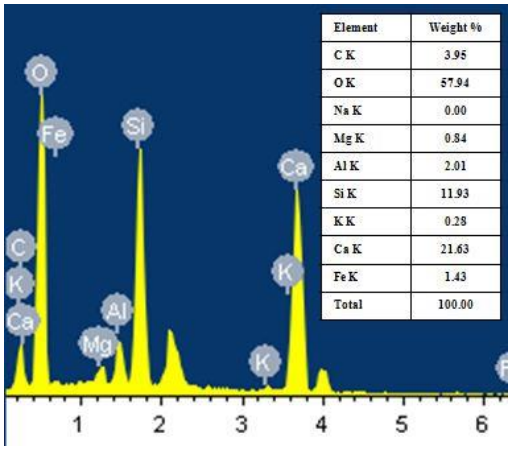

c) Spectrum2

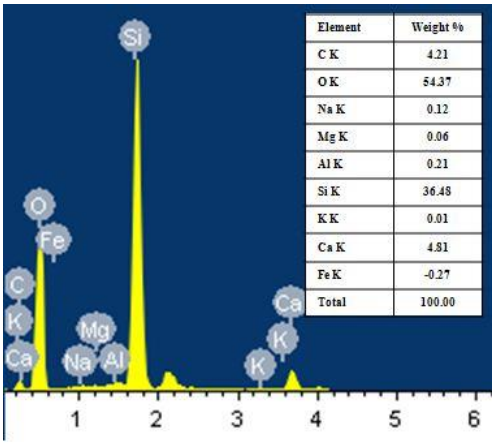

d) Spectrum3

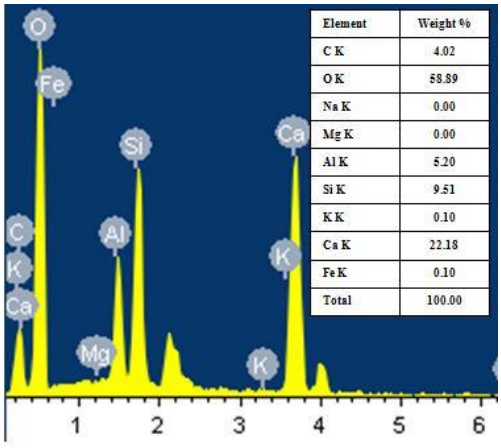

e) Spectrum4

Fig.4.63.SEM image of R20WFS20 after 90 days and EDS of spectrum 1 to 4

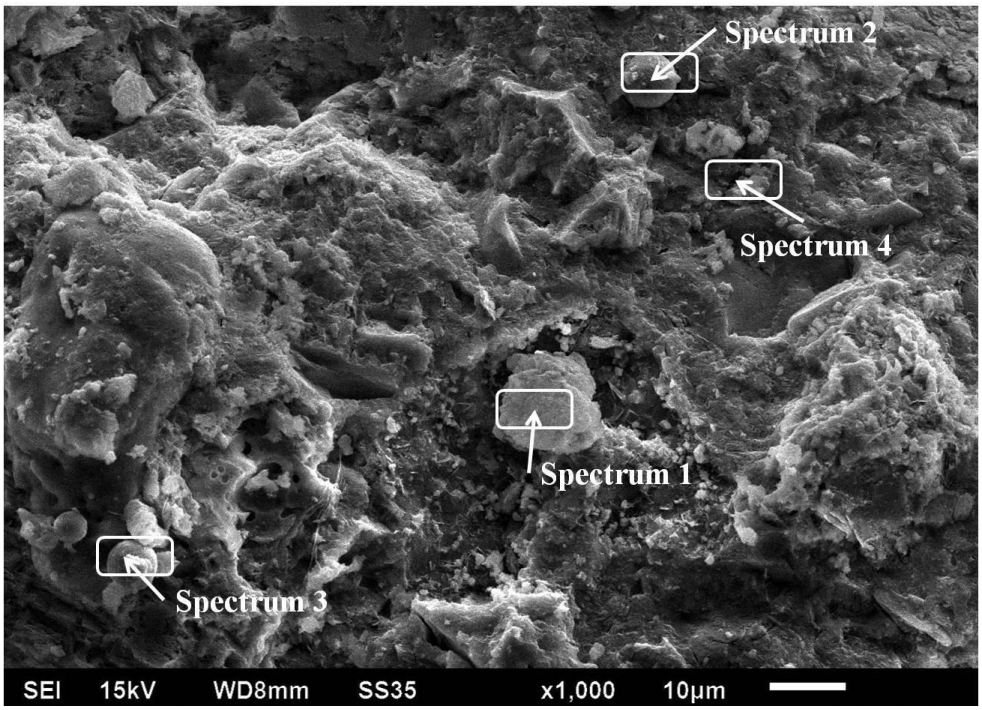

a) R30WFS30 at 90 days

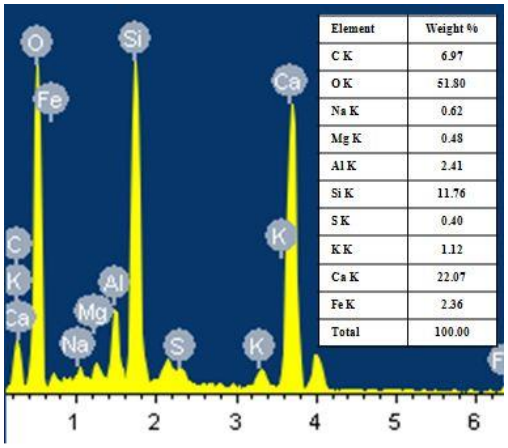

b) Spectrum1

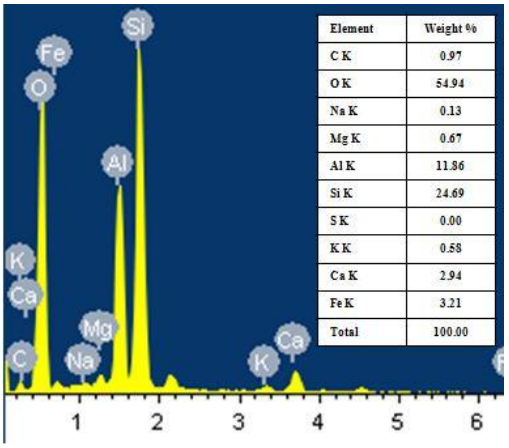

c) Spectrum2

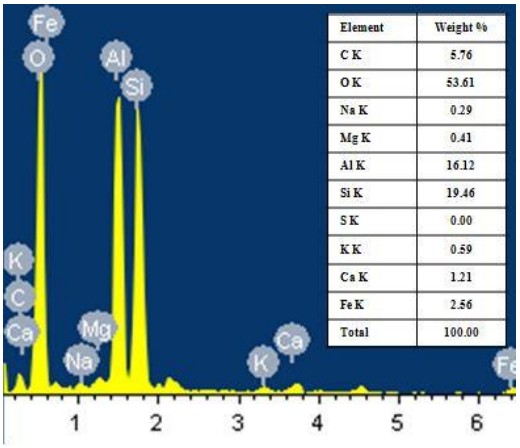

d) Spectrum3

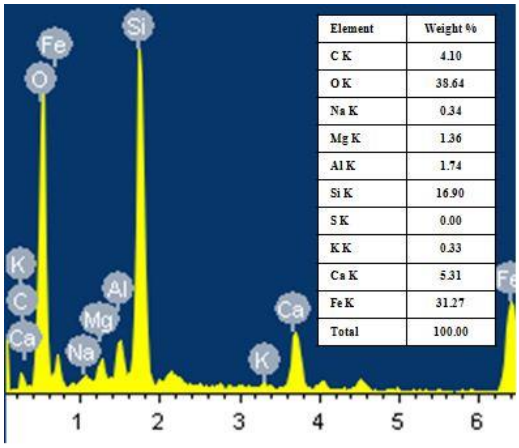

e) Spectrum4

Fig.4.64.SEM image of R30WFS30 after 90 days and EDS of spectrum 1 to 4

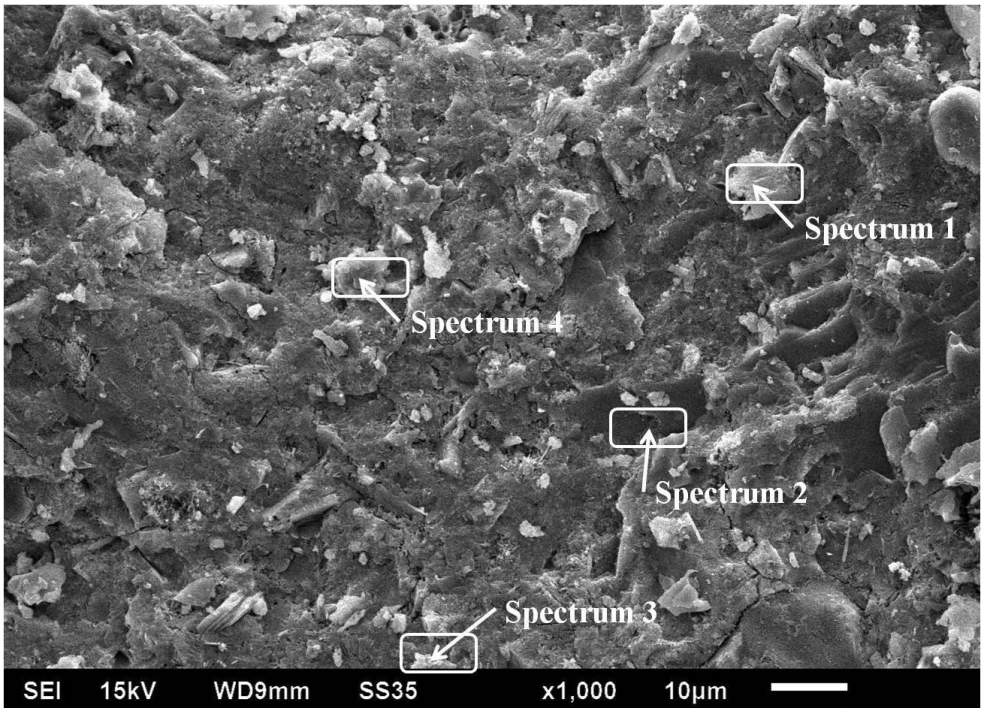

a) R0WFS0 at 365 days

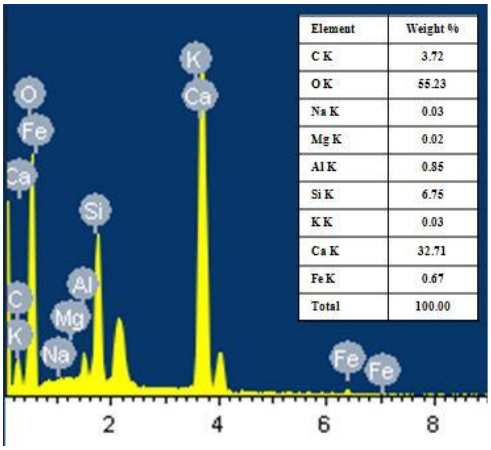

b) Spectrum1

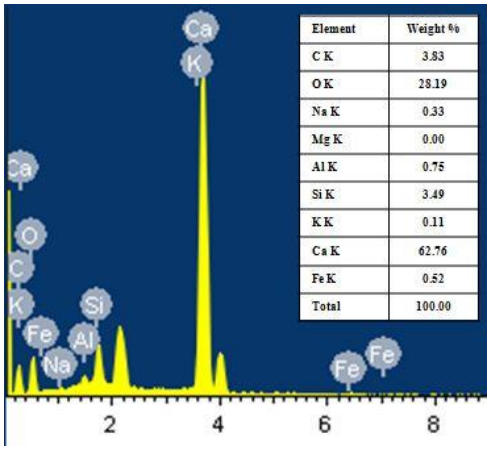

c) Spectrum2

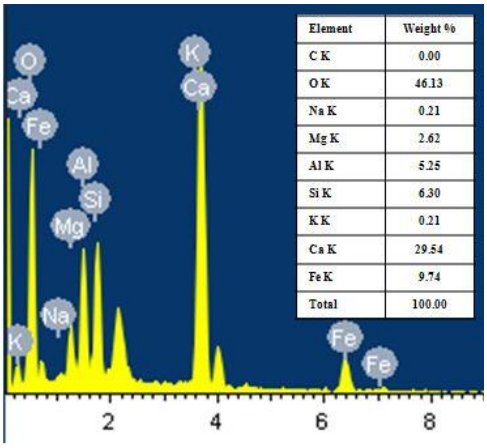

d) Spectrum3

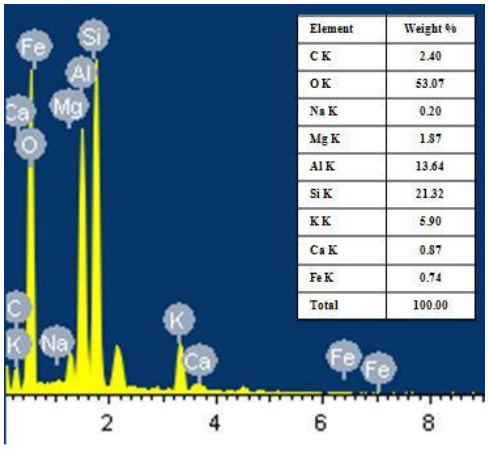

e) Spectrum4

Fig.4.65.SEM image of R0WFS0 after 365 days and EDS of spectrum 1 to 4

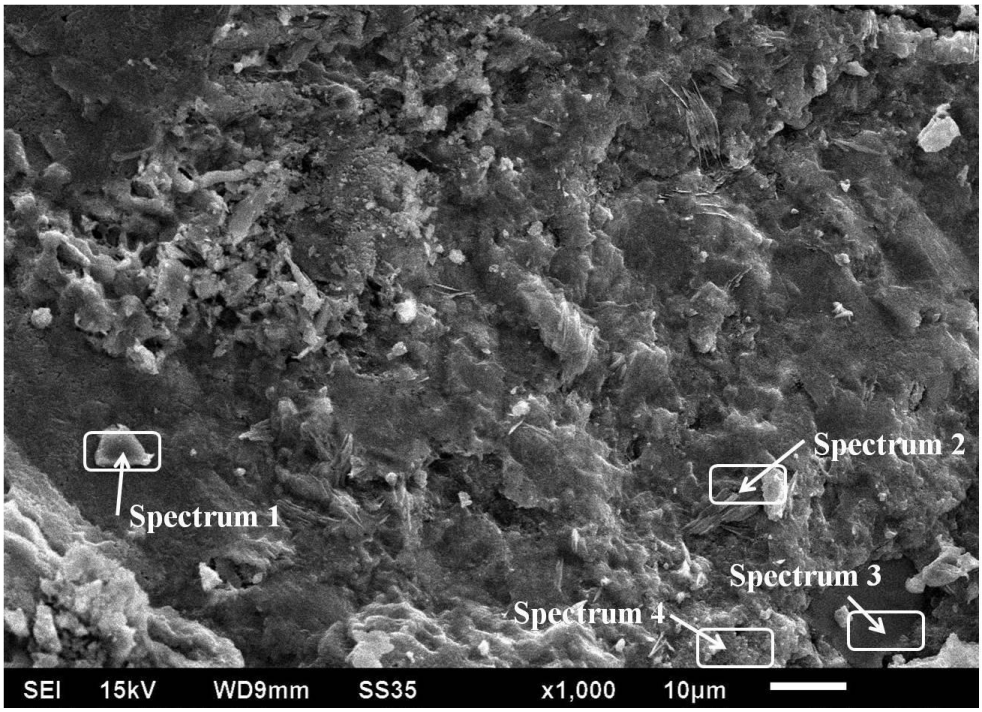

a) R10WFS10 at 365 days

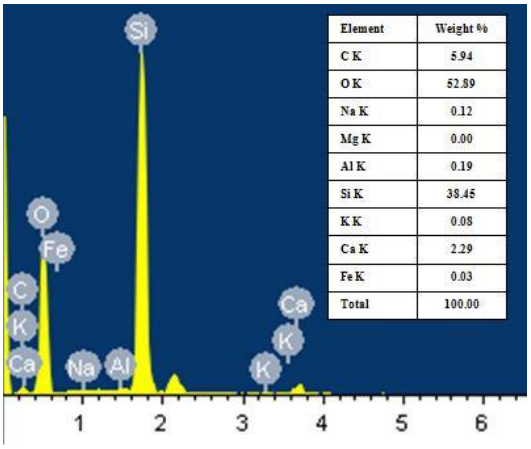

b) Spectrum1

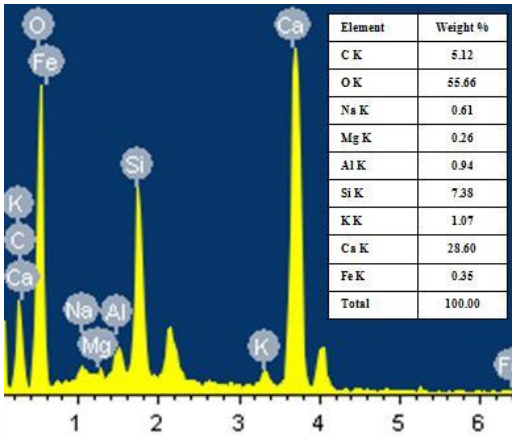

c) Spectrum2

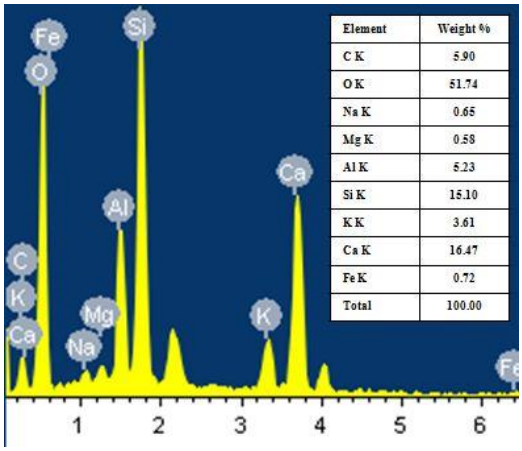

d) Spectrum3

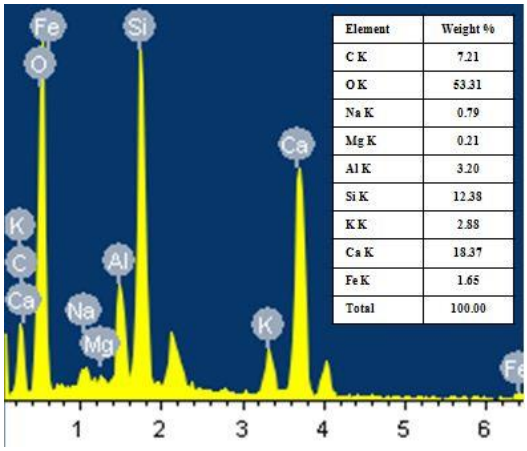

e) Spectrum4

Fig.4.66.SEM image of R10WFS10 after 365 days and EDS of spectrum 1 to 4

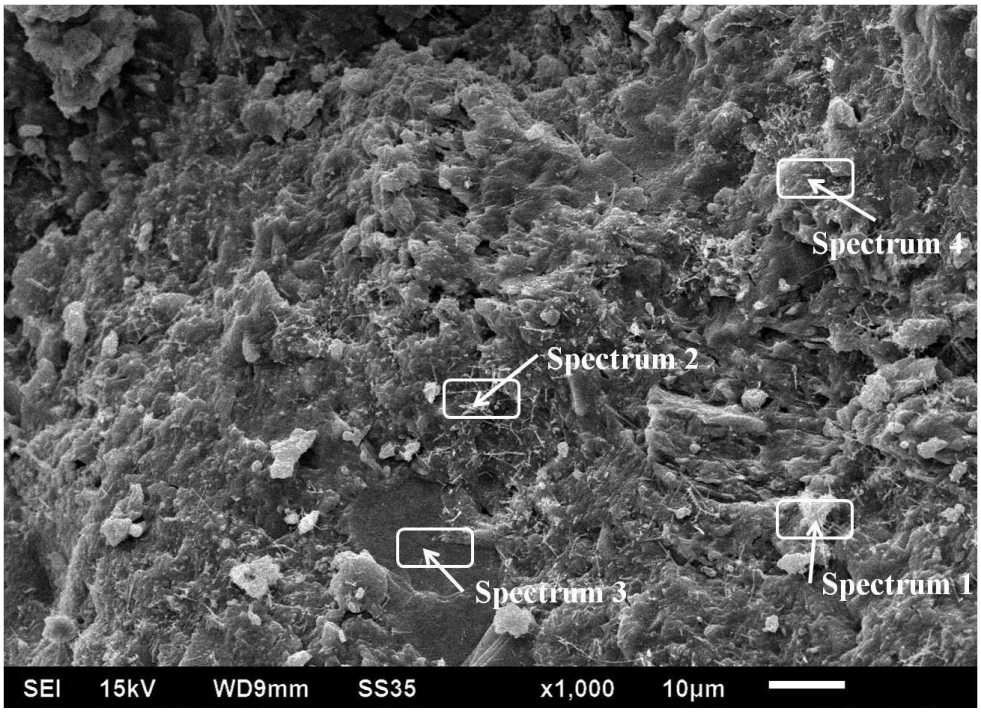

a) R20WFS20 at 365 days

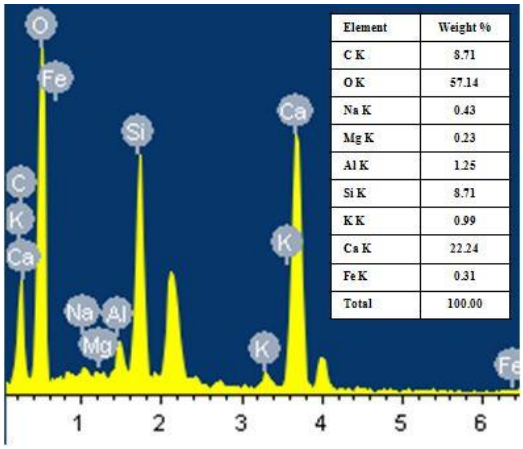

b) Spectrum1

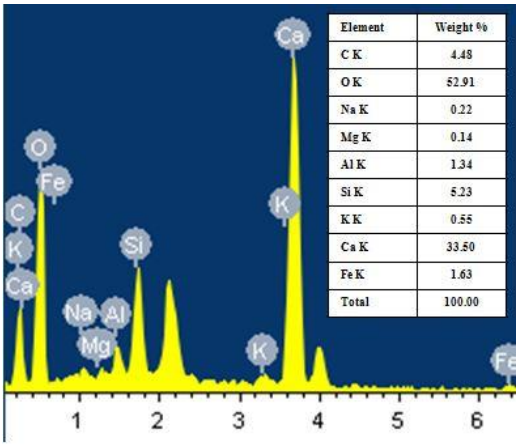

c) Spectrum2

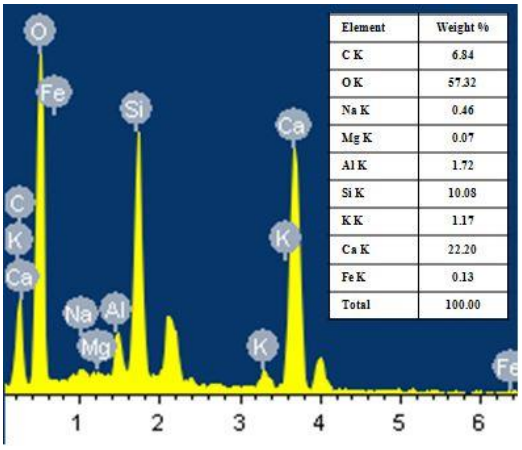

d) Spectrum3

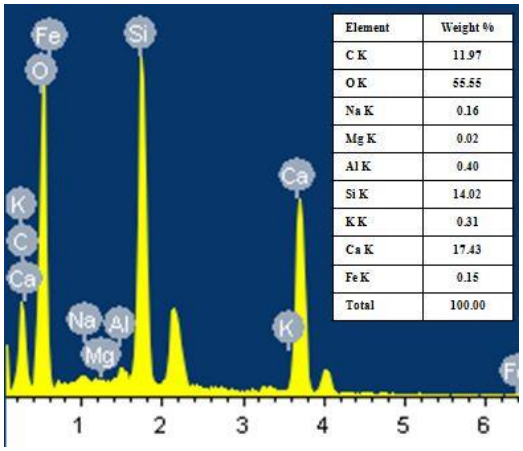

e) Spectrum4

Fig.4.67.SEM image of R20WFS20 after 365 days and EDS of spectrum 1 to 4

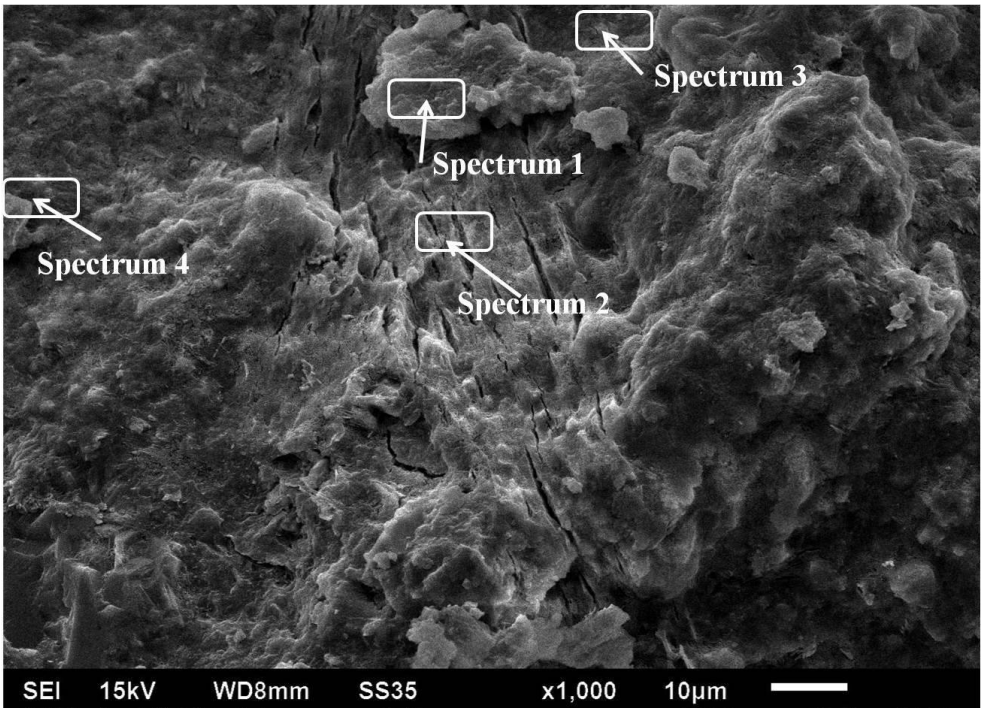

a) R30WFS30 at 365 days

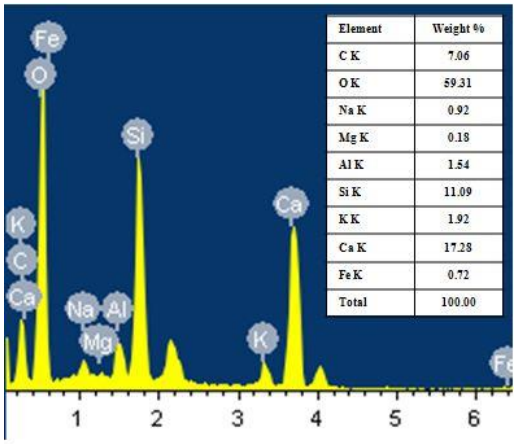

b) Spectrum1

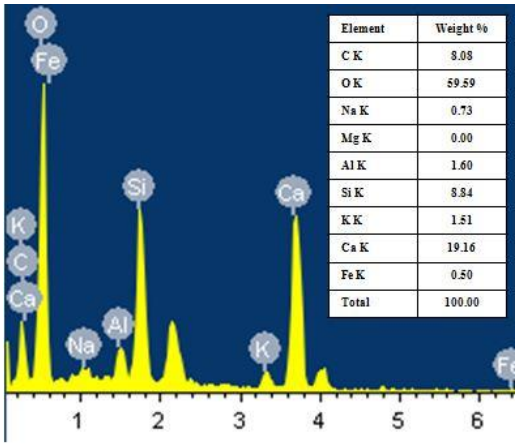

c) Spectrum2

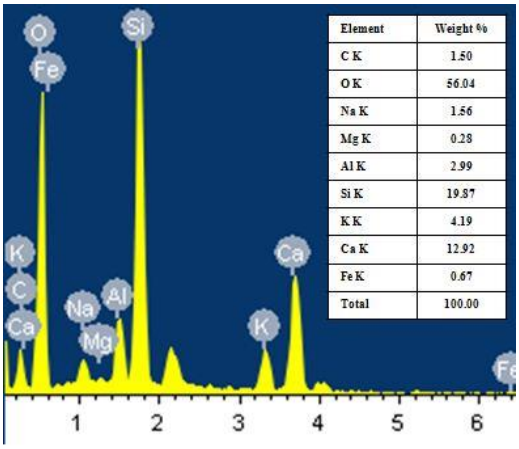

d) Spectrum3

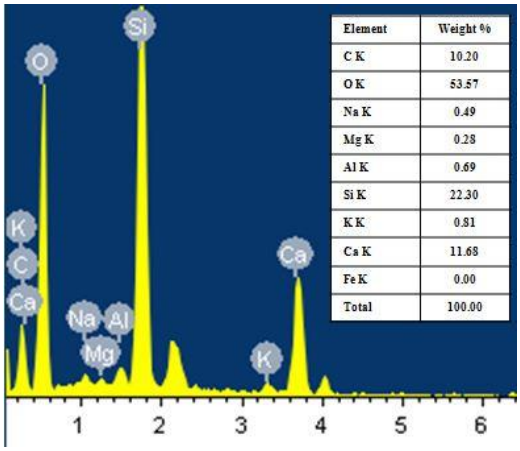

e) Spectrum4

Fig.4.68.SEM image of R30WFS30 after 365 days and EDS of spectrum 1 to 4

4.3.5.2 XRD

A non-destructive technique for determining the components present in any given material is X-ray diffraction. The specimens were processed in powder form for X-Ray diffraction analysis. Figures 4.69 to 4.74 show the X-ray diffraction pattern and analyses of RHA and WFS blended SCC mixes at ages 28 days and 365 days. The XRD experiments were performed at diffraction angles 2θ ranging from 5° to 80° in incremental of 2θ = 0.017°. In Figure 4.69, the presence of free silica in concrete mix was indicated by the silica oxide (SiO2) peak. The XRD investigation primarily revealed C-S-H and CH compounds in the SCC mixes. Figure 4.70 represented that additional compounds of Gismondine ($CaAl_2Si_2O4(H_2O)$) and Portlandite ($Ca(OH)_2$) were formed in R10WFS10 at 365 days of curing along with sharp peaks of Silica (SiO_2) and Calcite ($CaCO_3$). The minimum amount of calcium hydroxide ($Ca(OH)_2$) is present in every concrete mix, indicating that the hydration reaction consumes the most calcium. In the XRD analysis of R30WFS30, silica (SiO2) and calcite ($CaCO_3$) exhibited a number of sharp peaks in Figure 4.71. The white blocky crystals are considered to be gypsum and mirabilite, the small granular crystals are thenardite, and the bar-like particles are ettringite, according to the outcomes of the XRD and EDS analyses. In comparison to control concrete, the RHA and WFS blended SCC mixes had a comparatively high difference in the intensities of calcium silicate hydrate and portlandite at 365 days of curing age. Pore size refinement aided in filling the capillary pores, and as a result, permeability was decreased. The pozzolanic compounds formed during cement hydration improve the pore structure of concrete, which results in a more compact SCC.

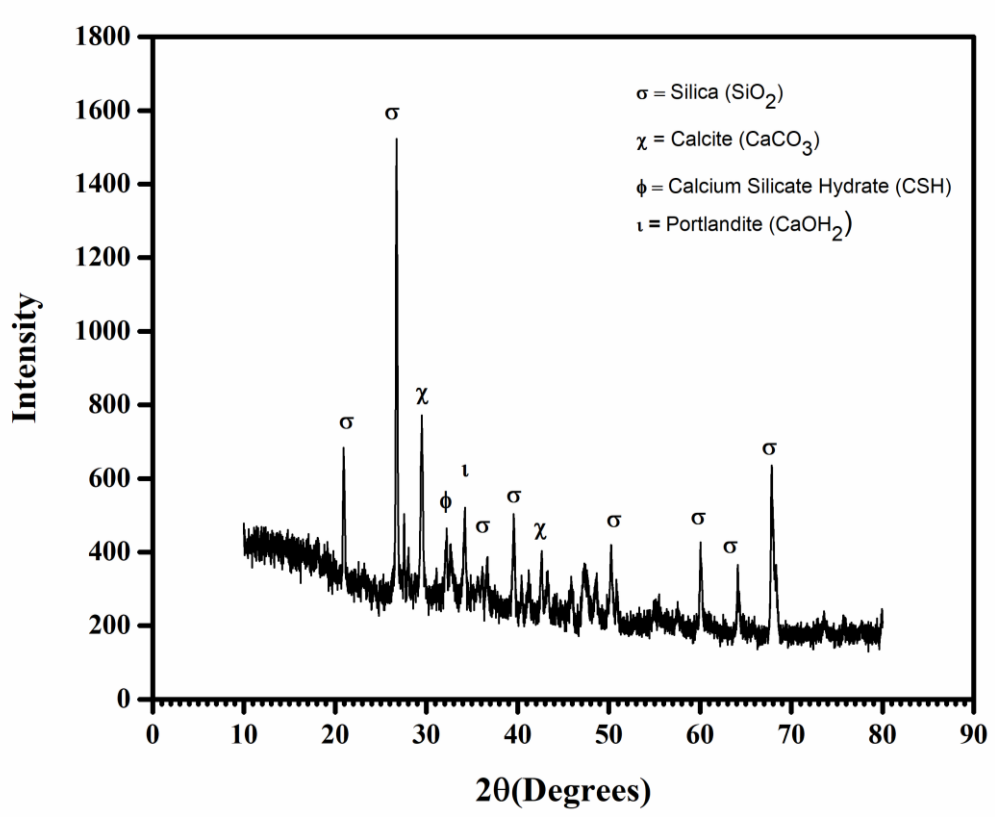

Fig.4.69. XRD pattern of R0WFS0 at 28 days

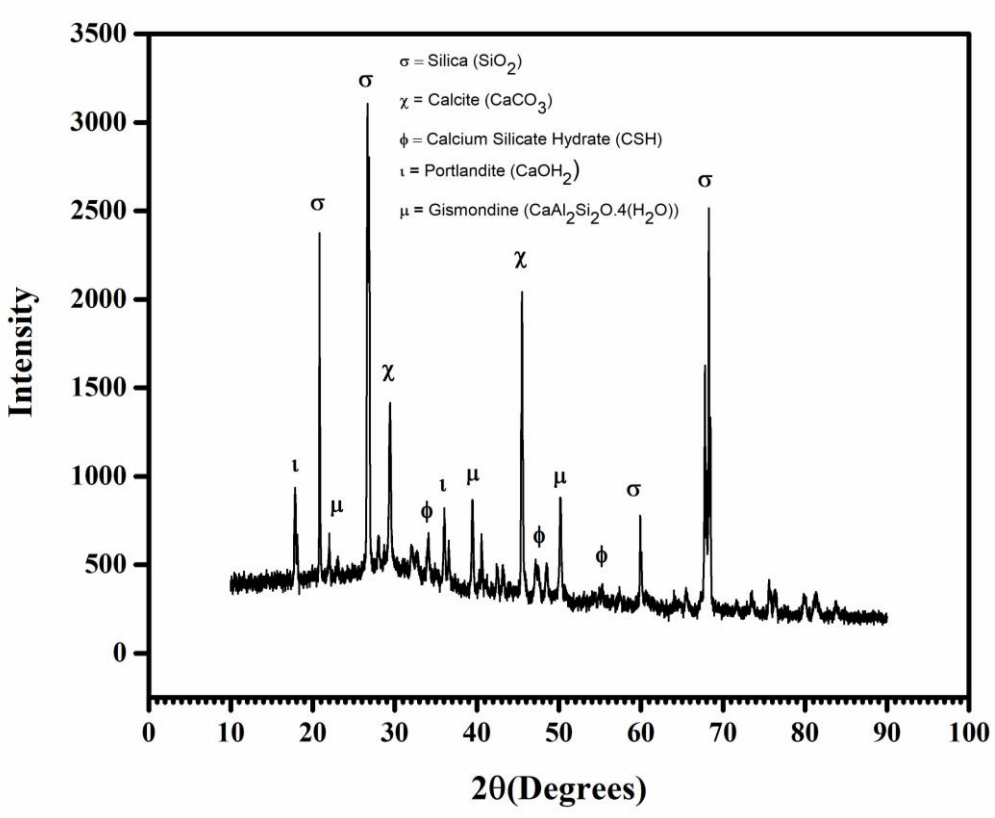

Fig.4.70. XRD pattern of R10WFS10 at 28 days

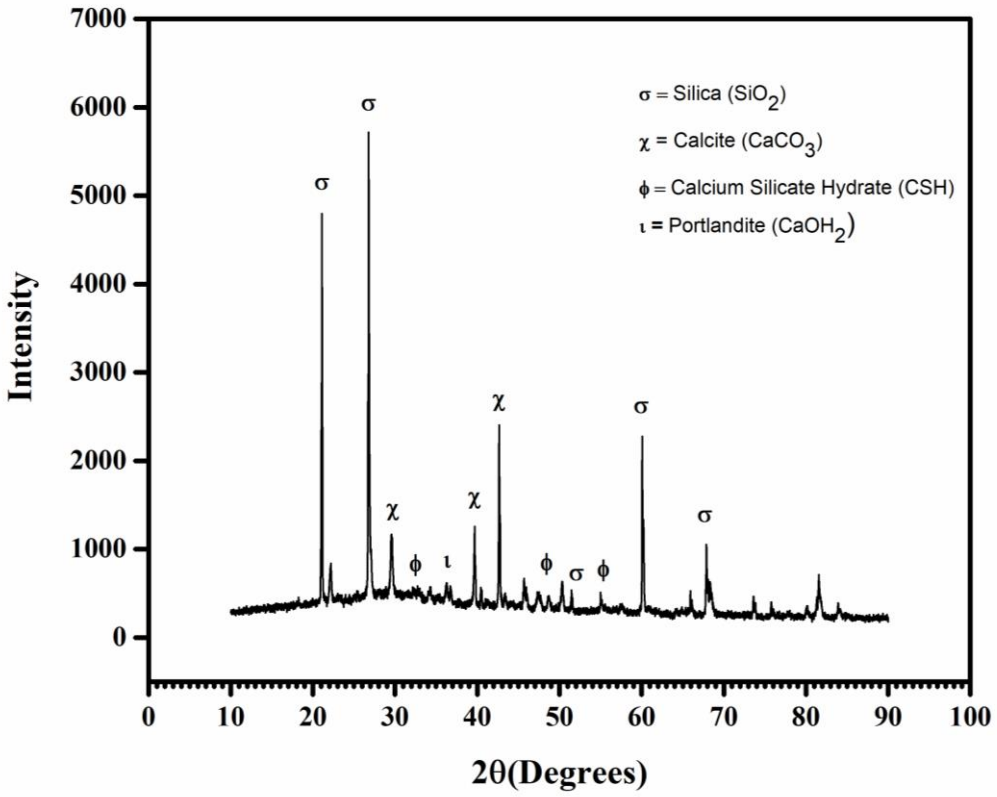

Fig.4.71. XRD pattern of R30WFS30 at 28 days

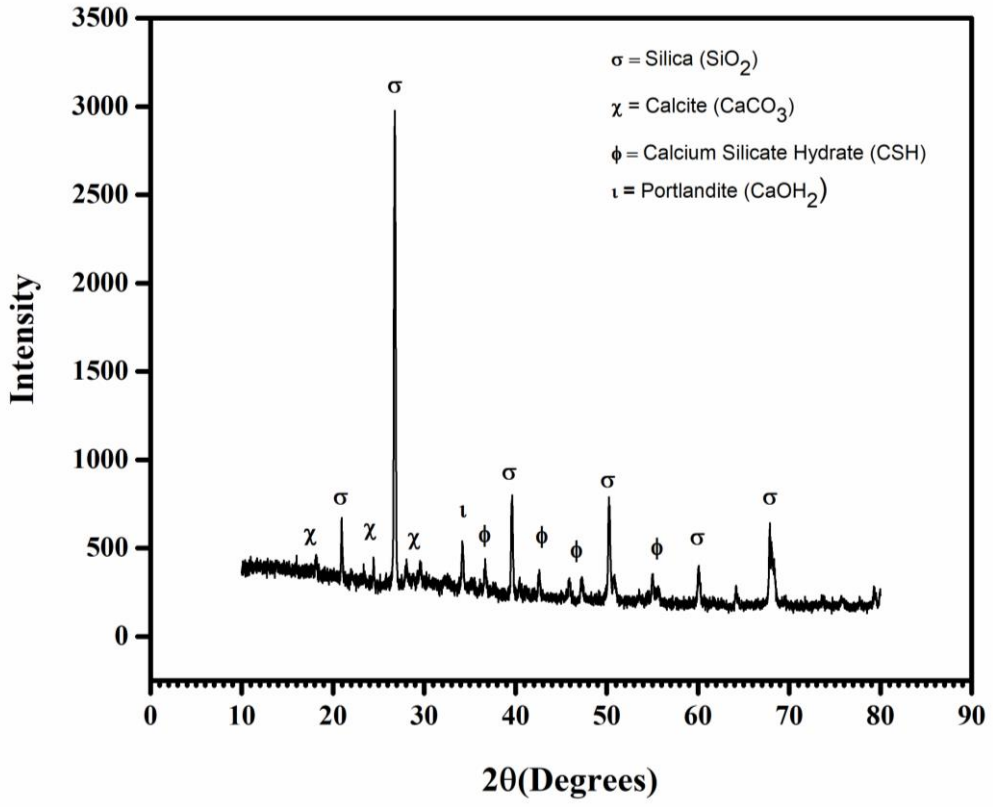

Fig.4.72. XRD pattern of R0WFS0 at 365 days

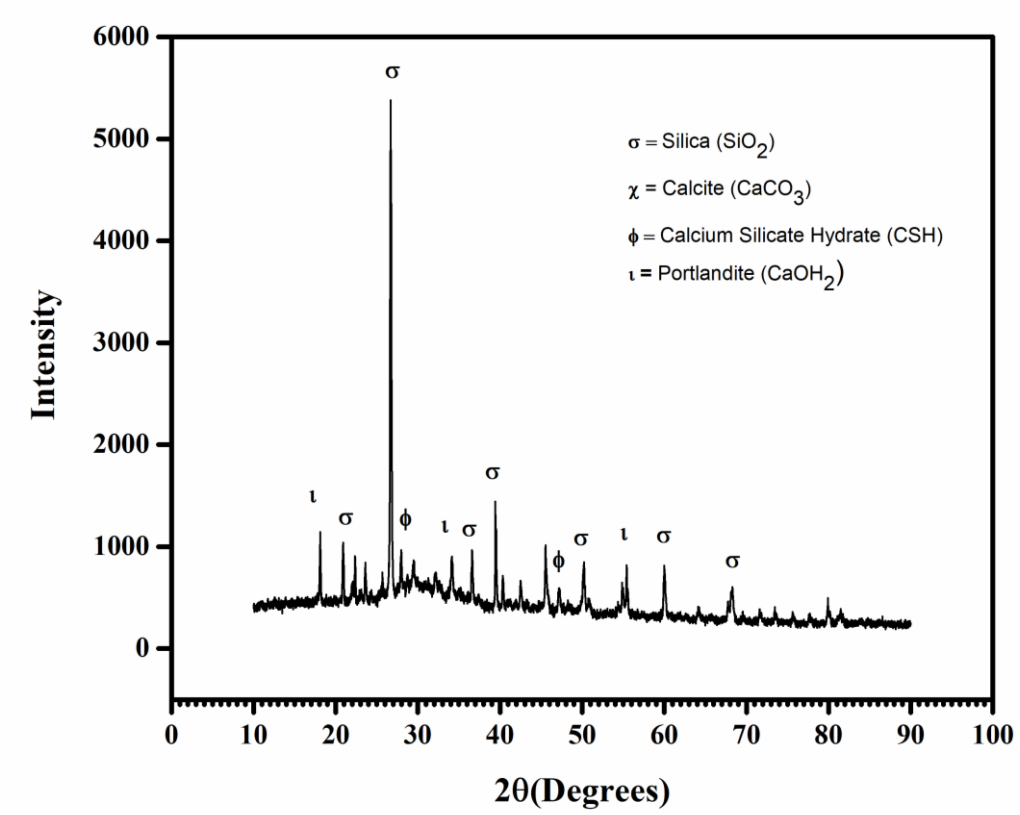

Fig.4.73. XRD pattern of R10WFS10 at 365 days

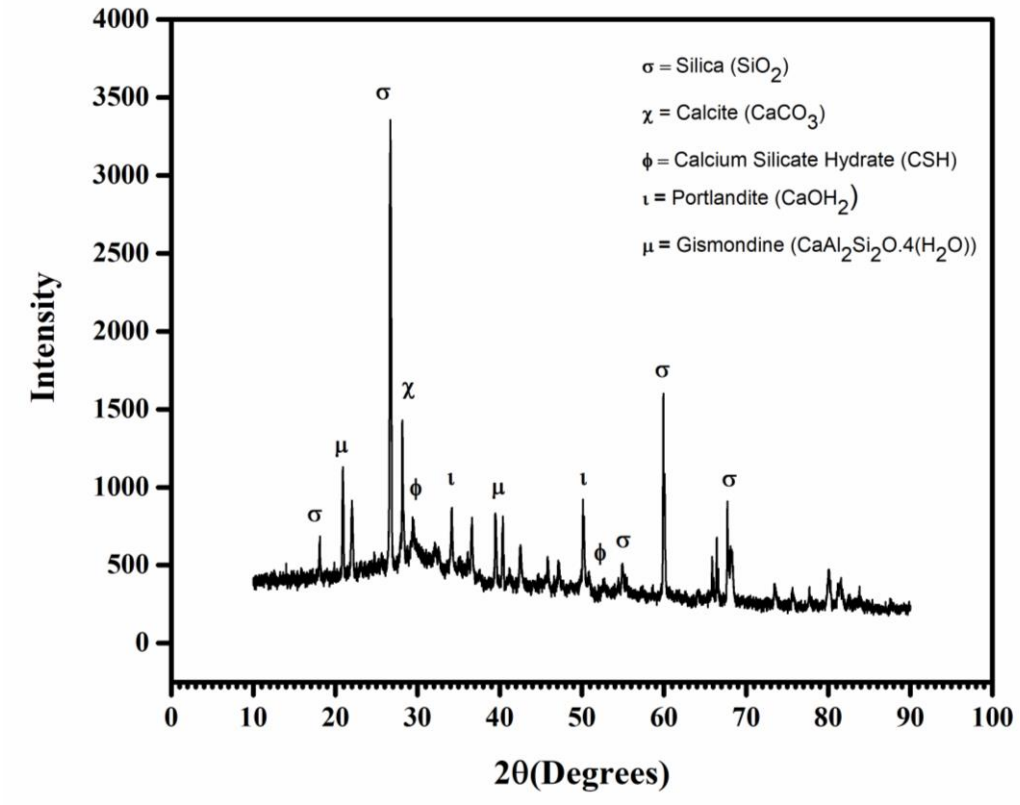

Fig.4.74. XRD pattern of R30WFS30 at 365 days

4.3.6 Statistical Analysis

The multiple linear regression statistical analysis of the compressive strength, tensile strength, RCPT and sorptivity of specimens of SCC blended with RHA and WFS is performed. Using statistical analysis for the concrete data received from the experimental work done in this study, a mathematical model was developed for the prediction of the strength and durability parameters of SCC. The correlation coefficient for the prediction of strength and durability characteristics at 7, 28, 90, and 365 days of age was obtained using the multiple linear regression models.The advantage of statistical models is that, after fitting, they can be used to make accurate predictions considerably more efficiently than other modelling approaches. Before an accurate assessment can be made, these databases must be provided with a statistically substantial amount of data.

MLR mathematical equation (4.6) is given by;

$$Y = A_0 + A_1 (AGE) + A_2 (PERCENTAGE) \pm \varepsilon \quad (4.6)$$

Where Y is the value of dependent variable

A_0 is y-intercept or constant in the equation

A_1 and A_2 are the regression coefficients for independent variables

ε is the error associated with the equation

In this equation variables are generally dependent on a number of independent variables to achieve more accurate results and this equation is commonly referred as the multivariable power equation. There is a relationship between value of each independent variable (age and percentage) and the dependent variable (Y).84 observations were obtained for the compressive strength and tensile strength in the regression modelling, and the MLR model was used to make the prediction. Similarly, 63 observations were made about the durability characteristics of RCPT and sorptivity at various curing ages and percentages of RHA and WFS in SCC. The standard errors and p-values for the intercept and regression coefficients are presented in Table 4.19. The regression coefficients and the intercept were found to have significant p values, which made them essential for the derivation of the MLR equation. The correlation between the values of a dependent variable obtained from actual and predicted values of MLR is also measured by the correlation coefficient (R).The correlation coefficient values in the equation showed a strong relationship between the observed and

projected values, confirming the model's accuracy. Therefore, it can be concluded that curing age and the proportions of RHA and WFS in the SCC mixes had an impact on compressive strength, tensile strength, RCPT, and sorptivity.

Y= 41.455 + 9.778 (Age) -1.908 (Percentage) R= 0.96 for Compressive Strength (4.7)

Y= 4.168 + 0.436 (Age) - 0.144 (Percentage) R= 0.90 for Tensile Strength (4.8)

Y= 2001.714 – 475.214 (Age) – 8.571 (Percentage) R= 0.86 for RCPT (4.9)

Y= 2.734 - 0.615 (Age) + 0.053 (Percentage) R= 0.97 for Sorptivity (4.10)

Table 4.19 Regression model results for strength and durability properties of RHA-WFS SCC mixes

	Compressive Strength		Tensile Strength		RCPT		Sorptivity	
	Standard Error	P-value	Standard Error	P-value	Standard Error	P-value	Standard Error	P-value
Intercept	1.177	0.000	0.095	0.000	100.371	0.000	0.094	0.000
Age	0.333	0.000	0.027	0.000	37.064	0.000	0.034	0.000
Percentage	0.186	0.000	0.015	0.000	15.131	0.573	0.014	0.001

4.4 SUMMARY

This chapter explained the results of the SCC mixes with RHA, WFS and combination of RHA and WFS as partial replacement of cement and fine aggregates, respectively. All the mixes exhibited fresh properties as per EFNARC with inclusion of RHA, WFS and RHA-WFS both in SCC mixes. The strength, and durability properties studied for various SCC mixes depicted durable SCC can be effectively produced with partial replacement of cement and fine aggregates with RHA, WFS and combination of RHA and WFS. Phase identification using SEM-XRD was also done to verify the results. The conclusions drawn from the study are discussed in detail in the next chapter.

CHAPTER 5

CONCLUSIONS

In this research study , the effect of waste foundry sand as partial replacement of river sand in self-compacting concrete, rice husk ash as partial replacement of cement in self-compacting concrete and combined effect of replacement of cement and river sand with waste foundry sand and rice husk ash in self-compacting concrete has been investigated. Various test for self-compacting concrete i.e. slump flow, L-box, V-funnel, and U-box tests were conducted. Strength tests such as compressive strength and splitting tensile strength, durability tests which included water absorption, porosity, chloride permeability, sorptivity, and resistance to sulphate attack were performed for all the self-compacting concrete mixes. Microstructure analysis using SEM and XRD was also performed for the mixes.

Experimental values show that waste foundry sand, rice husk ash, and combination of waste foundry sand and rice husk ash can be effectively utilized in production of self-compacting concrete. The utilisation of by-products is an environmental friendly way to dispose of vast amounts of materials that might otherwise harm the soil, water, and air. This study is pertinent to the worldwide effort to achieve sustainable development. Waste materials like RHA have the potential to partially replace cement in the production of concrete, reducing the carbon footprint associated with the cement industry. Following results are summarized below based on the experimental program.

5.1 INCORPORATING RHA AS CEMENT REPLACEMENT IN SCC

5.1.1 Fresh Properties

The RHA facilitates cohesion and improves the segregation of the mixes. However, all mixes have been designated as SCC. The research study showed that substituting RHA for SCC reduces passing and filling ability of the mixes.

5.1.2 Compressive Strength

Compressive strength showed a steady increase when cement was replaced with RHA up to 10%. At a 28-day age, concrete that used 15% RHA as a partial cement replacement achieved compressive strength that was comparable to control concrete. As a result, it has been stated that up to 15% of rice husk ash may be used as a cement

substitute in concrete to reduce pollution from rice husk open burning and cement manufacturing.

5.1.3 Tensile Strength

A similar phenomenon like compressive strength was noted in the splitting tensile strength. It demonstrated an increased trend on replacement of cement with RHA up to 10%. The effect of substituting cement with RHA in SCC on splitting tensile strength and compressive strength ratio became less prominent with age.

5.1.4 Water Absorption and Porosity

Water absorption and porosity decreased with the incorporation of RHA in all the mixes indicating a positive effect. Furthermore, data showed that RHA contributed to a reduction in capillarity absorption. RHA contributed to the increase in the compactness, density, and ability to fill voids in SCC mixtures to a considerable extent. The durability properties of SCC have significantly improved while using RHA partially in place of cement.

5.1.5 Sorptivity

The RHA sorptivity data revealed a similar pattern to those of water absorption. It was found that the sorptivity (both initial and secondary) showed decreasing variation as the RHA level reached up to 15%. After that threshold, the sorptivity began to increase. It can be concluded that when sorptivity values decrease, absorption rates and capillary volume decrease as well, resulting in less concrete deterioration.

5.1.6 Sulphate Attack

Inclusion of RHA displayed improved resistance to sulphate attack as pozzolanic reaction of RHA reduced porosity, permeability with age, and opposed the effect of sulphate attack to some extent on SCC mixes. While concrete strength develops with age, RHA displays a favourable pozzolanic response.

5.1.7 Rapid Chloride Permeability Test

The RCPT findings showed that the incorporation of RHA to all the mixes reduced the amount of charge that could pass through them because of matrix densification, better particle packing, and enhanced microstructure. When compared to the control mix, RHA proved to be beneficial in decreasing the penetration of chloride ions.

5.1.8 Microstructure

Analysis of the microstructure revealed an enhanced, more compact, and denser matrix with the incorporation of RHA. The microstructure was in agreement with the compressive strength and other durability properties.

5.1.9 XRD

X-ray diffraction (XRD) analysis depicted presence of Silica (SiO_2), Calcite ($CaCO_3$), Calcium Silicate Hydrate (C-S-H), portlandite ($Ca(OH)_2$). An XRD test was performed on the powdered samples of various hardened SCC mix proportions. In the XRD analysis of RHA0, silica (SiO2) had several sharp peaks, whereas calcite (CaCO3) displayed a single, prominent peak after 15% RHA was substituted for cement. The amorphous phase present in the SCC mixes did not show any clear peaks.

5.2 INCORPORATING WFS AS FINE AGGREGATE IN SCC

The results provided in the present study illustrates that WFS can be effectively utilized for the production of SCC. Although the strength of the SCC mixes was reduced still it is economical to develop SCC up to 48 MPa with 30 % replacement of fine aggregates. It is observed from test results that detrimental effect on durability can be compensated with the use of WFS in place of river sand up to 10% for the production of SCC. Hence, recycling of WFS in SCC helps to develop economical, greener and sustainable concrete.Re-usage of WFS as a partial replacement of fine aggregates in SCC will lower the volume of waste in landfill sites simultaneously conserving fine aggregates. As SCC doesn't require vibration, WFS has the potential to ensure sustainability by consuming less energy. The utilization of WFS will conserve the environment promoting the minimization of global warming leading to green and economical concrete.

5.2.1 Fresh Properties

All the mixes exhibited fresh properties and adequate fluidity as per EFNARC (2005). SCC mixes passed all the tests conducted for passing ability, filling ability. In the mixes, there was no visible bleeding or segregation. With the same water-cement ratio and superplasticizer content, the reduction in workability was seen for all SCC mixtures. Slump flow values lie between 774 and 608 mm for the SCC mixes. The results obtained from the slump flow test suggested that SCC mixes with WFS can be effectively utilized for various applications and lie within limits of EFNARC.

However, slump flow diameter of SCC reduced with increase in percentage replacement of WFS. Similarly, T_{500} slump flow time and V-funnel flow increased with the increase in the content of WFS. L-box and U-box were also influenced since the values steadily decreased as the amount of WFS increased.

5.2.2 Compressive Strength

There was a marginal reduction in compressive strength with the inclusion of WFS up to 10% as compared to the control mix at 28, 90, and 365 days of curing. SCC with a strength of above 47 MPa may be prepared with the use of WFS up to 30% as a substitute for river sand. Compressive strength of all the mixes improved with curing age without compromising the quality of the SCC mixes with WFS as partial replacement of river sand.

5.2.3 Tensile Strength

The splitting tensile strength at all ages decreased as the proportion of fine aggregates replaced with WFS increased because the increased specific surface area of inert WFS particles caused improper hydration and the formation of voids.

5.2.4 Water Absorption and Porosity

Water absorption and porosity increases with the increase in percentage level of WFS as a partial replacement of river sand whereas both values improved significantly at the age of 365 days of curing in comparison to results at 28 days of curing.

5.2.5 Sorptivity

The initial and secondary rates of absorption decreased according to the slope of water absorption (by capillarity) with age, and these values increased when WFS was added to SCC mixtures. There was an insignificant change in the values of secondary sorptivity at all ages. The pore refinement occurred with an increase in age due to hydration reactions at later ages.

5.2.6 Sulphate Attack

The compressive strength of sulphate attacked SCC specimens marginally decreased at an early age. On the contrary, relatively good strength and resistance to sulphate attack was observed at later ages. Hydration process of the mixes continued even in sulphate immersion environment leading to increased strength. Up to the age of 90 days, there was no mass change; however, at the age of 365 days after sulphate exposure, there was a negligible mass increase.

5.2.7 Rapid Chloride Permeability Test

The chloride permeability of SCC increases by incorporating WFS at all ages. In comparison to 28 days, RCPT data showed a significant improvement in pore structure after 365 days.

5.2.8 Microstructure

According to the SEM pictures, the microstructure becomes dense with curing time because the gel matrix fills in the micro-cracks, however as the amount of WFS in SCC mixes increases, the structure becomes heterogeneous and porous.

5.2.9 XRD

No sharp peaks were observed for the amorphous phase present in the WFS mixes. From the results, it was found that no additional compounds were formed in SCC mixes with the substitution of WFS. The XRD analyses demonstrated that the addition of WFS did not result in any qualitative modifications or the creation of new phases in the SCC mixes.

5.3 INCORPORATING RHA AND WFS AS PARTIAL REPLACEMENT OF CEMENT AND FINE AGGREGATES IN SCC

5.3.1 Fresh Properties

With the addition of RHA and WFS, the workability of the mix proportions (slump flow, T500, L-box, and U-box) reduced while V-funnel time increased. All the mixtures were within the prescribed limits of the EFNARC, which showed that RHA and WFS can be effectively used for the preparation of the SCC up to 30% RHA and WFS in place of the cement and fine aggregates.

5.3.2 Compressive Strength

There was a marginal improvement in compressive strength with inclusion of RHA and WFS up to 10% in comparison to control mix at 28, 90, and 365 days of curing. With the use of RHA and WFS up to 30% as a substitute for cement and fine aggregates, SCC with a strength more than 49 MPa can be prepared.

5.3.3 Tensile Strength

The interfacial interactions between the various SCC constituents are improved by partial replacement with 10% RHA and 10% WFS. The SCC mixes with 15% RHA and 15% WFS blends showed considerably higher splitting tensile strengths than the control mix after 365 days of curing.

5.3.4 Water Absorption and Porosity

Water absorption and porosity were decreased with the addition of RHA and WFS to the SCC mixes up to partial replacement levels of 15%. Comparing SCC mixes with 365 days of curing age to those with 28 days of curing age, water absorption and the volume of permeable pore space decreased with age.

5.3.5 Sorptivity

At all ages, there was marginal decrease in sorptivity values up to 10% of replacement level, thereafter values increased at 15% to 30% of replacement levels. The sorptivity value is decreased due to filling effect of finer pores and diminishing interconnected capillaries in the SCC specimens. Enhanced homogeneity and compact microstructure of SCC incorporating RHA and WFS are the cause of the sorptivity reduction. In this case, the lower permeability could have been caused by the higher paste volume and decreased aggregate content.

5.3.6 Sulphate Attack

It was determined that the final mass of the specimens showed no discernible difference. The compressive strength of SCC with 10% RHA and 10% WFS partial replacements was comparable at all ages, even after sulphate solution curing.

5.3.7 Rapid Chloride Permeability Test

The characteristics of chloride permeability for each of the blended mixtures were confirmed to be "low" and "very low". RCPT values reduced with incorporation of RHA and WFS in the SCC mixes at all ages.

5.3.8 Microstructure

The SEM images showed matrix densification with RHA and WFS usage in the SCC mixtures up to 10% replacement level. With curing age, the mixes showed higher compressive strength which was verified in SEM images. At 365 days of curing, the SCC mixes containing 15% RHA and 15% WFS blends had significantly improved mechanical and microstructure properties than the control mix.

5.3.9 XRD

In the SCC mixes, the XRD analysis mostly identified C-S-H and CH compounds. Additional compounds of Gismondine ($CaAl_2Si_2O4(H_2O)$) and Portlandite ($Ca(OH)_2$) were formed in RHA15 at 365 days of curing along with sharp peaks of Silica (SiO_2) and Calcite ($CaCO_3$).

REFERENCES

Arulrajah, A., Yaghoubi, E., Imteaz, M., and Horpibulsuk, S. (2017). "Recycled waste foundry sand as a sustainable subgrade fill and pipe-bedding construction material : Engineering and environmental evaluation." Sustainable Cities and Society, Elsevier B.V., 28, 343–349. doi:10.1016/j.scs.2016.10.009.

ACI -237 (2007) Self-Consolidating Concrete, Emerging Technology Series Committee ACI 237R-07.American Concrete Institute. Farmington Hills, MI.

Asavapisit, S., & Ruengrit, N. (2005). The role of RHA blended cement in stabilizing metal containing wastes. Cement and Concrete Composites, 3, 782- 787.

ACI Committee 318. (2019). Building Code Requirements Available for Public Review (ACI 318-19). ACI Materials Journal.

Atan, M. N., & Awang, H. (2011). The compressive and flexural strengths of self-compacting concrete using raw rice husk ash. Journal of Engineering Science and Technology, 6, 720–732.

Ahmadi, M. A, Alidoust, O., Sadrinejad, I., & Nayeri, M. (2007). Development of mechanical properties of self-compacting concrete contain rice husk ash. International Journal of Civil, Structural, Construction and Architectural Engineering, 1, 258–261.

Ashish, D. K., and Verma, S. K. (2021). Robustness of self-compacting concrete containing waste foundry sand and metakaolin: A sustainable approach. Journal of Hazardous Materials, Elsevier, 401(June 2020), 123329.

Ameri, F., Shoaei, P., Bahrami, N., Vaezi, M., & Ozbakkaloglu, T. (2019). Optimum rice husk ash content and bacterial concentration in self-compacting concrete. Construction and Building Materials, 222, 796–813. https://doi.org/10.1016/j.conbuildmat.2019.06.190

Ali, S., Ali, M., Akbar, H., & Ash, R. H. (2011). Utilization of Rice Husk Ash as viscosity modifying agent in Self Compacting Concrete. Construction and Building Materials, 25(2), 1044–1048. https://doi.org/10.1016/j.conbuildmat.2010.06.074

ASTM C 150/ C150M-15, (2015). Standard specification for portland cement. ASTM International, 1–9. https://doi.org/10.1520/C0150

ASTM C33/C33M − 18 Standard Specification for Concrete Aggregates, ASTM International, West Conshohocken, USA. Doi:10.1520/C0033_C0033M-18.

ASTM C 618 – 05, (2005). Standard Specification for Coal Fly Ash and Raw or Calcined Natural Pozzolan for Use in Concrete. AIP Conference Proceedings, 1479(1), 860–863. https://doi.org/10.1063/1.4756275

ASTM C 39/C 39M – 18, (2018) Standard Test Method for Compressive Strength of Cylindrical Concrete Specimens .https://doi.org/10.1520/C0039_C0039M-18

ASTM C496/C496M-17, (2017). Standard Test Method for Splitting Tensile Strength of Cylindrical Concrete Specimens. https://doi.org/10.1520/C0496_C0496M-17

ASTM C642-13, (2013). Standard Test Method for Density, Relative Density (Specific Gravity), and Absorption, 3–8.

ASTM C1585− 13, (2013). Standard Test Method for Measurement of Rate of Absorption of Water by Hydraulic- Cement Concretes1-, 41(147), 1–6. https://doi.org/10.1520/C1585-13.2

ASTM C1202-10. (2010). Standard Test Method for Electrical Indication of Concrete's Ability to Resist Chloride Ion Penetration. https://doi.org/10.1520/C1202-10

ASTM C1012 – 10, (2010). Standard Test Method for Length Change of Hydraulic-Cement Mortars Exposed to a Sulfate Solution. https://doi.org/10.1520/C1012_C1012M-10

ASTM C1610/C160M-17 Standard Test Method for Static Segregation of Self-Consolidating Concrete Using Column Technique, ASTM International, West Conshohocken, USA. Doi: 10.1520/C1610_C1610M-17.

ASTM C1611/C1611M-18 Standard Test Method for Slump Flow of Self-Consolidating Concrete, ASTM International, West Conshohocken, USA. Doi: 10.1520/C1611_C1611M-18.

ASTM C1621/C1621M-17 Standard Test Method for Passing Ability of Self-Consolidating Concrete by J-Ring , ASTM International, West Conshohocken, USA .doi:10.1520/C1621_C1621M-17.

ASTM C1617-17 Standard Test Method for Rapid Assessment of Static Segregation Resistance of Self-Consolidating Concrete Using Penetration Test , ASTM International, West Conshohocken, USA .doi:10.1520/C1712-17.

Aïssoun B, Khayat K, Gallias JL. (2016) Variations of sorptivity with rheological properties of concrete cover in self-consolidating concrete.. 2016; Construction and Building Materials 113:113–120. doi:10.1016/j.conbuildmat..03.006

Bhardwaj B., P. Kumar P., (2018). Waste foundry sand in concrete : A review, Constr. Build. Mater. doi:10.1016/j.conbuildmat.2017.09.010.

Bradshaw S.L., Benson C.H., Olenbush E.H., Melton J.S., (2015). Using foundry sand in green infrastructure construction. Green Streets and Highways 2010, ASCE 2011 280, 280–298.

Bouzoubaa, N., & Fournier, B. (2001). Concrete incorporating rice husk ash: compressive strength and chloride-ion durability. Report MTL 2001-5 (TR), CANMET, 17.

Bronzeoak Ltd. (2003). Rice Husk Ash Market Study. Available online at: www.berr.gov.uk/files/file15138.pdf.

Basha, E. A., Hashim, R., Mahmud, H. B., & Muntohar, A. S. (2005), Stabilization of residual soil with RHA and cement. Construction and Building Materials, 19, 448-453.

Bhanumathidas, N., & Mehta, P. K. (2004). Concrete mixtures made with ternary blended cements containing fly ash and rice husk ash: Fly ash, Silica fume, Slag and Neutral pozzolans in concrete. Proc., Int. Conf., CANMET, ACI SP-199, 1, 379–391.

Benachour, Y., Davy, C. A., Skoczylas, F., & Houari, H. (2008). Effect of high calcite filler addition upon microstructural, mechanical, Shrinkage and transport properties of a mortar. Cement and Concrete Research, 38, 727-736.

BIS: 4031-1989. (1989). Hydraulic cement, methods of physical tests (Part- 14) Bureau of Indi a Standards, New Delhi. Bureau of Indian Standards,New Delhi, (March).

IS 8112: 2013, (2013) Ordinary Portland cement, 43 Grade — Specification, Bureau of Indian Standards, New Delhi. Bureau of Indian Standards,New Delhi, (March).

BIS: 383:1970 (Reaafirmed 1997) Indian standard specification for coarse and fine aggregates from natural sources for concrete (Second Revision).

BIS 3812 (Part-1). (2013). Pulverised fuel ash — Specification. Bureau of Indian Satandards, New Delhi. (May), 1–12.

BIS: 516:1959 (Reaffirmed 1999) Indian Standard Methods of Tests for Strength for Strength of Concrete (Incorporating Amendment Nos 1&2). Edition 1.2 (1991-07)

BIS: 5816:1999 (Reaffirmed 2004) Indian Standard Method of Test for Splitting Tensile Strength of Concrete, First Revision.

Burgos DM, Guzmán Á, Torres N, Delvasto S. (2017). Chloride ion resistance of self-compacting concretes incorporating volcanic materials.Construction and Building Materials 156:565–573.

Basar H.M., Deveci N., (2012). The effect of waste foundry sand (WFS) as partial replacement of sand on the mechanical , leaching and micro-structural characteristics of ready-mixed concrete, Constr. Build. Mater. 35 508–515. doi:10.1016/j.conbuildmat.2012.04.078

Burgos, D. M., Guzmán, Á. & Delvasto, S. (2019). Assessment of the performance of SCC incorporating volcanic materials in a sodium sulfate environment. Construction and Building Materials, 195, 52–65. https://doi.org/10.1016/j.conbuildmat.2018 .11.007

Barger, G. S., Bayles, J., Blair, B., Brown, D., Chen, H., Conway, T., & Hawkins, P. (2001). Ettringite Formation and the Performance of Concrete. Portland cement Association, (2166), 1–16.

Booya E, Mermerdas K, Güneyisi E, Gesog M. (2015). Strength and permeability properties of self-compacting concrete with cold bonded fly ash lightweight aggregate. Construction and Building Materials.74:17–24.

Boudali S, Kerdal DE, Ayed K, Abdulsalam B, Soliman AM. (2016). Performance of self-compacting concrete incorporating recycled concrete fines and aggregate exposed to sulphate attack.; Construction and Building Materials 124:705–713.

Census of world casting production. (2019). Global Casting Production expands, American foundry society. Metal casting design & purchasing jan/feb 2019 pp 27-29.

Chindaprasirt, P., Rukzon, S., & Sirivivatnanon, V. (2008) Resistance to chloride penetration of blended Portland cement mortar containing palm oil fuel ash, rice husk ash and fly ash. Construction and Building Materials, 22, 932–938.

Chandrasekhar, S., Satyanarayana, K. G., Pramada, P. N., Raghavan, P., & Gupta, T. N. (2003). Review Processing, properties and applications of reactive silica from rice husk—an overview. Journal of Materials Science, 38, 3159–3168.

Cizer, O., Van Balen, K., Elsen, J., & Gemert, D.V. (2006). Carbonation and hydration of calcium hydroxide and calcium silicate binders with rice husk ash. In: 2nd International Symposium on Advances in Concrete through Science and Engineering September 11–13, Quebec City, Canada.

Chopra, D., Siddique, R., & Kunal. (2015). Strength, permeability and microstructure of self-compacting concrete containing rice husk ash. Biosystems Engineering, 130, 72–80.

Cachim, P., Velosa, A. L., and Ferraz, E. (2014). Substitution materials for sustainable concrete production in Portugal. KSCE Journal of Civil Engineering, 18(1), 60–66.

Chik, F. A. W., Bakar, B. H. A., Johari, M. A. M., & Jaya, R. P. (2011). Properties of concrete block containing rice husk ash. International Journal of Research & Reviews in Applied Sciences, 8, 57-64.

Carlos, F. R., Sagrario, M. R., & Teresa, B. V. M. (2006). Modelling of slaked lime-Metakaolin mortar engineering characteristics in terms of process variables. Cement and Concrete Composites, 28, 458–467.

Chhorn, C., Hong, S. J., & Lee, S. W. (2018). Relationship between compressive and tensile strengths of roller-compacted concrete. Journal of Traffic and Transportation Engineering (English Edition), 5(3), 215–223. https://doi.org/10.1016/j.jtte.2017.09.002

CCAA.(2011). Technical Note: Sulfate-Resisting Concrete. Cement concrete and aggregates, Australia. St Leonards, NSW; 2011.

Dyer P.P.O.L., Lima M.G.D., Klinsky M.G., Silva S.A., G.J.L. Coppio, (2018).Environmental characterization of Foundry Waste Sand (WFS) in hot mix asphalt (HMA) mixtures, Constr. Build. Mater. 171, 474–484. doi:10.1016/j.conbuildmat.2018.03.151.

Di Maria, F., Sisani, F., Contini, S., Ghosh, S. K., and Mersky, R. L. (2020). Is the policy of the European Union in waste management sustainable? An assessment of the Italian context. Waste Management, Elsevier Ltd, 103, 437–448.

Della, V. P., Kühn, I., & Hotza, D. (2002). Rice husk ash as an alternate source for active silica production. Materials Letters, 57(4), 818–821.

Dinakar P, Babu KG, Santhanam M. (2008). Durability properties of high volume fly ash self-compacting concretes. Cement and Concrete Composites. 30(10):880–886. doi:10.1016/j.cemconcomp.2008.06.011

ERNARC (2005). The European Guidelines for Self-Compacting Concrete, Specification,Production and Use. EFNARC (2005). https://doi.org/0 9539733 4 4

EN 206-9 (2010) Eurocode,Concrete Part 9: Additional rules for Self compacting concrete.

EFNARC. (2002). Specifications and guidelines for self-comApacting concrete. EFNARC, UK. 1-32.

Etxeberria M, Pacheco C, Meneses J M, Beerridi I. Properties of concrete using metallurgical industrial by-product as aggregate. Construction and Building Materials 2010; 24:1594-1600.

FIRST (2004) Foundry Sand Facts for Civil Engineers, May, U.S Department of Transportation, Federal Highway Administration, First Printing. FHWA-IF-04-004.

FAO. (2018). FAO Rice Market Monitor. Food and Agriculture Organization of the United States, 21(1), 1–38.

Farooque, K., Zaman, M., Halim, E., Islam, S., Hossain, M., Mollah, Y., & Mahmood, A. (2009). Characterization and utilization of rice husk ash (RHA) from rice mill of Bangladesh. Bangladesh Journal of Scientific and Industrial Research, 44, 157–162.

Farhan, N. A., Sheikh, M. N., and Hadi, M. N. S. (2020). Effect of steel fiber on engineering properties of geopolymer concrete. ACI Materials Journal, 117(3), 29–40.

GCCA, https://gccassociation.org/ (accessed June 18, 2019).

Gupta, C. K., Birgonda, S., Sachan, A. K., and Pooja. (2021). Self-compacting concrete with manufactured sand and recycled coarse aggregate. Indian Journal of Environmental Protection, 41(6), 627–634.

Ghasemi, Y., Emborg, M., and Cwirzen, A. (2018). Estimation of specific surface area of particles based on size distribution curve. Magazine of Concrete Research, 70(10), 533–540.

Guney, Y., Dursun, Y., Yalcin, M., Tuncan, A., and Donmez, S. (2010). “Re-usage of waste foundry sand in high-strength concrete.” Waste Management, Elsevier Ltd, 30(8–9), 1705–1713.

Ganeshan M., Sreevidya V., Salim P.M., (2016). Waste Foundry Sand as a Replacement for Fine Aggregate in High Strength Solid Masonry Blocks, 6878–6886. doi:10.15680/IJIRSET.2016.0505037.

Güneyisi E, Özturan T, Öznur H, Sabah D.(2014). Permeation characteristics of self-compacting concrete made with partially substitution of natural aggregates with rounded lightweight aggregates. Construction and Building Materials 59:1–9.

Gurumoorthy N., Arunachalam K., (2016). Micro and mechanical behaviour of Treated Used Foundry Sand concrete, Constr. Build. Mater. 123 184–190. doi:10.1016/j.conbuildmat.2016.06.143.

Habeeb, G. A., & Mahmud, H. B. (2010). Study on properties of rice husk ash and its use as cement replacement material. Materials Research, 13, 185–190.

Hwang, C. L., & Chandra, S. (1997). Waste materials used in concrete manufacturing. William Andrew. inc, 184-234.

He, R., Zheng, S., Gan, V. J. L., Wang, Z., Fang, J., & Shao, Y. (2020). Damage mechanism and interfacial transition zone characteristics of concrete under sulfate erosion and Dry-Wet cycles. Construction and Building Materials, 255, 119340. https://doi.org/10.1016/j.conbuildmat.2020.119340

Habeeb, G. A., Fayyadh, M. M. (2009). Rice husk ash concrete: the effect of RHA average particle size on mechanical properties and drying shrinkage. Australian Journal of Basic and Applied Science, 3, 1616–1622.

Ikumi T, Cavalaro SHP, Segura I.(2019). The role of porosity in external sulphate attack. Cement and Concrete Composites. 97:1–12. doi:10.1016/j.cemconcomp.2018.12.016

Jha, P., Sachan, A. K., and Singh, R. P. (2021). Properties of Concrete with Bagasse Ash and Stone Dust Exposed to Sulphate Attack." Lecture Notes in Civil Engineering, 135 LNCE (April), 29–37.

Jauberthie, R., Rendell, F., Tamba, S., & Cisse, I. (2000). Origin of the pozzolanic effect of rice husks. Construction and Building Materials, 14, 419–423.

Juma, A., Sai, R., Prakash, D. V. A. K., Haider, S., & Rao, S. K. (2012). An experimental study on synergic effect of sugar cane bagasse ash with rice husk ash on

self-compaction concrete. International Journal of Science and Advanced Technology, 2, 75-80

Kapoor K., Singh S.P., Singh B., (2016) .Durability of self-compacting concrete made with Recycled Concrete Aggregates and mineral admixtures, Construction and Building Materials, 128 67–76.

Kraus R.N., Naik T.R., Ramme B.W., Kumar, F. Ash, (2009). Use of foundry silica-dust in manufacturing economical self-consolidating concrete Foundry Dust, Constr. Build. Mater. 23 3439–3442. doi:10.1016/j.conbuildmat.2009.06.006.

Kannan, V., & Ganesan, K. (2015). Effect of tricalcium aluminate on durability properties of self-compacting concrete incorporating rice husk ash and metakaolin. ASCE Journal of Materials in Civil Engineering, DOI: 10.1061/ (ASCE) MT.1943-5533.0001330.

Kannan, V., & Ganesan, K. (2014). Chloride and chemical resistance of self compacting concrete containing rice husk ash and metakaolin. Construction and Building Materials, 51, 225–234.

Krishna, S. N. (2012). Rice husk ash – an ideal admixture for concrete in aggressive environments. 37th Conference on Our World in Concrete & Structures, 29-31 August 2012, Singapore.

Khatib J. M., Baig S., Bougara A., (2010). Booth, Foundry Sand Utilisation in Concrete Production.Second International Conference on Sustainable Construction Materials and Technologies.

Khadiry, S. M., Nayak, G. P., Aziz, T., Saurav, S., & Pai, B. H. V. (2014). Evaluation of properties of self-compacting concrete specimens having rice husk ash and shell lime powder as fillers. American Journal of Engineering Research, 3, 207-211.

Kosmatka, Steven H.; Wilson ML. (2002). Design and Control of Concrete Mixtures – The Guide to Applications, Methods and Materials. Portland cement Association.

Kolias, S., and Georgiou, C. (2005). “The effect of paste volume and of water content on the strength and water absorption of concrete.” *Cement and Concrete Composites*, 27(2), 211–216.

Le, H. T., Siewert, K., & Ludwig, H. M. (2015). Alkali silica reaction in mortar formulated from self-compacting high performance concrete containing rice husk ash. Construction and Building Materials, 88, 10–19.

Ling, S. K., & Kwan, A. K. H. (2016). Adding limestone fines as cementitious paste replacement to lower carbon footprint of SCC. Construction and Building Materials, 111, 326–336. https://doi.org/10.1016/j.conbuildmat.2016.02.072

Mehta, P. K. (1992). Rice husk as: a unique supplementary cementing material. In: Proceedings of the International Symposium on Advances in Concrete Technology; 1992 May; Athens, Greece. Canada: CANMET, 407-430.

Madrid, R., Nogueira, C., & Margarido, F. (2012). Production and characterisation of amorphous silica. In: 4th International Conference on Engineering for Waste and Biomass Valorisation, September 10-13, 2012 – Porto, Portugal.

Mohseni E., Naseri F., Amjadi R., Khotbehsara MM,.,Ranjbar M.M.,(2016).Microstructure and durability properties of cement mortars containing nano-TiO2 and rice husk ash, Constr. Build. Mater. 114 (2016) 656–664.

Memon, S. A., Shaikh, M. A., & Akbar, H. (2011). Utilization of Rice Husk Ash as viscosity modifying agent in self-compacting concrete. Construction and Building Materials, 25, 1044–1048.

Memon, S. A., Shaikh, M. A., & Akbar, H. (2008). Production of low cost self-compacting concrete using rice husk ash. In: First International Conference on Construction in Developing Countries (ICCIDC–I), August 4-5, 2008, Karachi,, Pakistan, 260–269.

Mostofinejad, D., Hosseini, S. M., Nosouhian, F., Ozbakkaloglu, T., & Nader Tehrani, B. (2020). Durability of concrete containing recycled concrete coarse and fine aggregates and milled waste glass in magnesium sulfate environment. Journal of Building Engineering, 29(January), 1–11. https://doi.org/10.1016/j.jobe.2020.101182

Molaei Raisi, E., Vaseghi Amiri, J., & Davoodi, M. R. (2018). Mechanical performance of self-compacting concrete incorporating rice husk ash. Construction and Building Materials, 177, 148–157. https://doi.org/10.1016/j.conbuildmat. 2018.05.053

Martins, M. A. B., Silva, L. R. R., Kuffner, B. H. B., Barros, R. M., and Melo, M. L. N. M. (2022a). Behavior of high strength self-compacting concrete with marble/granite processing waste and waste foundry exhaust sand, subjected to chemical attacks.Construction and Building Materials, Elsevier Ltd, 323(January), 126492.

Martins, M. A., Barros, R. M., da Silva, L. R. R., dos Santos, V. C., Lintz, R. C. C., Gachet, L. A., Melo, M. de L., and Martinez, C. B. (2022b). Durability indicators of high-strength self-compacting concrete with marble and granite wastes and waste foundry exhaust sand using electrochemical tests. Construction and Building Materials, Elsevier Ltd, 317(November 2021), 125907.

Makul, N. (2019). Combined use of untreated-waste rice husk ash and foundry sand waste in high-performance self-consolidating concrete. Results in Materials, Elsevier Ltd, 1(July), 100014.

Naik TR., Singh SS., and Ramme BW. (2001) Performance and leaching assessment of flow able slurry. Journal of Environmental Engineering 2001:359-368.

Nair, D., Fraaij, A., Klaassen, A., & Kentgens, A. (2008) A structural investigation relating to the pozzolanic activity of rice husk ashes. Cement and Concrete Research, 38, 861-869.

Neville, A. M. (1996). Properties of concrete, 4th edition. New York, USA: John Wiley & Sons, Inc.

Okamura H., and Ouchi M., (2003). Self-compacting concrete. Journal of Advanced Concrete Technology Vol. 1 pp. 5-15.

Prabhu G.G., Bang J.W., Lee B.J., Hyun J.H., Kim Y.Y., (2015). Mechanical and Durability Properties of Concrete Made with Used Foundry Sand as Fine Aggregate,

Hindawi Publishing Corporation Advances in Materials Science and Engineering Volume 2015, Article ID 161753, doi.org/10.1155/2015/161753.

Pathak N., Siddique R., (2012.) Effects of elevated temperatures on properties of self-compacting-concrete containing fly ash and spent foundry sand, Constr. Build. Mater. 34 512–521. doi:10.1016/j.conbuildmat.2012.02.026.

Prasad, C. S., Maiti, K. N., & Venugopal, R. (2000). Effect of rha in white ware composition. Ceramics International, 27, 629.

Parashar, A., Aggarwal, P., Saini, B., Aggarwal, Y., and Bishnoi, S. (2020). Study on performance enhancement of self-compacting concrete incorporating waste foundry sand.Construction and Building Materials, Elsevier Ltd, 251, 118875.

Pai, B. H. V., Nandy, M., Krishnamoorthy, A., Sarkar, P. K., & George, P. (2014). Comparative study of self-compacting concrete mixes containing fly ash and rice husk ash. American Journal of Engineering Research, 03, 150–154.

Park, K. B., Kwon, S. J., & Wang, X. Y. (2016). Analysis of the effects of rice husk ash on the hydration of cementitious materials. Construction and Building Materials, 105, 196–205. https://doi.org/10.1016/j.conbuildmat.2015.12.086

Prabhu G.G., Hyun J.H., Kim Y.Y., (2014). Effects of foundry sand as a fine aggregate in concrete production, Construction and building material. 70, 514–521. doi:10.1016/j.conbuildmat.2014.07.070.

Piasta W, Marczewska J, Jaworska M. (1985). Some aspects and mechanisms of sulphate attack. Structure.19–24.

Rahman, F.,Adil, W.,Raheel, M.,Saberian, M.,Li, J.,Maqsood, T. (2022). Experimental investigation of high replacement of cement by pumice in cement mortar: A mechanical, durability and microstructural study In: Journal of Building Engineering, 49, 1 – 14

Rao, A., Jha, K. N., and Misra, S. (2007). Use of aggregates from recycled construction and demolition waste in concrete.Resources, Conservation and Recycling, 50(1), 71–81.

Raju S.R., (2016) A Study on Compressive Strength of Self- Compacting Concrete Using Portland Slag Cement with Partial Replacement of Fine Aggregate by Foundry Sand, 4673–4680. doi:10.15680/IJIRSET.2016.0504010.

Reddy, D. V., & Marcelina, B. S. (2006). Marine durability characteristics of rice husk ash-modified reinforced concrete. In: International Latin American and Caribbean Conference for Engineering and Technology; 2006 Jun 21-23; Mayaguez, Puerto Rico. Puerto Rico: University of Puerto Rico at Mayagüez.

Rego, J. H. S., Nepomuceno, A. A., Figueiredo, E. P., Hasparyk, N. P., & Borges, L. D. (2015). Effect of particle size of residual rice-husk ash in consumption of Ca(OH)2. ASCE Journal of Materials in Civil Engineering, 27, 04014178 1-8.

Rahman, M. E., Muntohar, A. S., Pakrashi, V., Nagaratnam, B. H., & Sujan, D. (2014). Self-compacting concrete from uncontrolled burning of rice husk and blended fine aggregate. Materials and Design, 55, 410–415.

Rukzon, S., & Chindaprasirt, P. (2014). Use of Rice Husk-Bark Ash in Producing Self-Compacting Concrete, Advances in Civil Engineering, Hindawi Publishing, 14(325). Article ID 429727, 6 pages.

Ramasamy, V. (2011). Compressive strength and durability properties of rice husk ash concrete. KSCE Journal of Civil Engineering, 16, 93-102.

Siddique R. (2008). Waste Materials and By-Products in Concrete, Springer.

Siddique R., Singh G., (2011). Utilization of waste foundry sand (WFS) in concrete manufacturing, "Resources, Conserv. Recycl. 55 885–892. doi:10.1016/j.resconrec.2011.05.001.

Siddique R., Kaur G., Rajor A., (2010). Waste foundry sand and its leachate characteristics, Resources, Conservation and Recycling. doi:10.1016/j.resconrec.2010.04.006.

Siddique, R., and Noumowe, A. (2008). Utilization of spent foundry sand in controlled low-strength materials and concrete. Resources, Conservation and Recycling 53, 27–35.

Sahmaran M., Lachemi M.L., Erdem T.K., Yusel H.E., (2011).Use of spent foundry sand and fly ash for the development of green self-consolidating concrete, Materials and Structures 44 1193–1204. Doi: 10.1617/s11527-010-9692-7.

Stroeven P, Bui DD, & Sabuni E. (1999). Ash of vegetable waste used for economic production of low to high strength hydraulic binders. Fuel, 7, 153–159.

Sahu, A.K., Kumar, S and Sachan, A.K. (2003) Crushed stone waste as fine aggregates for concrete. The Indian Concrete Journal,; 1: 845-848.

Sua-Iam, G., & Makul, N. (2013). Utilization of limestone powder to improve the properties of self-compacting concrete incorporating high volumes of untreated rice husk ash as fine aggregate. Construction and Building Materials, 38, 455–464.

Siddique, R., & Khan, M. I. (2011). Supplementary Cementing Materials. Springer-Verlag Berlin Heidelberg. DOI: 10.1007/978-3-642-17866-5.

Safiuddin, M., West, J. S., & Soudki, K. A. (2012). Properties of freshly mixed self-consolidating concretes incorporating rice husk ash as a supplementary cementing material. Construction and Building Materials, 30, 833–842.

Sua-Iam, G., & Makul, N. (2014). Utilization of high volumes of unprocessed lignite-coal fly ash and rice husk ash in self-consolidating concrete. Journal of Cleaner Production, 78, 184–194.

Sua-Iam, G., & Makul, N. (2012). Self-Compacting Concrete Prepared Using Rice Husk Ash Waste from Electric Power Plants. Advanced Materials Research, 488-489, 258–262.

Sukumar, B., Nagamani, M., & Raghavan, R.S. (2008). Evaluation of strength at early ages of self-compacting concrete with high volume fly ash. Construction and Building Materials, 22, 1394-1401.

Safiuddin, M., West, J. S., & Soudki, K. A. (2010). Hardened properties of self-consolidating high performance concrete including rice husk ash. Cement and Concrete Composites, 32, 708–717

Sadrmomtazi, A., & Barzegar, A. (2010). Assessment of the effect of Nano-SiO2 on physical and mechanical properties of self-compacting concrete containing rice husk ash.Second international conference on sustainable construction material and technologies,Italy.

Sua-iam, G., Makul, N., Cheng, S., & Sokrai, P. (2019). Workability and compressive strength development of self-consolidating concrete incorporating rice husk ash and foundry sand waste – A preliminary experimental study. Construction and Building Materials, 228, 116813. https://doi.org/10.1016/j.conbuildmat.2019.116813

Smarzewski, P., Barnat-Hunek, D., and Jezierski, W. (2018). The Possibility of Using Boiler Slag as Coarse Aggregate in High Strength Concrete. KSCE Journal of Civil Engineering, 22(5), 1816–1826.

Smarzewski P., D. Barnat-hunek D., Jezierski W., (2016). Mechanical and durability related properties of high performance concrete made with coal cinder and waste foundry sand, (2016) Constr. Build. Mater. 121 9–17. doi:10.1016/j.conbuildmat.2016.05.148.

Siddique R., Aggarwal Y., Aggarwal P., Kadri E., Bennacer R., (2011). Strength, durability, and micro-structural properties of concrete made with used-foundry sand (UFS), Constr. Build. Mater. 25 1916–1925. doi:10.1016/j.conbuildmat.2010.11.065.

Singh G., Siddique R., (2012). Effect of waste foundry sand (WFS) as partial replacement of sand on the strength, ultrasonic pulse velocity and permeability of concrete, Constr. Build. Mater. 26 416–422. doi:10.1016/j.conbuildmat.2011.06.041.

Siddique R., Schutter G.De, Noumowe A., (2009). Effect of used-foundry sand on the mechanical properties of concrete, Constr. Build. Mater. 23 976–980. doi:10.1016/j.conbuildmat.2008.05.005.

Siddique R., Kadri E., (2011).Effect of metakaolin and foundry sand on the near surface characteristics of concrete, Constr. Build. Mater. 1–10. doi:10.1016/j.conbuildmat.2011.03.012.

Santhanam M, Cohen MD, Olek J. (2001).Sulfate attack research. Cement and Concrete Research. 2001; 31(6):845–851. Doi: 10.1016/S0008-8846(01)00510-5

The Institute of Indian Foundrymen, https://www.indianfoundry.org/cms-index.php (accessed June 18, 2019).

Tao, J. (2005). Preliminary study on the water permeability and microstructure of concrete incorporating nano-SiO2. Cement and Concrete Research, 35, 1943-1947.

Torres A., Bartlett L., Pilgrim C., (2017). Effect of foundry waste on the mechanical properties of Portland Cement Concrete, Constr. Build. Mater. 135 674–681. doi:10.1016/j.conbuildmat.2017.01.028.

Xu, W., Lo, T. Y., & Memon, S. A. (2012). Microstructure and reactivity of rich husk ash. Construction and Building Materials, 29, 541-547.

Xu, A., Shayan, A., Baburamani, P., (1998). ARRB Transport Research, L., & National Interest Service (Australia). (1998). Test methods for sulfate resistance of concrete and mechanism of sulfate attack : a state-of-the-art review. Review Report, (5), 38.

Zhang, M. H., & Malhotra, V. M. (1996). High-performance concrete incorporating rice husk ash as a supplementary cementing materials. ACI Materials Journal, 93, 629-636.

Zareei, S. A., Ameri, F., Dorostkar, F., & Ahmadi, M. (2017). Rice husk ash as a partial replacement of cement in high strength concrete containing micro silica: Evaluating durability and mechanical properties. Case Studies in Construction Materials, 7(October 2016), 73–81. https://doi.org/10.1016/j.cscm.2017.05.001

Zhu, W., & Bartos, P. J. M. (2003). Permeation properties of self-compacting concrete, Cement and Concrete Research, 33(September 2002), 921–926. https://doi.org/10.1016/S0008-8846 (02)01090-6

Zhang, M.H., Lastra, R., & Malhotra, V.M. (1996). Rice-husk ash paste and concrete: some aspects of hydration and the microstructure of the interfacial zone between the aggregate and paste. Cement and Concrete Research, 26, 963–977.